

Musculoskeletal Modelling to Analyse and Treat Anterior Cruciate Ligament Deficiency

Nur Liyana Binti Azmi

Imperial College London

Department of Bioengineering

A thesis submitted in fulfilment of the requirements for the degree of Doctor of Philosophy
at Imperial College London and the Diploma of Imperial College

September 2017

Abstract

Anterior cruciate ligament (ACL) deficiency results in knee instability that includes an increase in internal tibial rotation and anterior tibial translation (ATT) as ACL is the primary restraint to anterior shear and internal rotation. Clinically, ACL deficient (ACLD) patients undergo surgery or/and rehabilitation programmes depending on their ability to cope or otherwise. However, the ACL reconstructed (ACLR) knees may still have residual instability in ATT and tibial internal rotation. Functional electrical stimulation (FES) has been used in conventional physiotherapy for ACL deficiency, including strengthening the muscles around the knee. The rehabilitation treatment focuses on strengthening the quadriceps muscle because it gets weakened after ACL injury or ACL reconstruction. However, stimulating the hamstrings, especially the biceps femoris long head (BFLH) with its insertion on the fibular head is a candidate to reduce the knee instability of ACLD and ACLR by applying a posterior pull and external rotation to the tibia. This thesis proposes that knee instability in ACLD subjects can be reduced by stimulating the BFLH muscle with FES. Here, a musculoskeletal modelling approach was used to simulate the function of FES. A new optimisation method was developed which allowed the inclusion of FES. There are three main studies present in this thesis. First, a pilot study was conducted in which healthy control subjects walked with and without FES of BFLH. It was found that selective activation of the BFLH can reduce the anterior tibial shear and tibial internal rotation torque at the knee in healthy subjects. Second, a validation study for the algorithm used in the musculoskeletal model was conducted in which the effect of FES stimulation of the BFLH on gluteus maximus activations was tested using electromyography (EMG). This study concluded that there were statistical correlations between peak and impulse of gluteus maximus activation between FES activation level and muscle activity of gluteus maximus as quantified by both EMG and the musculoskeletal model. In the final study, the validated model was used to compare the internal rotation torque, anterior shear force, speed and gluteus medius and gluteus maximus muscle activation between control, ACLD and ACLR groups during stance phase with and without FES stimulated on BFLH. This study found that the activation of BFLH with FES during stance phase was able to reduce the knee instability of the patient groups and triggered the compensatory mechanism for each patient group to react differently. Therefore, besides quadriceps, the rehabilitation treatment should focus on appropriate timed activation of the BFLH to improve the quality of life of patients.

Table of contents

Abstract	2
Table of contents	3
List of Figures	5
List of Tables	9
Abbreviations	10
Acknowledgements	11
Declaration of Originality	12
CHAPTER 1 THESIS MOTIVATION AND SCOPE	13
1.1 Problem Statement and Motivation	14
1.2 Aim and Scope	15
1.3 Thesis Objectives	15
1.4 Thesis Outline	16
CHAPTER 2 LITERATURE REVIEW AND BACKGROUND	17
2.1 Functional Anatomy of Anterior Cruciate Ligament (ACL)	18
2.2 Knee Muscles and the ACL	22
2.3 Anterior Cruciate Ligament Deficiency (ACLD)	24
2.4 Treatment of ACL Injury	27
2.5 Reconstruction Surgery	28
2.6 Functional Electrical Stimulation (FES)	30
2.7 Conclusion	35
CHAPTER 3 MUSCULOSKELETAL MODELLING TO INVESTIGATE THE USE OF FES AT THE KNEE	36
3.1 Introduction	37
3.2 Materials and Methods	38
3.3 Results	47
3.4 Discussion	65
3.5 Conclusion	68
CHAPTER 4 VALIDATION OF THE FES MODEL DURING GAIT	69
4.1 Introduction	70
4.2 Methods and Materials	71
4.3 Results	75
4.4 Discussion	83

4.5 Conclusion	85
CHAPTER 5 MUSCULOSKELETAL MODEL TO INVESTIGATE THE USE OF FES AT THE ACLD AND ACLR KNEE	86
5.1 Introduction	87
5.2 Materials and Methods	89
5.3 Results	94
5.4 Discussion	110
5.5 Conclusion	116
CHAPTER 6 DISCUSSION AND CONCLUSIONS	117
6.1 Key findings	118
6.2 The role of FES in rehabilitation	120
6.3 FES and muscle learning	122
6.4 Muscle learning and its application in medicine or physiotherapy	123
6.5 Conclusions	124
APPENDIX A : Ethics	125
APPENDIX B : Gluteus maximus muscle activations predicted from modelling and the measured EMG. These results are summarised in Chapter 4.	134
DISSEMINATION	149
REFERENCES	150

List of Figures

Figure 2.1 Posterior aspect of a left knee (© Primal Pictures. All rights reserved. Primal Pictures, an informa business www.primalpictures.com www.anatomy.tv) highlighting the femoral origin of the anterior cruciate ligament.	18
Figure 2.2 Anterior aspect of a left knee (© Primal Pictures. All rights reserved. Primal Pictures, an informa business www.primalpictures.com www.anatomy.tv) highlighting the tibial insertion of the anterior cruciate ligament.	19
Figure 2.3 Caudal view of tibial plateau of a right cadaveric specimen. The ACL insertion site is marked, and its relation with the medial tibial spine and anterior horn of the lateral meniscus is shown (The Journal of Arthroscopic & Related Surgery, Anatomic Single- and Double-Bundle Anterior Cruciate Ligament Reconstruction Flowchart, 26, 2010, page 263, Carola F. van Eck, Bryson P. Lesniak, Verena M. Schreiber, Freddie H. Fu. Copyright © 2010 Arthroscopy Association of North America. Published by Elsevier Inc. All rights reserved. "With permission of Springer")	20
Figure 2.4 Rotation and translation motions of the knee joint (Sports Medicine, A 'Plane' Explanation of Anterior Cruciate Ligament Injury Mechanisms, Carmen E. Quatman et. al, 40, 2010, page 731, Copyright © 2010, Adis Data Information BV "With permission of Springer") ..	21
Figure 2.5 Hamstring muscles (© Primal Pictures. All rights reserved. Primal Pictures, an informa business www.primalpictures.com www.anatomy.tv)	23
Figure 2.6 Quadriceps muscles (© Primal Pictures. All rights reserved. Primal Pictures, an informa business www.primalpictures.com www.anatomy.tv).....	24
Figure 2.7 Multiplanar loading mechanism of a noncontact anterior cruciate ligament injury. Image reproduced with permission from Levine et al. (2013)	25
Figure 3.1 Stimulation pulse width intensity level.....	39
Figure 3.2 The FES stimulation setting.....	40
Figure 3.3 Schematic of stimulation output normalised to maximum stimulation level.....	41
Figure 3.4 The FES device and the switch.....	41
Figure 3.5 Lab set-up	42
Figure 3.6 Optical motion tracking markers and FES electrode positioning	43
Figure 3.7 Peak tibial internal torque (Nm/BW) across twelve subjects during normal and FES gait	47
Figure 3.8 Tibial internal rotation torque (Nm/BW) (mean ± SD) of subject 1 during normal and FES gait.....	48
Figure 3.9 Tibial internal rotation torque (Nm/BW) (mean ± SD) of subject 2 during normal and FES gait.....	48
Figure 3.10 Tibial internal rotation torque (Nm/BW) (mean ± SD) of subject 3 during normal and FES gait.....	49
Figure 3.11 Tibial internal rotation torque (Nm/BW) (mean ± SD) of subject 4 during normal and FES gait.....	49
Figure 3.12 Tibial internal rotation torque (Nm/BW) (mean ± SD) of subject 5 during normal and FES gait.....	50
Figure 3.13 Tibial internal rotation torque (Nm/BW) (mean ± SD) of subject 6 during normal and FES gait.....	50
Figure 3.14 Tibial internal rotation torque (Nm/BW) (mean ± SD) of subject 7 during normal and FES gait.....	51
Figure 3.15 Tibial internal rotation torque (Nm/BW) (mean ± SD) of subject 8 during normal and FES gait.....	51

Figure 3.16 Tibial internal rotation torque (Nm/BW) (mean \pm SD) of subject 9 during normal and FES gait.....	52
Figure 3.17 Tibial internal rotation torque (Nm/BW) (mean \pm SD) of subject 10 during normal and FES gait.....	52
Figure 3.18 Tibial internal rotation torque (Nm/BW) (mean \pm SD) of subject 11 during normal and FES gait.....	53
Figure 3.19 Tibial internal rotation torque (Nm/BW) (mean \pm SD) of subject 12 during normal and FES gait.....	53
Figure 3.20 (a) Tibial adduction torque (Nm/BW) and (b) tibial flexion torque (Nm/BW) during normal and FES gait for all subjects (mean \pm SD, n=12).....	55
Figure 3.21 Anterior shear force (BW) (mean \pm SD) of subject 1 during normal and FES gait.....	57
Figure 3.22 Anterior shear force (BW) (mean \pm SD) of subject 2 during normal and FES gait.....	58
Figure 3.23 Anterior shear force (BW) (mean \pm SD) of subject 3 during normal and FES gait.....	58
Figure 3.24 Anterior shear force (BW) (mean \pm SD) of subject 4 during normal and FES gait.....	59
Figure 3.25 Anterior shear force (BW) (mean \pm SD) of subject 5 during normal and FES gait.....	59
Figure 3.26 Anterior shear force (BW) (mean \pm SD) of subject 6 during normal and FES gait.....	60
Figure 3.27 Anterior shear force (BW) (mean \pm SD) of subject 7 during normal and FES gait.....	60
Figure 3.28 Anterior shear force (BW) (mean \pm SD) of subject 8 during normal and FES gait.....	61
Figure 3.29 Anterior shear force (BW) (mean \pm SD) of subject 9 during normal and FES gait.....	61
Figure 3.30 Anterior shear force (BW) (mean \pm SD) of subject 10 during normal and FES gait....	62
Figure 3.31 Anterior shear force (BW) (mean \pm SD) of subject 11 during normal and FES gait....	62
Figure 3.32 Anterior shear force (BW) (mean \pm SD) of subject 12 during normal and FES gait....	63
Figure 3.33 Predicted peak anterior shear force across twelve subjects using standard and revised optimisation methods	63
Figure 3.34 Knee joint compressive forces (mean \pm SD, n=12) using standard and revised optimisation: (a) medial, (b) lateral, (c) total force.	64
Figure 4.1 EMG and FES electrode positions.....	74
Figure 4.2 Model predictions of gluteus maximus muscle activations (mean \pm SD, n=15). Standard optimisation refers to muscle activations during normal walking, and revised optimisation presents the muscle activations during FES applied walking	75
Figure 4.3 Gluteus maximus EMG measurements (mean \pm SD, n=15) in normal walking and FES applied walking.....	76
Figure 4.4 Correlations between predicted peak gluteus maximus activation and its measured peak EMG signals in each sub-phase of the stance phase: (a)-(d). The four datapoints in each graph represent normal walking, and FES applied walking with FES currents of 40 mA, 60 mA and 80 mA.....	77
Figure 4.5 Correlations between predicted gluteus maximus activation impulse (area under the curve) and measured EMG impulse in each sub-phase of the stance phase : (a)-(d). The four datapoints in each graph represent normal walking, and FES applied walking with FES currents of 40 mA, 60 mA and 80 mA.	80
Figure 5.1 Internal rotation torque (Nm/BW) (mean \pm SD) for control (n=8), ACLD (n=4) and ACLR (n=4) groups during normal gait and FES gait.....	96
Figure 5.2 Internal rotation torque (Nm/BW) (mean \pm SD) for control (n=8), ACLD (n=4) and ACLR (n=4) groups during normal gait.....	96
Figure 5.3 Internal rotation torque (Nm/BW) for control group (mean \pm SD,n=8) during normal gait and FES gait.....	97
Figure 5.4 Internal rotation torque (Nm/BW) for ACLD group (mean \pm SD, n=4) during normal gait and FES gait	97

Figure 5.5 Internal rotation torque (Nm/BW) for ACLR groups (mean \pm SD, n=4) during normal gait and FES gait	98
Figure 5.6 Mean shear force (BW) curves (mean \pm SD) for 8 control healthy subjects, 4 ACLD subjects and 4 ACLR subjects.....	99
Figure 5.7 Shear force (BW) (mean \pm SD) for subject ACLD1 (Full Tear)	100
Figure 5.8 Shear force (BW) (mean \pm SD) for subject ACLD2 (Partial Tear)	101
Figure 5.9 Shear force (BW) (mean \pm SD) for subject ACLD3 (Full Tear)	101
Figure 5.10 Shear force (BW) (mean \pm SD) for subject ACLD4 (Partial Tear)	102
Figure 5.11 Shear force (BW) (mean \pm SD) for subject ACLR1	102
Figure 5.12 Shear force (BW) (mean \pm SD) for subject ACLR2	103
Figure 5.13 Shear force (BW) (mean \pm SD) for subject ACLR3	103
Figure 5.14 Shear force (BW) (mean \pm SD) for subject ACLR4	104
Figure 5.15 Gluteus maximus muscle activation (mean \pm SD) for 8 control subjects	106
Figure 5.16 Gluteus maximus muscle activation (mean \pm SD) for 4 ACLD subjects	107
Figure 5.17 Gluteus maximus muscle activation (mean \pm SD) for 4 ACLR subjects.....	107
Figure 5.18 Gluteus medius muscle activation (mean \pm SD) for 8 control subjects	108
Figure 5.19 Gluteus medius muscle activation (mean \pm SD) for 4 ACLD subjects.....	109
Figure 5.20 Gluteus medius muscle activation (mean \pm SD) for 4 ACLR subjects.....	109
Figure B.1 Gluteus maximus model predictions of subject 1 in normal walking and FES applied walking.....	134
Figure B.2 Gluteus maximus EMG measurement of subject 1 in normal walking and FES applied walking.....	134
Figure B.3 Gluteus maximus model predictions of subject 2 in normal walking and FES applied walking.....	135
Figure B.4 Gluteus maximus EMG measurement of subject 2 in normal walking and FES applied walking.....	135
Figure B.5 Gluteus maximus model predictions of subject 3 in normal walking and FES applied walking.....	136
Figure B.6 Gluteus maximus EMG measurement of subject 3 in normal walking and FES applied walking.....	136
Figure B.7 Gluteus maximus model predictions of subject 4 in normal walking and FES applied walking.....	137
Figure B.8 Gluteus maximus EMG measurement of subject 4 in normal walking and FES applied walking.....	137
Figure B.9 Gluteus maximus model predictions of subject 5 in normal walking and FES applied walking.....	138
Figure B.10 Gluteus maximus EMG measurement of subject 5 in normal walking and FES applied walking.....	138
Figure B.11 Gluteus maximus model predictions of subject 6 in normal walking and FES applied walking.....	139
Figure B.12 Gluteus maximus EMG measurement of subject 6 in normal walking and FES applied walking.....	139
Figure B.13 Gluteus maximus model predictions of subject 7 in normal walking and FES applied walking.....	140
Figure B.14 Gluteus maximus EMG measurement of subject 7 in normal walking and FES applied walking.....	140
Figure B.15 Gluteus maximus model predictions of subject 8 in normal walking and FES applied walking.....	141

Figure B.16 Gluteus maximus EMG measurement of subject 8 in normal walking and FES applied walking.....	141
Figure B.17 Gluteus maximus model predictions of subject 9 in normal walking and FES applied walking.....	142
Figure B.18 Gluteus maximus EMG measurement of subject 9 in normal walking and FES applied walking.....	142
Figure B.19 Gluteus maximus model predictions of subject 10 in normal walking and FES applied walking.....	143
Figure B.20 Gluteus maximus EMG measurement of subject 10 in normal walking and FES applied walking.....	143
Figure B.21 Gluteus maximus model predictions of subject 11 in normal walking and FES applied walking.....	144
Figure B.22 Gluteus maximus EMG measurement of subject 11 in normal walking and FES applied walking.....	144
Figure B.23 Gluteus maximus model predictions of subject 12 in normal walking and FES applied walking.....	145
Figure B.24 Gluteus maximus EMG measurement of subject 12 in normal walking and FES applied walking.....	145
Figure B.25 Gluteus maximus model predictions of subject 13 in normal walking and FES applied walking.....	146
Figure B.26 Gluteus maximus EMG measurement of subject 13 in normal walking and FES applied walking.....	146
Figure B.27 Gluteus maximus model predictions of subject 14 in normal walking and FES applied walking.....	147
Figure B.28 Gluteus maximus EMG measurement of subject 14 in normal walking and FES applied walking.....	147
Figure B.29 Gluteus maximus model predictions of subject 15 in normal walking and FES applied walking.....	148
Figure B.30 Gluteus maximus EMG measurement of subject 15 in normal walking and FES applied walking.....	148

List of Tables

Table 2.1 Motor unit recruitment during voluntary contraction and NMES contraction (from Maffiuletti, 2010)	32
Table 3.1 Anthropometric data.....	39
Table 3.2 Marker positions.....	43
Table 3.3 Peak tibial internal rotation torque (Nm/BW) during normal and FES gait.....	47
Table 3.4 Peak tibial adduction torque (Nm/BW) and peak tibial flexion torque (Nm/BW) during normal and FES gait.....	54
Table 3.5 Peak anterior shear force (BW) and muscle activation	56
Table 3.6 Difference mean peak internal rotational torque (Nm/BW).....	57
Table 3.7 Knee joint compressive forces (BW) during normal and FES gait.....	65
Table 4.1 Anthropometric data of the subjects.....	72
Table 4.2 Peak gluteus maximus activations calculated by musculoskeletal modelling and as measured by EMG during the stance phase of normal walking and FES applied walking. <i>c</i> values of 0.10, 0.15 and 0.20 in models represent FES currents of 40 mA, 60 mA and 80 mA, respectively (mean \pm SD), N=15).....	77
Table 4.3 Peak gluteus maximus activations calculated by musculoskeletal modelling and as measured by EMG during initial contact (0-3% of stance phase) of normal walking and FES applied walking.	78
Table 4.4 Peak gluteus maximus activations calculated by musculoskeletal modelling and as measured by EMG during loading response (4-19% stance phase) of normal walking and FES applied walking	78
Table 4.5 Peak gluteus maximus activations calculated by musculoskeletal modelling and as measured by EMG during mid stance (20-50% stance phase) of normal walking and FES applied walking.....	79
Table 4.6 Peak gluteus maximus activations calculated by musculoskeletal modelling and as measured by EMG during terminal stance (51-100% stance phase) of normal walking and FES applied walking	79
Table 4.7 Gluteus maximus activation impulse calculated by musculoskeletal modelling and as measured by EMG during the stance phase of normal walking and FES applied walking. <i>c</i> values of 0.10, 0.15 and 0.20 in models represent FES currents of 40 mA, 60 mA and 80 mA, respectively (mean \pm SD, n=15).....	81
Table 4.8 Gluteus maximus activation impulse calculated by musculoskeletal modelling and as measured by EMG during initial contact (0-3% stance phase)	81
Table 4.9 Gluteus maximus activation impulse calculated by musculoskeletal modelling and as measured by EMG during loading response (4-19% stance phase).....	82
Table 4.10 Gluteus maximus activation impulse calculated by musculoskeletal modelling and as measured by EMG during mid stance (20-50% stance phase).....	82
Table 4.11 Gluteus maximus activation impulse calculated by musculoskeletal modelling and as measured by EMG during loading response (51-100%).....	83
Table 5.1 Patients' anthropometric data.....	90
Table 5.2 Control subjects' anthropometric data	91
Table 5.3 Testing normality of data for height, mass and age for ACLD, ACLR and control groups using Shapiro Wilk's test and Levene's test	91
Table 5.4 Testing for statistical difference of height, mass and age between ACLD, ACLR and control groups (using ANOVA for height and age and Kruskal-Wallis for mass)	91

Table 5.5 Peak internal rotation torque (Nm/BW) for 8 control subjects, 4 ACL deficient subjects and 4 ACL reconstructed subjects during stance phase (* $p < 0.05$)	95
Table 5.6 Percentage difference between mean peak internal rotation torque in normal gait and FES gait for all groups	95
Table 5.7 Magnitude error (M), Phase error (P) and combined error (C) (Sprague and Geers' metric) for the comparison of internal rotation torque of the measured waveform, $m(t)$ and calculated waveform, $c(t)$	99
Table 5.8 Peak anterior shear force (BW) for 8 control subjects, 4 ACL deficient subjects and 4 ACL reconstructed subjects (* $p < 0.05$).....	100
Table 5.9 Mean speed (m/s) of 8 control subjects, 4 ACL deficient subjects and 4 ACL reconstructed subjects (* $p < 0.05$).....	105
Table 5.10 Percentage difference between mean speed in normal gait and FES gait for all groups	105
Table 5.11 Peak gluteus maximus muscle activation for 8 control subjects, 4 ACLD subjects and 4 ACLR subjects (* $p < 0.05$)	106
Table 5.12 Peak gluteus medius activation for 8 control subjects, 4 ACLD subjects and 4 ACLR subjects (* $p < 0.05$).....	108

Abbreviations

ACL	anterior cruciate ligament
AM	anteromedial
AMB	anteromedial band
ACLD	anterior cruciate ligament deficiency
ACLR	anterior cruciate ligament reconstruction
ATT	anterior tibial translation
BFLH	biceps femoris long head
BW	body weight
CP	cerebral palsy
DN	ACLD group in normal gait
DF	ACLD group in FES gait
EMG	electromyography
FES	functional electrical stimulation
GRF	ground reaction force
HN	control group in normal gait
MCL	medial collateral ligament
OA	osteoarthritis
PL	posterolateral
PLB	posterolateral band
RN	ACLR group in normal gait
RF	ACLR group in FES gait
SCI	spinal cord injury
SD	standard deviation
TKA	total knee arthroplasty

Acknowledgements

Alhamdulillah, All praises to Allah.

I would like to thank my supervisor, Prof Anthony Bull, for his invaluable guidance and constant support throughout the ups and downs of my degree.

I would also like to thank all the members of the Biomechanics group (in no particular order: Ziyun, Aida, Rui, Max, Christian, Lance, Vassia, Sam, Suzy, Daniel, Darshan and others) who are always helpful in sharing knowledge, positive feedbacks, constructive comments, advices and supports in so many way.

I would also like to express my thanks to surgeons, Mr Chimney and Mr Rahul for helping me recruiting the patient subjects for my study. Thank you to all the individuals who participated in my experiments. This thesis would not have been possible without your help.

I am grateful to both my sponsors, Ministry of Higher Education Malaysia and International Islamic University of Malaysia who opened the door for me to pursue a PhD degree.

Thank you to all my friends (again, in no particular order: Kak Hasyimah, kak Akhma, Jannah, Ashikin, Sumayyah, Yona and others) who always helped me in various ways throughout my journey in London. A kind thanks also to kak Haida and the PR group (also, in no particular order: Ros, Hafiza, Saira, Amnah, Dinah and others) for all the support and positive advices.

Finally, a special thanks to the most important people in my life; my lovely mom (Habshah Midi), my dad (Azmi Jaafar), Azfar, Izzati, Syahmi, Sabrina and my entire family who have always been there for me and always made the best prayers for me. I would not be able to finish this thesis without them.

Alhamdulillah.

Thank you.

Declaration of Originality

The thesis comprises only my original work, except where due acknowledgment is made in the text.

Copyright Declaration

‘The copyright of this thesis rests with the author and is made available under a Creative Commons Attribution Non-Commercial No Derivatives licence. Researchers are free to copy, distribute or transmit the thesis on the condition that they attribute it, that they do not use it for commercial purposes and that they do not alter, transform or build upon it. For any reuse or redistribution, researchers must make clear to others the licence terms of this work

CHAPTER 1

Thesis Motivation and Scope

This chapter provides a general overview of the subject matter of this thesis and provides the thesis aim, scope and structure.

1.1 Problem Statement and Motivation

Anterior cruciate ligament (ACL) injury is one of the most common types of knee injuries which occur to both men and women, especially to those active in sport. ACL injury causes knee instability mainly in anterior tibial translation (ATT) and internal rotation. ACL deficient patients can be divided into copers and non-copers. Coping is achieved by avoiding muscular contraction that produces an anterior shear force, for example, avoiding full contraction of the quadriceps especially during the early stance phase and when the knee is at full extension (Escamilla et al., 2012). An alternative coping mechanism counteracts quadriceps contraction through co-contraction of the hamstrings (Rudolph et al., 2001; Sinkjaer et al., 1991) and through the adaptation of muscle firing (Andriacchi et al., 2005). The copers are able to return to pre-injury activity without surgical intervention and non-copers require surgery to achieve the same outcome. It has been reported that 44% of ACL reconstructed patients returned to sport (Ardern et al., 2011) and 24% of young people (10-25 years old) who had ACL reconstruction had a second ACL injury (Paterno et al., 2010). As the muscle interactions, especially quadriceps and hamstrings can help in improving knee stability, stimulating the right muscle at the right time is important. Enhancing muscle interactions and stimulation may help non-copers to become copers. Optimisation of muscle contraction through functional electrical stimulation (FES) offers the prospect of mitigating the destabilising effects of ACL deficiency.

Most clinical studies have focused on strengthening the quadriceps muscles of ACL deficient patients with FES but these have overlooked the beneficial effect of activating the hamstrings. FES has been used to stimulate hamstrings, semitendinosus and biceps femoris, to reduce ATT, however, this was only used in healthy subjects and not ACL patients (Chen et al., 2013). The selection of semitendinosus is surprising, because it is located on the medial side of the knee and so is not positioned to help in reducing internal rotation torque. Also, ACL reconstruction surgery mostly uses semitendinosus as a graft and consequently, the semitendinosus muscle becomes weaker after the surgery. However, stimulating the lateral hamstrings will result in a posterior pull and external rotation on the tibia. The biceps femoral long head (BFLH) is ideally placed to achieve this.

However, the interplay between knee stabilisation and musculoskeletal system restraint with FES stimulating BFLH is not known for ACL deficient and ACL reconstruction patients. As such, the value of BFLH muscle activation, activated with FES which has the potential to reduce knee instability, needs to be investigate. A new musculoskeletal model

needs to be introduced to estimate the BFLH muscle contraction with FES; this could then be used to simulate and analyse ACL deficient patients focussing on their knee joint stability in the plane of articulation in order to include rotational and translational effects.

Quantifying the level of muscle stimulation through FES is challenging as conventional recording of muscle activity using electromyography (EMG) is not possible to the stimulation artefacts. Previous studies removed the stimulation artefact by using a shut-down circuit and an adaptive filter or extracted the volitional EMG from a partially paralyzed muscle and used this to control other muscle stimulation (Frigo et al., 2000; Thorsen et al., 1999). However, none of these have been able to totally eliminate FES artefacts from the EMG signals (Frigo et al., 2000; Sennels et al., 1997) or to control the EMG-controlled FES stimulation to stimulate only the targeted paretic muscle, or to negate the stimulation of other muscles located near to the paretic muscles (Thorsen et al., 1999). An alternative method needs to be introduced to solve this problem. Instead of designing a new device or system to extract the stimulation artefact, an alternative method to quantify FES stimulation could be conceived whereby the effect of FES stimulation of one muscle on the muscle activations of other muscles could be investigated. To date, no study has been able to adequately address this problem.

1.2 Aim and Scope

The aim of this study is to investigate the ability of FES stimulation of BFLH to reduce the knee instability of ACL deficient and ACL reconstructed patients by means of in vivo physical experiments and computational musculoskeletal modelling.

1.3 Thesis Objectives

The objectives of this thesis are to :

- a. formulate a musculoskeletal mathematical model to investigate the optimum levels of BFLH activation during FES gait in reducing the anterior shear force to zero;
- b. validate the musculoskeletal model in (a) that quantifies and evaluates the effect of FES on selected muscles through measuring EMG of muscles that are not affected by the FES stimulation artefact; and
- c. utilise this knowledge to enhance knee stability in the ACL deficient and ACL reconstructed groups by using FES.

1.4 Thesis Outline

This thesis is subdivided into six chapters.

Chapter 2 presents literature review on the musculoskeletal modelling, biomechanics of the ACL deficient and ACL reconstructed patients and its current treatment.

Chapter 3 introduces the pre-study of musculoskeletal modelling on the ability of the FES stimulation of the BFLH of the healthy subjects in reducing the anterior shear force and internal tibial rotation torque.

Chapter 4 explains the validation of the novel cost function to simulate neuromuscular electrical stimulation during gait.

Chapter 5 compares the differences in kinematics between healthy, ACL deficient and ACL reconstructed groups in walking with and without FES stimulation of the BFLH by means of physical experiments and musculoskeletal modelling.

Chapter 6 presents the overall discussion of this thesis and proposes future work.

CHAPTER 2

Literature Review and Background

This chapter presents a literature review on the functional anatomy of anterior cruciate ligament (ACL) deficient and ACL reconstructed patients and their current treatments.

2.1 Functional Anatomy of Anterior Cruciate Ligament (ACL)

The anterior cruciate ligament (ACL) is located between the two condyles of the tibiofemoral joint and crosses the posterior cruciate ligament in an anterior-posterior direction (Figure 2.1 and Figure 2.2).

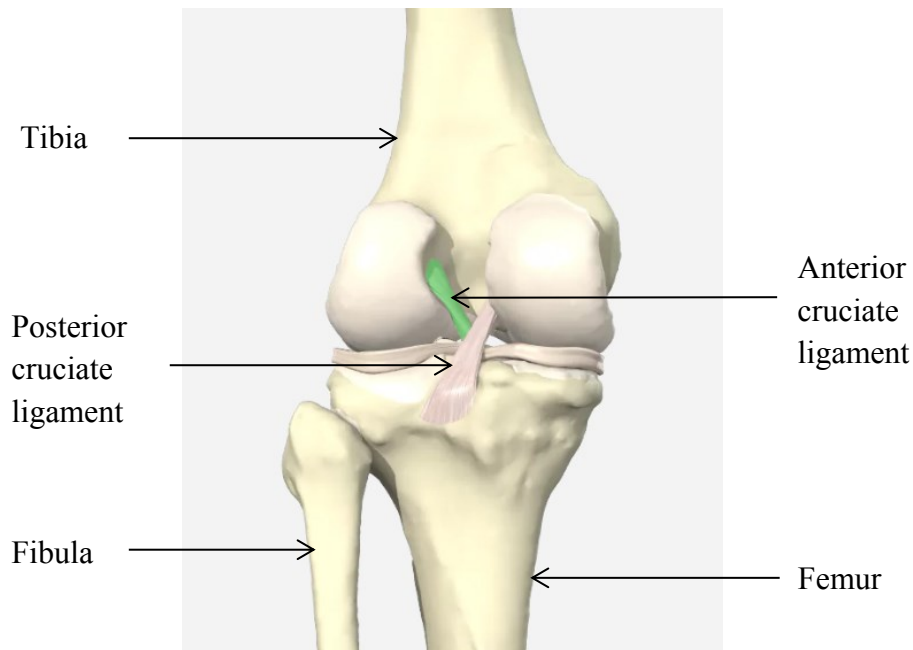


Figure 2.1 Posterior aspect of a left knee (© Primal Pictures. All rights reserved. Primal Pictures, an informa business www.primalpictures.com www.anatomy.tv) highlighting the femoral origin of the anterior cruciate ligament.

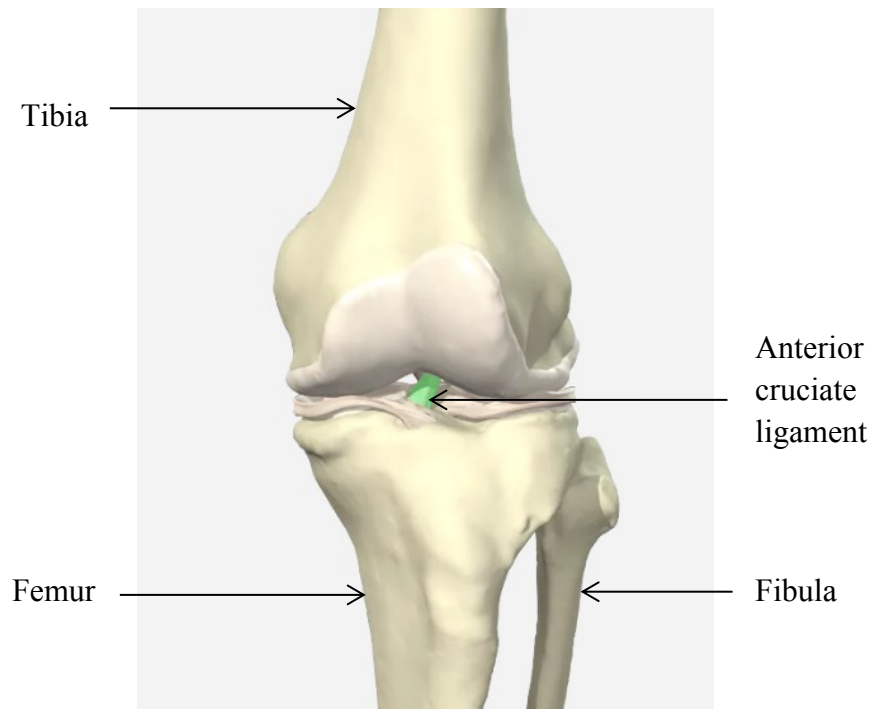


Figure 2.2 Anterior aspect of a left knee (© Primal Pictures. All rights reserved. Primal Pictures, an informa business www.primalpictures.com www.anatomy.tv) highlighting the tibial insertion of the anterior cruciate ligament.

The ACL origin is on the posterior part of the medial surface of the lateral femoral condyle and inserts on a wide depressed area in front of and lateral to the anterior tibial spine (medial intercondylar tubercle) with some variable fibers attached to the base of the spine (Girgis et al., 1975). The tibial spines are lodged in the intercondylar notch (Figure 2.3) (AM : anteromedial, PL : posterolateral).

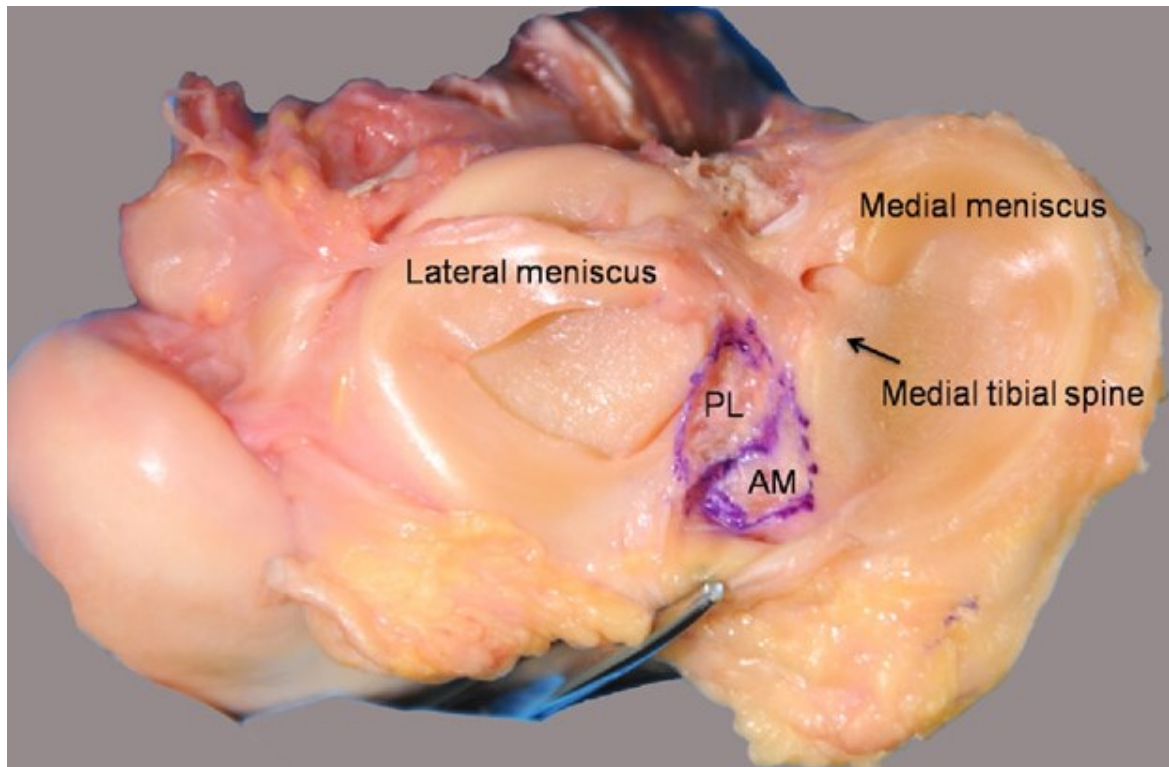


Figure 2.3 Caudal view of tibial plateau of a right cadaveric specimen. The ACL insertion site is marked, and its relation with the medial tibial spine and anterior horn of the lateral meniscus is shown (The Journal of Arthroscopic & Related Surgery, Anatomic Single- and Double-Bundle Anterior Cruciate Ligament Reconstruction Flowchart, 26, 2010, page 263, Carola F. van Eck, Bryson P. Lesniak, Verena M. Schreiber, Freddie H. Fu. Copyright © 2010 Arthroscopy Association of North America. Published by Elsevier Inc. All rights reserved. "With permission of Springer")

The tibiofemoral knee joint motion occurs in all three planes (sagittal, frontal and transverse) with six degrees of freedom (three rotations and three translations) between the femoral and tibial plateau (Figure 2.4) (Woo et al., 2006). The primary function of the ACL is to restraint anterior tibial translation (ATT) (Noyes et al., 1983b), where ATT occurs across a range of knee flexion angles, activities, and muscle activations. The secondary function of the ACL is to resist tibial internal rotation and varus rotations (adduction) (Gao et al., 2010; Logan et al., 2004b).

The ACL has two functional portions which are the anteromedial (AMB) and posterolateral (PLB) bands. The terminology of the bundles is based on their tibial insertion. The AMB fibres originate on the most proximal part of the femoral origin and insert on the anteromedial aspect of the tibial insertion site. The PLB fibres originate on the most distal aspect of the femoral origin and insert on the posterolateral aspect of the tibial insertion site. The AMB is the more significant restraint to anterior tibial translation of the

knee (Girgis et al., 1975), while the PLB is an important restraint to tibial internal rotation of the knee (Yagi M, 2002). The load sharing between these two bands complement each other (Wu et al., 2009) to provide restraint across a large range of knee joint flexion. The distribution of strain between the bundles and over the cross section of the ACL is not uniform and depends on the position of the tibiofemoral joint, muscle contraction, and externally applied loads to the limb, in particular, ground reaction forces. When the knee is extended, the femoral attachment of the ACL is in a vertical position, the PLB is tight, and the AMB is moderately lax. In contrast, when the knee is flexed, the femoral attachment of the ACL becomes more horizontally orientated, causing the AMB to tighten and the PLB to loosen (Zantop et al., 2007).

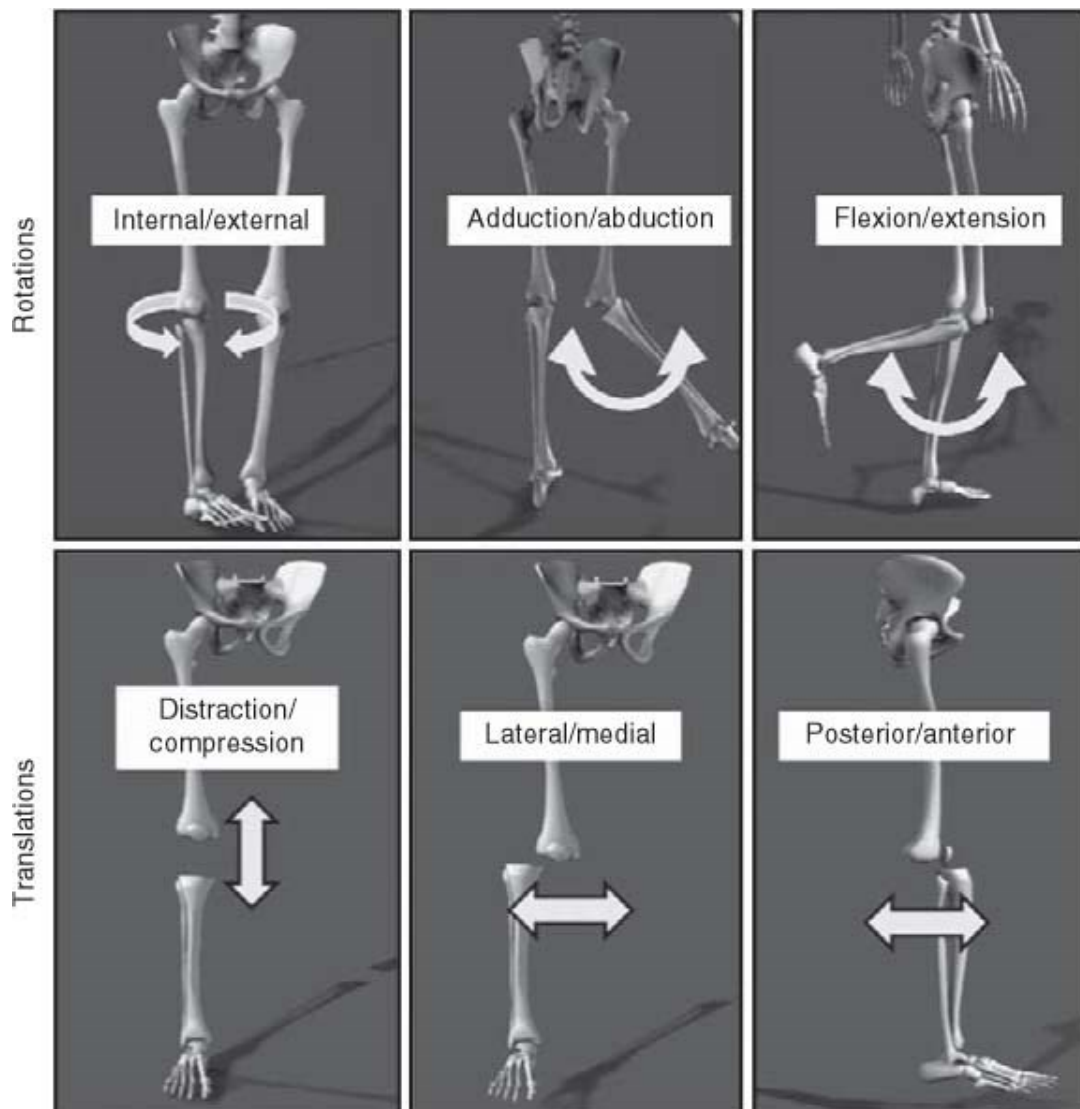


Figure 2.4 Rotation and translation motions of the knee joint (Sports Medicine, A 'Plane' Explanation of Anterior Cruciate Ligament Injury Mechanisms, Carmen E. Quatman et. al, 40, 2010, page 731, Copyright © 2010, Adis Data Information BV "With permission of Springer")

The ACL can resist anterior tibial translation in response to a combined internal tibial torque and valgus torque; therefore, in response to this combined rotatory load, the knee undergoes anterior tibial subluxation when the ligament is deficient (Fukuda et al., 2003; Gabriel et al., 2004).

The articular rotational motion of the knee occurs about the centre of the medial tibial plateau (Amis et al., 2005). Knee joint movements are not only related to the surface of the tibia but also muscle activity (Shelburne et al., 2004). Knee stability is achieved by a good collaboration between the primary active and the passive knee stabilizers, which are the muscles and the ligaments (Shelburne et al., 2005).

2.2 Knee Muscles and the ACL

Muscles that dynamically resist anterior tibial translation act as ACL agonists, whereas muscles that dynamically produce anterior tibial translation act as ACL antagonists (Elias et al., 2003). Because the hamstring muscles attach on the proximal tibia and exert a force with a posterior orientation when the knee is flexed, they are considered the primary ACL agonists (Li et al., 1999; MacWilliams et al., 1999; More et al., 1993), restraining ATT and reducing ACL strain (Li et al., 1999; Renstrom et al., 1986). Hamstrings can be divided into biarticular (semitendinosus, semimembranosus, and long biceps femoris) and monoarticular (short biceps femoris) knee flexor muscles that act on both the medial (semitendinosus and semimembranosus) and lateral (long biceps femoris and short biceps femoris) side of the joint (Figure 2.5). During knee flexion, the hamstrings activations moves the lateral part of the tibia more than the medial portion, because of its geometric location and because of the more mobile lateral tibial plateau (Kwak et al., 2000; Victor et al., 2010). Biceps femoris in particular assists in rotating the tibia externally when the knee is semi-flexed (between 20° to 50°) (Besier et al., 2003).

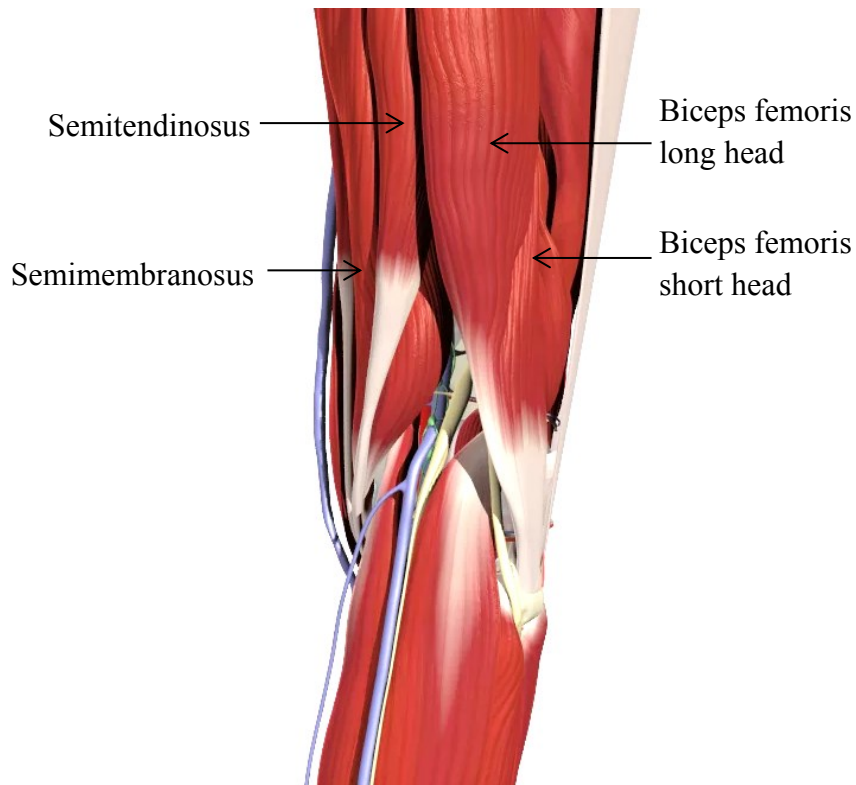


Figure 2.5 Hamstring muscles (© Primal Pictures. All rights reserved. Primal Pictures, an informa business www.primalpictures.com www.anatomy.tv)

Conversely, the quadriceps muscles are considered ACL antagonists; they are the strongest muscles across the knee and are attached through the quadriceps tendon to the patella. The quadriceps has four main muscles namely the vastus lateralis, rectus femoris, vastus medialis, and vastus intermedius (Figure 2.6). As quadriceps contract, they extend the knee through apply a force to the patellar tendon. This applies an ATT and thus an intact knee will produce a force in the ACL when the quadriceps is contracted.

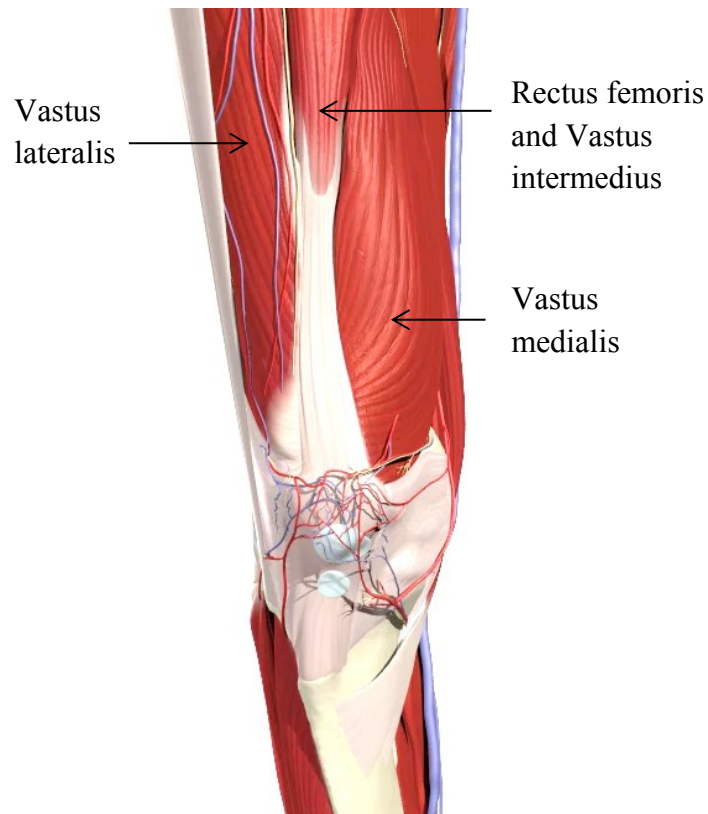


Figure 2.6 Quadriceps muscles (© Primal Pictures. All rights reserved. Primal Pictures, an informa business www.primalpictures.com www.anatomy.tv)

2.3 Anterior Cruciate Ligament Deficiency (ACLD)

ACL injury is prevalent especially in young athletes (Donnelly et al., 2012). ACL injury is commonly caused by non-contact injury (indirect force). The defining features of the non-contact injury are that it results from the athlete's own movements, which typically are disturbed by a physical or cognitive perturbation either during or immediately before the injury event (Marshall, 2010). ACL injury is clinically diagnosed through manipulating the knee to elicit translations and rotations that would normally be resisted by an intact ACL. The Lachman test applies an anterior drawer force to the tibia at 20° flexion which can then be diagnostic of an ACL injury if ATT is increased compared to a healthy knee. Combined rotational instability due to ACLD is tested with the “pivot shift test” which involves applying a combined internal tibial and valgus torque throughout the range of flexion-extension (Matsumoto, 1990). The pivot shift is then observed as a sudden combined rotation and translation motion that is not present in the healthy knee (Bull et al., 1998).

The mechanism of non-contact ACL injury typically involves multiplanar loading including anterior tibial shear force, knee abduction and internal or external tibial rotation

moments (Figure 2.7) (Levine et al., 2013). More than half of the athletes injured their ACL during a sidestepping sport manoeuvre (Donnelly et al., 2012; Griffin et al., 2006).

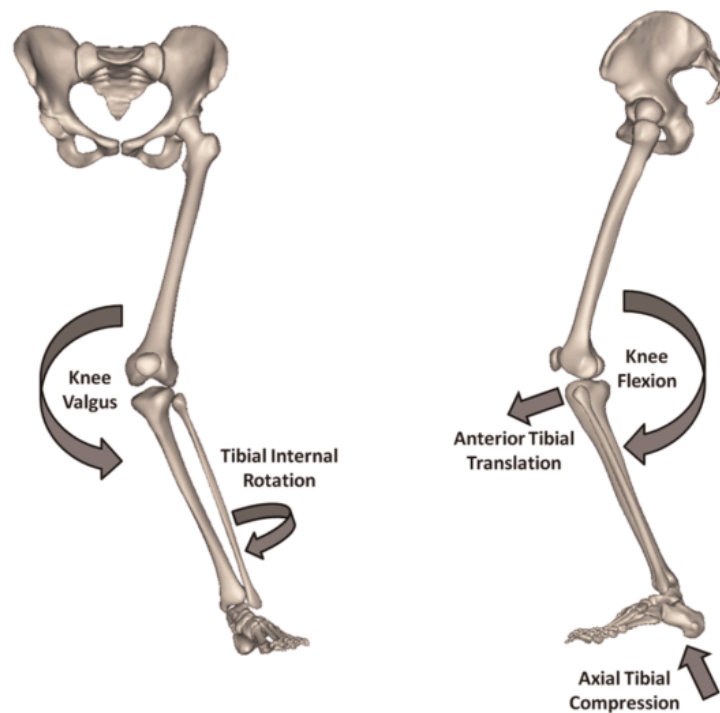


Figure 2.7 Multiplanar loading mechanism of a noncontact anterior cruciate ligament injury. Image reproduced with permission from Levine et al. (2013)

Most ACLD patients are not able to return to sport, because of continued episodes of knee giving way (non-copers). The ACL injury can lead to severe disability affecting sporting activities (77%), routine activities (44%) and walking (31%) (Noyes et al., 1989). ACLD results in increased ATT and internal tibial rotation and therefore the secondary restraints are more highly loaded, for example, resistance to ATT is provided by the long superficial medial collateral ligament (MCL) (Masouros et al., 2010; Shelburne et al., 2004). This causes the secondary restraint to stretch and fail over time (Wen et al., 2000).

Other changes to the joint occur due to ligament injury and these are particularly significant when loaded in gait (Dyrby et al., 2004; Shimokochi et al., 2008). These changes are not found during non-weightbearing activities (e.g. passive leg flexion). When the ACL is injured, the rotational axis moves further medial and thus there is a large translation of the lateral compartment (Amis et al., 2005; Georgoulis et al., 2003; Logan et al., 2004a). This is because the axis of rotation of the tibial plateau of ACL injury is no longer at the centre of the medial plateau, but at the outside of the medial tibial plateau (Amis et al., 2005; Bull et al., 2002).

This offset of internal tibial rotation axis has been observed in ACL deficient knees during walking (Andriacchi et al., 2005; Georgoulis et al., 2003) and also in ACL reconstructed knees (Gao et al., 2010). However, there is some literature that found the opposite in that the axis of rotation was on the lateral side during normal walking (Koo et al., 2008), however, these studies did not use the same methods or kinematics descriptions. In particular the use of instantaneous rotational axes to describe the known combination of flexion, anterior–posterior translation and internal–external rotation that occur during walking (Dyrby et al., 2004) causes confusion in the literature. It is important to understand the movement strategies of ACL deficient subjects during the mid-stance phase of gait at which point these complex movements occur.

The normal function of the knee requires a subtle balance between stability and mobility of the ligaments, joint surfaces and muscles spanning the joint (Dyrby et al., 2004; Koo et al., 2008). When the ACL is ruptured, the mechanics of the knee joint are greatly altered by adaptive changes in patterns of gait. For example, hamstring co-contraction, in addition to their primary role as knee flexors, providing synergistic action to the ACL by preventing excessive anterior displacement and internal rotation of the tibia (Hirokawa et al., 1992). There are also complementary strategies from other ligaments and musculotendon units, for example, the MCL and posteromedial capsule complement the ACL deficient knee secondarily by controlling anterior translation on the medial side of the joint. These complementary strategies are a reason why some ACL deficient patients are able to walk with normal gait patterns. However, some patients do not have this complementary function either because the ligament is completely destroyed or they have lost other complementary mechanisms. Therefore, ACL deficient patients can be divided into two groups: the copers and the non-copers. The copers are able to return to pre-injury activity without surgical intervention and non-copers require surgery to achieve the same outcome.

There are different coping strategies exist among the copers: quadriceps avoidance or hamstring facilitation. In quadriceps avoidance, the patients avoid contracting the quadriceps to reduce the amount of knee flexion moment and to limit ATT. These modified processes occur especially during weight acceptance (less 40° of knee flexion and 20-40% of stance phase) and midstance (full knee extension, 40-60% of stance phase) (Andriacchi, 1990; Berchuck et al., 1990). A partial ACL tear can lead to a complete tear depending on the amount of the tear, a subtle change in anterior translation and the occurrence of re-injury with giving-way. Besides, ACL injury can lead to meniscal or

chondral injury as well as osteoarthritis (Georgoulis et al., 2003). Where ‘quadriceps avoidance’ does not occur an alternative coping mechanism comes into play. ACL deficient copers have a functional adaptation in which the knee is flexed more which then positions the hamstrings to prevent abnormal anterior translation and internal or external rotation of the tibia through contraction in this flexed position (Beard et al., 1996).

2.4 Treatment of ACL Injury

The initial course of treatment of ACL injury includes rest, anti-inflammatory measures and activity modification. After the swelling resolves and normal range of motion and strength is achieved, a clinical test will be conducted as described previously, including the Lachman test (Logan et al., 2004b) and pivot shift test (Matsumoto, 1990). These clinical assessments will then define the type of treatment that the patient will undergo including only non-operative treatment as well as reconstruction surgery (Fitzgerald et al., 2000). Patients who have multiple injuries are normally required to undergo reconstruction surgery, where these other injuries can include other ligament tears, meniscal injuries or chondral lesions. Conversely, patients with low-risk activity levels, isolated ACL injuries, and mild pathologic laxity may be successfully treated without surgery. Each patient will be evaluated separately, because of the complexity of the functional deficit and condition of other tissues.

If a non-operative approach is chosen, the main treatment focus is to maintain the strength, balance, and range of motion in order to avoid further injury. During this treatment, many patients choose to use a sports brace and limit their participation in activities that require a lot of pivoting, cutting or jumping. The non-operative practice consists of several activities to improve functional of the knee.

Some ACL injuries involve on a partial ligament tear and these are primarily treated non-operatively, because the remaining ACL can provide a near-intact function. However, as with secondary restraints, there is a risk that the remaining ACL might further tear after certain types of activity introducing additional injuries to other structures of the joint. In the literature it has been shown that a one quarter tear does not progress to full tear, in a half tear 50% of the patients progress to a full tear and 86% of a three quarter tear progress to a full tear (Noyes et al., 1989). Copers should not progress to a full tear. However, the decision to undergo surgery cannot be based solely on the proportion of ligament that is intact.

2.5 Reconstruction Surgery

Anterior cruciate ligament reconstruction (ACLR) surgery is a commonly performed procedure, particularly in athletes who want to return to competitive sport following an ACL injury. The decision to reconstruct is based on the clinical assessment, including the clinical tests described previously, the condition of the ACL as possibly quantified through medical imaging and the state of the other knee joint structures. Giving way as assessed by the pivot shift is a strong indication for reconstruction surgery as this is correlated with progression to osteoarthritis, a severe ACL tear, and other ligament injuries (Frank et al., 1997).

There is a variety of grafts used for reconstruction surgery, including allografts and autografts. The most commonly used grafts are autografts, in particular the patellar tendon bone to bone graft and a hamstrings graft (quadruple semitendinosus-gracilis tendon graft) (Brand et al., 2000). Both of the grafts have their strengths and weaknesses, with, for example, some papers showing residual ATT under complex loading (Woo et al., 2002). The surgical positioning is also important, for example, if the surgery places the graft too close to the central axis of the tibia and femur it is inadequate in resisting rotatory loads (Kanamori et al., 2000; Woo et al., 2002; Yagi M, 2002). Therefore, more laterally placed grafts have been advocated in some instances (Kanamori et al., 2000; Woo et al., 2002). Other techniques have included using a graft with multiple insertion points at both the tibia and femur to replicate the function of the separate bundles. These are termed, variously, double-bundle, or anatomic reconstructions (van Eck et al., 2010) (Kondo et al., 2008). Double bundle reconstruction replicated the native ACL anatomy by reconstruction the 2 main functional bundles, the AMB, taut through full range of knee motion, and the PLB, taut mainly toward extension. The different behaviour of the 2 bundles should affect knee kinematics, and the AMB, which is closer to the line of knee axial rotation, controls mainly anterior laxity while the PLB, which is more divergent to the axis, controls rotation. The latter should also be involved in controlling the pivot-shift phenomenon, which is a combination of abnormal rotation and translation (Aglietti et al., 2009; Yagi et al., 2007; Zantop et al., 2007). Even though there is evidence that the double bundle reconstruction is superior to single bundle reconstruction, it is difficult to compare between single and double graft because they are not necessarily have a same procedure (van Eck et al., 2010).

Despite the success of the ACL reconstruction, the current surgical treatment of ACL injury is costly, with variable outcomes (Hewett et al., 2013) and is associated with high

risk of post-traumatic osteoarthritis within two decades of injury (Murray et al., 2012). While few athletes are able to resume sports at the same level without surgery, the surgical reconstruction is also not always successful at returning patients to their pre-injury activity level. Furthermore, those athletes who successfully return to activity are at high risk of a second knee injury with notably less favourable outcomes.

There is a lack of evidence that the outcomes of surgical treatment are better than those of nonsurgical treatment with respect to knee function, sports participation, or the early onset of knee osteoarthritis (Grindem et al., 2014). A systematic review recently reported fear of re-injury to be a more dominant reason for not returning to sport after ACL reconstruction than problems with the reconstructed knee (Ardern et al., 2011). Even though 44% of ACL reconstructed patients have been reported to return to sport (Ardern et al., 2011), and 24% of young people (10-25 years old) who had ACL reconstruction had a second ACL injury (Paterno et al., 2010).

Reconstruction of the ACL with synthetic material, whether for total, permanent replacement, a scaffold for ingrowth of host tissue, or a stent to protect an allograft or autograft as it heals, has not proven to be satisfactory for treatment of a torn ACL (Beynon et al., 2005). However, bio-enhanced repair using a collagen-based scaffold and autologous blood has shown a significant decrease in risk of post-traumatic osteoarthritis, which makes it the first and so far only possible ACL injury treatment with the potential to lower the risk of osteoarthritis after an ACL injury (Kiapour et al., 2014). However, this method is still new and is not used clinically.

Similar to the ACL deficient knee, the ACL reconstructed knee required rehabilitation activities following surgery. It is interesting to know that hamstring exercises are not detrimental to ACL repairs or reconstruction and can be included early in the rehabilitation program after ACL surgery as these do not load the joint in ATT. However, the hamstrings are not capable of masking the potentially harmful effects of simultaneous quadriceps contraction on freshly repaired or reconstructed ACLs unless the knee flexion angle exceeds 30° (Renstrom et al., 1986). As knee stability is related to muscle strength, it is interesting to know if any contraction of knee muscle of the ACL deficient patient is able to treat these ACL patients to restore knee stability by using electrical stimulation without undergo any surgery.

2.6 Functional Electrical Stimulation (FES)

FES has been used in the clinical arena to strengthen weak muscles by applying low level electrical currents (Peckham, 1987). FES has been widely used clinically to contract the paralyzed or paretic muscles of upper motor neuron lesions such as spinal cord injury (SCI) patients (Lynch et al., 2008), cerebral palsy (Carmick, 1997), Parkinson's and multiple sclerosis. Neuromuscular electrical stimulation (NMES) assists in strengthening weak muscle in orthopaedic conditions. Both FES and NMES have the same function in that they assist in contracting the weak muscles; the difference is that FES contracts muscle to assist in any functional activities (eg walking) while NMES contracts muscle during a static position (eg sitting at a certain knee flexion angle). NMES has been used to restore quadriceps strength of the ACL deficient patient following surgery. This is because the quadriceps muscles are often affected by arthrogenic muscle inhibition after ACL reconstruction, which limits volitional contraction. NMES directly recruits the motor neurons to produce better quadriceps strength gains than voluntary exercise alone. Functional outcomes are improved with increased strength gains of the quadriceps (Palmieri-Smith et al., 2008).

Based on previous studies, ACL deficient and ACL reconstructed knees may still have residual instability in ATT and tibial internal rotation. The combination of the conforming surface of tibia and the muscles of the knee are able to reduce these knee instabilities. The important thing is to find the right muscle to contract which is able to assist in stabilising the knee movements of the patients. The stimulation of hamstrings using a functional knee brace with FES has been shown to assist a patient in walking (Solomonow, 2006). The literature has also proposed using FES to contract the hamstrings to reduce ATT (Chen et al., 2013), however, this was only tested in healthy subject. There is no other study in the open literature that explores the contraction of the hamstrings with FES in order to restore the knee stability in ACLD and ACLR patients. Stimulating the hamstrings, especially the biceps femoris long head (BFLH) with its insertion on the fibular head is a candidate to target to apply a posterior pull and external rotation to the tibia.

Based on a review by Maffiuletti (2010), there are two aspects for physiological considerations with the use of NMES which are: the differences in motor unit recruitment pattern between NMES and voluntary contractions, and the involvement of the nervous system during peripheral NMES. These physiological aspects also apply to FES.

The first physiological consideration is the differences in motor unit recruitment pattern between NMES and voluntary contractions. NMES stimulates synchronous recruitment which stimulates all muscle units at the same time. In contrast, the nervous system stimulates muscles in a sequential manner. The recruitment of motor units during NMES is without obvious sequencing related to unit types which is referred as the “disorderly” recruitment (Gregory et al., 2005) and thus, NMES (20-40Hz) needs a higher FES frequency than the nervous system (6-8Hz) to stimulate muscle (Lynch et al., 2008). NMES also tends to recruit fast twitch muscle fibres over slow twitch muscle fibres, because fast twitch muscle fibres have larger diameter axon that can be recruited before the smaller slow fast twitch muscle fibres. The large-diameter axons, mostly located in superficial muscles such as vastus medialis, are more easily excited by electrical stimuli because they have the lowest threshold of activation (Maffiuletti, 2010). Increasing the NMES current intensity or prolonging the duration of NMES in a rehabilitation could depolarise the new fibres located at a greater, which is deeper, distance from the electrode, while the closer, superficial, ones maintain their contractile activity. Both these effects of synchronous recruitment and preferential recruitment of fast twitch muscle fibres contribute to muscle fatigue. It is known that muscle fatigue increases with pulse frequency. Lower amplitude stimulation with longer pulse durations reduces fatigue. Muscle fatigue can also be reduced through training; FES training can increase muscle volume and increase muscle strength. Higher frequency with intermittent FES electrical pulses contributes to less muscle fatigue compared to low frequency intermittent FES electrical pulses (Matsunaga et al., 1999). Pulse frequency, pulse amplitude and pulse duration (Ferrarin et al., 2000) are all parameters that can be tuned for the orthopaedic patient, as appropriate for their physical condition, such as injury, recent surgery or impaired activation in performing high-intensity voluntary contractions. Table 2.1 shows the differences in motor unit recruitment during voluntary and NMES contractions (Maffiuletti, 2010).

Table 2.1 Motor unit recruitment during voluntary contraction and NMES contraction (from Maffiuletti, 2010)

Characteristics	Voluntary contraction	NMES contraction
Temporal	Asynchronous	Synchronous
Spatial	Dispersed	Superficial
	Rotation is possible	Spatially fixed
	Quasi-complete (even at the the maximum)	Largely incomplete (even at the maximum)
Orderly	Selective (slow to fast)	No, nonselective/random/disorderly (slow and fast)
Consequence	Partially fatiguing	Extremely fatiguing

The second physiological consideration is the involvement of the nervous system during NMES which contributes to the clinical gains observed during motor recovery. NMES increases cortical activity (Smith et al., 2003) and NMES increases spinal motoneuron recruitment (Collins, 2007). High training intensities would mainly promote supraspinal adaptations which train populations of slow and fast muscle fibers. Wide pulse (1 ms) high frequency (50-100Hz) (Collins, 2007) NMES would likely result in changes at the spinal level which train the slow fibers. However, these suggestions in the literature need further investigation by controlled studies in both healthy and patient populations (Maffiuletti, 2010).

The goal of ACL reconstruction surgery is to improve anterior translational and internal rotation knee stability but even after ACL reconstruction, sagittal translation may remain elevated. There are no specific muscle-related criteria that have been shown to correlate significantly with a successful return to sports activities after ACL reconstruction other than, simply, muscle strength (Micheo et al., 2010). However, it is recognised that functional stability and good muscle function are important aspects that need to be addressed after reconstruction surgery before return to sports activities (Kvist, 2004). This can be done with NMES. There is some evidence of a beneficial effect of NMES together with conventional rehabilitation exercises (volitional training) in improving muscle strength and function two months after ACL reconstruction surgery (Imoto et al., 2011).

NMES has been used clinically in the early postoperative surgery phase (Noyes et al., 2006). The activities involved mostly focus on strengthening the quadriceps as these are affected by arthrogenic muscle inhibition. Six months after reconstruction surgery, the quadriceps have a muscle deficit of 19-44% and hamstring having muscle deficit of less than a 10% (Kvist, 2004). Training with NMES while the patient is in a sitting position with a steadily held knee flexion angle has been used from 3 to 14 weeks postoperatively (Kim et al., 2010). Various researchers recommend different time periods for the use of NMES, citing, for example, the significant muscle weakening in the first six weeks as evidence for the use of NMES in that period (Imoto et al., 2011). Treatment times and durations vary from 30 minutes to 10 hours per day or by, for example, performing 15 repetitions over a daily or every other day (Snyder-Mackler et al., 1994; Snyder-Mackler et al., 1995; Snyder-Mackler et al., 1991). These different NMES parameters may have an impact on the clinical outcomes of treatment and the lack of consistency in the literature make it difficult for clinicians to select appropriate parameters (Kim et al., 2010). There is evidence that treatment with NMES in combination with conventional rehabilitation exercises results in greater quadriceps strength compared to doing volitional training alone (Bax et al., 2005; Palmieri-Smith et al., 2008), however, others suggest that NMES provides no benefit, perhaps due to the work effort and overall training intensity (Kim et al., 2010) and wide variety of parameters utilised across trials (Risberg et al., 2004). Also, the different injury/surgical condition of each individual will affect the treatment outcome (Maffiuletti, 2010).

Studies have used NMES with extremely different frequencies of between 35 to 70Hz (Imoto et al., 2011; Kim et al., 2010; Paillard, 2008). Higher frequencies (above 50Hz) have been shown to deliver at sensory intensity (DeSantana et al., 2008), while lower frequencies (lower 10Hz) have been shown to deliver at motor intensity (DeSantana et al., 2008). Most studies used NMES with a frequency of 40 Hz which is claimed suitable for eliciting reflectors. The suitable pulse duration should be around 200 to 350 microseconds (Imoto et al., 2011). The stimulus can be made more comfortable for the patient by slowing the rising and falling edges of the stimulation with a ramp time of 1-2 seconds being suitable but some users with severe spasticity require a ramp time of 6s or above (DeSantana et al., 2008). This demonstrates that stimulation with 40Hz, 200 to 350 microseconds with 1-2 seconds ramp times of rising and falling edges are suitable to

provide sufficient muscle contractions. Therefore, in this thesis the stimulation parameters will be set according to these parameters.

There are some drawbacks with the clinical approach described above. First, NMES is generally delivered at a fixed joint angle where the effects of NMES are considered to be poorly related to functional activities of daily living or to sporting activities that occur over a range of knee joint flexion angles. Second, NMES is mostly used during the early post-operative phase, where potential benefits even 6 months after surgery, at which point rehabilitation post ligament reconstruction surgery is increased, could help to improve the thigh musculature before return to sports activities. In particular, the hamstrings muscles have less deficit after surgery compared to quadriceps muscles, and so, based on their physiological line of action and strength, stimulating these during walking could further improve knee instability by reducing the ATT.

There is robust evidence of a beneficial effect of NMES for ACL rehabilitation. Using NMES has shown that the quality of quadriceps activation is greater compared to rehabilitation treatment without NMES treatment. However, there are no significant differences in endurance, maximum voluntary isometric torque, function or quality of life (Monaghan et al., 2010). Overall, while NMES stimulation may potentially strengthen quadriceps muscles, this does not appear to be a requirement for successful ACL reconstruction rehabilitation (Wright et al., 2008). Treatment with FES during activity could potentially provide better knee stability and performance for ACL deficient and ACL reconstructed patients.

The interplay between knee stabilisation and musculoskeletal system restraint with FES stimulating BFLH is not known for ACL deficient and ACL reconstructed patients. Besides, the level of BFLH muscle activation activated with FES that can reduce the knee instability needs to be investigate. Quantifying this level of activation can be achieved through the use of musculoskeletal modelling and so a new model needs to be developed to estimate BFLH muscle contraction with FES to then be used to analyse ACL deficient patients focussing on their knee joint stability in the plane of articulation, focusing on the key effects in rotation and translation.

2.7 Conclusion

Knee stability is achieved by a good collaboration between the active and the passive knee stabilisers, which are the muscles and the ligaments. The injured ACL causes increased translation and rotational laxity on the lateral side of the tibia. The reconstructed ACL also suffers from residual rotational instability. Quadriceps strengthening can assist in addressing inhibition atrophy, but there is no work that has properly explored the potential of stimulating hamstrings using FES, especially BFLH, to reduce the knee instability of ACL deficient and as well as ACL reconstructed patients. In addition, the prospect of enhancing BFLH interactions at the knee may enable non-copers to become copers and potentially reduce the need for surgery. Knee injury is associated with adaptive changes in walking that can be detected using gait analysis. However, gait analysis on its own does not fully characterise knee mechanics and since muscle forces cannot be measured directly, a lower limb musculoskeletal model is required to understand knee mechanics in gait. Current musculoskeletal models do not allow the imposition of muscle stimulation using FES and therefore a modification of such models is required to investigate the contraction of BFLH with FES and explore its ability to reduce knee instability of ACL deficient and ACL reconstructed knees.

CHAPTER 3 ¹

Musculoskeletal Modelling to Investigate the Use of FES at the Knee

This chapter introduces a modification of musculoskeletal modelling to enable the assessment of the ability of FES to stimulate muscles around the knee to change the local articular loading. The study is focused on biceps femoris long head (BFLH) of healthy subjects and the loading of interest is anterior shear force and internal tibial rotation torque.

¹Part of this chapter has been published as “Azmi NL, Ding Z, Xu R, Bull AMJ (2018) Activation of biceps femoris long head reduces tibiofemoral anterior shear force and tibial internal rotation torque in healthy subjects. PLoS ONE 13(1): e0190672. <https://doi.org/10.1371/journal.pone.0190672>”

3.1 Introduction

As described full in Chapter 2, healthy loading of the tibiofemoral joint of the knee during activities of daily living including gait involves significant tibial anterior shear and tibial internal rotation torque (Andersen et al., 1997), in particular during the stance phase of gait (Escamilla et al., 2012). The anterior cruciate ligament (ACL) is the primary restraint to anterior shear and a major secondary restraint to internal tibial rotation (Noyes et al., 1983b). Therefore, ACL deficiency through sports trauma results in anterior tibial translation instability and tibial internal rotational instability of the knee (Duthon et al., 2006).

Knee movement is a function of external forces and of muscle forces (Shelburne et al., 2005). In ACL-deficiency, knee joint stability is provided through the action of concavity compression of the tibiofemoral articulation on the medial side, where the compressive forces push together the concave surfaces of the joints (Amis et al., 2005). However, this stability mechanism is not present at the lateral knee compartment as the lateral tibial plateau is convex, which, combined with the convex femoral condyle, results in an unstable and more mobile compartment. As a result, during normal knee joint loading with a tibial rotational torque, the rotational axis of the knee moves medially creating an excessive translation of the lateral compartment (Amis et al., 2005; Bull et al., 1999; Gao et al., 2010; Shimokochi et al., 2008). These excessive movements then cause secondary conditions including damage to the other passive restraints to these motions, such as cartilage, menisci, and the collateral ligaments (Noyes et al., 1980; Noyes et al., 1983a; Shao et al., 2011). ACL deficiency is implicated with an increase in the rate of osteoarthritis (Lohmander et al., 2007; Solomonow, 2006) and limits athletes in their activity (Catalfamo et al., 2010).

As described in Chapter 2, there is a subset of ACL deficient patients who are able to return to pre-injury activity without surgical intervention; these are termed copers. Non-copers require surgery to achieve the same outcome. A third group is that of non-copers who undergo ACL reconstruction surgery, where there is a residual internal rotation instability.

Coping is achieved through avoiding muscular contraction that produces an anterior shear force through, for example, avoiding full contraction of the quadriceps especially during

the early stance phase and when the knee is at full extension (Escamilla et al., 2012). An alternative coping mechanism counteracts quadriceps contraction through co-contraction of the hamstrings (Rudolph et al., 2001; Sinkjaer et al., 1991) and through the adaptation of muscle firing (Andriacchi et al., 2005). The underpinning hypothesis of this work is to adapt muscle firing through functional electrical stimulation (FES) in order to restore normal ATT at the lateral compartment of the knee by causing specific muscles to contract.

The main muscles involved in the movement of the knee are the quadriceps, gastrocnemius and hamstrings. Of these, the hamstrings afford the most potential to reduce anterior tibial shear force and thus restore ATT to normal (Liu et al., 2000; Markolf et al., 2004; Shelburne et al., 2005) as they are anatomically located to apply a posterior pull to the tibia (Yanagawa et al., 2002). Biceps femoris long head (BFLH) is the best candidate for selective activation in order to resist the peaks of anterior shear force and internal rotation moments during the stance phase of gait (Shelburne et al., 2005). It has been shown in a modelling study that activation of biceps femoris is able to decrease the anterior tibial shear force when knee flexion is less than 40° (Biscarini et al., 2013). Additionally, because BFLH attaches to the fibular head on the lateral aspect of the knee, it is expected that it will also be able to resist the large internal rotation moment and hence the large pathological motion of the lateral compartment in ACL deficiency (Amis et al., 2005; Gao et al., 2010). Thus, it is hypothesized that activation of BFLH is able to restore knee stability in non-copers to allow them to become copers.

The aim of this chapter is to:

1. modify a musculoskeletal model to investigate the effect of FES of the BFLH on internal rotation torque and anterior tibial shear force at the knee;
2. explore the optimal level of muscle activation to reduce internal rotation torque and anterior tibial shear force; and
3. test the use of FES on BFLH in healthy control subjects.

3.2 Materials and Methods

Physical Experiments

An Imperial College Research Ethics application was submitted previously and ethics approval was granted in 2014. The full application is shown in Appendix A. Written

informed consent was obtained from all participants. In this pilot study, twelve healthy subjects (5 male, 7 female; height 1.67 ± 0.09 m; mass 66.74 ± 16.75 kg; age 26.08 ± 2.39 years) underwent level walking without and with FES (Table 3.1).

Table 3.1 Anthropometric data

Subject	Gender	Height (m)	Mass (kg)	Age (year)
1	Male	1.61	61.00	25
2	Female	1.68	54.10	26
3	Female	1.60	48.90	28
4	Female	1.62	54.20	25
5	Female	1.59	54.40	30
6	Male	1.63	62.70	28
7	Male	1.87	93.00	27
8	Male	1.77	85.50	26
9	Male	1.67	88.30	23
10	Female	1.74	88.50	27
11	Female	1.58	54.50	21
12	Female	1.71	55.80	27
Mean		1.67	66.74	26.08
SD		0.09	16.75	2.39

The FES electrodes (Odstock 2 Channel Stimulator, Odstock Medical Ltd., UK) were placed over the right BFLH with one electrode at the bottom of the BFLH and one at the centre, with a distance of two hand widths between them. The frequency of the stimulator was set to the manufacturer recommended level of 40 Hz and stimulation current was initially set to a minimum value of 40 mA. The intensity was then adjusted to the maximum level that the subject was able to comfortably withstand. The intensity level stimulation pulse width potentially ranged from level 0 to 9 (0 to 350 μ s), yet in this case pulse durations were varied between level 4 and 8 on a subject-specific basis; this is within the suitable pulse durations for NMES as described in Chapter 2 (Imoto et al., 2011) (Figure 3.1).



Figure 3.1 Stimulation pulse width intensity level

The stance phase that was analysed in this study started from the point at which the right heel stepped on the force plate (initial contact). All subjects underwent a practice session using the FES before the trials were recorded. This practice session ensured that the subject adapted to the stimulation while their right foot stepped on the force plate. The FES stimulation current was set up to start from one second of ramp up, followed by four seconds of maximum current and then end up with one second of ramp down (Figure 3.2 and Figure 3.3). The stimulator was manually started by the subject pressing the hand switch button, and timed so that the stimulation current was at its maximum value from when the right foot stepped on the force plate, through heel strike, until toe off. As there were multiple stance phases before the right leg stepped on the force plate, 4 seconds of stimulation ensured that the peak of stimulation occurred throughout the stance phase whilst on the force plate. The subject was advised to press the hand switch button (Figure 3.4) and wait for 1 second before starting to walk from one walking end of the walkway, which is 2.39 metres long, to the other (Figure 3.5). The ramp time of 1 second set at the beginning and end of the stimulation is to provide comfort to the patient throughout the stimulation applied to the muscle (DeSantana et al., 2008).



Figure 3.2 The FES stimulation setting

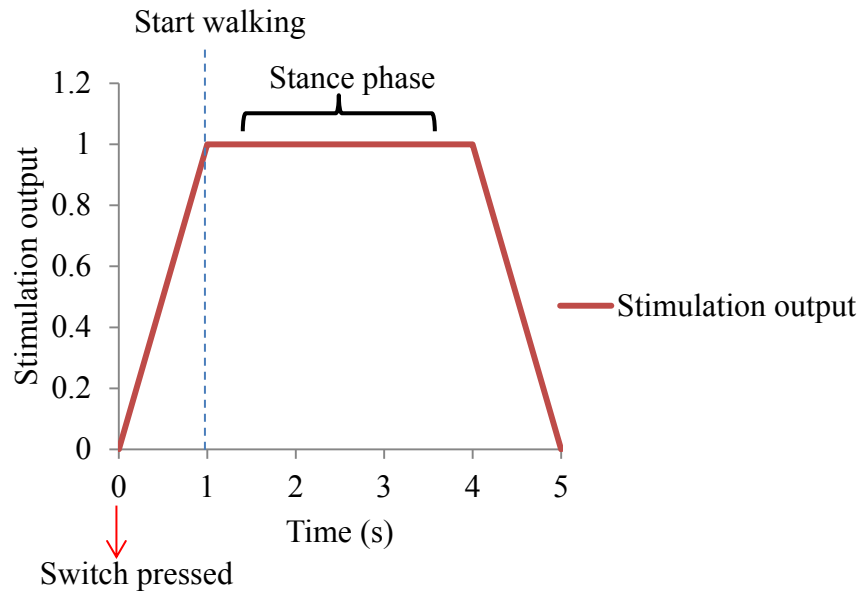


Figure 3.3 Schematic of stimulation output normalised to maximum stimulation level

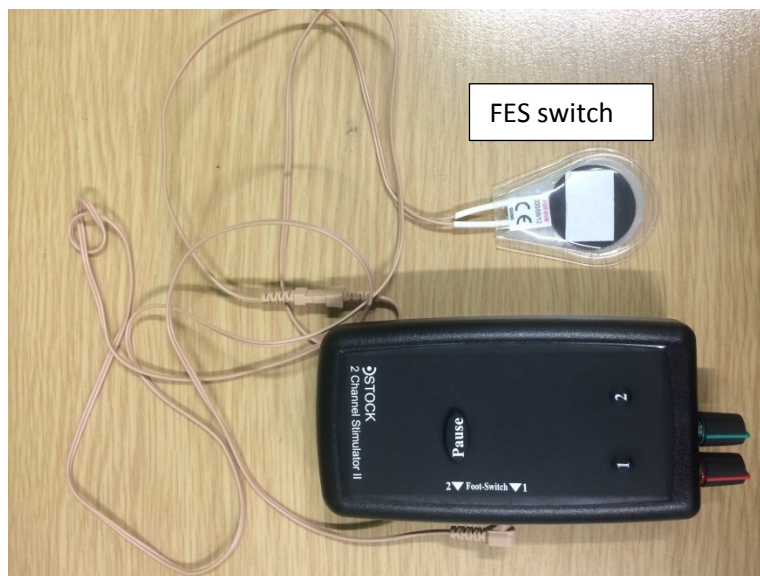


Figure 3.4 The FES device and the switch

The subjects walked for six trials for normal gait and six for FES gait, of which a random selection of three trials each were used for data analysis. All subjects started with normal gait, following by FES trials.

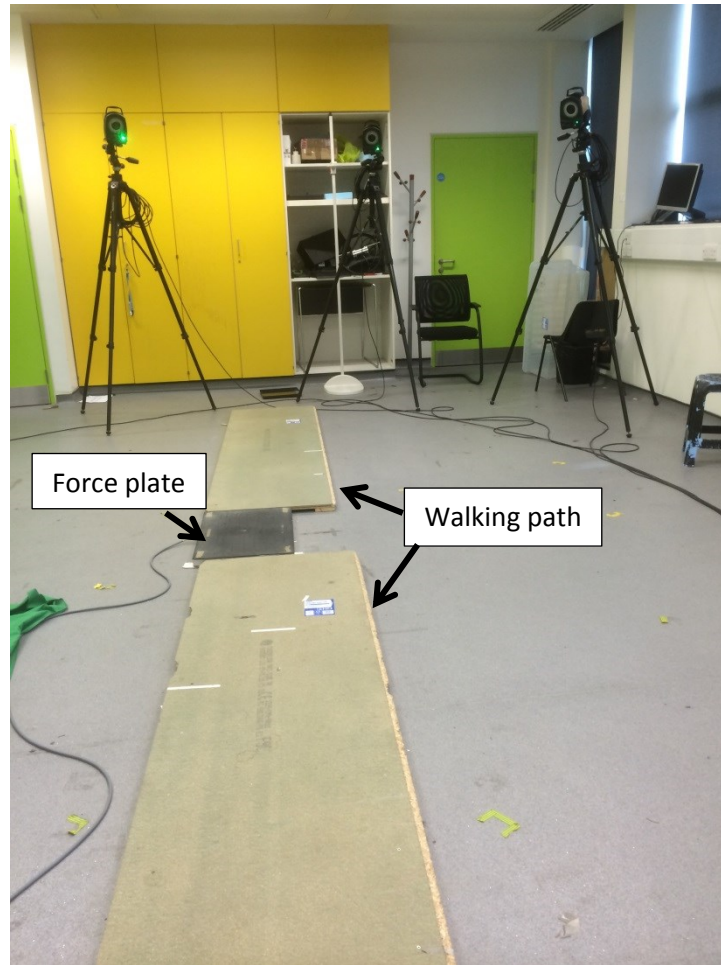


Figure 3.5 Lab set-up

Walking speed, tibial internal rotation torque, and anterior shear force were the gait measures of interest, where speed is included, because muscle activity changes are influenced by speed of walking (Arnold et al., 2013). Ground reaction forces (GRF) were recorded at 1000 Hz from a force plate (Kistler Type 9286BA, Kistler Instrument AG, Winterthur, Switzerland). A ten-camera motion analysis system (Vicon Motion Systems Ltd, Oxford, UK) recorded the motion of the right lower limb at 200 Hz; eighteen retro-reflective markers were attached to the foot, thigh and pelvis with an additional two clusters of three markers attached to the shank and thigh (Duffell et al., 2014) (Figure 3.6) (Table 3.2).

Table 3.2 Marker positions

Marker	Location
RASIS	Right anterior superior iliac spine
LASIS	Left anterior superior iliac spine
RPSIS	Right posterior superior iliac spine
LPSIS	Left posterior superior iliac spine
FLE	Lateral femoral epicondyle
FME	Medial femoral epicondyle
T1, T2, T3	Additional markers placed on the thigh segment
FAM	Apex of the lateral malleolus
TAM	Apex of the medial malleolus
S1, S2, S3	Additional markers placed on the shank segment
FCC	Calcaneus
FMT	Tuberosity of the fifth metatarsal
FM2	Head of the second metatarsal
TF	Additional marker placed on the foot

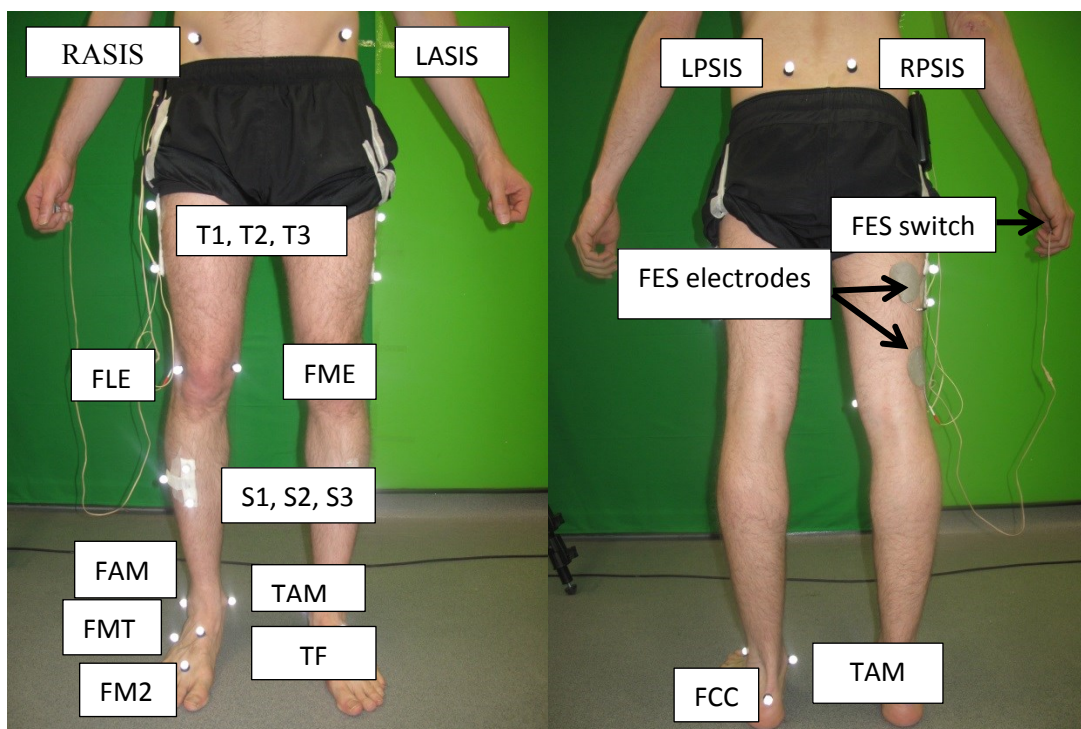


Figure 3.6 Optical motion tracking markers and FES electrode positioning

Lower limb musculoskeletal model

Musculoskeletal modelling allows the quantification of internal forces such as muscle and joint forces with gait data input. There is one commercial musculoskeletal modelling software available, Anybody (Damsgaard et al., 2006). This software has an accurate lower limb model which has been validated for various tasks with implementation of

different muscle recruitment methods and a focus on the knee (Marra et al., 2015). However, there is no clear method to modify the internal algorithms to allow the modelling of FES. In addition, there are two open source musculoskeletal modelling software packages available, OpenSim (Delp et al., 2007) and Freebody (Cleather et al., 2015; Ding et al., 2016). Of these, Freebody is the most flexible in that all the code is written in C++ and Matlab, allowing full modification of the code. In addition, as this study is focusing on ACL surgery at the knee, it is important to use a model that allows physiological and pathological joint translations at the knee to be modelled. OpenSim assumes a fixed centre of rotation and so is unable to model these translations.

Therefore, the open source musculoskeletal modelling software, Freebody V2.1 (Cleather et al., 2015; Ding et al., 2016), was used in this study. The segment-based lower limb model consists of the foot, shank, thigh, pelvis and patella segments. The patella is assumed to be massless in the model. Its position and orientation were determined based on the knee flexion angles and the length of patella ligament.

The model inputs are the kinematics data from the retro reflective markers and the kinetic data from the force plate, as can be obtained from any standard gait lab. The model calculates the intersegmental forces and torque at the proximal end of each segment (Dumas et al., 2004). The internal rotation torque was obtained from the inverse dynamics method. Each subject's anatomical geometry was created by linear scaling of an MRI-based anatomical dataset (Ding et al., 2016). The definition of the parameters of the linear scaling law is based on a study by Nolte et al., (2016): the pelvis width was calculated as the distance between the right and left anterior iliac spine landmarks; the segment lengths were defined as the distance between the hip joint centre and the midpoint between the lateral and medial femoral epicondyles, the shank segment from the femoral epicondyle midpoint and the midpoint between the tibial and fibula malleoli, and the foot segment as from the mid malleoli and distal end of the second metatarsal (Nolte et al., 2016).

The dataset consists of 163 muscle elements representing 38 lower limb muscles. The muscle attachment sites, joint centres of rotation and tibiofemoral contact points were manually digitized from the MR imaging of a male subject (1.83 m, 96 kg, 44 years) (Ding et al., 2016). The model quantifies the muscular and joint reaction forces experienced by the lower limb during the recorded movement through minimisation of a cost function

(Crowninshield et al., 1981) (Equation 3.1). This optimisation is termed *standard optimisation* throughout this thesis:

$$\text{Min} \sum_{i=1}^{163} \left(\frac{f_i}{f_{max_i}} \right)^3 \quad \text{Equation 3.1}$$

where f_i is the muscle force of muscle element i ($i=1, \dots, 163$) and f_{max_i} is the maximal muscle force of muscle element i , which is determined by multiplying published physiological cross-sectional areas of muscle element i by an assumed maximum muscle stress of 31.39 N/cm² (Yamaguchi, 2001), constrained by the equations of motion of the whole lower limb (Equation 3.2):

$$\begin{bmatrix} S_i \\ M_i \end{bmatrix} = \begin{bmatrix} m_i E_{3 \times 3} & 0_{3 \times 3} \\ m_i c_i & I_i \end{bmatrix} \begin{bmatrix} a_i - g \\ \ddot{\theta}_i \end{bmatrix} + \begin{bmatrix} 0_{3 \times 1} \\ \dot{\theta}_i \times I_i \dot{\theta}_i \end{bmatrix} \begin{bmatrix} E_{3 \times 3} & 0_{3 \times 3} \\ d_i & E_{3 \times 3} \end{bmatrix} \begin{bmatrix} S_{i-1} \\ M_{i-1} \end{bmatrix} \quad \text{Equation 3.2}$$

where i is the segment number or joint number (numbering from distal to proximal), S_i the proximal intersegmental forces, S_{i-1} the distal inter-segmental forces, M_i the proximal intersegmental moments (notional joint moments), M_{i-1} the distal intersegmental moments (notional joint moments), I_i the inertia tensor, $\ddot{\theta}_i$ the angular acceleration about center of motion (COM), $\dot{\theta}_i$ the angular velocity about center of motion (COM), a_i the linear acceleration of COM, m_i the segment mass, $E_{3 \times 3}$ the identity matrix, c_i the vector from the proximal joint to the segment COM and d_i is the vector from the proximal to the distal joint.

In order to quantify the effect of higher muscle activation of BFLH produced by the FES at the knee, a revised optimisation method is proposed (Equation 3.3):

$$\text{min} \sum_{i=1}^{162} \left(\frac{f_i}{f_{max_i}} \right)^3 \quad \text{Equation 3.3}$$

where f_i is the muscle force of muscle element i ($i=1, \dots, 162$) and f_{max_i} is the maximal muscle force of muscle element i .

In the revised optimisation method, the muscle element is reduced to 162 because the muscle force of BFLH, f_{26} is set as a constant value during the stance phase to replicate the

physical stimulation of the muscle by FES. This value is set at a muscle activation, c , times the maximum force of BFLH, $f_{BFLH_{max}}$, where $f_{26} = c \times f_{BFLH_{max}}$. As the attachment sites of BFLH are on the shank and thigh segments, the equations of motion of the shank and thigh segments (Equation 3.2) were modified by the inclusion of an additional term to give (Equation 3.4):

$$\begin{bmatrix} S_i \\ M_i \end{bmatrix} = \begin{bmatrix} m_i E_{3 \times 3} & 0_{3 \times 3} \\ m_i c_i & I_i \end{bmatrix} \begin{bmatrix} a_i - g \\ \ddot{\theta}_i \end{bmatrix} + \begin{bmatrix} 0_{3 \times 1} \\ \dot{\theta}_i \times I_i \dot{\theta}_i \end{bmatrix} + \begin{bmatrix} E_{3 \times 3} & 0_{3 \times 3} \\ d_i & E_{3 \times 3} \end{bmatrix} \begin{bmatrix} S_{i-1} \\ M_{i-1} \end{bmatrix} - \begin{bmatrix} (c \times f_{BFLH_{max}}) \cdot n_{BFLH} \\ (c \times f_{BFLH_{max}}) \cdot (r_{BFLH} \times n_{BFLH}) \end{bmatrix} \quad \text{Equation 3.4}$$

where S_i the revised proximal intersegmental forces, S_{i-1} the revised distal inter-segmental forces, M_i the revised proximal intersegmental moments (notional joint moments), M_{i-1} the revised distal intersegmental moments (notional joint moments), c is a constant, $f_{BFLH_{max}}$ the maximum force of BFLH, n_{BFLH} the line of action of BFLH and r_{BFLH} the moment arm of BFLH. In this study, c was increased in increments of 0.05 until the peak anterior tibial shear was reduced to zero, where c is a value between 0 and 1, to make sure that the BFLH force does not exceed its maximum activation value. The increment of BFLH activation theoretically causes a reduction in tibial internal torque, which was calculated as the product of the increment of BFLH muscle force and its moment arm at the time frame at which peak anterior tibial shear was occurred.

Data Analysis

The walking speed (as calculated from the stance phase only), knee joint torque, anterior shear force, and knee contact force were averaged over three trials and presented as a mean value. Knee joint torque and knee contact force were presented in the tibial coordinate frame. The stance phase was expressed in a 0-100% duration with a step interval of 1% using cubic spline data interpolation. To test the hypothesis that the peak of the tibial internal rotation torque and the anterior shear force were reduced by applying the FES over the BFLH, the differences between normal gait and FES gait were compared using a one-tail paired-samples t-test with an α level of 0.05. All data processing and analysis was conducted in MATLAB (The Mathworks Inc., Natick, MA).

3.3 Results

FES gait mean walking speed (as calculated from the stance phase only) 0.25 ± 0.04 m/s was lower than that during normal gait (0.27 ± 0.03 m/s; $p=0.036$). The peak value of the tibial internal rotation torque across all subjects was 0.0012 ± 0.0010 Nm/BW during normal gait. It was reduced by 63% to 0.0005 ± 0.0004 Nm/BW ($p=0.032$) when BFLH was stimulated by FES (Table 3.3) (Figure 3.7).

Table 3.3 Peak tibial internal rotation torque (Nm/BW) during normal and FES gait

Peak internal rotation torque (Nm/BW)		
Subject	Normal gait	FES gait
1	0.0006	0.0006
2	0.0003	0.0004
3	0.0009	0.0001
4	0.0037	-0.0001
5	0.0007	0.0007
6	0.0028	-0.0004
7	0.0007	0.0009
8	0.0010	0.0004
9	0.0010	0.0008
10	0.0015	0.0009
11	0.0010	0.0007
12	0.0007	0.0005
Mean	0.0012	0.0005
SD	0.0010	0.0004

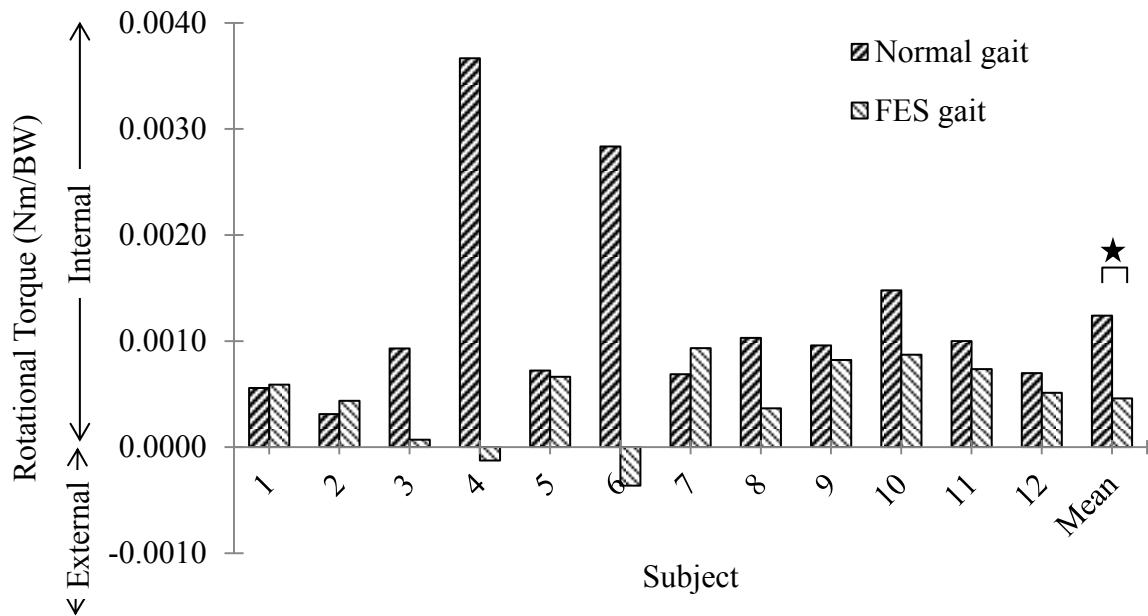


Figure 3.7 Peak tibial internal torque (Nm/BW) across twelve subjects during normal and FES gait

Figure 3.8-3.19 shows the tibial internal rotation torque of all subjects during normal and FES gait.

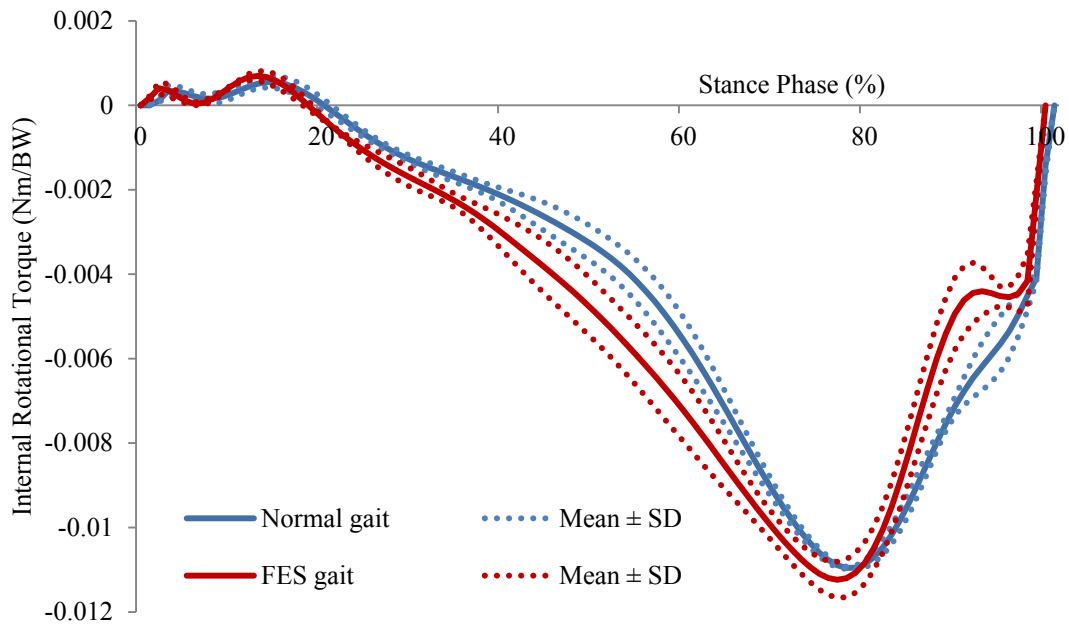


Figure 3.8 Tibial internal rotation torque (Nm/BW) (mean \pm SD) of subject 1 during normal and FES gait

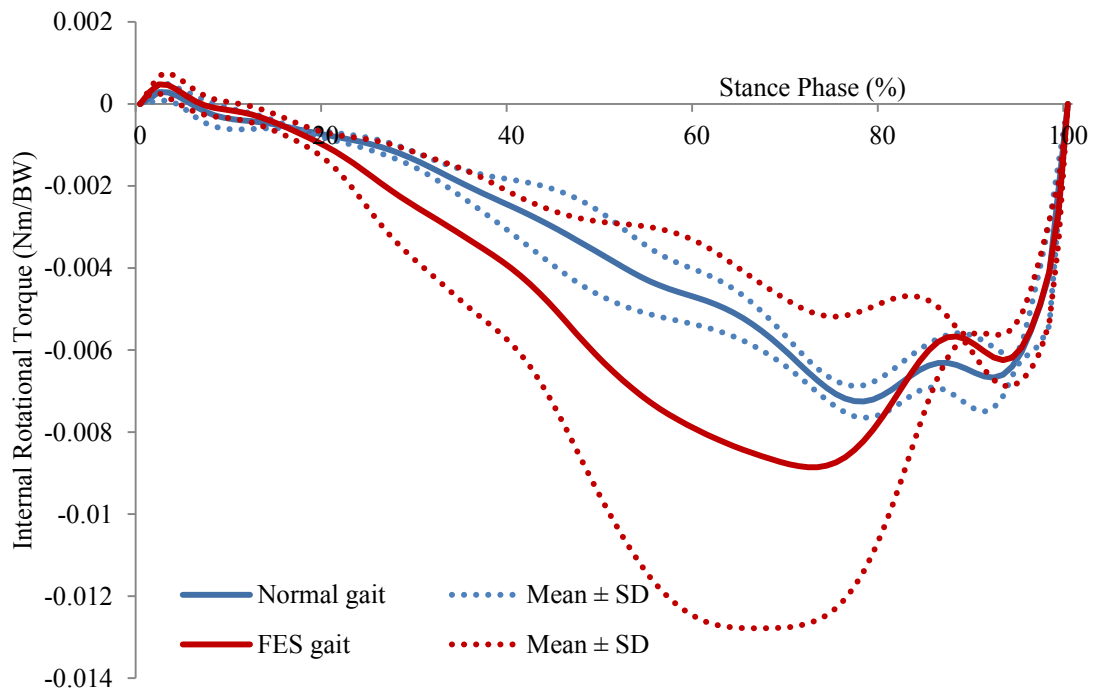


Figure 3.9 Tibial internal rotation torque (Nm/BW) (mean \pm SD) of subject 2 during normal and FES gait

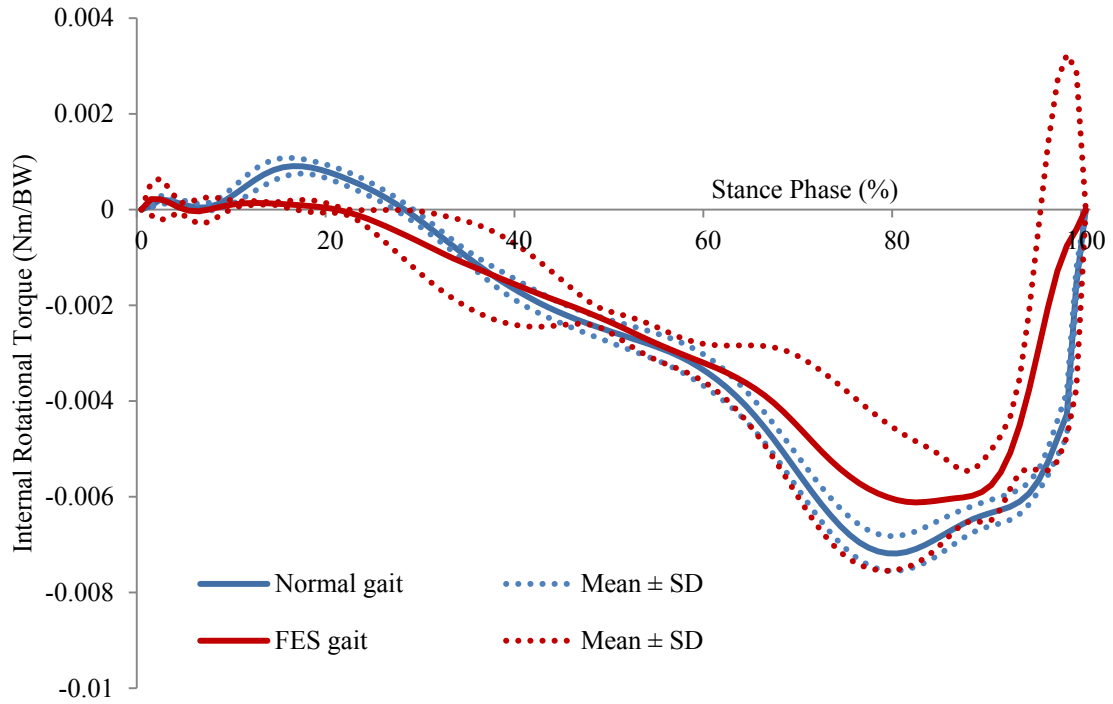


Figure 3.10 Tibial internal rotation torque (Nm/BW) (mean \pm SD) of subject 3 during normal and FES gait

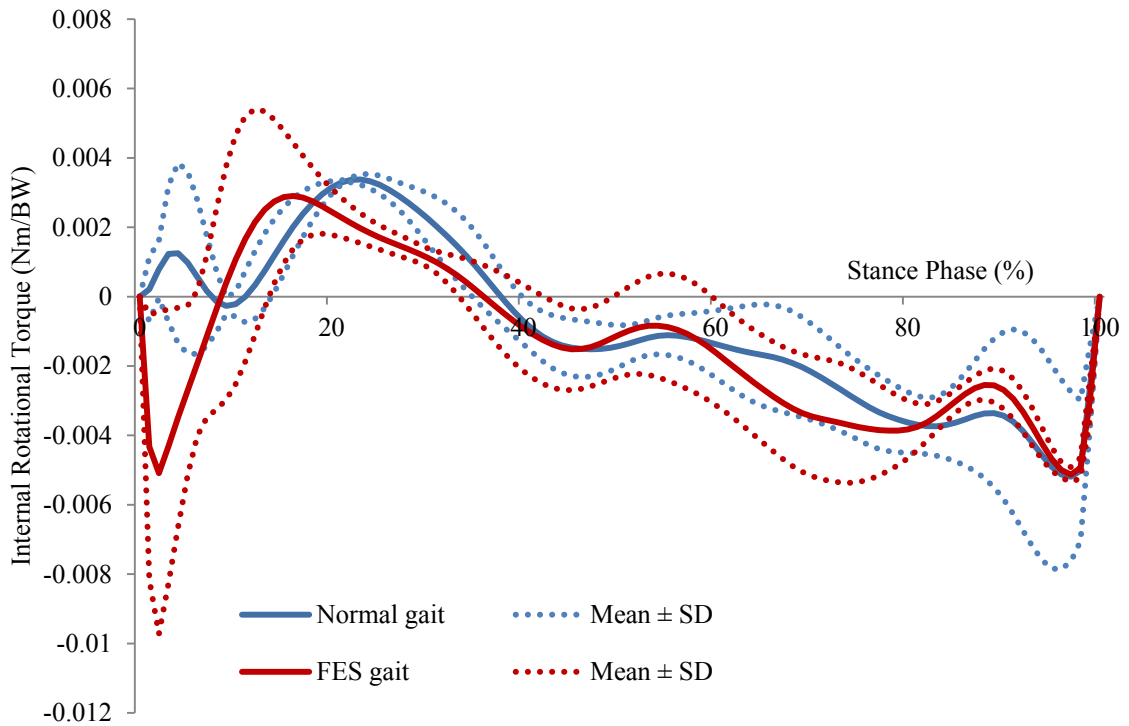


Figure 3.11 Tibial internal rotation torque (Nm/BW) (mean \pm SD) of subject 4 during normal and FES gait

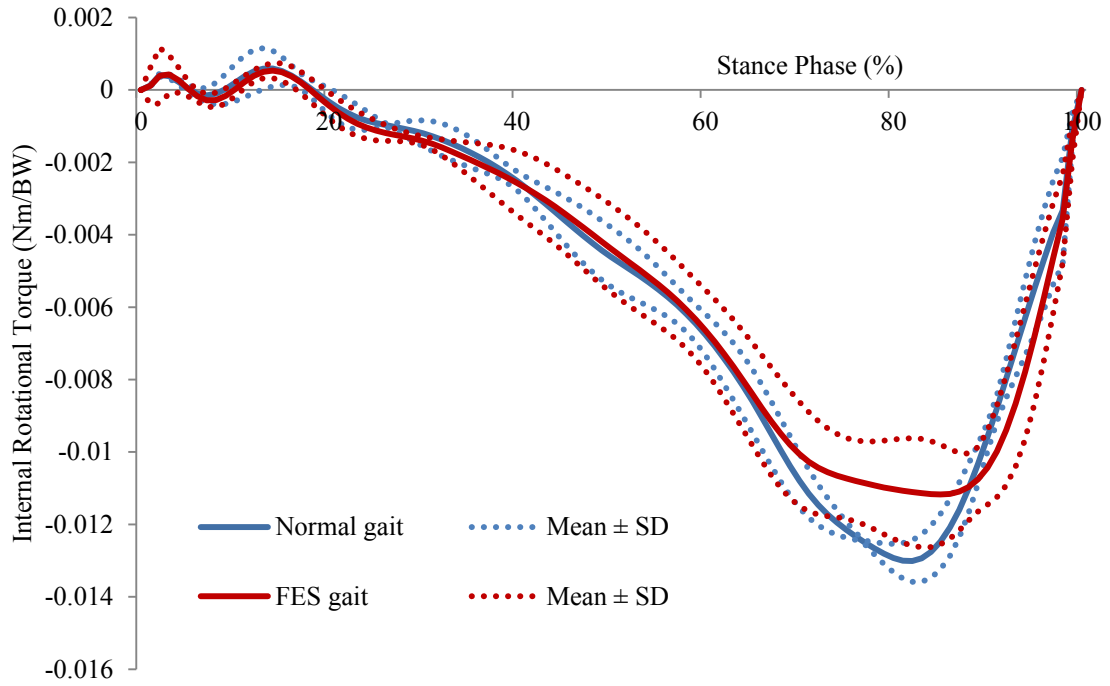


Figure 3.12 Tibial internal rotation torque (Nm/BW) (mean \pm SD) of subject 5 during normal and FES gait

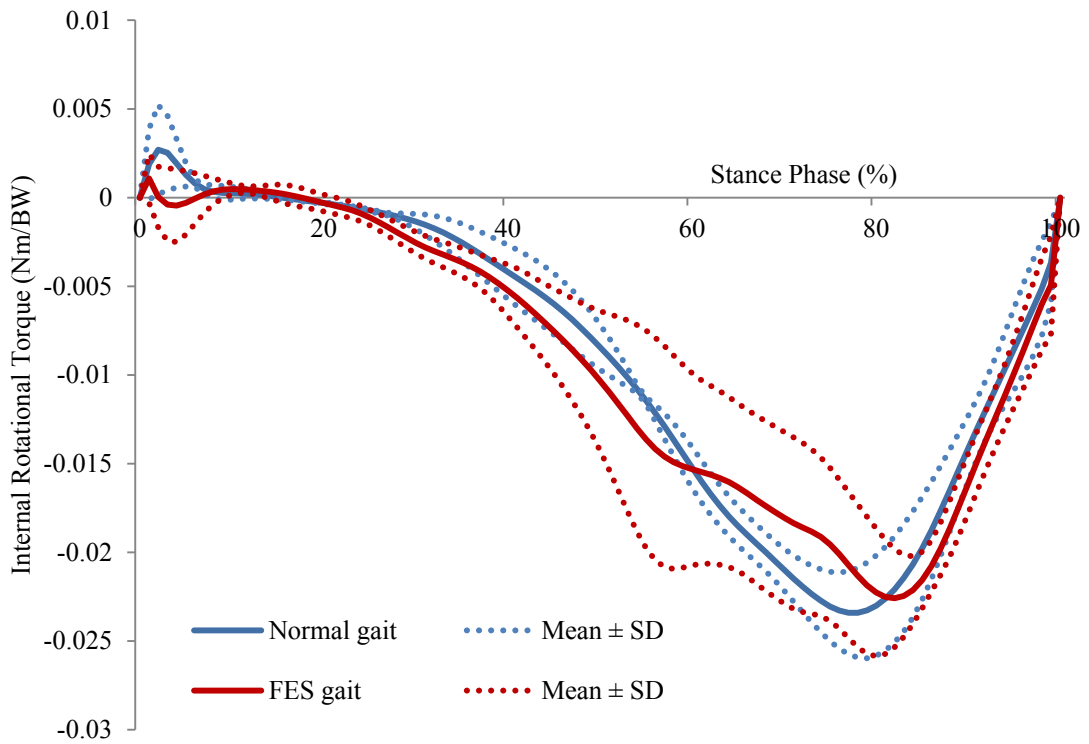


Figure 3.13 Tibial internal rotation torque (Nm/BW) (mean \pm SD) of subject 6 during normal and FES gait

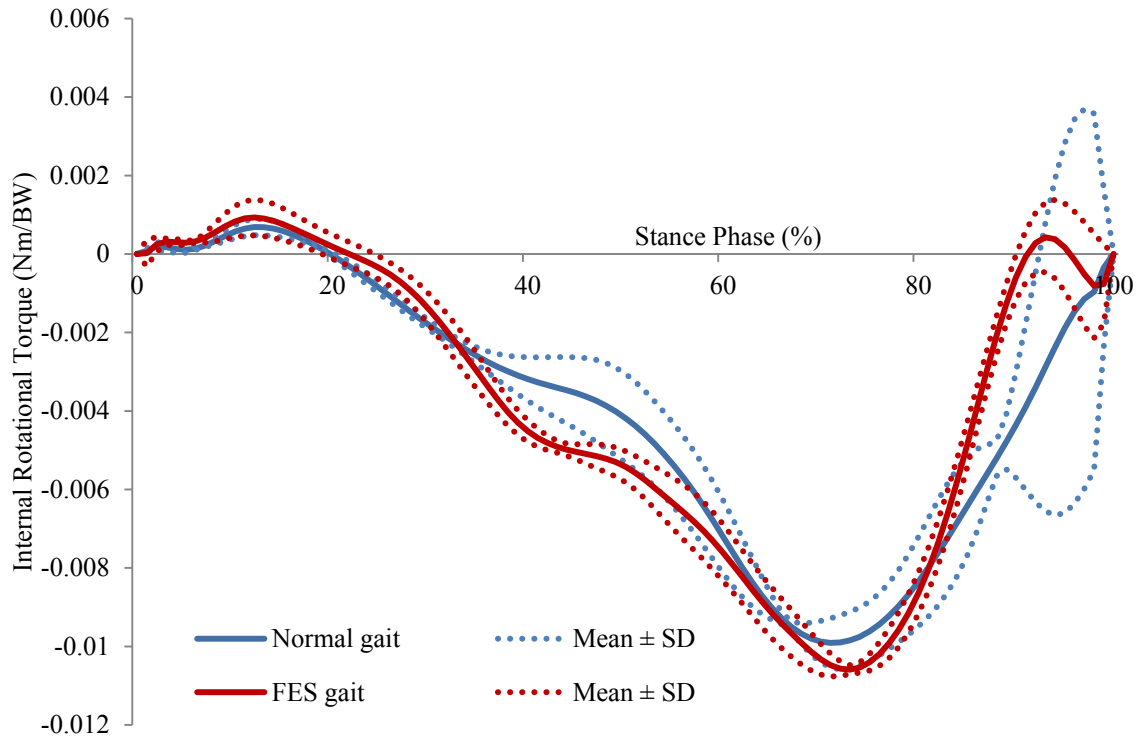


Figure 3.14 Tibial internal rotation torque (Nm/BW) (mean \pm SD) of subject 7 during normal and FES gait

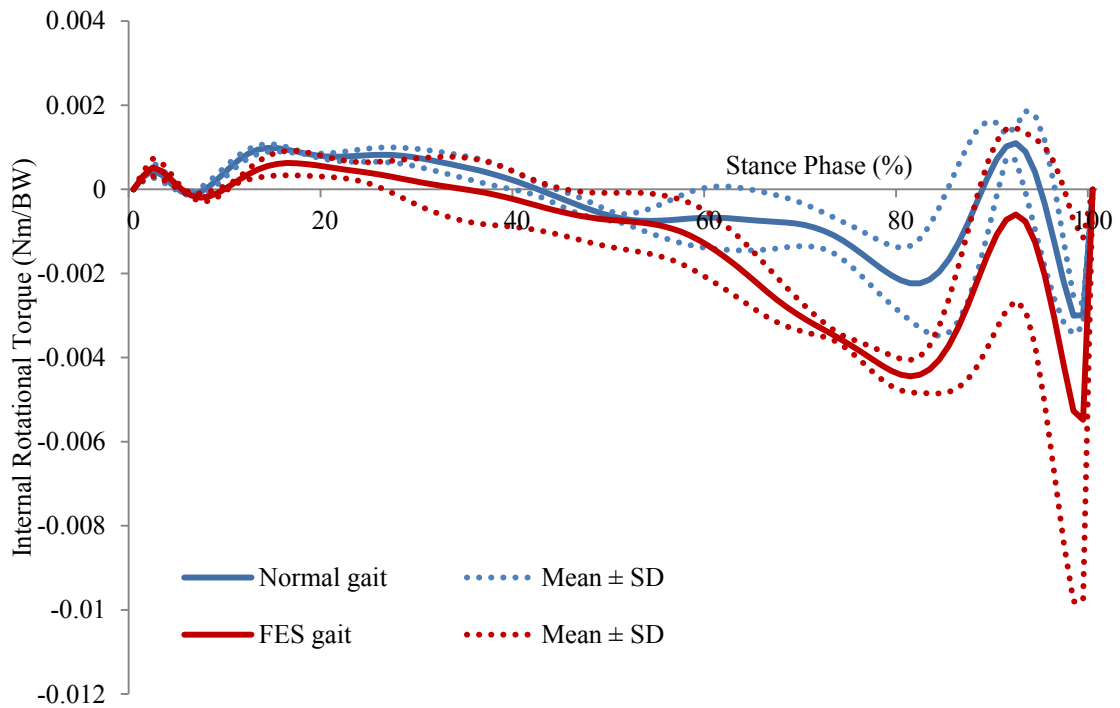


Figure 3.15 Tibial internal rotation torque (Nm/BW) (mean \pm SD) of subject 8 during normal and FES gait

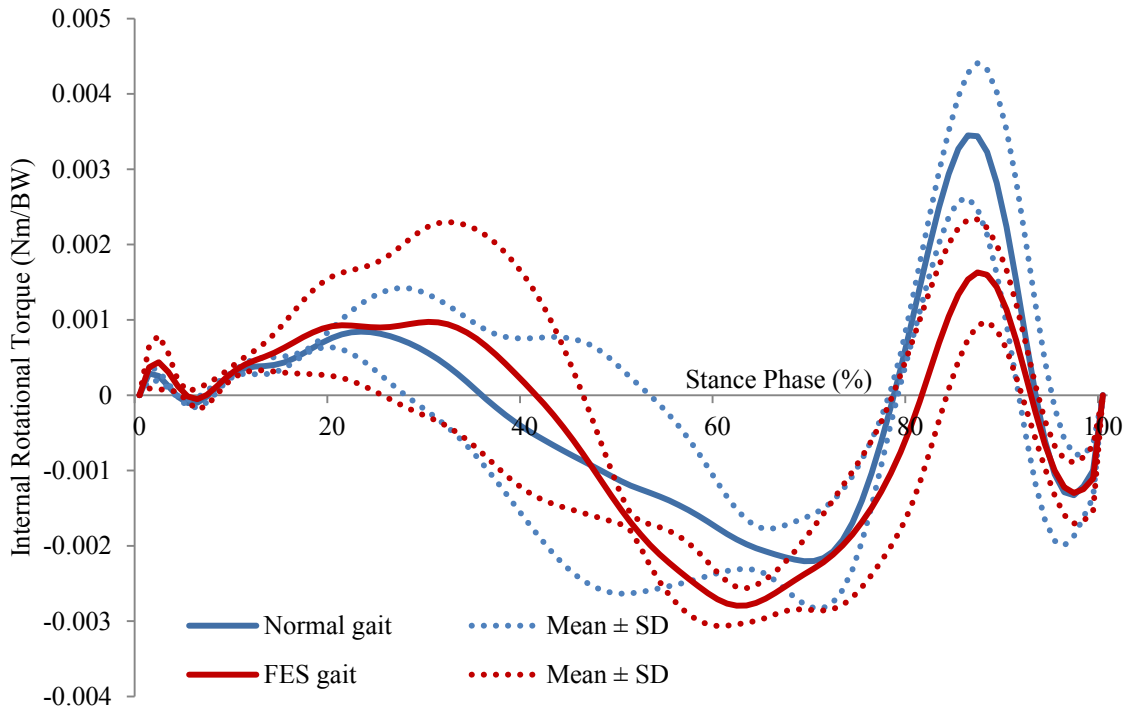


Figure 3.16 Tibial internal rotation torque (Nm/BW) (mean \pm SD) of subject 9 during normal and FES gait

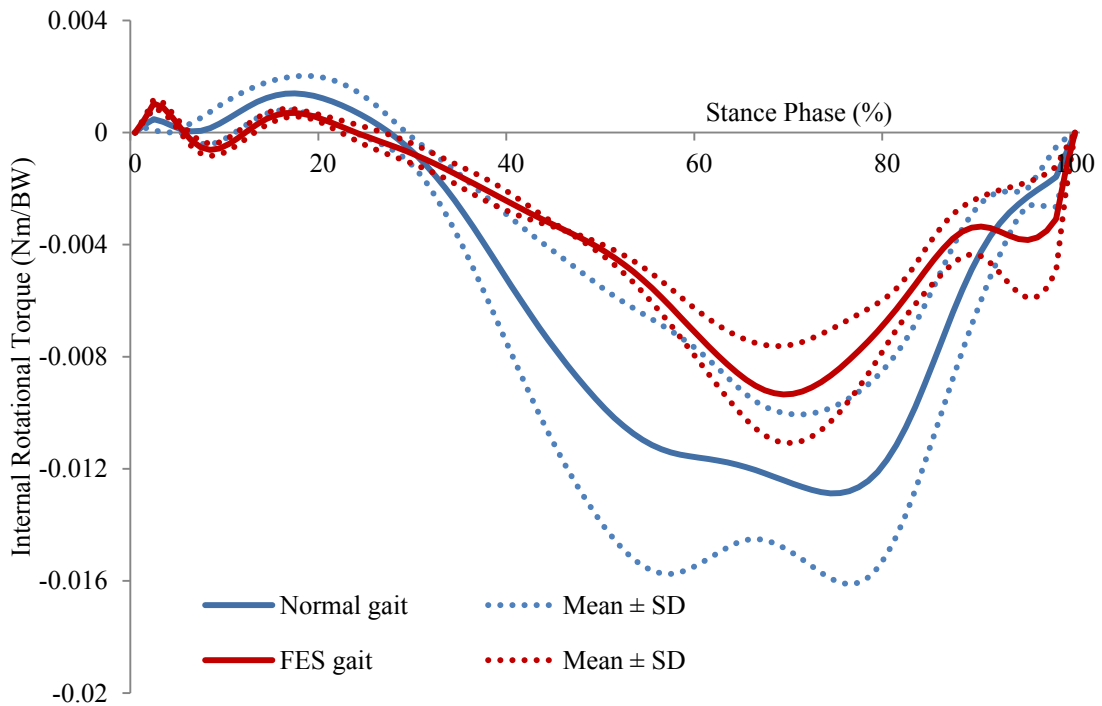


Figure 3.17 Tibial internal rotation torque (Nm/BW) (mean \pm SD) of subject 10 during normal and FES gait

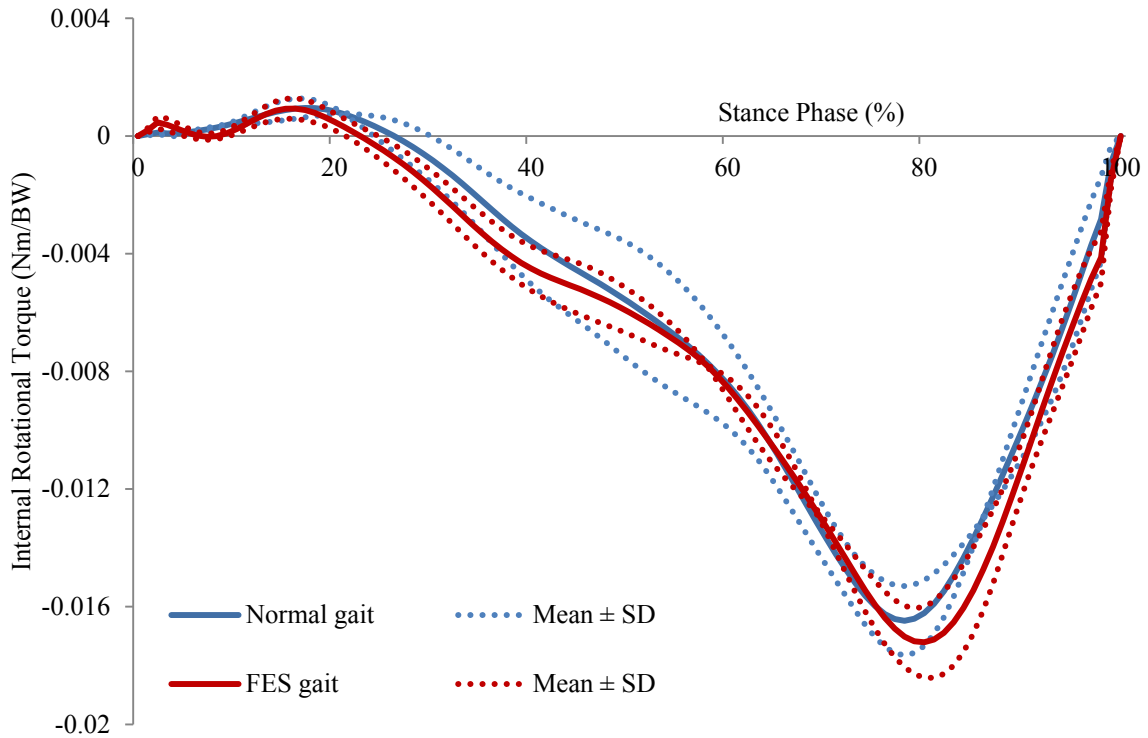


Figure 3.18 Tibial internal rotation torque (Nm/BW) (mean \pm SD) of subject 11 during normal and FES gait

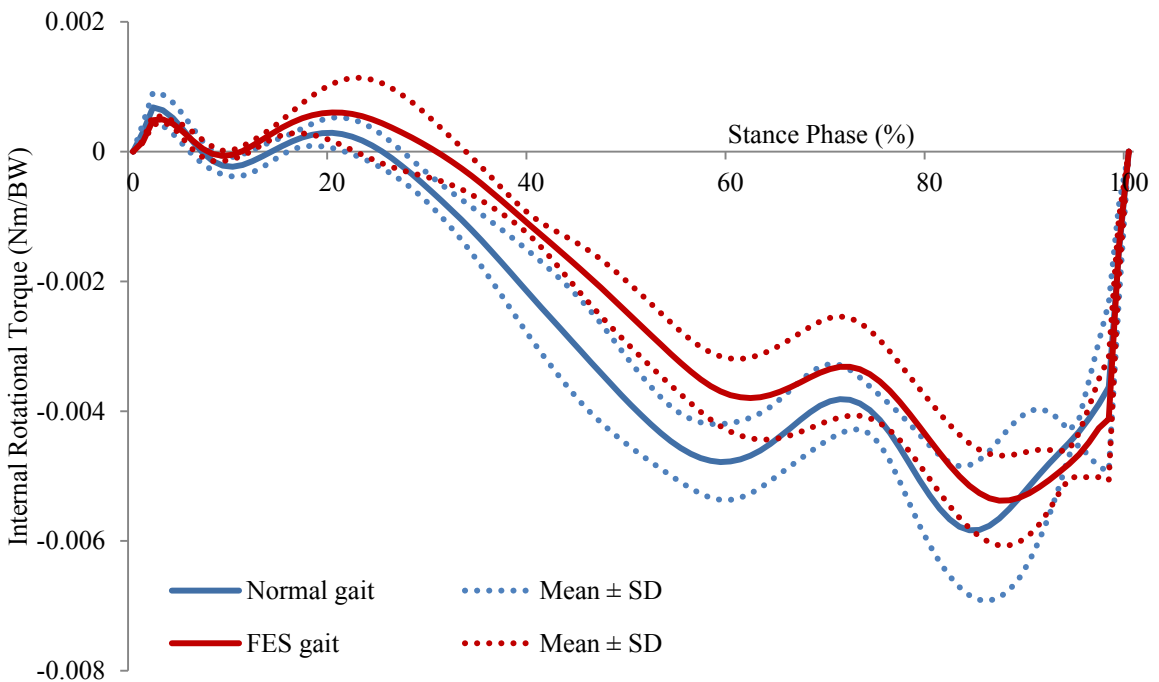


Figure 3.19 Tibial internal rotation torque (Nm/BW) (mean \pm SD) of subject 12 during normal and FES gait

The first peak of adduction torque and flexion torque were not significantly different during FES gait compared to normal gait ($p=0.3457$ and $p=0.2623$, respectively; Table 3.4, Figure 3.20).

Table 3.4 Peak tibial adduction torque (Nm/BW) and peak tibial flexion torque (Nm/BW) during normal and FES gait

Subjects	Peak adduction torque (Nm/BW)		Peak flexion torque (Nm/BW)	
	Normal gait	FES gait	Normal gait	FES gait
1	0.0361	0.0344	0.0464	0.0397
2	0.0427	0.0411	0.0589	0.0516
3	0.0326	0.0338	0.0643	0.0514
4	0.0232	0.0298	0.1193	0.0952
5	0.0480	0.0466	0.0755	0.0933
6	0.0592	0.0546	0.0477	0.1804
7	0.0446	0.0434	0.0300	0.0310
8	0.0095	0.0122	0.0704	0.0594
9	0.0152	0.0080	0.0352	0.0429
10	0.0452	0.0440	0.0616	0.0571
11	0.0401	0.0415	0.0477	0.0498
12	0.0375	0.0394	0.0564	0.0543
Mean	0.0361	0.0357	0.0594	0.0672
SD	0.0142	0.0136	0.0232	0.0405

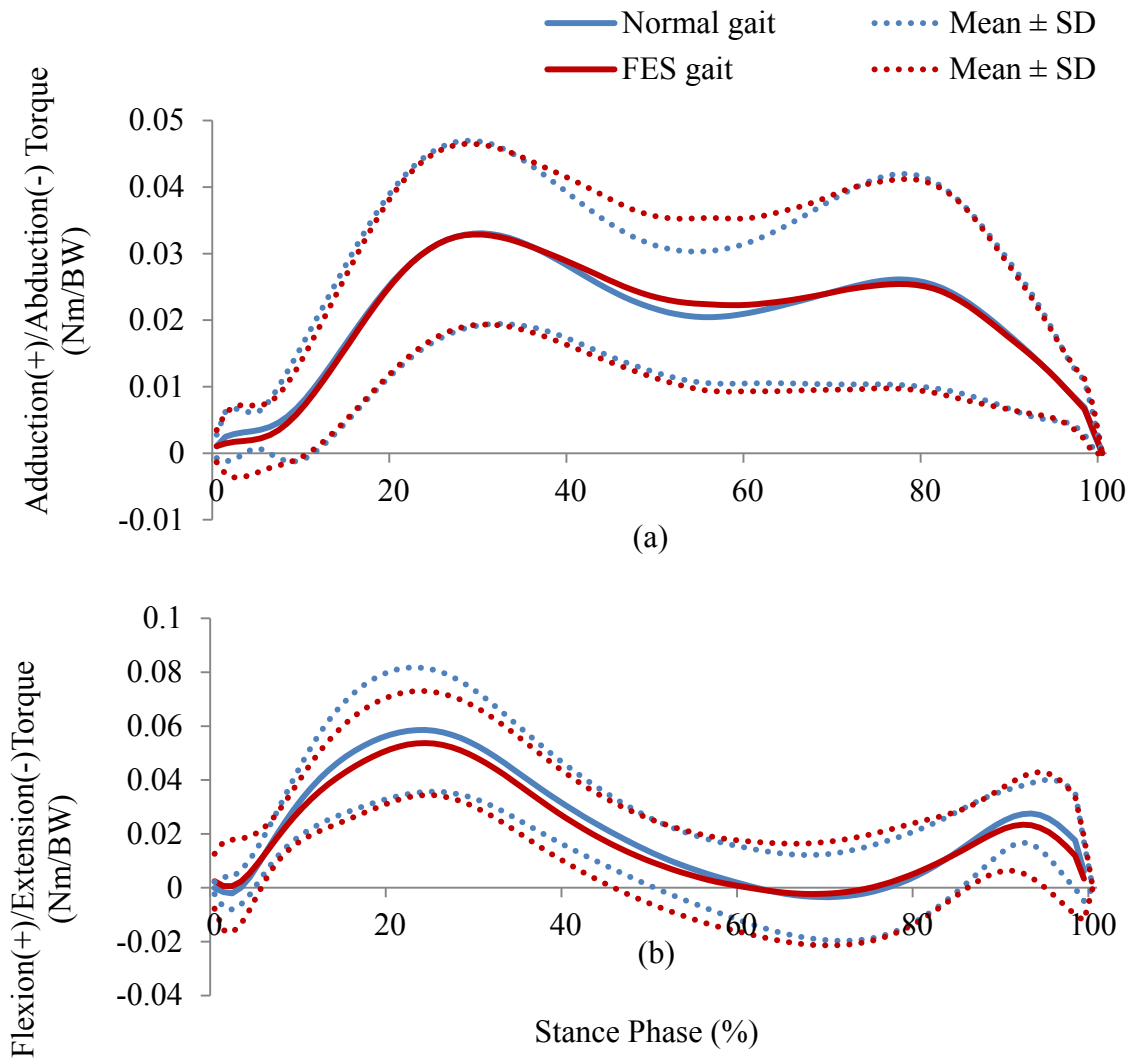


Figure 3.20 (a) Tibial adduction torque (Nm/BW) and (b) tibial flexion torque (Nm/BW) during normal and FES gait for all subjects (mean \pm SD, n=12)

In the standard optimisation method, the peak anterior shear force occurred at 18.8% ($\pm 6.0\%$) of stance phase with a mean value of 0.289 ± 0.077 BW. The muscle activation of BFLH at peak anterior shear was 0.015 ± 0.021 (Table 3.5).

Table 3.5 Peak anterior shear force (BW) and muscle activation

Subject	Peak anterior shear force during normal gait (BW)	% stance phase	BFLH muscle activation	<i>c</i>	Peak anterior shear force during FES gait (BW) (<i>c</i> =0.208)
1	0.288	26.0	0.002	0.20	-0.030
2	0.187	23.0	0.016	0.15	-0.330
3	0.310	20.0	0.000	0.15	-0.140
4	0.423	19.0	0.000	0.10	-0.620
5	0.278	26.0	0.000	0.40	-0.498
6	0.178	15.0	0.067	0.25	-0.272
7	0.201	5.0	0.054	0.30	0.078
8	0.265	16.0	0.013	0.20	-0.176
9	0.275	23.0	0.016	0.20	-0.116
10	0.420	15.0	0.000	0.20	-0.132
11	0.348	23.0	0.001	0.20	-0.247
12	0.297	15.0	0.013	0.15	-0.221
Mean	0.289	18.8	0.015	0.208	-0.225
SD	0.077	6.0	0.021	0.084	0.192

Increasing BFLH activation incrementally resulted in an incremental reduction in the anterior shear force for all subjects (Figure 3.21-Figure 3.32). The activation of BFLH (expressed as *c* value) required to reduce the peak anterior shear force to zero in the revised optimisation ranged from 0.15 to 0.40 with a mean *c* value of 0.208 ± 0.084 (Table 3.5). Applying the mean value of 0.208 to all subjects, reduced the peak anterior shear force to below zero in 11/12 subjects and was 0.078 BW for the other subject (Table 3.5; Figure 3.33). At the time frame at which peak anterior shear force occurred, the reduction in tibial internal torque was calculated as the product of the increment of BFLH muscle force and its moment arm at that time frame. This level of muscle activation at 0.208 caused a reduction of the internal rotational torque of 0.023 ± 0.0167 Nm/BW ($p < 0.001$) (Table 3.6).

Table 3.6 Difference mean peak internal rotational torque (Nm/BW)

Subject	Mean peak internal rotational torque (Nm/BW)		
	Normal gait	FES gait	Difference (FES gait – normal gait)
1	0.0049	0.0376	0.0327
2	0.0080	0.0294	0.0214
3	0.0004	0.0302	0.0298
4	0.0000	0.0216	0.0215
5	0.0051	0.0660	0.0609
6	0.0181	0.0605	0.0424
7	0.0350	0.0333	-0.0017
8	0.0100	0.0313	0.0213
9	0.0044	0.0173	0.0129
10	0.0025	0.0163	0.0138
11	0.0487	0.0486	0.0000
12	0.0205	0.0365	0.0160
Mean	0.0131	0.0357	0.0226
SD	0.0145	0.0150	0.0167

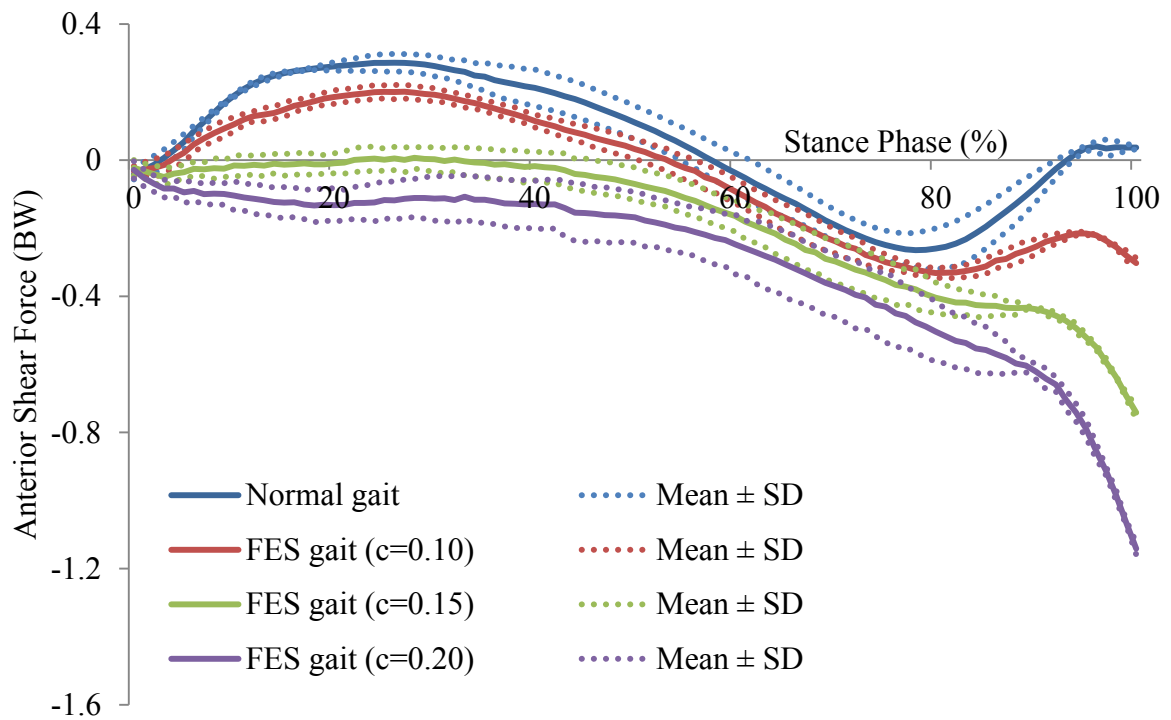


Figure 3.21 Anterior shear force (BW) (mean ± SD) of subject 1 during normal and FES gait

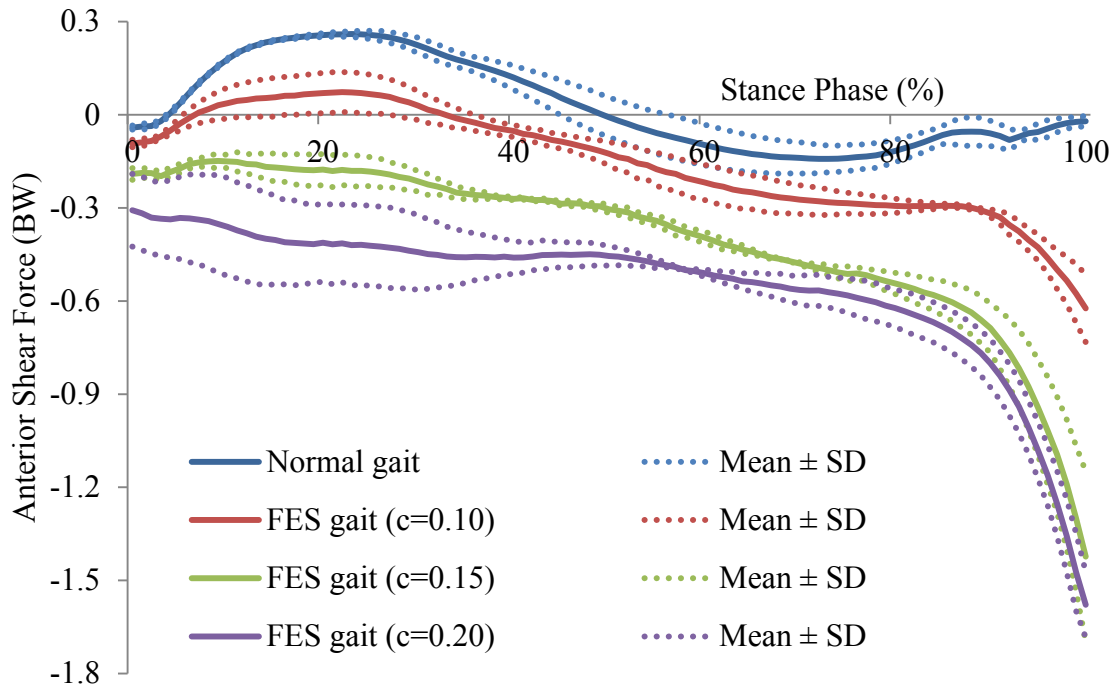


Figure 3.22 Anterior shear force (BW) (mean \pm SD) of subject 2 during normal and FES gait

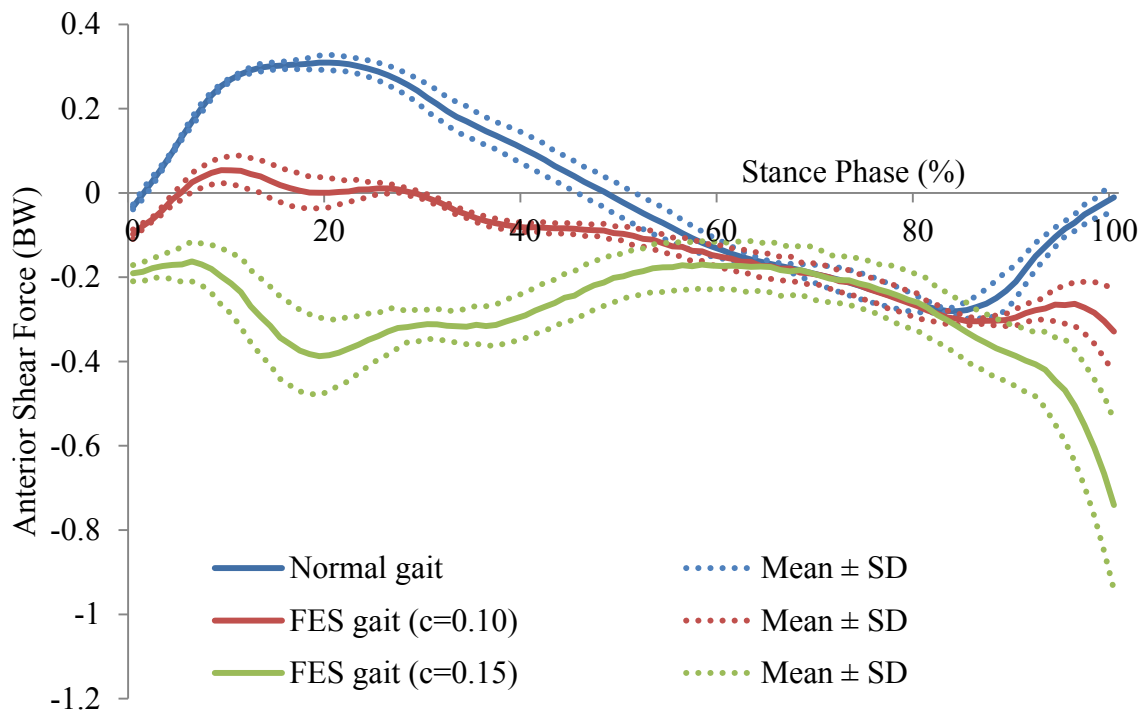


Figure 3.23 Anterior shear force (BW) (mean \pm SD) of subject 3 during normal and FES gait

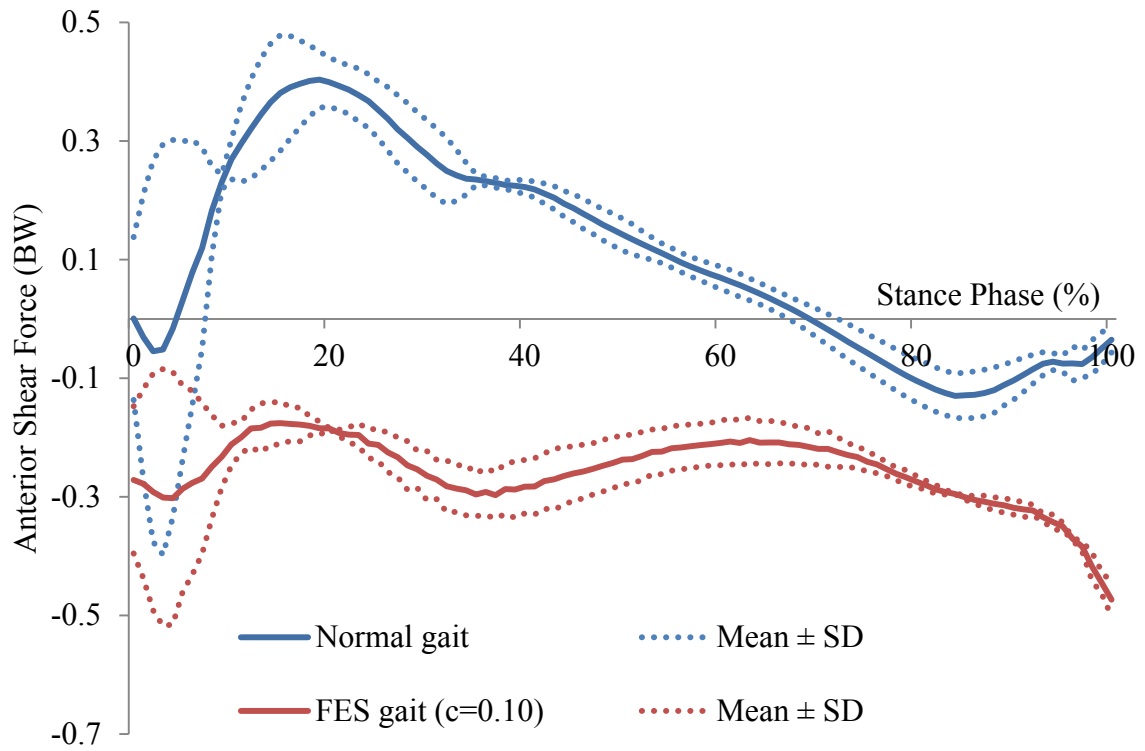


Figure 3.24 Anterior shear force (BW) (mean \pm SD) of subject 4 during normal and FES gait

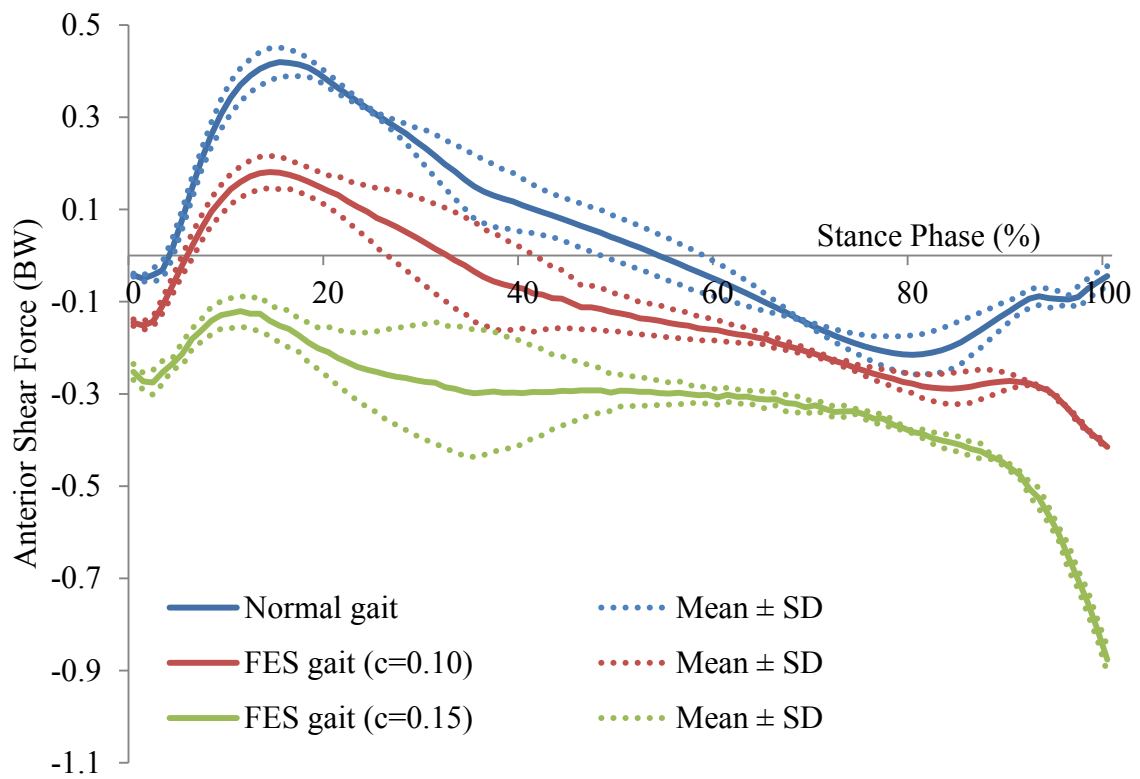


Figure 3.25 Anterior shear force (BW) (mean \pm SD) of subject 5 during normal and FES gait

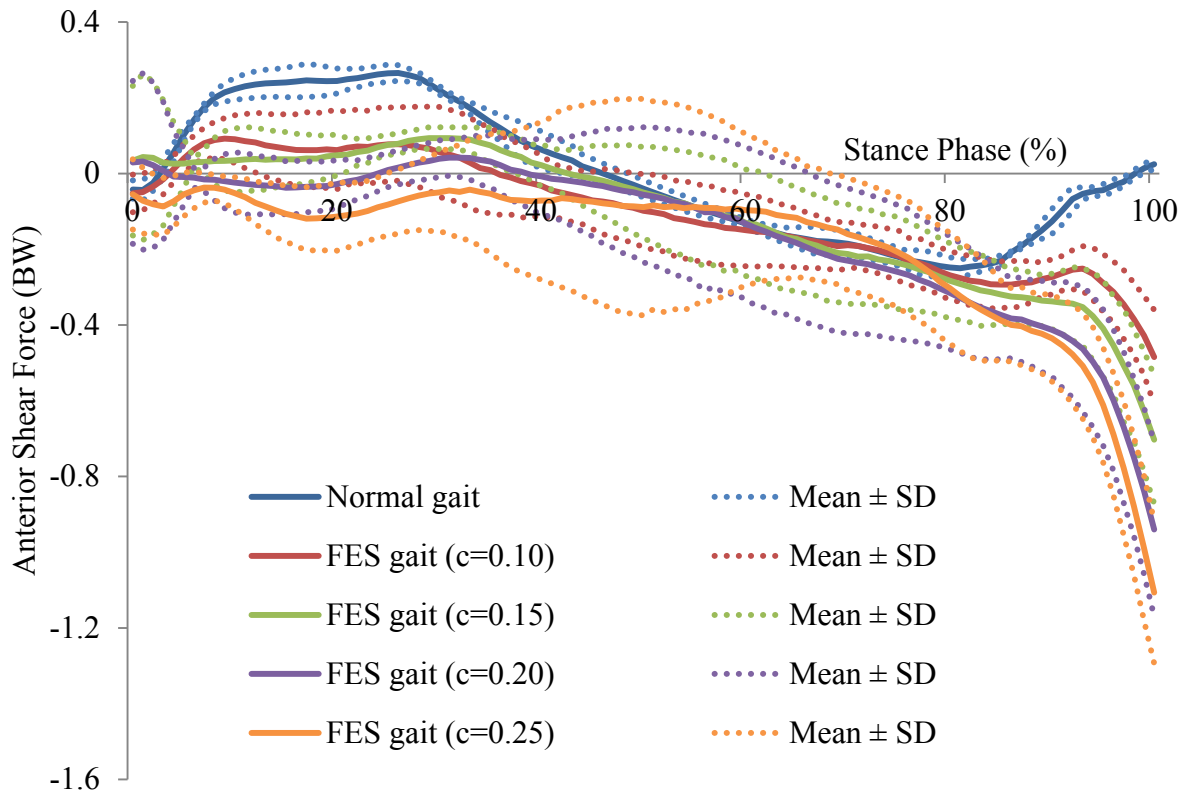


Figure 3.26 Anterior shear force (BW) (mean \pm SD) of subject 6 during normal and FES gait

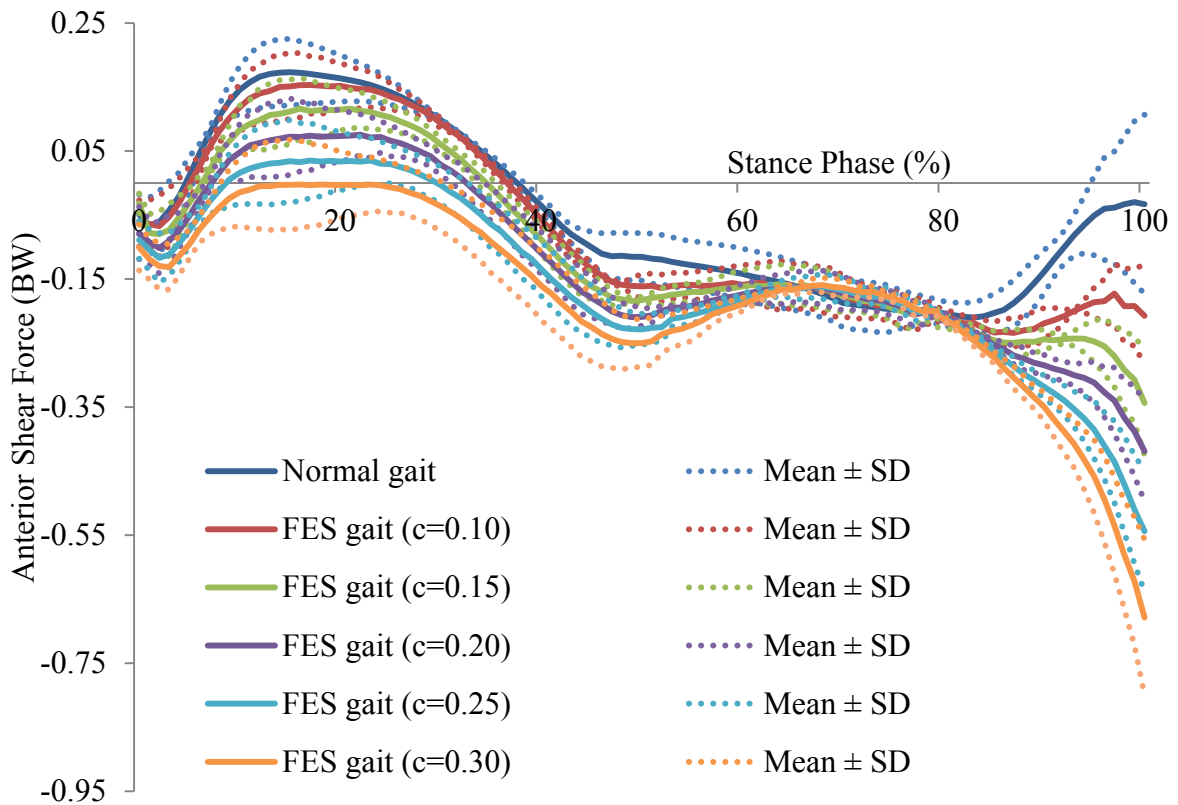


Figure 3.27 Anterior shear force (BW) (mean \pm SD) of subject 7 during normal and FES gait

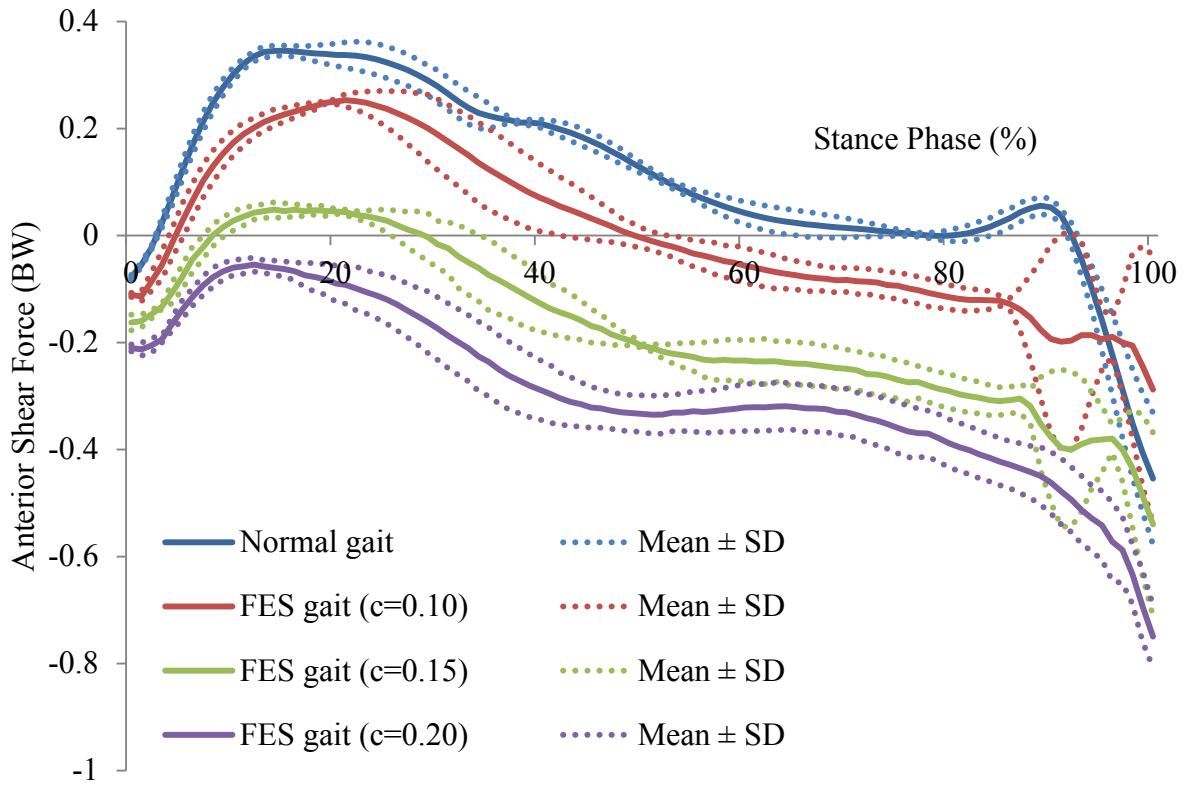


Figure 3.28 Anterior shear force (BW) (mean \pm SD) of subject 8 during normal and FES gait

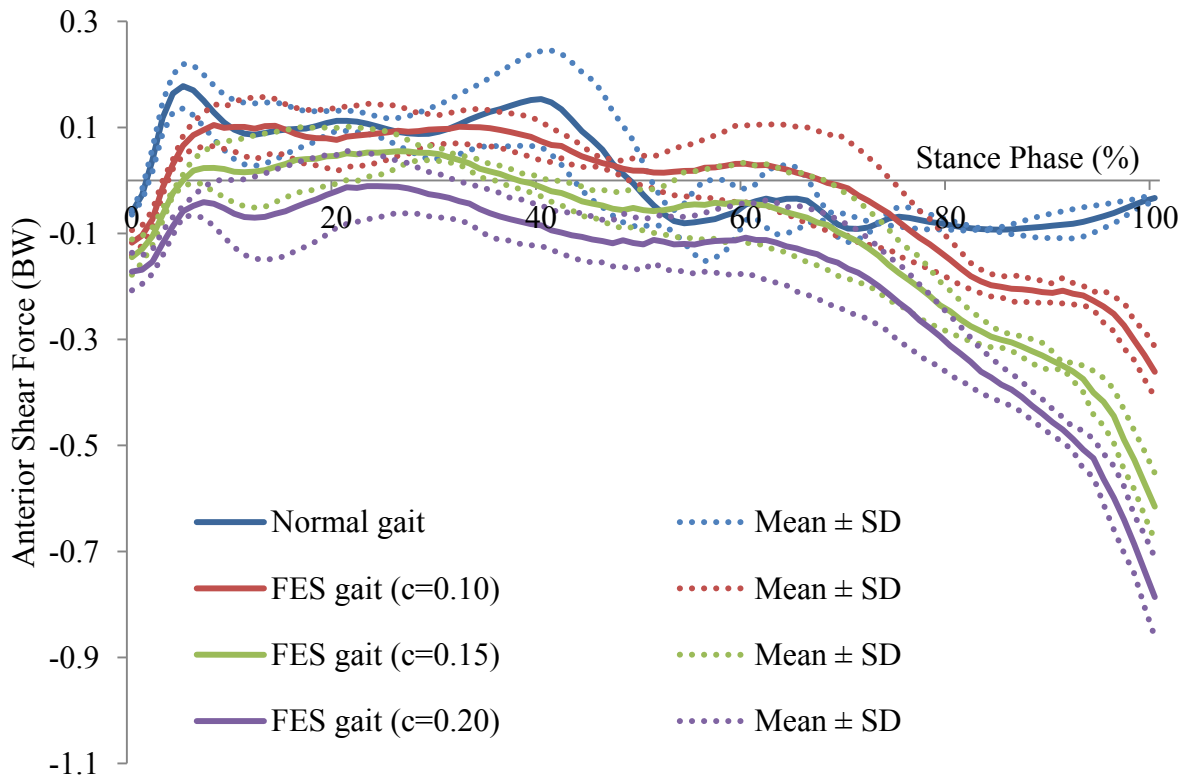


Figure 3.29 Anterior shear force (BW) (mean \pm SD) of subject 9 during normal and FES gait

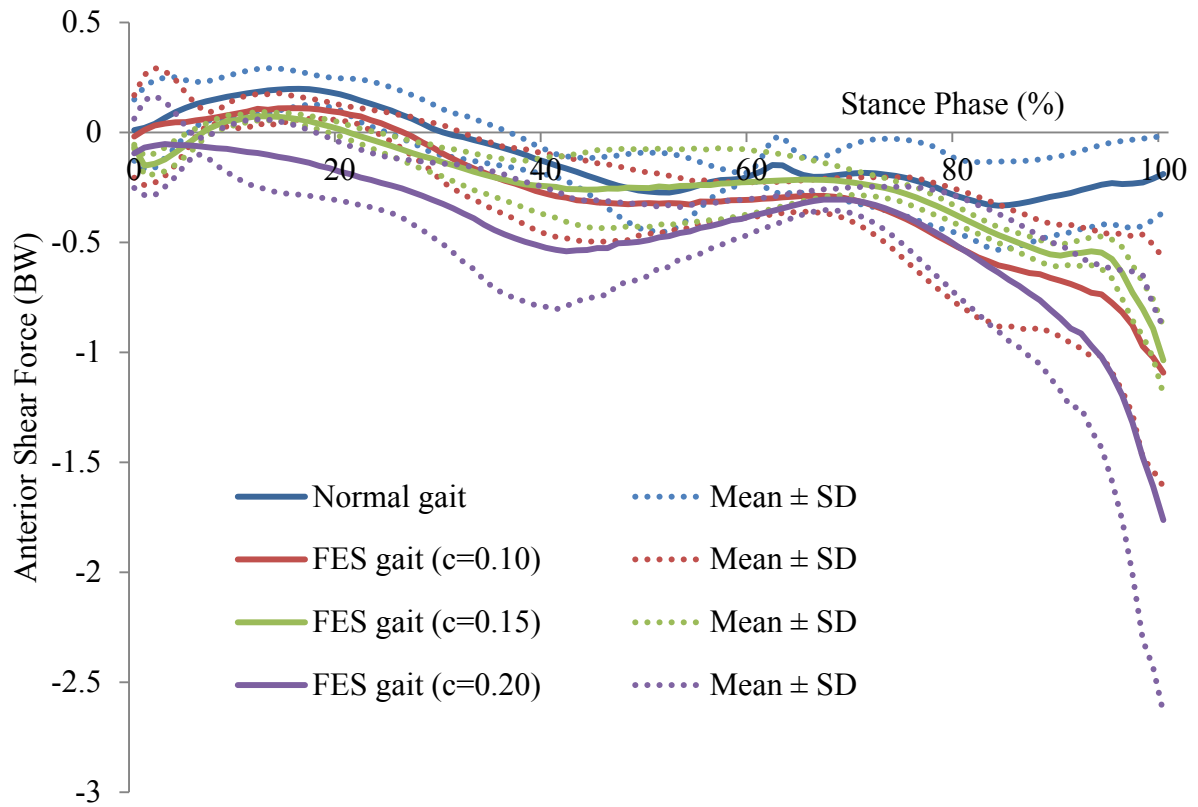


Figure 3.30 Anterior shear force (BW) (mean \pm SD) of subject 10 during normal and FES gait

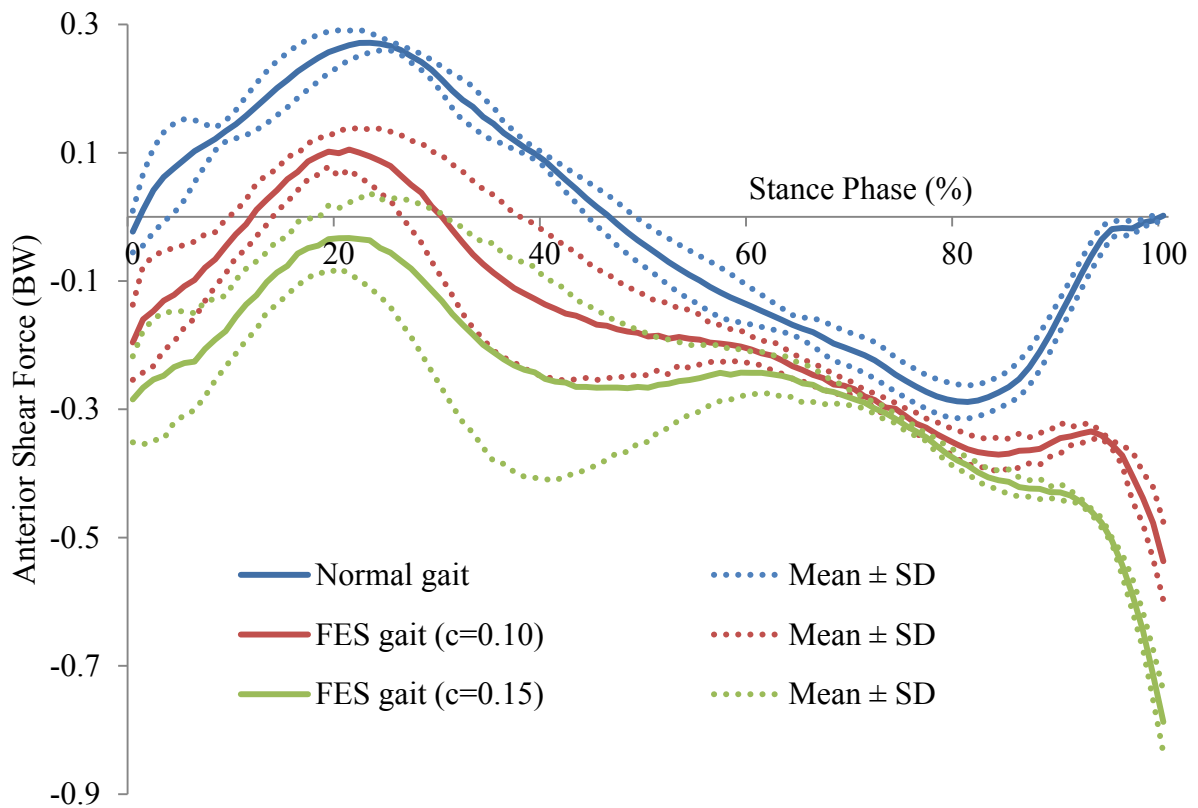


Figure 3.31 Anterior shear force (BW) (mean \pm SD) of subject 11 during normal and FES gait

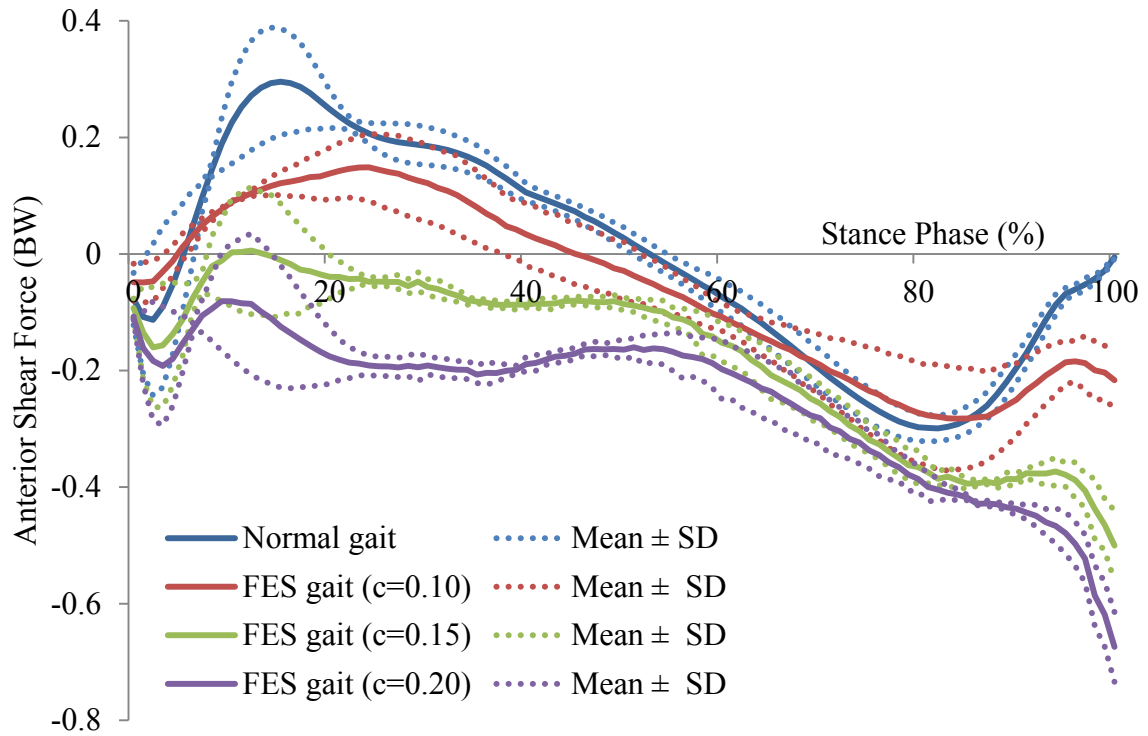


Figure 3.32 Anterior shear force (BW) (mean \pm SD) of subject 12 during normal and FES gait

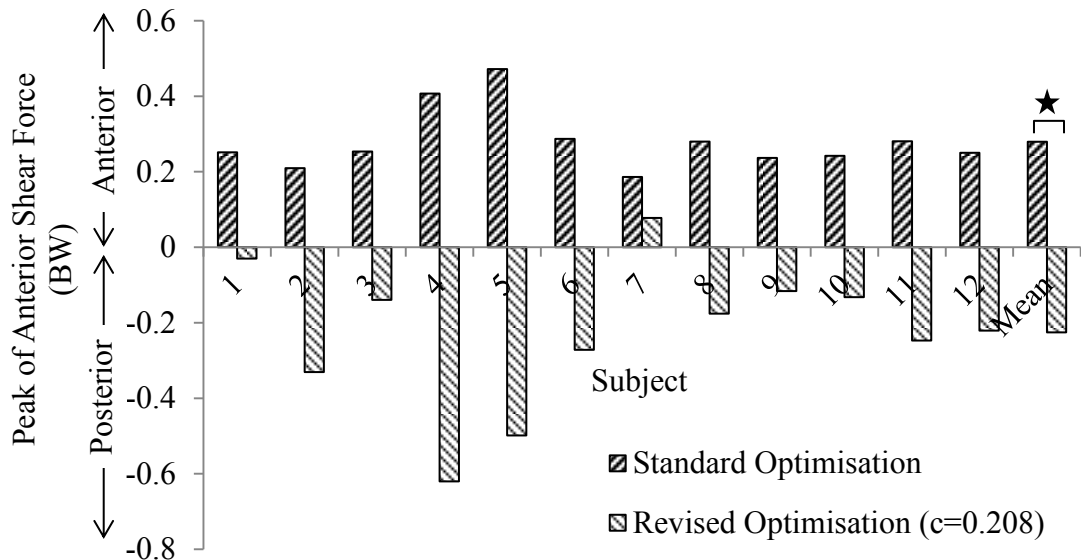


Figure 3.33 Predicted peak anterior shear force across twelve subjects using standard and revised optimisation methods

There was no significant difference for the first peak of medial knee compressive force ($p=0.2373$, Figure 3.34a). The first peak of lateral knee compressive force was increased by 276% ($p<0.0001$, Figure 3.34b) during FES gait compared to normal gait, resulting in an increase in overall knee compressive force of 144% ($p=0.0003$, Figure 3.34c).

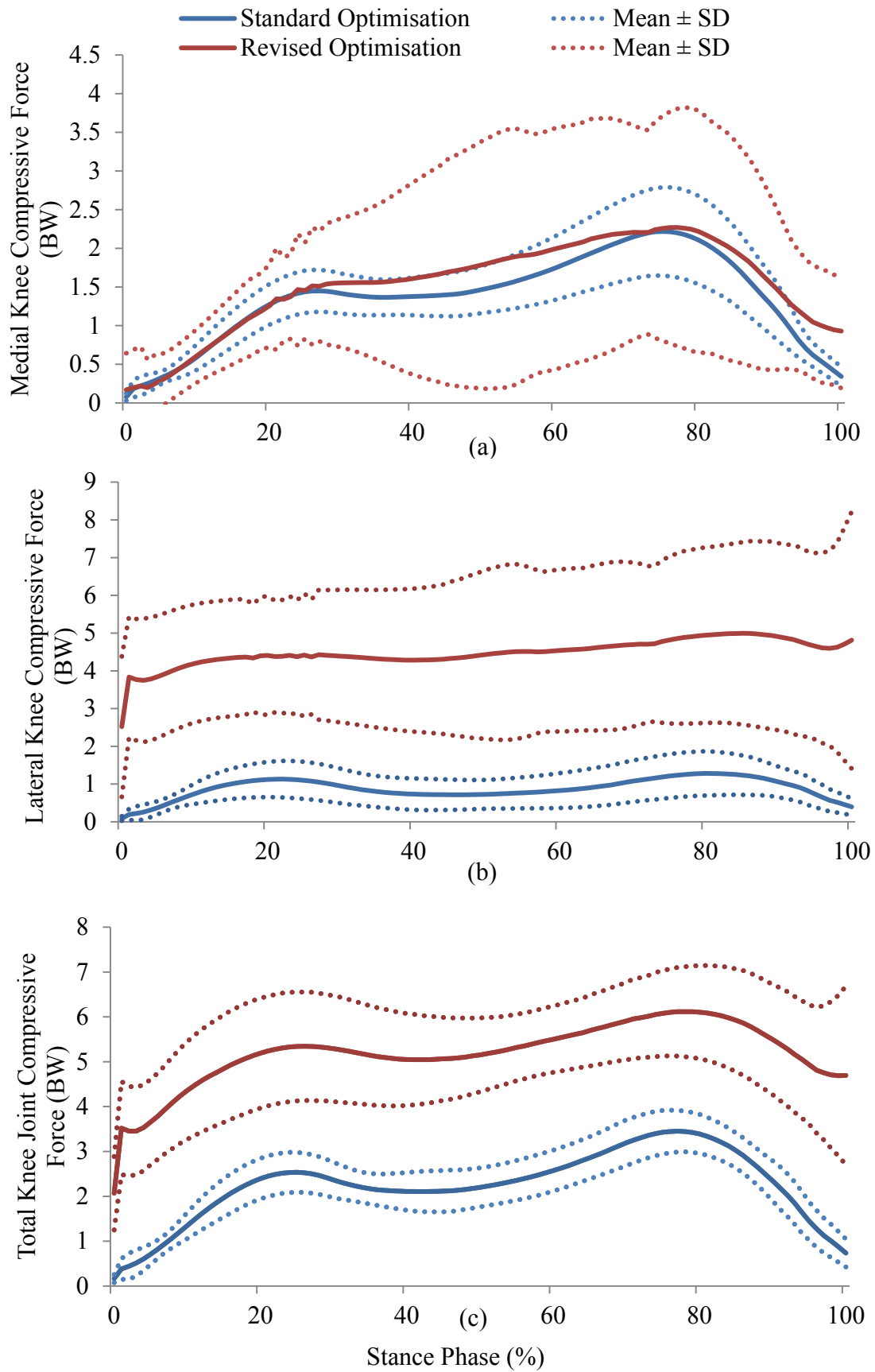


Figure 3.34 Knee joint compressive forces (mean \pm SD, n=12) using standard and revised optimisation: (a) medial, (b) lateral, (c) total force.

Table 3.7 Knee joint compressive forces (BW) during normal and FES gait

Subjects	Medial compressive force (BW)		Lateral compressive force (BW)		Total compressive force (BW)	
	Normal gait	FES gait	Normal gait	FES gait	Normal gait	FES gait
1	1.44	1.18	0.75	3.90	2.16	5.02
2	1.61	1.54	0.93	4.43	2.46	5.94
3	1.49	1.47	1.12	5.11	2.52	6.57
4	1.57	1.47	2.29	5.30	3.63	6.71
5	1.80	2.04	1.09	5.17	2.81	7.17
6	1.80	6.10	0.74	7.15	2.17	13.25
7	1.54	1.33	0.65	2.31	2.12	3.61
8	0.93	0.79	1.48	3.68	2.27	4.39
9	1.13	0.98	1.60	3.09	2.64	4.07
10	1.70	1.55	0.95	3.26	2.53	4.58
11	1.59	1.58	0.93	4.79	2.40	6.08
12	1.65	1.50	1.44	4.40	3.07	5.83
Mean	1.52	1.79	1.16	4.38	2.56	6.10
SD	0.26	1.39	0.47	1.27	0.44	2.52

3.4 Discussion

In healthy gait, the hamstrings, including BFLH, have their maximum activation during the swing phase. In late and terminal swing the hamstrings reduce the intensity of their activity so that excessive knee flexion is avoided at the end of the phase. Immediately after heel strike the ACL becomes loaded when the joint is close to maximum extension. Non-coping ACL deficient subjects maintain, or increase, hamstrings activity at this point through co-contraction, in order to achieve normal gait (Rudolph et al., 2001; Shelburne et al., 2005). This theory of hamstrings co-contraction has been used in the development of technology to combine an ACL knee brace with hamstrings stimulation using FES to assist those with knee instability (Solomonow, 2006). It is likely that the selective activation of BFLH will be achievable through the use of such technology. Other work has shown that selective activation of muscles on the lateral aspect of the knee such as biceps femoris can also be used to delay medial knee osteoarthritis (Hodges et al., 2016). In this chapter, co-contraction was created through the stimulation of BFLH throughout the stance phase.

This chapter tested, using a combined modelling and experimental approach, the hypothesis that selective activation of the BFLH, one of the hamstrings, can theoretically and practically reduce the anterior tibial shear and tibial internal rotation torque at the knee. The hypothesis was derived due to the anatomy of the muscle, which attaches on the

fibular head that articulates with the lateral tibia and so has the potential to resist a large internal rotation moment and hence the pathological motion of the lateral compartment that occurs in ACL deficiency (Amis et al., 2005; Gao et al., 2010). We found that the anterior shear force and the tibial internal rotation torque were reduced when BFLH was stimulated with FES. However, BFLH stimulation does not affect the knee adduction torque and flexion torque (Fig 3.20 (a) and (b), $p > 0.01$). The pulsewidth of the FES stimulation across subjects ranged from 4 to 8 and there is no correlation between the levels of pulsewidth with their body mass.

The modelling approach developed here used two optimisation methods to solve the muscle indeterminacy problem; both of these show that the peaks of reduction of tibial internal rotation torque occurred during weight acceptance, near full knee extension, which this is the time when the ACL is loaded.

The reduction of the tibial internal rotation torque also indirectly affects the value of the anterior shear force (More et al., 1993). Theoretically, as BF inserts on the fibula, its activation in a flexed knee is able to pull the tibia posteriorly. In this study, the peak anterior shear force was significantly reduced when FES was applied during weight acceptance, before full knee extension. This work is consistent with the model simulation by Shelburne et al (2005) and the experimental study by Chen et al (2013) showing that by increasing the muscle activation of the hamstrings, ATT was reduced by 0.2cm with the knee in 20° to 50° of flexion. Also, in healthy gait body weight is transferred onto the forward limb in the weight acceptance phase. In contrast, for FES gait, the posterior pull of the extra activation of the BFLH by the FES resulting in slower than normal gait, as found in our study. After 80% of stance phase the posterior shear forces became elevated and, therefore to mitigate any detrimental posterior forces, the recommendation from this work would be that stimulation should stop after 80% of stance phase. This has been shown clearly in the results for all subjects (Figure 3.21-3.32) especially subject 7 (Figure 3.27).

Here, the modelling cost function was modified from its standard form by assigning a weighting, c , to simulate BFLH stimulation. The value of c for each subject that reduced anterior shear force to zero was found and the mean value of c across all was 0.208. This mean value was then used, resulting in only one subject having a very small positive anterior shear force, demonstrating that the use of a mean value to simulate external

activation using FES is appropriate. This opens the way to clinical application without required significant personalisation of FES stimulation. The one subject with a higher c to decrease anterior shear force was the tallest and heaviest subject. This work also follows the literature in which a similar c value of 0.25 was used to simulate the electrically stimulated muscle activation of gluteus medius to reduce the medial knee joint reaction force (Rane et al., 2016). In the literature hamstrings activation without FES has shown that 56% of the maximal hamstring muscle force could reduce the ATT to a normal level during the stance phase of gait (Liu et al., 2000). That study modelled motions in the sagittal plane only and so cannot be compared for tibial internal rotation. Focusing on ATT only would suggest that the hamstrings on the medial side could also reduce anterior shear force and this has been shown in other modelling studies (Shelburne et al., 2005). However, as these do not assess tibial internal rotation torque, their results cannot be compared here.

It should be noted that over activation of the hamstrings resulted in a higher knee contact force due to the co-contraction of the quadriceps muscles to overcome the flexion torque due to the hamstrings activation. This has been addressed by Catalfamo et al. (2010) who found that a 50% of stimulation of biceps femoris is more appropriate for reducing ATT compared to 100% stimulation due to the pathological increase in knee joint forces and this chapter has provided further evidence for this.

This study has some limitations. Firstly, the experimental order was not randomised which may cause bias in the results. Secondly, the test cohort comprised only healthy control subjects; future work should focus on conducting experiments in ACL deficient subjects to test the applicability of this method in a clinical cohort. This is addressed in Chapter 5. It is expected that the results in such a cohort to be amplified as an ACL deficient subject would have reduced ability of the passive stabilisers to resist the ATT and internal rotation torque, thus emphasising the effect of the musculature. However, a confounding factor in ACL deficient subjects is that they already demonstrate altered muscle activation patterns that might result in a different pattern of internal rotation torque and anterior shear force (Berchuck et al., 1990; Gao et al., 2010; Rudolph et al., 1998). Thus, the following chapters will address these further discussed to cover these issues. The effect of activation of BFLH in ACL deficient subjects and also the timing of activation and the effect of stimulation of other muscles will be presented in Chapter 4 and 5. An investigation of compensatory muscle activations due to selective activation of BFLH, perhaps through the

use of electromyography is presented in Chapter 4. Secondly, the model used in this study is a non-subject specific model. The use of subject specific models would enable parameters such as muscle volume, maximum muscle stress and lines of action to be customised. This would enable, potentially, a greater fidelity of output to be achieved from the modelling. Thirdly, the use of static optimisation to determine the muscle forces needs to be further validated, as it may not reflect in vivo muscle force generation (Anderson et al., 2001), particularly in the FES condition. Finally, the application of a constant muscle activation for the whole of stance phase as achieved here is neither desirable, nor practical because muscle activation is changing accordingly during stance phase. Technology to allow selective activation at the peak of anterior tibial shear should be developed for appropriate clinical use.

3.5 Conclusion

This chapter presented a study which is the first to have shown that selective activation of the long head of biceps femoris can reduce the anterior tibial shear and tibial internal rotation torque at the knee in healthy subjects. A musculoskeletal model was modified to allow this analysis to take place. This approach opens the way for new rehabilitation therapies for ACL deficient subjects using functional electrical stimulation. The level of muscle activation predicted from the model to reduce the anterior tibial shear and tibial internal rotation torque in this chapter will be used for a study with ACL deficient and ACL reconstruction patients which will be presented in Chapter 5.

CHAPTER 4²

Validation of the FES Model during Gait

This chapter explains the validation of the novel cost function to simulate functional electrical stimulation (FES) during gait. This chapter introduces a new method of validation that avoids functional electrical stimulation (FES) artefacts to allow the simultaneous measurement of EMG signals by identifying a pair of muscles where the stimulation of one is likely to have an effect on the activity of the second muscle.

²Part of this chapter has been submitted for peer review publication, entitled “Validation of a musculoskeletal gait model to study the role of functional electrical stimulation”, with authors: Nur Liyana Azmi, Ziyun Ding and Anthony M J Bull

4.1 Introduction

Functional electrical stimulation (FES) has been used clinically to strengthen weak muscles by applying low level electrical currents (Peckham, 1987). FES can be used to treat patients with spinal cord injuries (SCI), anterior cruciate ligament (ACL) injuries and cerebral palsy (CP). For patients with SCI, short electrical pulses of FES stimulating paralyzed muscles are able to improve motor function (Lynch et al., 2008); for ACL injuries, FES on selected lateral hamstring muscles can improve knee stability (Chen et al., 2013); and for CP, FES assists in reducing spasticity or contracting the involuntary muscle (Kerr et al., 2004). Inverse dynamics-based musculoskeletal modelling enables the quantification of muscle and joint forces based on measured inputs such as kinematics and external forces. Such models have been used preclinically to test FES's ability in altering joint loading at the knee (Chapter 3) (Rane et al., 2016; Xu et al.). As these models require the use of an objective function to solve the indeterminacy of the musculoskeletal system that has more muscles available than necessary to drive the motion, the objective function should represent an appropriate physiological constraint. In the case of FES, alternative objective functions have been proposed (Rane et al., 2016; Xu et al.), yet these have not been validated to date. In Chapter 3, an alternative objective function was introduced to investigate the activation level of the biceps femoris long head (BFLH) in reducing the internal rotational torque and anterior shear at the knee in healthy subjects.

Validation of musculoskeletal models is challenging (Erdemir et al., 2007). Validation can be achieved at the level of tendon forces, bone forces or joint contact forces using invasive devices, for example instrumented prostheses (Fregly et al., 2012) or tendon transducers (Bull et al., 2005). Non-invasive approaches are achievable by using surface electromyography (EMG) to validate the muscle activations calculated from the musculoskeletal model (Crowninshield et al., 1981; Erdemir et al., 2007). However, when combined with FES currents, EMG signals are affected. This has been partially addressed by others, where, for example, a shut-down circuit and an adaptive filter were used to remove the stimulation artefacts in a study using FES for tetraplegic patients (Sennels et al., 1997). Others have extracted the volitional EMG from a partially paralyzed muscle and used this to control other muscle stimulation (Frigo et al., 2000; Thorsen et al., 1999). However, none of these have been able to totally eliminate FES artefacts from the EMG signals (Frigo et al., 2000; Sennels et al., 1997).

The ability to apply FES and measure EMG simultaneously would likely only be possible if the muscle receiving stimulation through FES is located at a distance from the muscle whose EMG is being measured. It is therefore necessary to identify such a pair of muscles, where the stimulation of one is likely to have an effect on the activity of the second muscle.

As shown in Chapter 3 stimulation of the BFLH thigh muscle using FES has been used clinically to treat ACL deficient and ACL reconstructed patients (Snyder-Mackler et al., 1991), to improve spinal cord injury patients in walking (Mohr et al., 1997), and in cerebral palsy to assist in standing (Carmick, 1997). BFLH acts as a knee flexor, but can also compensate for weak hip extensors such as gluteus maximus (Jonkers et al., 2003). In addition, the primary compensatory muscles for hamstrings weakness are gluteus maximus, the vasti (Komura et al., 2004) and iliacus psoas (Ardestani et al., 2016). The vasti are located near to BFLH and the measured signal with EMG could easily be affected by FES current. The iliacus psoas is not superficial and so cannot be measured by surface EMG. Therefore, a likely clinically-relevant candidate for muscle stimulation is BFLH and it is hypothesised that gluteus maximus will then increase its activity, and is sufficiently far removed from BFLH to allow its activity to be measured with EMG. The hypothesis of this chapter is that FES-assisted activation of BFLH during gait increases the activation of gluteus maximus, and that the EMG signals of gluteus maximus are clean from FES artefacts, because of its distance from the FES electrodes.

The aim of this chapter is to

1. understand the compensatory gluteus maximus muscle activations due to activation of BFLH with FES; and
2. validate a musculoskeletal model that quantifies and evaluates the effect of FES on BFLH through measuring EMG of gluteus maximus muscles.

4.2 Methods and Materials

The hypotheses were tested through the application of three different FES current stimulation levels (40 mA, 60 mA and 80 mA) to the BFLH of healthy subjects and through the simultaneous measurement of the EMG of gluteus maximus. In this pilot study, fifteen healthy subjects (6 males and 9 females; mean height 1.64 ± 0.12 m; mass 64.0 ± 12.46 kg; age 26.9 ± 3.39 years) participated in the study (Table 4.1). This study was

approved by the institutional research ethics committee of Imperial College London (Date: 4 August 2014) and written informed consent was obtained from all participants.

Table 4.1 Anthropometric data of the subjects

Subject	Height (m)	Mass (kg)	Age (year)
1	1.59	69.00	22
2	1.82	71.20	26
3	1.59	51.50	33
4	1.71	63.50	27
5	1.53	70.80	30
6	1.54	58.10	28
7	1.73	68.40	25
8	1.67	62.80	24
9	1.53	50.20	20
10	1.65	52.70	27
11	1.77	68.20	28
12	1.89	100.90	26
13	1.62	60.80	31
14	1.51	55.50	30
15	1.54	56.30	27
Mean	1.64	63.99	26.93
SD	0.12	12.46	3.39

Data Collection

Kinematic and kinetic data were captured in a motion analysis laboratory. Eighteen retro-reflective markers were placed on the pelvis and the right lower limb (Duffell et al., 2014) (Figure 3.6 and Table 3.2 in Section 3.2). Their trajectories were captured at 200 Hz using a ten-camera motion capture system (Vicon Motion Systems Ltd, Oxford, UK). Ground reaction forces of the right lower limb were measured at 1000 Hz from a force plate (Kistler Type 9286BA, Kistler Instrument AG, Winterthur, Switzerland). After six over ground walking trials, FES electrodes (Odstock 2 Channel Stimulator, Odstock Medical Ltd., UK) were placed on the subject's BFLH: one at the bottom and the other at the centre of the BFLH, with a distance of two hand widths between them. The FES pulse widths could be set at a level of between 0 to 350 μ s, corresponding to a manufacturer-defined range of 0-9. This was set with an average level of three according to subjects' tolerance towards the current stimulations. The frequency of the stimulator was 40 Hz as recommended by the FES manufacturer, and the intensity was adjusted to the maximum

level that each subject was able to comfortably withstand (Lynch et al., 2008). Similar to the initial over ground walking trial, subjects walked in a self-selected comfortable speed with three FES stimulation currents, which were initialised at 40 mA and increased to 60 mA and finally to 80 mA. The subjects were allowed to rest between trials. Walking trials were repeated six times at each current level. The stimulation current was set to start with one second of ramp up, followed by four seconds of maximum current level and then ending with one second of ramp down. The stimulator was manually started by the subject and timed so that the stimulation current was at its maximum value when the right foot stepped on the force plate, through heel strike and toe off.

Surface EMG sensors (Delsys, Trigno Wireless EMG System, USA) were placed according to SENIAM recommendations (Hermens et al., 2000) on the BFLH (the electrodes were placed halfway along the line between the ischial tuberosity and the lateral epicondyle of the tibia) and gluteus maximus (the electrodes were placed halfway along the line between the sacral vertebrae and the greater trochanter) of the right leg (Figure 4.1). The skin was treated with isopropyl alcohol prior to sensor application to ensure low impedance. For the first trial, an EMG sensor was attached over the BFLH. This was then replaced with the FES electrodes for the second and subsequent walking trials. Raw EMG data was band-pass filtered (30-300Hz), whole wave rectified, and normalized to the maximum EMG signal of each particular subject (Buchanan et al., 2004).

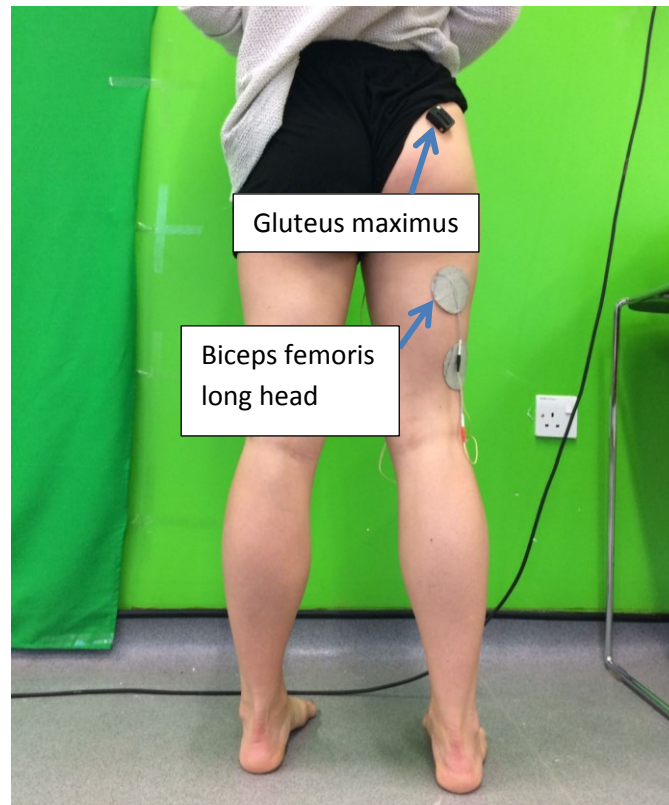


Figure 4.1 EMG and FES electrode positions

Lower Limb Musculoskeletal Model

Similar to Chapter 3, the open source musculoskeletal modelling software Freebody V2.1 was used in this chapter (Cleather et al., 2015; Ding et al., 2016). The same standard optimisation (Equation 3.1 & Equation 3.2) was performed using the standard cost function in order to minimize the sum of the cubed muscle activations (Crowninshield et al., 1981):

Optimisation Method

In order to simulate the effect of three FES current levels applied to BFLH, the same revised optimisation method (Equation 3.3 & Equation 3.4) in Chapter 3 was used. In this chapter, the c value to present 40mA, 60mA and 80mA current stimulations was set as 0.10, 0.15 and 0.20, respectively; these were all higher than the muscle activation of BFLH predicted from standard optimisation.

Data Analysis

Stance phase was expressed over a 0-100% duration with a step interval of 1%. This was then further divided into four sub-phases (Perry et al., 2010): initial contact (0-3%), loading response (4-19%), mid stance (20-50%) and terminal stance (51-100%).

The gluteus maximus activations predicted from the model and its EMG signals were averaged over three trials and presented as a mean value. Correlations of determination (R^2) were calculated between the predicted gluteus maximus muscle activations and its EMG data in terms of their peak values and the areas under the curve in each sub-phase of the stance. All data were analysed using MATLAB (R2015b, The MathWorks Inc., USA).

4.3 Results

All subjects tolerated all tests at 40mA and 60mA stimulation. One subject did not tolerate 80mA stimulation, therefore, data at 80mA are presented from 14/15 subjects. In normal walking and in FES applied walking, the gluteus maximus muscle activation predicted from models across all subjects is shown in Figure 4.2 and its EMG measurement is shown in Figure 4.3. Higher c values in the optimisation function contribute to greater gluteus maximus activation. A similar trend of its activity was found from the measured EMG. The gluteus maximus muscle activations predicted from modelling and the measured EMG of all subjects are shown in Appendix B.

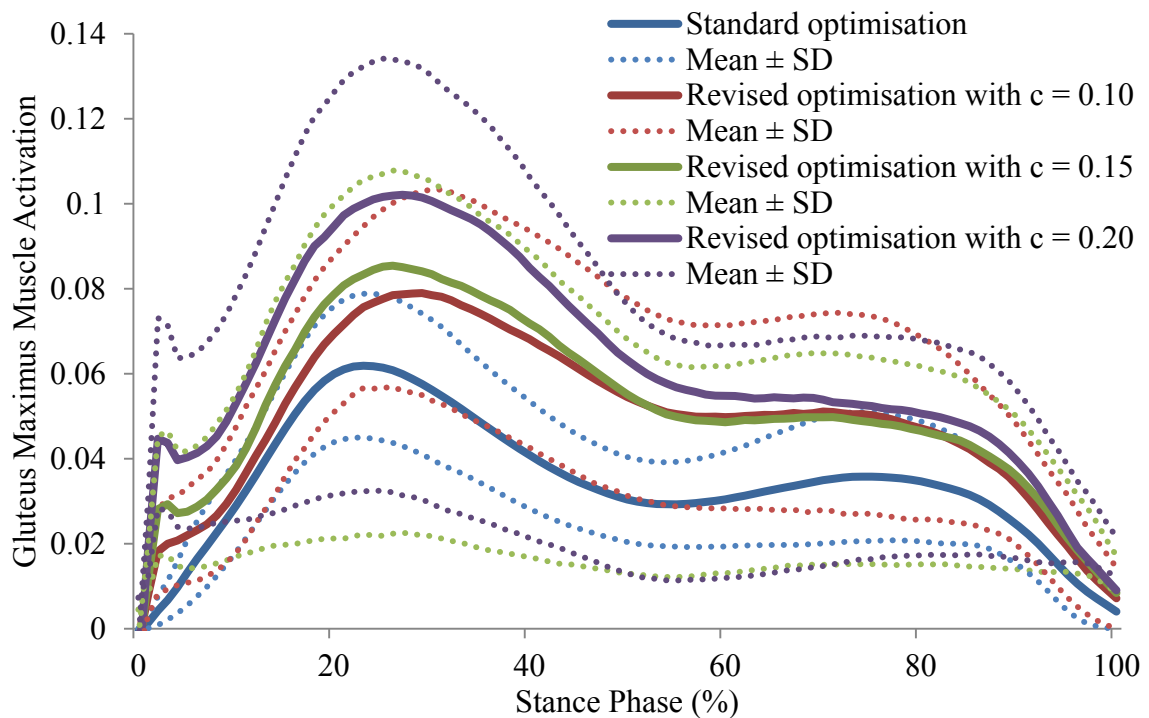


Figure 4.2 Model predictions of gluteus maximus muscle activations (mean \pm SD, n=15). Standard optimisation refers to muscle activations during normal walking, and revised optimisation presents the muscle activations during FES applied walking

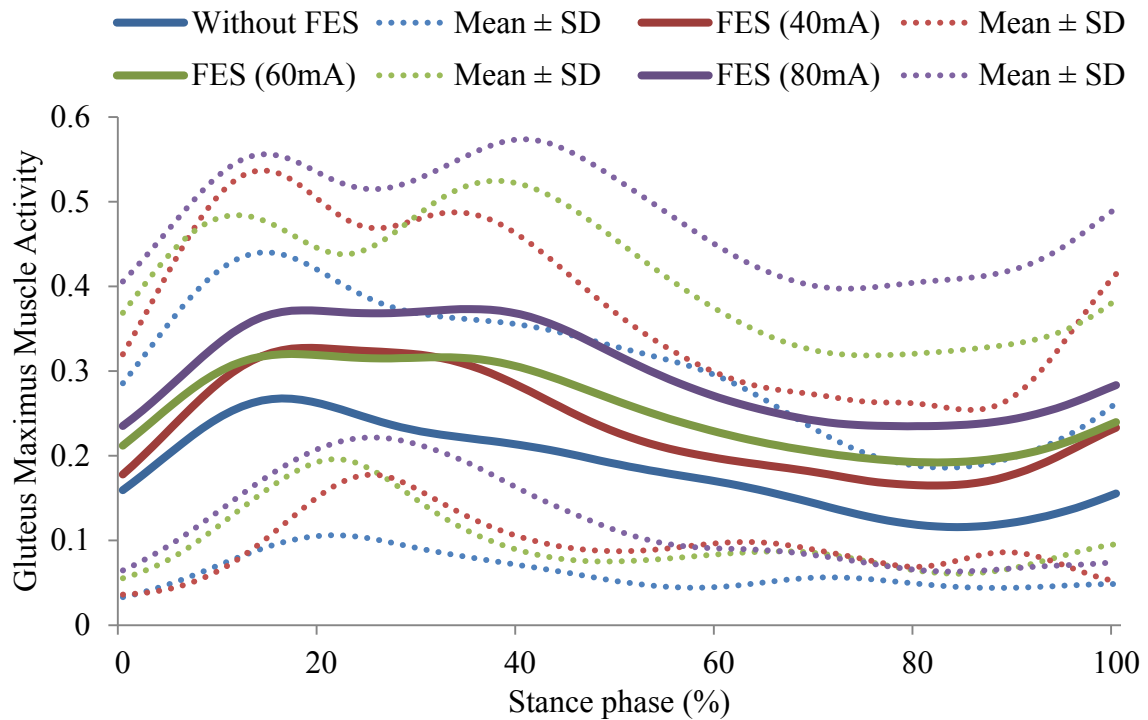
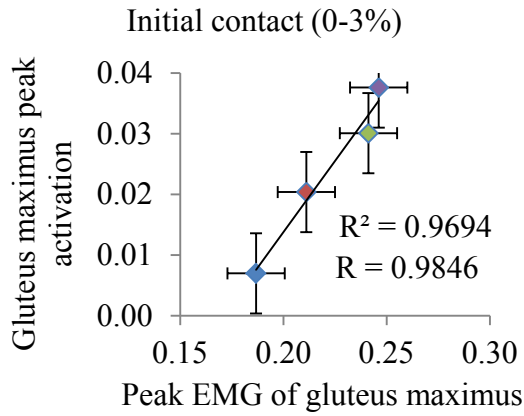
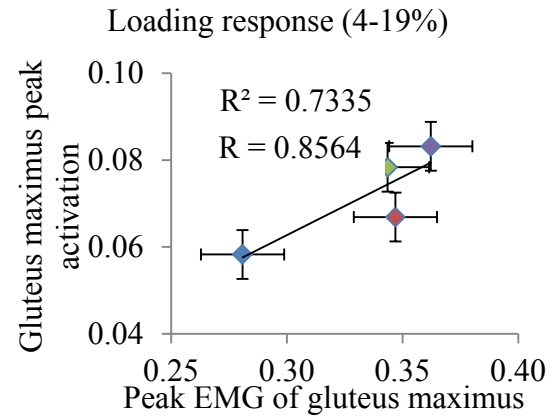


Figure 4.3 Gluteus maximus EMG measurements (mean±SD, n=15) in normal walking and FES applied walking

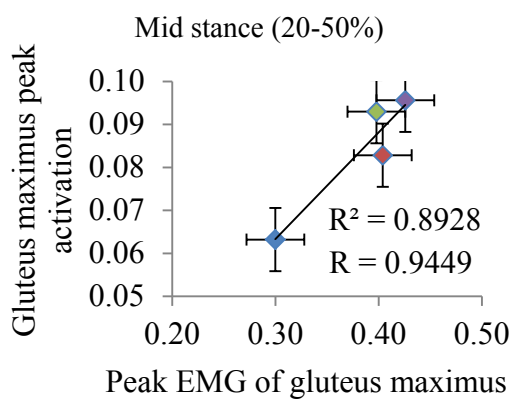
Predicted peak activation and maximum EMG measurement of the gluteus maximus are highly correlated, with the R^2 values ranging from 0.73 to 0.99 and R values ranging from 0.86 to 0.995 (Figure 4.4, Table 4.2). The peak gluteus maximus activations for all subjects calculated by musculoskeletal modelling and as measured by EMG are shown below during the four sub-phases: initial contact (Table 4.3), loading response (Table 4.4), mid stance (Table 4.5) and terminal stance (Table 4.6).



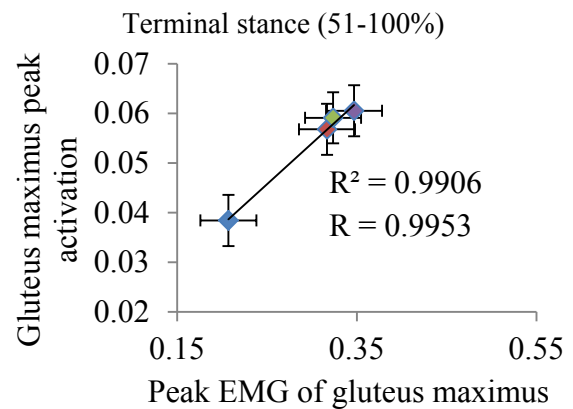
(a) Initial contact (0-3%)



(b) Loading response (4-19%)



(c) Mid stance (20-50%)



(d) Terminal stance (51-100%)

● Standard Optimisation, Without FES ● $c=0.10$, 40 mA ● $c=0.15$, 60 mA ● $c=0.20$, 80 mA

Figure 4.4 Correlations between predicted peak gluteus maximus activation and its measured peak EMG signals in each sub-phase of the stance phase: (a)-(d). The four datapoints in each graph represent normal walking, and FES applied walking with FES currents of 40 mA, 60 mA and 80 mA

Table 4.2 Peak gluteus maximus activations calculated by musculoskeletal modelling and as measured by EMG during the stance phase of normal walking and FES applied walking. c values of 0.10, 0.15 and 0.20 in models represent FES currents of 40 mA, 60 mA and 80 mA, respectively (mean \pm SD), N=15)

Stance phase (%)	Model predictions				EMG			
	No FES	$c=0.10$	$c=0.15$	$c=0.20$	No FES	40mA	60 mA	80mA
0-3%	0.01 ± 0.01	0.02 ± 0.01	0.03 ± 0.02	0.04 ± 0.03	0.19 ± 0.15	0.21 ± 0.17	0.24 ± 0.17	0.25 ± 0.19
4-19%	0.06 ± 0.02	0.07 ± 0.02	0.08 ± 0.02	0.08 ± 0.04	0.28 ± 0.17	0.35 ± 0.21	0.34 ± 0.17	0.36 ± 0.20
20-50%	0.06 ± 0.02	0.08 ± 0.26	0.09 ± 0.02	0.10 ± 0.04	0.30 ± 0.17	0.40 ± 0.19	0.40 ± 0.20	0.43 ± 0.23
51-100%	0.04 ± 0.14	0.06 ± 0.02	0.06 ± 0.01	0.06 ± 0.02	0.21 ± 0.14	0.32 ± 0.18	0.32 ± 0.15	0.35 ± 0.23

Table 4.3 Peak gluteus maximus activations calculated by musculoskeletal modelling and as measured by EMG during initial contact (0-3% of stance phase) of normal walking and FES applied walking.

Subject	Model predictions				EMG			
	No FES	c = 0.1	c = 0.15	c = 0.20	No FES	40 mA	60 mA	80 mA
1	0.0067	0.0132	0.0105	0.0219	0.2064	0.1674	0.2205	0.1980
2	0.0033	0.0169	0.0470	0.0484	0.4374	0.3727	0.4399	0.5887
3	0.0094	0.0387	0.0562	0.0892	0.0607	0.1189	0.1541	0.1747
4	0.0186	0.0276	0.0427	0.0604	0.0615	0.0395	0.0523	0.0502
5	0.0087	0.0205	0.0377	0.0713	0.2016	0.1490	0.3373	0.3693
6	0.0065	0.0210	0.0239	0.0649	0.3151	0.1929	0.3528	0.3951
7	0.0152	0.0386	0.0551	0.0716	0.1257	0.1506	0.1536	0.1492
8	0.0039	0.0220	0.0404	0.0000	0.0851	0.0695	0.1215	0.0000
9	0.0007	0.0081	0.0130	0.0183	0.5052	0.3752	0.3688	0.4386
10	0.0031	0.0055	0.0027	0.0008	0.2422	0.2976	0.2287	0.2357
11	0.0022	0.0079	0.0135	0.0174	0.0887	0.0917	0.0825	0.0825
12	0.0041	0.0109	0.0053	0.0030	0.0048	0.1166	0.1270	0.0694
13	0.0128	0.0322	0.0412	0.0056	0.2341	0.7000	0.7020	0.5776
14	0.0057	0.0179	0.0314	0.0452	0.1800	0.2570	0.1846	0.2450
15	0.0039	0.0246	0.0308	0.0462	0.0531	0.0678	0.0916	0.1184
Mean	0.0070	0.0204	0.0301	0.0376	0.1868	0.2111	0.2411	0.2462
SD	0.0051	0.0106	0.0177	0.0299	0.1446	0.1718	0.1731	0.1874

Table 4.4 Peak gluteus maximus activations calculated by musculoskeletal modelling and as measured by EMG during loading response (4-19% stance phase) of normal walking and FES applied walking

Subject	Model predictions				EMG			
	No FES	c = 0.1	c = 0.15	c = 0.20	No FES	40 mA	60 mA	80 mA
1	0.0374	0.0481	0.0584	0.0610	0.2416	0.2398	0.3335	0.2980
2	0.0591	0.0539	0.0759	0.0914	0.6203	0.6306	0.6015	0.8103
3	0.0700	0.0933	0.1006	0.1370	0.2583	0.3507	0.2667	0.3599
4	0.0716	0.0717	0.0823	0.0973	0.3089	0.2770	0.3346	0.3029
5	0.0528	0.0656	0.0835	0.0951	0.3281	0.3571	0.3727	0.4143
6	0.0392	0.0508	0.0678	0.0846	0.3594	0.2978	0.3796	0.4967
7	0.0795	0.1033	0.1298	0.1513	0.1886	0.2190	0.1803	0.2309
8	0.0534	0.0676	0.0838	-	0.1297	0.0963	0.1887	-
9	0.0317	0.0417	0.0532	0.0644	0.5969	0.5010	0.4866	0.5761
10	0.0522	0.0499	0.0555	0.0665	0.4164	0.4119	0.3199	0.3706
11	0.0792	0.0608	0.0558	0.0733	0.1306	0.1979	0.2157	0.1997
12	0.0712	0.0568	0.0622	0.0538	0.0069	0.1822	0.2531	0.1461
13	0.0433	0.0709	0.0770	0.0502	0.2474	0.9044	0.7592	0.5781
14	0.0637	0.0775	0.0878	0.0966	0.3147	0.4336	0.3181	0.4327
15	0.0697	0.0913	0.1015	0.1249	0.0648	0.1042	0.1431	0.2169
Mean	0.0583	0.0669	0.0783	0.0832	0.2808	0.3469	0.3435	0.3622
SD	0.0155	0.0182	0.0212	0.0378	0.1738	0.2127	0.1657	0.2017

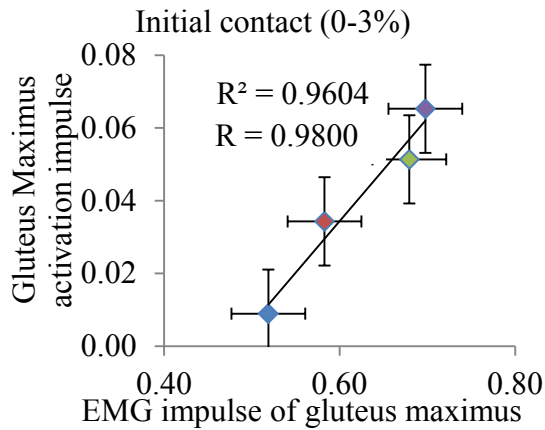
Table 4.5 Peak gluteus maximus activations calculated by musculoskeletal modelling and as measured by EMG during mid stance (20-50% stance phase) of normal walking and FES applied walking

Subject	Model predictions				EMG			
	No FES	c = 0.1	c = 0.15	c = 0.20	No FES	40 mA	60 mA	80 mA
1	0.0406	0.0655	0.0680	0.0751	0.2172	0.2448	0.3192	0.2989
2	0.0599	0.0649	0.0833	0.1005	0.5295	0.6142	0.5583	0.7291
3	0.0751	0.0977	0.1191	0.1496	0.2471	0.3387	0.2614	0.3137
4	0.0733	0.0757	0.0896	0.1129	0.4989	0.5782	0.6926	0.5679
5	0.0611	0.0837	0.0920	0.1023	0.3789	0.5510	0.4303	0.4486
6	0.0422	0.0549	0.0728	0.0884	0.2981	0.4358	0.5146	0.6428
7	0.0809	0.1098	0.1382	0.1645	0.1569	0.1728	0.1296	0.1892
8	0.0642	0.1493	0.1182	-	0.1260	0.0956	0.1738	-
9	0.0372	0.0543	0.0678	0.0788	0.5427	0.4904	0.4662	0.5483
10	0.0594	0.0522	0.0608	0.0723	0.4063	0.3603	0.3082	0.3554
11	0.0949	0.0811	0.0860	0.1025	0.4905	0.6739	0.8420	0.7558
12	0.0738	0.0857	0.1027	0.0856	0.0066	0.1938	0.2577	0.1696
13	0.0423	0.0759	0.0828	0.0546	0.2145	0.6904	0.4827	0.4999
14	0.0654	0.0861	0.0992	0.1085	0.3242	0.4005	0.3767	0.6350
15	0.0776	0.1057	0.1141	0.1386	0.0617	0.2183	0.1539	0.2322
Mean	0.0632	0.0828	0.0930	0.0956	0.2999	0.4039	0.3978	0.4258
SD	0.0169	0.0256	0.0222	0.0399	0.1724	0.1924	0.2020	0.2247

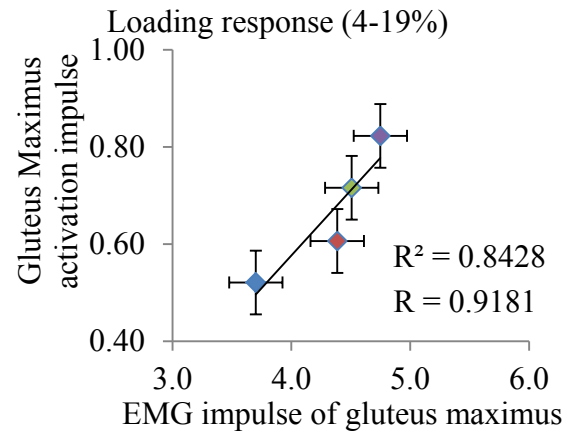
Table 4.6 Peak gluteus maximus activations calculated by musculoskeletal modelling and as measured by EMG during terminal stance (51-100% stance phase) of normal walking and FES applied walking

Subject	Model predictions				EMG			
	No FES	c = 0.1	c = 0.15	c = 0.20	No FES	40 mA	60 mA	80 mA
1	0.0433	0.0541	0.0609	0.0694	0.1402	0.1609	0.1537	0.1758
2	0.0386	0.0470	0.0563	0.0582	0.2142	0.2834	0.3043	0.4208
3	0.0195	0.0446	0.0544	0.0619	0.1693	0.4209	0.3428	0.3577
4	0.0328	0.0421	0.0490	0.0553	0.2350	0.2854	0.2765	0.2039
5	0.0626	0.0824	0.0832	0.0873	0.3285	0.3932	0.4493	0.5004
6	0.0298	0.0396	0.0456	0.0490	0.2985	0.3345	0.4934	0.6462
7	0.0427	0.0584	0.0689	0.0822	0.0595	0.1398	0.0812	0.0938
8	0.0620	0.1241	0.0647	-	0.0667	0.0470	0.1571	-
9	0.0232	0.0370	0.0418	0.0528	0.3612	0.3177	0.3574	0.3533
10	0.0210	0.0376	0.0456	0.0557	0.1752	0.1641	0.2104	0.1816
11	0.0428	0.0694	0.0704	0.0745	0.4821	0.5291	0.6890	0.6782
12	0.0563	0.0660	0.0808	0.0746	0.0045	0.2315	0.2553	0.1211
13	0.0263	0.0366	0.0368	0.0442	0.1417	0.3257	0.3324	0.4466
14	0.0309	0.0505	0.0637	0.0645	0.3494	0.3195	0.4278	0.7476
15	0.0447	0.0625	0.0645	0.0785	0.0796	0.7991	0.3229	0.2767
Mean	0.0384	0.0568	0.0591	0.0605	0.2071	0.3168	0.3236	0.3469
SD	0.0140	0.0231	0.0138	0.0210	0.1346	0.1804	0.1526	0.2262

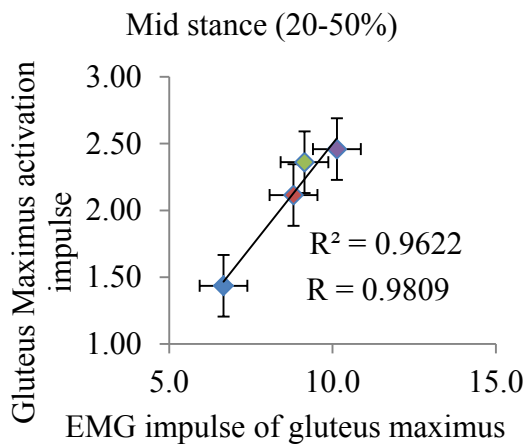
Predicted gluteus maximus activation impulse and measured EMG impulse were highly correlated, with the R² values ranging from 0.84 to 0.96 and R values ranging from 0.92 to 0.98 (Table 4.7, Figure 4.5). The predicted gluteus maximus activation impulses for all subjects calculated by musculoskeletal modelling and as measured by EMG are shown below during the four sub-phases: initial contact (Table 4.8), loading response (Table 4.9), mid stance (Table 4.10) and terminal stance (Table 4.11).



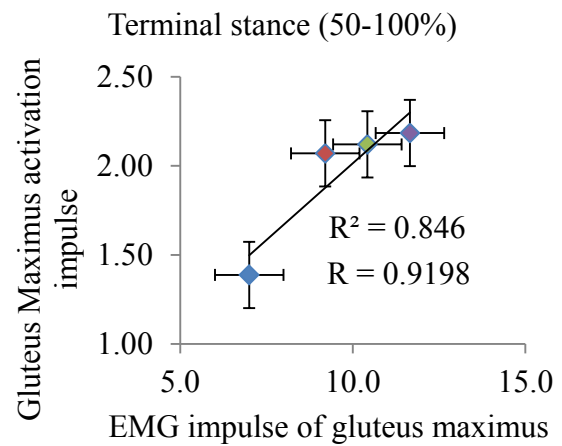
(a) Initial contact (0-3%)



(b) Loading response (4-19%)



(c) Mid stance (20-50%)



(d) Terminal stance (51-100%)

● Standard Optimisation, Without FES ● c=0.10, 40 mA ● c=0.15, 60 mA ● c=0.20, 80 mA

Figure 4.5 Correlations between predicted gluteus maximus activation impulse (area under the curve) and measured EMG impulse in each sub-phase of the stance phase : (a)-(d). The four datapoints in each graph represent normal walking, and FES applied walking with FES currents of 40 mA, 60 mA and 80 mA.

Table 4.7 Gluteus maximus activation impulse calculated by musculoskeletal modelling and as measured by EMG during the stance phase of normal walking and FES applied walking. c values of 0.10, 0.15 and 0.20 in models represent FES currents of 40 mA, 60 mA and 80 mA, respectively (mean \pm SD, $n=15$)

Impulse (area under the curve)								
Stance phase (%)	Model predictions				EMG			
	No FES	$c=0.10$	$c=0.15$	$c=0.20$	No FES	40mA	60 mA	80mA
0-3%	0.01 ± 0.01	0.03 ± 0.02	0.05 ± 0.03	0.07 ± 0.05	0.52 ± 0.41	0.58 ± 0.47	0.68 ± 0.50	0.70 ± 0.53
4-19%	0.52 ± 0.16	0.61 ± 0.22	0.72 ± 0.26	0.82 ± 0.39	3.70 ± 2.50	4.39 ± 3.11	4.51 ± 2.47	4.75 ± 2.82
20-50%	1.44 ± 0.40	2.11 ± 0.67	2.36 ± 0.52	2.46 ± 0.71	6.66 ± 3.92	8.81 ± 4.37	9.14 ± 5.06	10.13 ± 5.02
51-100%	1.39 ± 0.49	2.07 ± 0.87	2.12 ± 0.60	2.18 ± 0.66	7.00 ± 4.22	9.20 ± 3.78	10.42 ± 5.99	11.66 ± 8.01

Table 4.8 Gluteus maximus activation impulse calculated by musculoskeletal modelling and as measured by EMG during initial contact (0-3% stance phase)

Subject	Model predictions				EMG			
	No FES	$c = 0.1$	$c = 0.15$	$c = 0.20$	No FES	40 mA	60 mA	80 mA
1	0.0067	0.0252	0.0195	0.0408	0.5851	0.4686	0.6034	0.5416
2	0.0053	0.0305	0.0838	0.0869	1.1871	1.0062	1.2213	1.6309
3	0.0106	0.0502	0.0803	0.1357	0.1509	0.3283	0.4396	0.5008
4	0.0232	0.0446	0.0733	0.1052	0.1612	0.1078	0.1433	0.1361
5	0.0142	0.0398	0.0740	0.1308	0.5739	0.4296	0.9964	1.0902
6	0.0116	0.0395	0.0433	0.1160	0.8909	0.5577	1.0421	1.1590
7	0.0195	0.0676	0.0941	0.1293	0.3369	0.4040	0.4325	0.3965
8	0.0036	0.0286	0.0588	-	0.2330	0.1942	0.3279	-
9	0.0009	0.0137	0.0213	0.0283	1.4360	1.0606	1.0301	1.2293
10	0.0028	0.0060	0.0023	0.0008	0.6448	0.8059	0.6383	0.6455
11	0.0013	0.0104	0.0190	0.0250	0.2651	0.2660	0.2389	0.2359
12	0.0045	0.0166	0.0045	0.0059	0.0133	0.3213	0.3334	0.1986
13	0.0179	0.0607	0.0791	0.0088	0.6783	1.9226	1.9901	1.7222
14	0.0083	0.0326	0.0580	0.0838	0.4739	0.6790	0.5041	0.6571
15	0.0038	0.0485	0.0588	0.0819	0.1507	0.1891	0.2492	0.3208
Mean	0.0089	0.0343	0.0513	0.0653	0.5187	0.5827	0.6794	0.6976
SD	0.0070	0.0182	0.0308	0.0502	0.4062	0.4703	0.4952	0.5272

Table 4.9 Gluteus maximus activation impulse calculated by musculoskeletal modelling and as measured by EMG during loading response (4-19% stance phase)

Subject	Model predictions				EMG			
	No FES	$c = 0.1$	$c = 0.15$	$c = 0.20$	No FES	40 mA	60 mA	80 mA
1	0.3818	0.4089	0.4507	0.5215	3.4903	3.2564	4.5640	4.0907
2	0.4461	0.3716	0.6632	0.8107	8.6482	8.4022	8.4650	11.3717
3	0.6868	1.0475	1.0642	1.5948	2.7124	3.7753	3.3626	4.4312
4	0.7403	0.7186	0.8600	1.0561	2.5093	1.9397	2.3986	2.2264
5	0.4904	0.6222	0.8572	1.1659	4.1206	3.5202	5.4174	5.9583
6	0.3302	0.4985	0.5921	0.9417	5.1323	3.5865	5.5030	6.7490
7	0.7875	0.9779	1.2896	1.4553	2.5950	3.0250	2.5182	3.1617
8	0.4554	0.5093	0.6747	-	1.7673	1.3344	2.5753	-
9	0.2241	0.2869	0.4224	0.6036	8.6359	7.0236	6.9129	8.1673
10	0.3561	0.4432	0.4326	0.4918	5.5620	5.7966	4.4702	5.0174
11	0.6121	0.4832	0.5192	0.7037	1.5227	1.9084	1.9210	1.9098
12	0.7118	0.5134	0.4122	0.3321	0.0953	2.3686	3.1595	1.6087
13	0.4973	0.7403	0.7500	0.4473	3.5940	12.6670	10.2996	8.1813
14	0.5410	0.6390	0.7873	0.9714	4.2007	5.8683	4.1160	5.6586
15	0.5542	0.8358	0.9644	1.2467	0.9342	1.3243	1.9318	2.7013
Mean	0.5210	0.6064	0.7160	0.8229	3.7013	4.3864	4.5077	4.7489
SD	0.1637	0.2212	0.2600	0.3903	2.5012	3.1124	2.4722	2.8231

Table 4.10 Gluteus maximus activation impulse c calculated by musculoskeletal modelling and as measured by EMG during mid stance (20-50% stance phase)

Subject	Model predictions				EMG			
	No FES	$c = 0.1$	$c = 0.15$	$c = 0.20$	No FES	40 mA	60 mA	80 mA
1	1.1129	1.7377	1.9267	2.0478	5.7420	6.5876	6.8776	8.0239
2	1.1892	1.7144	2.1222	2.4872	7.9708	11.7158	11.9261	14.6580
3	1.4209	2.3039	2.8262	3.4820	5.5470	6.1278	6.1180	6.2914
4	1.4841	1.9267	2.3292	2.8964	12.2588	13.9100	16.1900	13.1195
5	1.5868	2.1972	2.5012	2.8109	10.5906	14.6508	12.1451	13.1308
6	1.0737	1.4469	1.8409	2.1838	7.2700	11.6775	14.0564	17.1528
7	1.8484	2.7216	3.3788	4.1312	2.1529	2.2632	2.2129	2.4549
8	1.5969	3.9877	2.9228	-	2.3289	2.1797	2.5492	-
9	0.8004	1.3501	1.6109	1.9947	12.2161	12.2459	12.0267	12.7004
10	1.2206	1.4365	1.6682	2.0316	8.1255	7.2035	5.6180	6.9437
11	2.2018	2.2533	2.3206	2.7793	10.5644	15.9879	19.3070	16.9269
12	1.8384	2.2469	2.7065	2.3191	0.1416	5.2896	5.7015	3.9898
13	0.8883	1.6425	1.8767	1.4404	4.6849	7.8228	7.7078	14.6079
14	1.4232	2.0965	2.5059	2.8516	8.7739	9.0316	10.3453	15.8534
15	1.8466	2.6582	2.8773	3.4227	1.5999	5.3900	4.3499	6.1497
Mean	1.4355	2.1147	2.3609	2.4586	6.6645	8.8056	9.1421	10.1335
SD	0.3951	0.6710	0.5203	0.7133	3.9167	4.3652	5.0619	5.0211

Table 4.11 Gluteus maximus activation impulse calculated by musculoskeletal modelling and as measured by EMG during loading response (51-100%)

Subject	Model predictions				EMG			
	No FES	$c=0.1$	$c=0.15$	$c=0.20$	No FES	40 mA	60 mA	80 mA
1	1.5848	2.2420	2.4382	2.8301	4.9354	5.2356	5.9163	5.4256
2	1.3551	1.7552	2.1042	2.2494	8.7736	11.6922	13.7329	19.2199
3	0.7089	1.2752	1.5405	1.8903	5.4198	14.6855	12.0843	13.2736
4	1.4286	1.7313	1.9114	2.2258	5.4779	5.4473	5.5621	4.8838
5	2.3375	3.1810	3.4315	3.6535	10.2224	14.2096	21.6455	22.9398
6	0.9445	1.3374	1.5961	1.7755	11.9562	12.0004	21.9256	27.5479
7	1.5624	2.0171	2.2333	2.4978	1.9945	5.3127	3.1256	3.0359
8	1.9017	4.4751	2.0074	-	2.7235	2.0077	5.0485	-
9	0.9539	1.4767	1.6521	1.8894	13.9756	12.1630	12.6562	13.3778
10	0.6536	0.9934	1.2514	1.2292	7.0164	7.0765	7.5348	7.6651
11	1.6688	2.4234	2.5521	2.5723	11.5626	9.8446	11.8356	12.1854
12	1.9420	2.4464	2.9493	2.8995	0.1771	6.4401	3.9369	2.1436
13	0.9680	1.3935	1.3773	1.4418	6.5591	8.7490	12.1121	20.1439
14	1.1485	2.0233	2.4619	2.7559	11.6877	12.3313	14.2151	17.1329
15	1.6551	2.2825	2.3032	2.8576	2.5143	10.8367	5.0272	5.8717
Mean	1.3876	2.0702	2.1206	2.1845	6.9997	9.2021	10.4239	11.6565
SD	0.4865	0.8749	0.6006	0.6554	4.2159	3.7786	5.9868	8.0102

4.4 Discussion

This chapter has experimentally validated an algorithm implemented in a musculoskeletal model to simulate the effect of FES stimulation and has shown that FES-assisted activation of BFLH during gait proportionally increases the activation of gluteus maximus.

Gluteus maximus, together with gastrocnemius, are the muscles which compensate for weakness of the BFLH to restore control at the hip during stance phase (Jonkers et al., 2003). Other studies have shown that the primary compensatory muscles for hamstrings weakness are gluteus maximus, the vasti (Komura et al., 2004) and iliopsoas (Ardestani et al., 2016). In this chapter, the gluteus maximus was chosen as the candidate for measuring EMG for two reasons: it is positioned at a distance from BFLH and it shares function with BFLH as a hip extensor (Kendall et al., 1993; Perry et al., 2010). The results show that FES artefact signals from the stimulated BFLH did not affect the EMG readings at gluteus maximus.

Both mean peak gluteus maximus muscle activation predicted from the models and mean peak gluteus maximus activity from EMG measurement occurred during mid stance (20-

50% of stance phase; Table 4.2); prior work has also shown that this takes place in mid stance (Winter et al., 1987).

In this study, the musculoskeletal modelling cost function was modified from its standard form by assigning and weighting a variable, c , to simulate the BFLH as previously presented in Chapter 3. In Chapter 3, the value of c for each subject that reduced anterior shear force to zero was found and the mean value of c across all subjects was 0.208 for 40mA FES current stimulation. In this chapter, the FES current stimulation was set to three different levels. The c values chosen for the FES gait set of 40, 60 and 80 mA were 0.10, 0.15 and 0.20 respectively. These were chosen to mimic the incremental increase in BFLH activation caused by the different levels of FES current stimulation and to reach the level of 0.20 which corresponds to the level found in Chapter 3. The incremental increase in BFLH activation was found from the increasing EMG signals of the gluteus maximus.

This study has found statistical correlations between peak and impulse of gluteus maximus activation between modelling and EMG signals (Figure 4.4, Figure 4.5). These correlations provide a level of validation for the algorithm used in the musculoskeletal model and show that FES stimulation potentially can be tuned to a level to achieve different outcomes. This dose-response relationship can be harnessed for clinical benefit in many different lower limb pathologies.

The literature highlights that during loading response, when the hamstrings action is reduced, the gluteus maximus activity should be increased to provide hip stability (Perry et al., 2010). Interestingly, in the study shown here, gluteus maximus activity increased with increasing activation of the BFLH using FES during walking. This increased activity of the gluteus maximus activity occurred because the BFLH and gluteus maximus actions are multi joint processes. The gluteus maximus and hamstrings are the hip extensor and knee flexors respectively and have increasing activity in late swing to control the forward movement of the swinging lower limb (Winter et al., 1987). Moreover, the hip extensor muscles have two functions, firstly to decelerate the limb's momentum in terminal swing to prepare for stance, and secondly to restrain the forward momentum of the pelvis and trunk as the limb is loaded (Perry et al., 2010). In addition, during stance phase, the primary muscles controlling the hip are the extensors and abductors, which include the gluteus maximus. The extra activation of the BFLH with FES in this study forced gluteus maximus activity to be activated from late mid swing through the loading response more

than usual. As the hamstrings and gluteus maximus have a complementary role as the plantar flexors, this might also change not only the kinematics of the foot (Jonkers et al., 2003) but also of the knee and hip during early stance phase. Both BFLH and gluteus maximus also assist in lateral rotation of the tibia. These multi-joint actions provide an explanation for why the extra activation of BFLH with FES contributes to such large changes to gluteus maximus muscle activity.

There are some limitations to this study. Firstly, the trials were not in a randomised order which may introduce an experimental bias. Secondly, FES was not comfortable for some subjects and the stimulation pulse width was set differently according to subject tolerance and could be due to different muscle thicknesses between subjects. None of the subjects complained about the pain caused by the FES during the study until the FES current was set to 80mA; at this highest level it was possible that some subjects may have changed their walking patterns, however, this was not analysed in this study. Thirdly, there may also have been a cross talk in EMG measurements due to electrode placement of the EMG sensors. This minor difference in EMG placement on the gluteus maximus may have caused the EMG sensors to pick up signals from neighbouring muscles. This study assumed that any signal interference from neighbouring muscles would be minimal in comparison to the gluteus maximus. Lastly, this study also does not take into account any differences in cadence or walking speed, which may affect the results, particularly at higher values of FES current. In the future, other muscles should be considered, for example the gastrocnemius and the tibialis anterior, which may also compensate for the extra stimulation of BFLH muscles and will present more complete results.

4.5 Conclusion

This chapter presents the investigation to show how the activation of the BFLH correlates with the muscle activity of the gluteus maximus. The results from this study also validate a musculoskeletal modelling method that can simulate FES during gait. This musculoskeletal model can be used to predict muscle activation for any clinical study using FES including the use of FES to reduce the knee instability of the ACL deficient knee during stance phase, which will be presented in Chapter 5.

CHAPTER 5

Musculoskeletal model to investigate the use of FES at the ACLD and ACLR knee

This chapter compares the differences in kinematics and kinetics between healthy, ACL deficient and ACL reconstructed subjects during the stance phase of gait with and without FES stimulation of the BFLH by means of physical experiments and musculoskeletal modelling.

5.1 Introduction

As described in Chapter 2, an ACL tear or rupture results in an increase in tibiofemoral laxity of the knee in which the tibia has greater anterior tibial translation (ATT) and internal rotation than the normal movement of a healthy knee with an intact ACL. ACL deficient (ACLD) patients not only have this abnormal laxity, but also have a tibial anterior translation and external rotation offset relative to their contralateral knee (Andriacchi et al., 2005). For these individuals it is hypothetically possible that the abnormal articular kinematics due to the loss of the ACL can be compensated by appropriate muscle firing during walking. This could not only restore knee stability, but also potentially avoid further degenerative changes of the knee, such as meniscal tears and articular cartilage degeneration.

The maximum peak values of the anterior tibial shear occurs during mid stance (20-50% of the stance phase) at approximately 25% of stance phase (Alkjaer et al., 2011) and maximum internal tibial rotational torques occur during heel strike (0-3% of the stance phase) (Andriacchi et al., 2005). Despite these known loading conditions and the known function of the ACL, some ACLD patients can functionally cope with their injury (copers) and others do not (non-copers). The copers are able to return to pre-injury activity without surgical intervention and non-copers require surgery to achieve the same outcome. The copers limit ATT by: reducing their quadriceps contraction and maintaining lower levels of knee joint flexion (Berchuck et al., 1990) or by having a higher knee flexion combined with hamstrings contraction to prevent abnormal ATT and to reduce internal rotation torque (Benedetti et al., 1999). Non-copers are known to have reduced compression and anterior shear force at the knee joint (Alkjaer et al., 2011) and have difficulty to even flex their knees (Rudolph et al., 1998).

The treatment for ACL injury is based on the level of injury diagnosed by surgeons; treatment is either rehabilitation alone, or ACL reconstruction (ACLR) surgery plus rehabilitation. Rehabilitation for ACL injury is focused on strengthening of the quadriceps muscles due to the 'quadriceps avoidance' mechanism for ACL rupture that causes quadriceps atrophy (Berchuck et al., 1990).

ACLR is a highly successful procedure, yet there are residual instabilities that still occur post surgery (Woo et al., 2002); this may be due to the surgical procedure itself, or due to a combination of the surgery and rehabilitation (Brandsson et al., 2002; Papannagari et al.,

2006). This means that some patients do not return to their pre-injury sports level post surgery. However, for those who do return to sport the re-rupture rate is high (Paterno et al., 2010). Furthermore, ACLR surgery does not consistently reduce other degenerative changes at the joint, such as of the meniscus and cartilage. Researchers have suggested that this could be a consequence of the knee joint kinematics that have not been fully restored by the reconstructive surgery and rehabilitation.

Based on the geometry of the knee joint of the patients, an alternative method to restore knee stability is by activating the hamstrings, especially the biceps femoris long head (BFLH), at the appropriate point in the gait cycle. An electromyographic (EMG) study of ACLD and ACLR patients found an increased activity of the biceps femoris muscle that indicates a protective mechanism (Ciccotti et al., 1994), protecting the ACL reconstruction and protecting the knee from elevated internal rotation torques and anterior shear; when a posterior force is applied by activating the BFLH, external rotation of the tibia occurs and internal rotation torque is reduced. This is evidenced in clinical studies that show that ACL copers stabilize their knees by increased their co-contraction of hamstrings (Alkjaer et al., 2003; Boerboom et al., 2001), however, one study disputes this (Rudolph et al., 2001). The interplay between knee stabilisation and musculoskeletal system restraint with functional electrical stimulation (FES) of the BFLH is not known for ACLD and ACLR patients. The effect of activation of BFLH with FES has the potential to reduce the knee instability of these patients. As described previously in this thesis (Chapter 3), another variable of interest with respect to BFLH activation is gait speed (Arnold et al., 2013) (Czerniecki et al., 1988) as hamstring muscle forces increase with walking speed (Neptune et al., 2005) and, therefore, the activation of BFLH with FES is possibly influenced by the gait speed. Also, gluteus maximus and gluteus medius are muscles that support the whole body during mid stance phase (Anderson et al., 2003) and the results of Chapter 4 show that gluteus maximus muscle forces increase with increased activation of BFLH.

In Chapter 3, the selective activation of BFLH was able to reduce the anterior tibial shear and tibial internal rotation torque at the knee in healthy subject during early stance phase. In Chapter 4, the modified musculoskeletal model which was introduced in Chapter 3 was validated by evaluating the measured EMG signal of the gluteus maximus while activating the BFLH with FES. In this chapter, the validated musculoskeletal model is used to predict and analyse the effect of activating during stance phase BFLH with FES in three groups: ACLD patients, ACLR patients, and control group.

The aims of this chapter are to:

1. simulate the ACLD and ACLR behaviour during stance phase using the validated musculoskeletal model (Chapter 4);
2. investigate the effectiveness of activating BFLH using FES in increasing knee stability in ACLD and ACLR subjects; and
3. compare knee stability between the control healthy group and the two patient groups.

5.2 Materials and Methods

Subject recruitment and selection

This pilot study was approved by the Health Research Authority (HRA), following a submission to the HRA, attendance at the London - Queen Square Research Ethics Committee and confirmation that Imperial College Healthcare NHS Trust and Imperial College London could host this study. Full details are provided in Appendix A. Subjects were recruited through posters at Imperial College London: South Kensington Campus, St Mary's Hospital Campus and Charing Cross Hospital Campus. The participating surgeons provided the clinical assessment of the state of the patient, as either ACLD or ACLR, confirmed by medical imaging (magnetic resonance imaging; MRI). Standard clinical decision-making took place prior to participating in the study and the study did not influence any treatment. The study inclusion criteria were that:

either the injury or the ACL reconstruction surgery had to have occurred a minimum of 6 months prior to joining the study, as this is appropriate rehabilitation time post ACL reconstruction (Devita et al., 1998); and

subjects must be aged between 18 and 60 years.

The exclusion criteria were:

any known allergy to adhesives;

any psychiatric illness that limits the ability to give informed consent;

pregnancy;

patients with implanted electronic device (for example, cardiac demand pacemakers) unless under specialised medical supervision;

poorly controlled epilepsy; and

known musculoskeletal lower limb conditions other than ACL deficiency.

Participant information sheet and consent forms were then emailed to the patients who met the inclusion and exclusion criteria. They were given at least 24 hours to decide whether or not to participate in this study. Patients who agreed to participate were later contacted by the researcher to set the date and time for the study at which point signed informed consent was taken. Participants were free to withdraw at any time.

Eight patients (7 male, 1 female; mean height 1.76 ± 0.06 m; mass 79.8 ± 11.5 kg; age 27.25 ± 5.91) participated in this study. Eight healthy control subjects were selected who closely matched the patient group's height, mass and age (6 male, 2 female; mean height 1.76 ± 0.13 m; mass 76.28 ± 13.21 kg; age 28.5 ± 3.70 years). The patients consisted of: 4 subjects with unilateral ACLD and 4 subjects with unilateral ACLR. The anthropometric data of patients and control subjects are shown in Table 5.1 and Table 5.2.

Table 5.1 Patients' anthropometric data

Patient	Type of injury	Gender	Age (Year)	Height (m)	Mass (kg)	Injury date	Experiment date	Duration time between injury/surgery (months)
ACLD group								
1	ACLD1 (Full tear)	Male	33	1.63	72.5	08.2016	17.01.2017	6
2	ACLD2 (Partial tear)	Male	30	1.77	79.5	12.2015	11.01.2017	24
3	ACLD3 (Full tear)	Male	29	1.90	80.0	03.2016	28.01.2017	10
4	ACLD4 (Partial tear)	Male	21	1.72	75.2	04.2016	27.07.2017	15
Mean (ACLD)			28.25	1.75	76.80	-	-	13.75
SD (ACLD)			5.12	0.11	3.59	-	-	7.76
ACLR group (all hamstrings grafts)								
5	ACLR1	Male	28	1.77	80.0	2011	18.01.2017	72
6	ACLR2	Male	21	1.76	95.7	08.2016	14.02.2017	6
7	ACLR3	Female	25	1.68	68.8	03.2015	16.03.2017	24
8	ACLR4	Male	35	1.81	74.7	2003	02.06.2017	168
Mean (ACLR)			27.25	1.76	79.8	-	-	67.5
SD (ACLR)			5.91	0.06	11.5	-	-	72.6
Mean all patients (ACLD and ACLR)			27.75	1.75	78.3	-	-	40.6
SD patients (ACLD and ACLR)			5.15	0.08	8.08	-	-	55.7

Table 5.2 Control subjects' anthropometric data

Control subject	Gender	Age (Year)	Height (m)	Mass (kg)
1	Male	26	1.89	100.9
2	Male	31	1.63	62.7
3	Female	30	1.53	70.8
4	Male	28	1.77	68.2
5	Male	26	1.83	92.0
6	Female	25	1.73	68.4
7	Male	26	1.82	71.2
8	Male	36	1.92	76.0
Mean		28.5	1.76	76.28
SD		3.70	0.13	13.21

Parametric one-way analysis of variance (ANOVA) for normally distributed data with equal error variances and nonparametric Kruskal Wallis tests for other data were used to test the null hypothesis that the three groups (ACLD, ACLR, control) means were equal with respect to height, mass and age. Normality was tested using the Shapiro Wilk's test and Levene's test was used to test for equal error variances. Based on these tests, height and age were normally distributed and mass were not normally distributed (Table 5.3). Therefore, for height and age ANOVA was used and for mass the Kruskal-Wallis test was used to test for statistical difference between the groups. No statistical differences were found (Table 5.4).

Table 5.3 Testing normality of data for height, mass and age for ACLD, ACLR and control groups using Shapiro Wilk's test and Levene's test

3 groups	Shapiro Wilk's (<i>p</i> -value)	Levene's (<i>p</i> -value)
Height	0.728	0.312
Mass	0.050	0.238
Age	0.152	0.323

Table 5.4 Testing for statistical difference of height, mass and age between ACLD, ACLR and control groups (using ANOVA for height and age and Kruskal-Wallis for mass)

3 groups	ANOVA (<i>p</i> -value)	Kruskal-Wallis (<i>p</i> -value)
Height	0.983	-
Mass	-	0.513
Age	0.703	-

The study was divided into two parts: in vivo physical experiments and computational musculoskeletal modelling.

In vivo experiments

The experimental protocol was similar to the protocol for Chapters 3 and 4. The experiment took place in the motion lab in the Royal School of Mines at the Imperial College London South Kensington Campus. On arriving in the lab, the height and mass of the subjects were measured. Retro-reflective markers were placed on lower limb landmarks and three-dimensional marker trajectories (as per Chapter 3, Table 3.2) were measured at 200 Hz using a 10-camera motion capture system (Vicon Motion Systems Ltd, Oxford, UK).

The safety guidelines for conducting FES were carefully explained to the subjects including how to halt FES stimulation during the study. The FES electrodes were attached over the BFLH as follows: one FES electrode was attached at the distal part of the muscle and the other electrode was placed at the centre, with a distance of two hand widths between them (as in Chapter 3, Figure 3.6). FES was set to 40 Hz and 40mA of current stimulation. These levels were chosen as in Chapter 3, where the FES was able to reduce the anterior shear force and the internal rotation torque. The surface stimulation electrode used was 7 cm in diameter. Each subject was set to a different level of pulse widths (with the average level of 4.22, maximum level 6 and minimum level 3) according to their tolerance of the stimulation level.

Subjects performed at least five trials of walking at a self-selected pace on a walkway with FES (FES gait) and without FES (normal gait). The walkway contained a force plate (Kistler Type 9286BA, Kistler Instrument AG, Winterthur, Switzerland) to measure ground reaction force. Control subjects walked on the walkway so that their right limb struck the force plate. Patient subjects stepped on the force plate with their affected (i.e. injured or reconstructed) limb. GRFs and EMG signals were simultaneously measured at 1000 Hz from the force plate and EMG system (Delsys, Trigno Wireless EMG system, USA). In this pilot study, the last three trials were chosen for analysis as this represents the trials where the subjects had the greatest opportunity to adapt to the walking task.

The stimulation of the FES current was set to start with 1 second of ramp up, followed by 4 seconds of maximum current level and then ending with 1 second of ramp down. The current was set to an asymmetrical biphasic waveform, because this gives stronger contraction compared to the symmetrical biphasic (Lynch et al., 2008). The stimulator was manually started by the subject and timed so that the stimulation current was at its

maximum value when the right foot stepped on the force plate, through heel strike and toe off.

Lower Limb Musculoskeletal model

The lower limb musculoskeletal model was used as described in Chapters 3 and 4.

As for those chapters, the standard cost function was used for the activity without using the FES. To simulate the stimulation of the FES during activities towards the BFLH in the revised optimisation, the muscle force of BFLH was set as a constant value, c , where c was set to 0.2 as the mean value found in Chapter 3 that reduced the anterior shear force to zero and the internal rotation torque to zero.

Data Analysis

The anterior tibial shear force, internal tibial rotational torque, gait speed, gluteus medius and gluteus maximus muscle activations were averaged over three trials and presented as mean values in the tibial coordinate frame. The gluteus medius and gluteus maximus muscle activations were predicted from the model. The anterior tibial shear force, internal tibial rotational torque, gluteus medius and gluteus maximus muscle activations were normalised to body weight (BW). The stance phase was expressed in a 0-100% duration with a step interval of 1% using cubic spline data interpolation (MATLAB, the Mathworks Inc., Natick, USA). To test the hypothesis that the knee peak internal tibial rotational torque, peak anterior tibial shear force and speed were reduced and gluteus medius and gluteus maximus muscle activations were increased by applying FES to the BFLH, the gait data without FES (normal gait) and with FES (FES gait) for all three groups were compared using the non-parametric one way ANOVA, Kruskal-Wallis test at $\alpha=0.05$. When significant differences were observed, Tukey's post hoc test was used with Bonferroni correction. All tests were calculated in MATLAB (R2015b, The Mathworks Inc., Natick, MA).

Sprague and Geers metric was used to calculate the difference in internal rotational torque in terms of the magnitude (M), phase (P) and combined (C) errors between groups. This method was devised as a modification of Geers' metric to enable the comparison of measured and experimental curves in biomechanics. Based on the Sprague and Geers metric, $m(t)$ is the measured history and $c(t)$ is the calculated history. The time integrals are defined as follows (Schwer, 2007):

$$\begin{aligned}
v_{mm} &= (t_2 - t_1)^{-1} \int_{t_1}^{t_2} m(t)^2 dt, \\
v_{cc} &= (t_2 - t_1)^{-1} \int_{t_1}^{t_2} c(t)^2 dt, \\
v_{mc} &= (t_2 - t_1)^{-1} \int_{t_1}^{t_2} m(t)c(t)dt,
\end{aligned}
\tag{Equation 5.1}$$

where $t_1 < t < t_2$ is the time interest response for the waveforms.

In this pilot study, the internal rotational torque of the patient group (ACLD or ACLR) was set as the measured curve, $m(t)$ and the internal rotational torque of the control group was set as the calculated curve, $c(t)$. The M , P and C values are defined as follows (Schwer, 2007; Sprague et al., 2003):

$$M = \sqrt{v_{cc} / v_{mm}} - 1 \tag{Equation 5.2}$$

which is insensitive to phase differences because it is based upon the area under the squared response histories, with the -1 providing a zero metric value when the two areas

are identical;
$$P = \frac{1}{\pi} \cos^{-1} \frac{v_{mc}}{\sqrt{v_{mm} v_{cc}}} \tag{Equation 5.3}$$

which is insensitive to magnitude differences (Sprague et al., 2003); and

$$C = \sqrt{M^2 + P^2}$$

This formula therefore enables magnitude and phase metrics to be combined (Geers, 1984).

If values of M and P are below 0.20 then this indicates that there is a high level of similarity between the two waveforms. Values for M and P between 0.20-0.30 indicate that there is a medium level of similarity the two waveforms. Values higher than 0.30 indicate that there is low level of similarity between the two waveforms (Geers, 1984). Positive M indicates that the $m(t)$ waveform is lagging relative to the $c(t)$ waveform.

5.3 Results

Internal rotation torque

All the curves of the internal rotation torques for control, ACLD and ACLR groups during normal gait and FES gait are shown in Figure 5.1. The peak values of the internal rotation

torque for all groups are shown in Table 5.5. There was a significant difference between the three groups for peak internal rotation torque during normal gait ($p=0.040$). There was a significant difference in peak internal rotation torque between the control group during normal gait and the ACLD and ACLR groups during FES gait ($p=0.038$).

Table 5.5 Peak internal rotation torque (Nm/BW) for 8 control subjects, 4 ACL deficient subjects and 4 ACL reconstructed subjects during stance phase ($*p < 0.05$)

Subject	Internal rotation torque (Nm/BW)					
	Normal gait ($p=0.04$)*			FES gait		
	Control*	ACLD	ACLR	Control	ACLD*	ACLR ($p=0.038$)*
1	0.0079	0.0009	0.0015	0.0087	0.0011	0.0012
2	0.0025	0.0006	0.0025	0.0018	0.0001	0.0027
3	0.0017	0.0030	0.0001	0.0017	0.0019	0.0001
4	0.0032	0.0021	0.0016	0.0031	0.0016	0.0020
5	0.0015	-	-	0.0014	-	-
6	0.0031	-	-	0.0028	-	-
7	0.0032	-	-	0.0034	-	-
8	0.0032	-	-	0.0021	-	-
Mean	0.0033	0.0016	0.0014	0.0031	0.0012	0.0015
SD	0.0020	0.0011	0.0010	0.0023	0.0008	0.0011

Table 5.5 shows that the peak internal rotation torque for the control group in normal gait (mean = 0.0033 ± 0.0020 Nm/BW) is higher than the ACLD group (mean = 0.0016 ± 0.0011 Nm/BW; $p=0.073$) and ACLR group (mean = 0.0014 ± 0.0010 Nm/BW; $p=0.048$) in normal gait (Figure 5.2). The internal rotation torques of the control group (Figure 5.3) and the ACLD group (Figure 5.4) are higher in normal gait compared to FES gait by 4.69% and by 27.78% but the internal rotational torque of the ACLR group (Figure 5.5) is higher in FES gait compared to the normal gait by 6.18% (Table 5.6).

Table 5.6 Percentage difference between mean peak internal rotation torque in normal gait and FES gait for all groups

Group	Control	ACLD	ACLR
Differences	-4.69%	-27.78%	6.18%

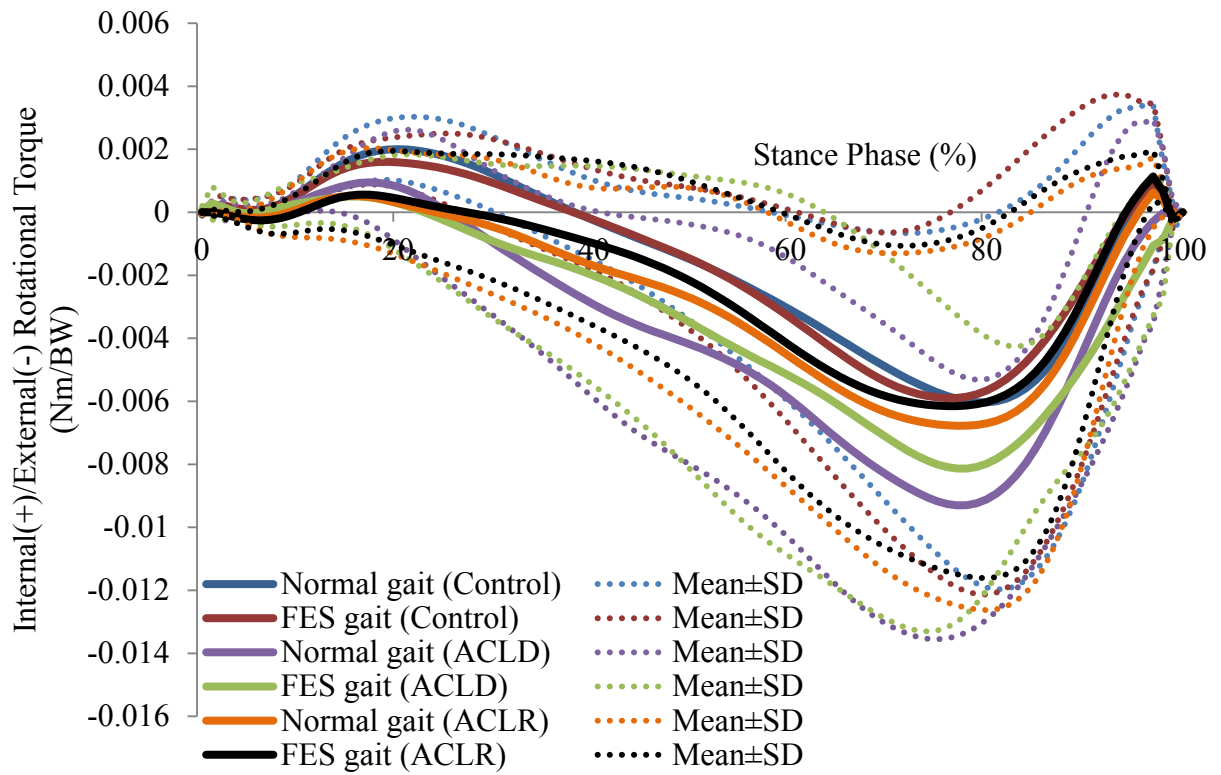


Figure 5.1 Internal rotation torque (Nm/BW) (mean ± SD) for control (n=8), ACLD (n=4) and ACLR (n=4) groups during normal gait and FES gait

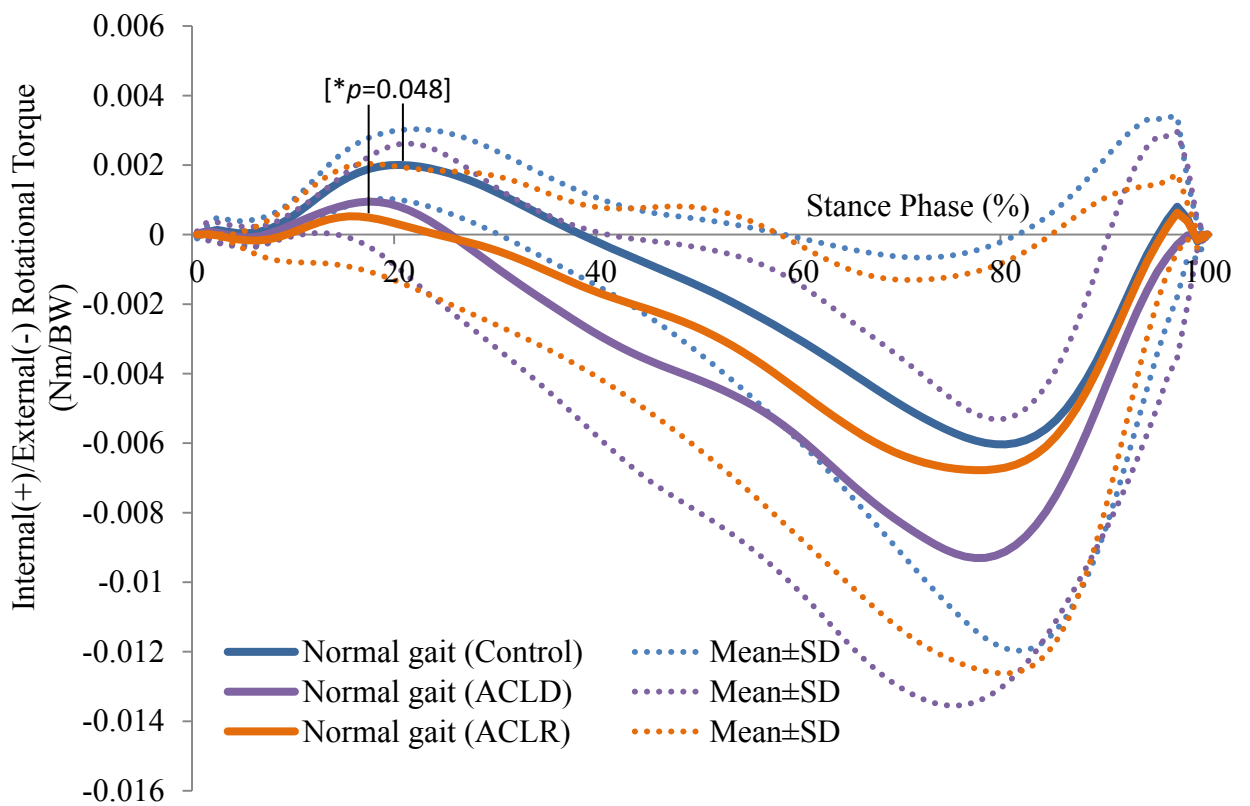


Figure 5.2 Internal rotation torque (Nm/BW) (mean ± SD) for control (n=8), ACLD (n=4) and ACLR (n=4) groups during normal gait

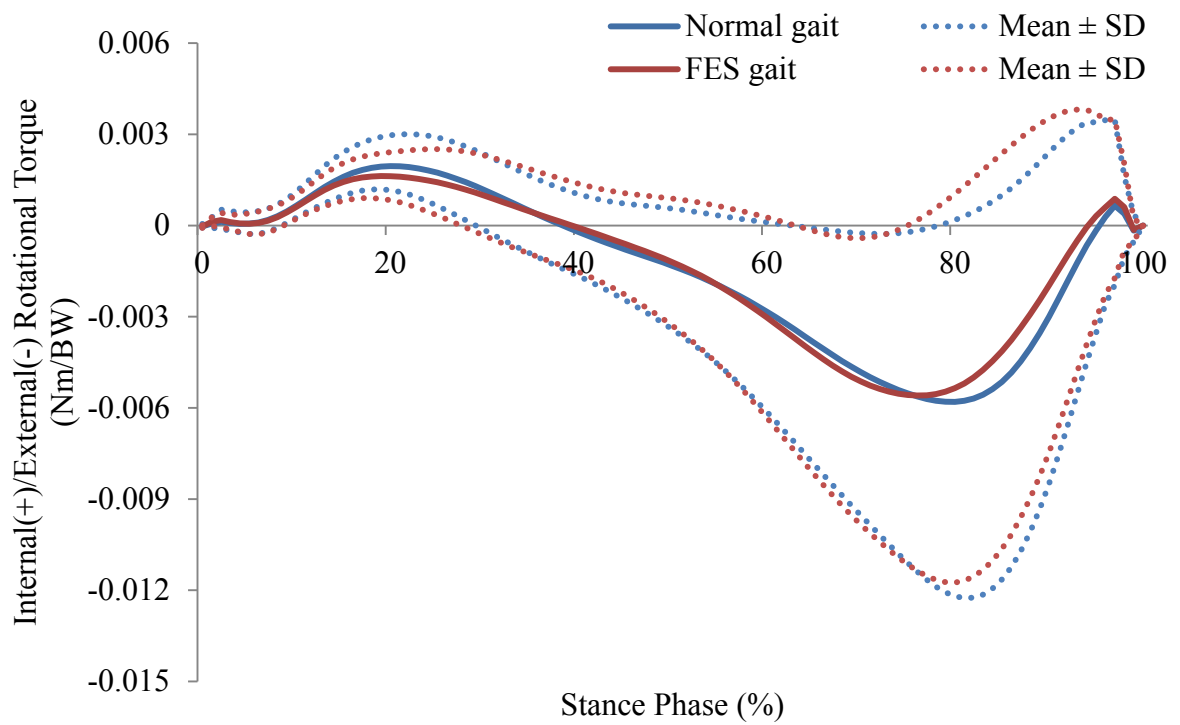


Figure 5.3 Internal rotation torque (Nm/BW) for control group (mean \pm SD, n=8) during normal gait and FES gait

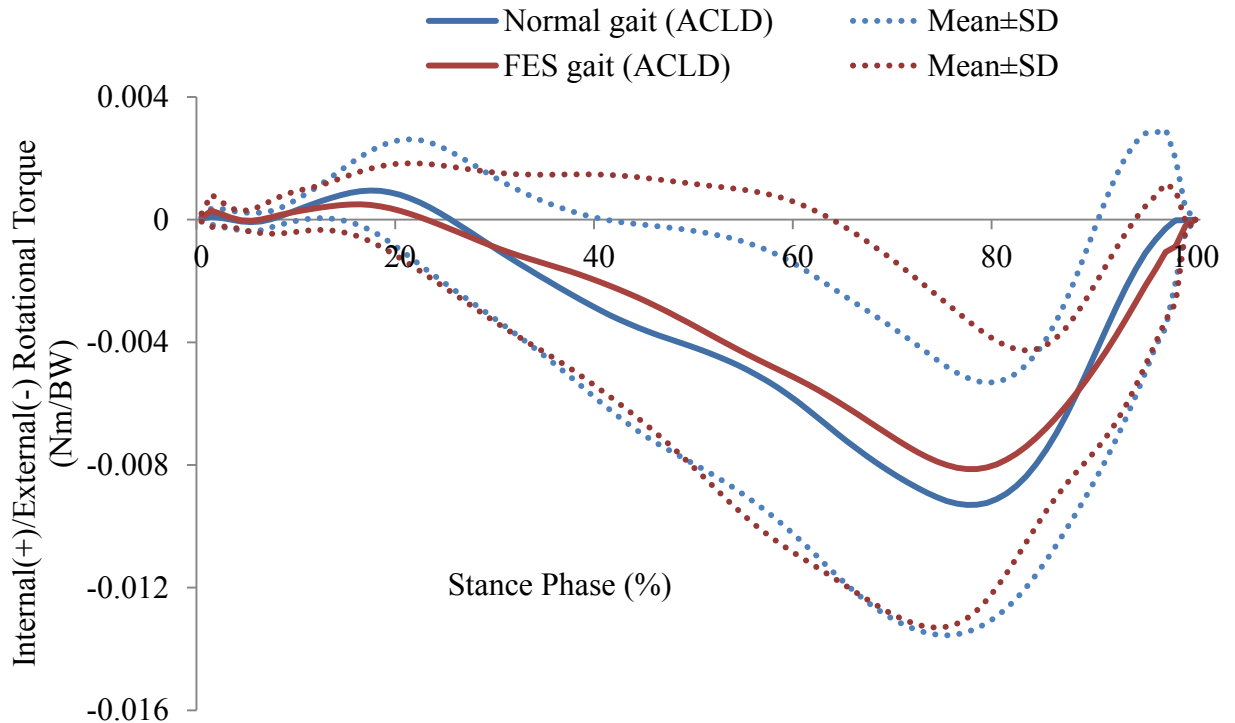


Figure 5.4 Internal rotation torque (Nm/BW) for ACLD group (mean \pm SD, n=4) during normal gait and FES gait

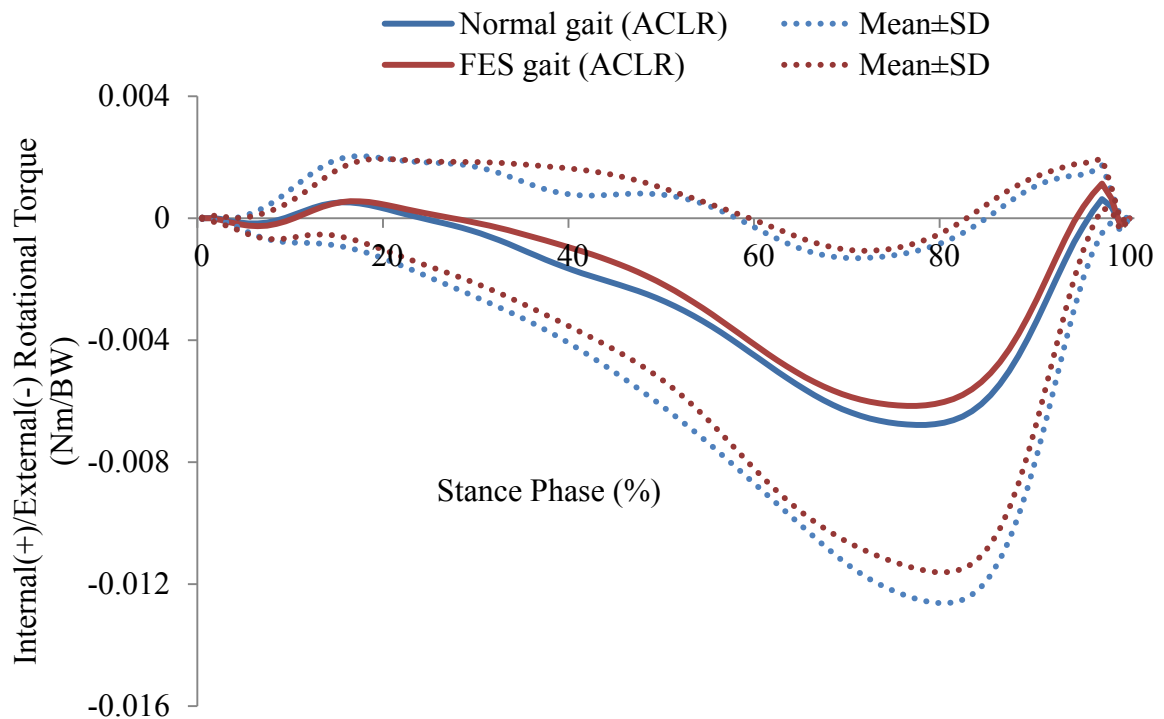


Figure 5.5 Internal rotation torque (Nm/BW) for ACLR groups (mean \pm SD, n=4) during normal gait and FES gait

Sprague and Geers metric (Internal rotation torque)

Internal rotation torque curve of the control group during normal gait (HN) and the internal rotation torque curve of the ACLR group during FES gait (RF) were highly similar in magnitude ($M=0.09$) but highly dissimilar in terms of phase ($P=0.54$; Table 5.7). Internal rotation torque of the control group during normal gait (HN) and the internal rotation torque of the ACLD group during FES gait (DF) were highly dissimilar in terms of magnitude ($M=0.39$) and phase ($P=0.52$; Table 5.7).

There are also high levels of differences in the internal rotation torque curves between the ACLD group during normal gait (DN) and ACLD group during FES gait (DF) ($P=0.59$) and also with ACLR group during FES gait (RF) ($P=0.58$; Table 5.7).

There are high levels of similarity between the internal rotation torque curve of the ACLR during normal gait (RN) and ACLR group during FES gait (RF) (Table 5.7) in terms of magnitude error ($M=0.07$) but not in terms of the phase error ($P=0.59$).

Table 5.7 Magnitude error (M), Phase error (P) and combined error (C) (Sprague and Geers' metric) for the comparison of internal rotation torque of the measured waveform, $m(t)$ and calculated waveform, $c(t)$

Measured waveform, $m(t)$	HN		DN		RN
	DF	RF	DF	RF	RF
Calculated waveform, $c(t)$					
M	0.39	0.09	-0.17	-0.34	-0.07
P	0.52	0.54	0.59	0.58	0.59
C	0.65	0.55	0.61	0.67	0.59

Anterior shear force

Anterior shear forces of the three groups are shown in Figure 5.6. Peak values of anterior shear forces are shown in Table 5.8. There is a significant difference between the peak anterior shear force in the control group during normal gait and the ACLD and ACLR during FES gait ($p=0.002$). There is a higher peak anterior shear force in the control group during normal gait compared to the ACLD group during FES gait ($p=0.003$).

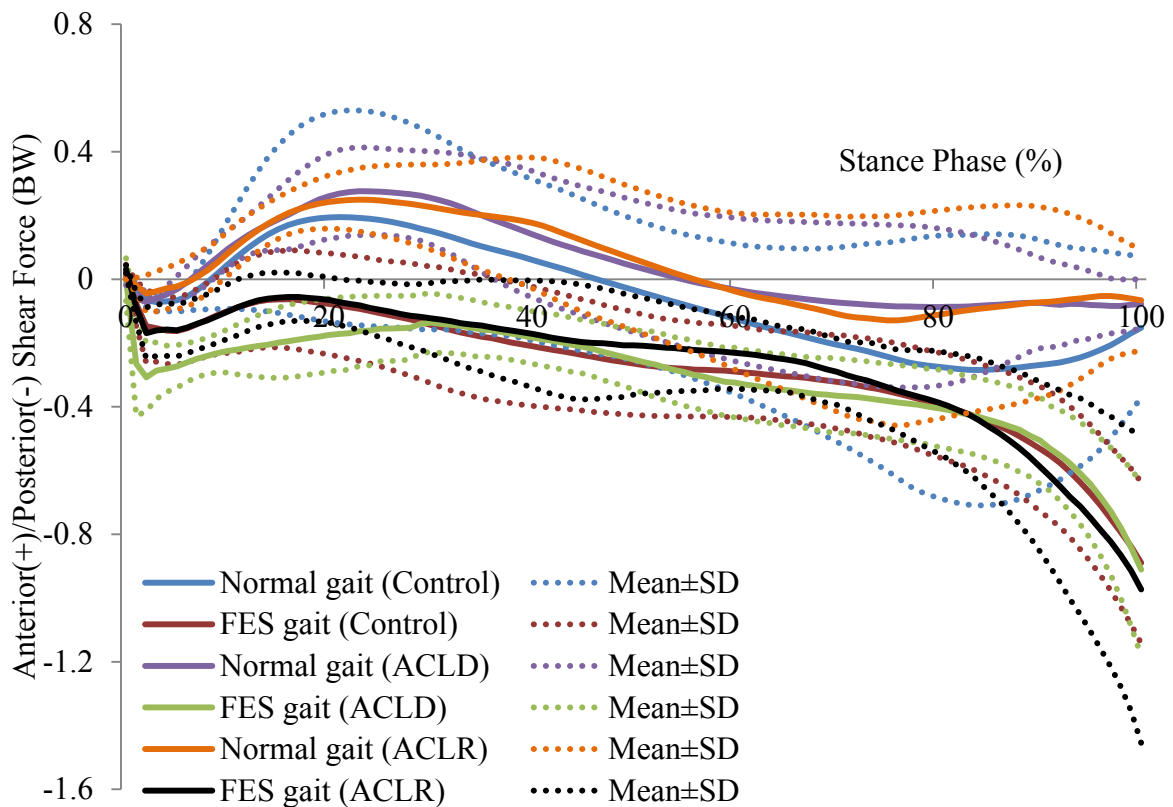


Figure 5.6 Mean shear force (BW) curves (mean \pm SD) for 8 control healthy subjects, 4 ACLD subjects and 4 ACLR subjects

Table 5.8 Peak anterior shear force (BW) for 8 control subjects, 4 ACL deficient subjects and 4 ACL reconstructed subjects (* $p < 0.05$)

Subject	Anterior shear force (BW)					
	Normal gait			FES gait		
	Control*	ACLD	ACLR	Control	ACLD* ($p=0.003$)*	ACLR ($p=0.002$)*
1	0.238	0.378	0.246	0.152	-0.517	-0.013
2	0.461	0.190	0.039	0.034	-0.166	-0.093
3	0.325	0.468	0.329	0.006	-0.047	-0.071
4	0.229	0.180	0.133	0.053	-0.255	0.064
5	0.013	-	-	0.028	-	-
6	0.383	-	-	0.006	-	-
7	0.324	-	-	0.052	-	-
8	0.242	-	-	0.033	-	-
Mean	0.277	0.304	0.187	0.045	-0.246	-0.028
SD	0.125	0.123	0.110	0.043	0.173	0.061

The anterior shear force curves for all ACLD subjects during normal and FES gait are shown in Figure 5.7, Figure 5.8, Figure 5.9 and Figure 5.10. The anterior shear force curves for all ACLR subjects during normal and FES gaits are shown in Figure 5.11, Figure 5.12, Figure 5.13 and Figure 5.14.

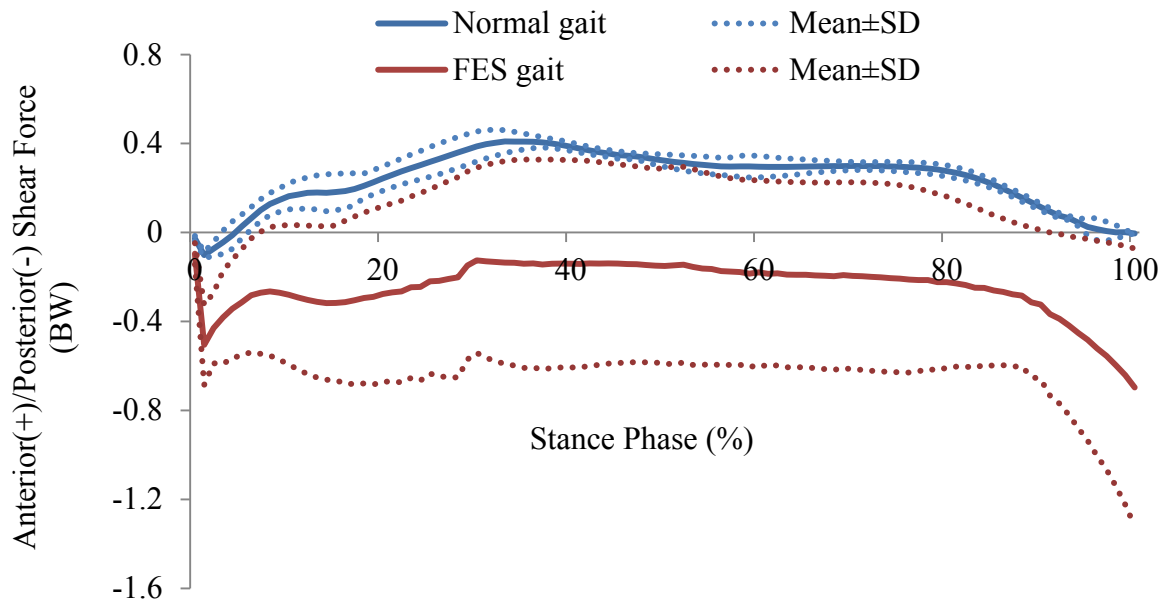


Figure 5.7 Shear force (BW) (mean \pm SD) for subject ACLD1 (Full Tear)

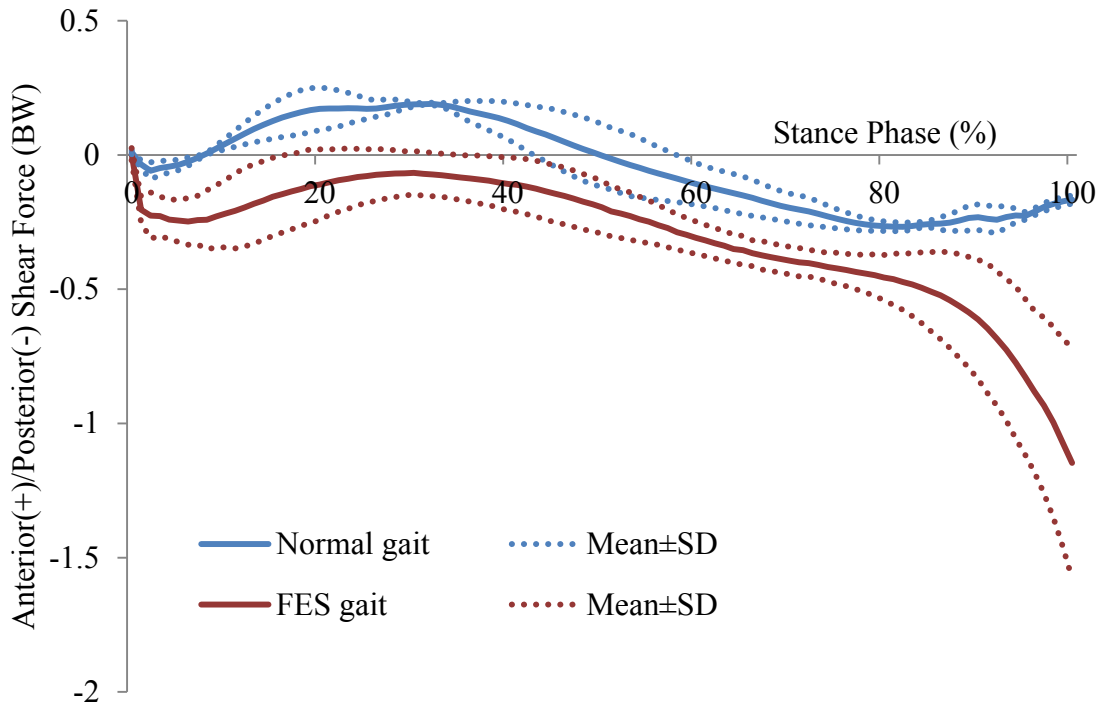


Figure 5.8 Shear force (BW) (mean \pm SD) for subject ACLD2 (Partial Tear)

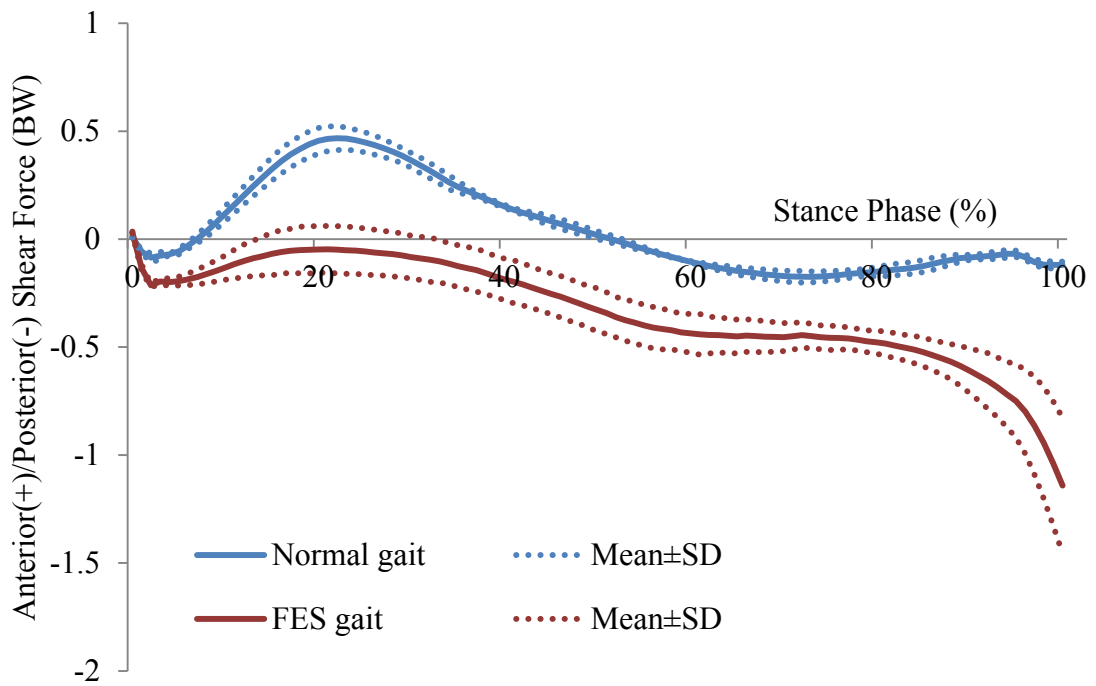


Figure 5.9 Shear force (BW) (mean \pm SD) for subject ACLD3 (Full Tear)

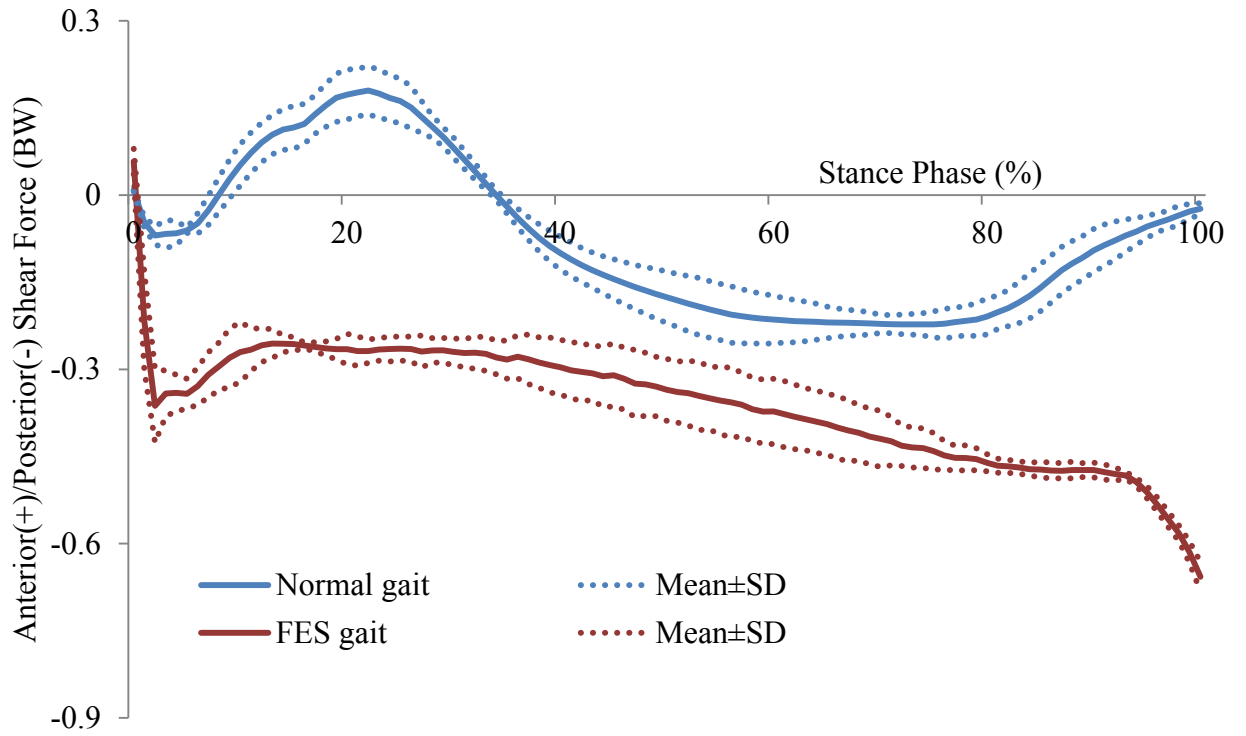


Figure 5.10 Shear force (BW) (mean \pm SD) for subject ACLD4 (Partial Tear)

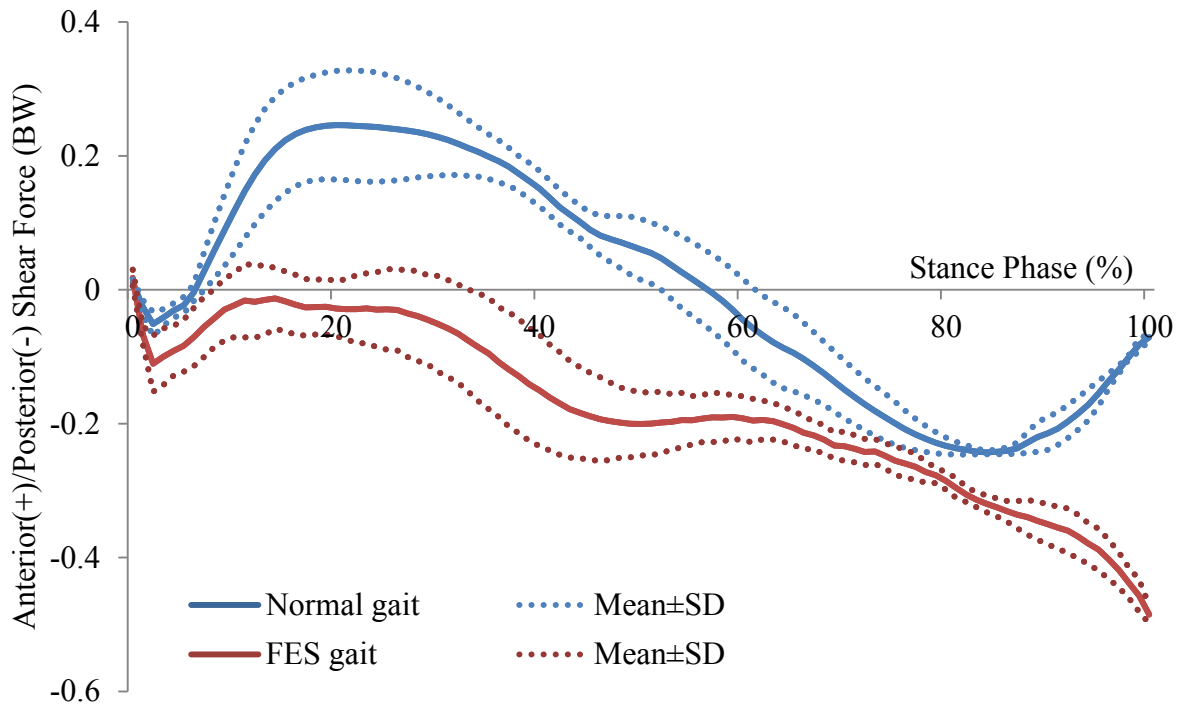


Figure 5.11 Shear force (BW) (mean \pm SD) for subject ACLR1

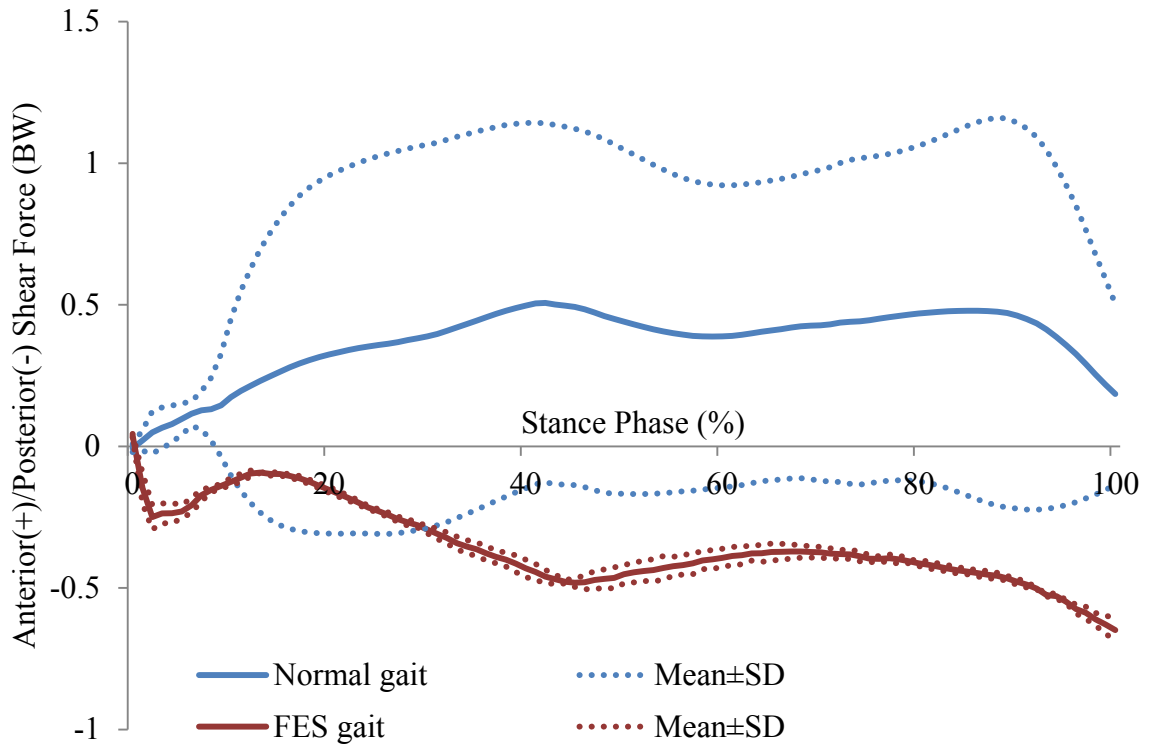


Figure 5.12 Shear force (BW) (mean \pm SD) for subject ACLR2

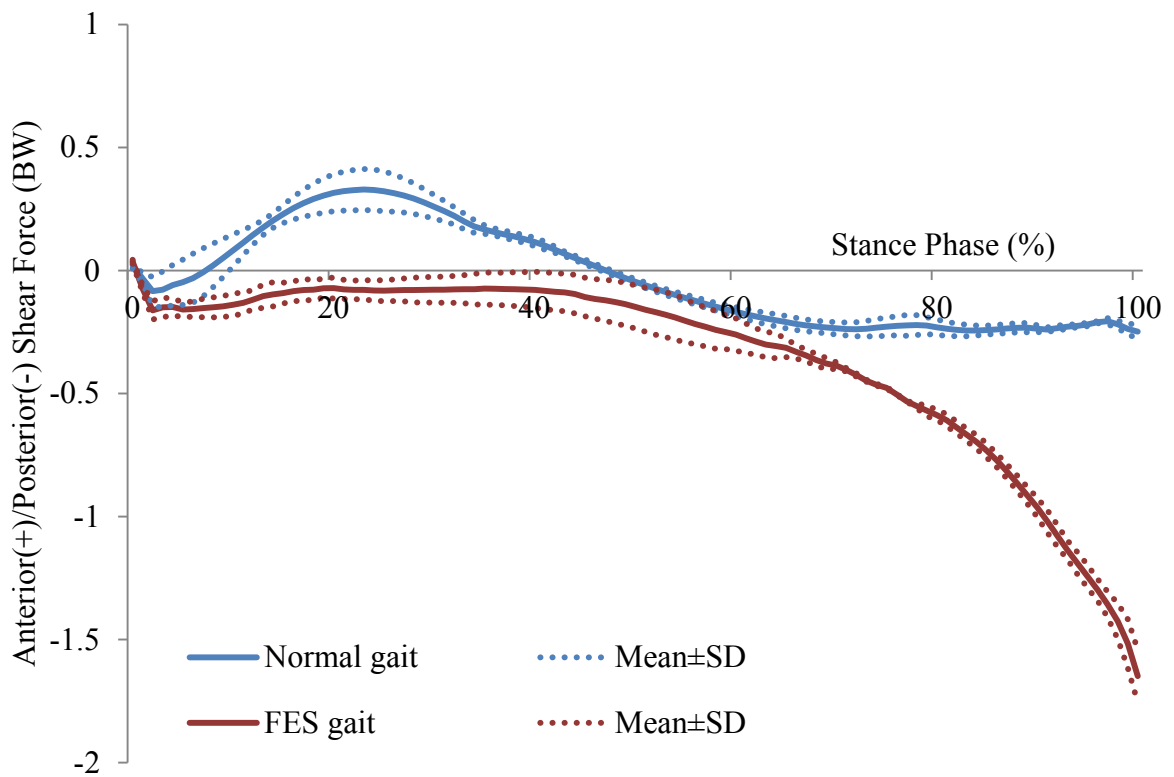


Figure 5.13 Shear force (BW) (mean \pm SD) for subject ACLR3

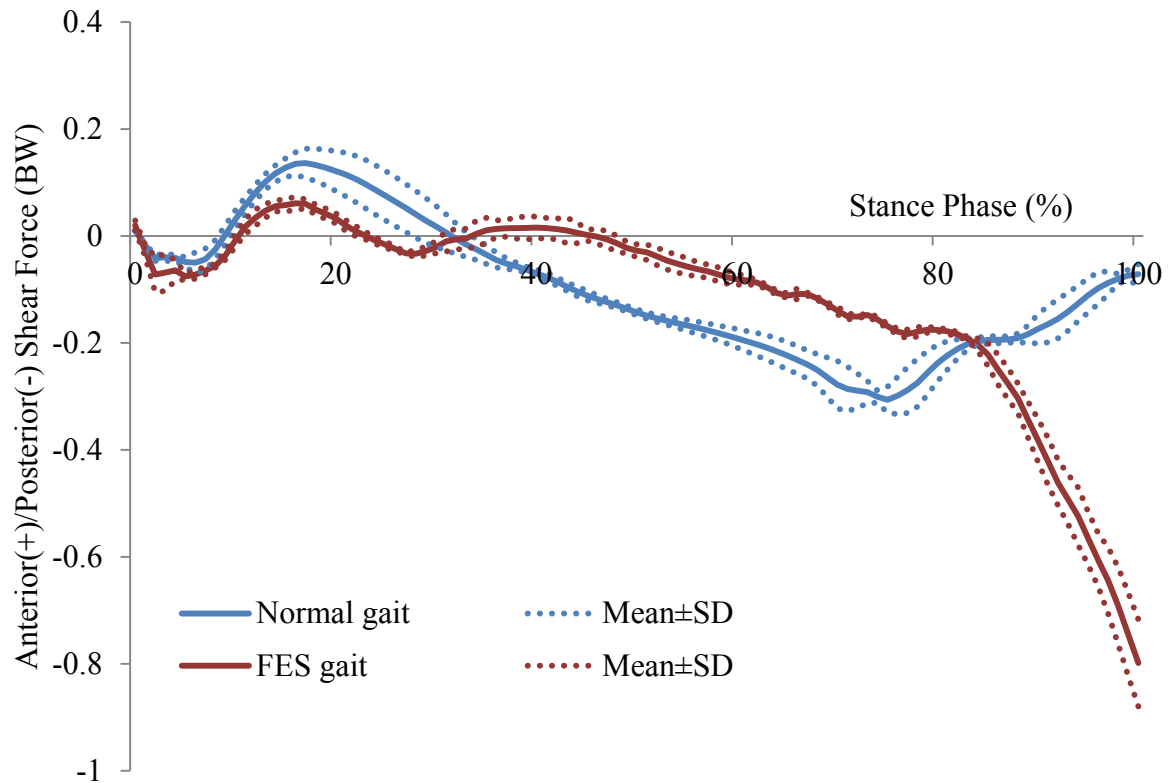


Figure 5.14 Shear force (BW) (mean \pm SD) for subject ACLR4

Speed

The speed (as calculated from the stance phase only) results are shown in Table 5.9.

There is a significant difference in speed between the control group during normal gait and the ACLD and the ACLR groups during FES gait ($p=0.029$). There is significantly higher speed in the control group during normal gait compared to the ACLD group during FES gait ($p=0.023$). There is a significant difference in speed between groups in FES gait ($p=0.047$) and there is significantly higher speed in the control group during FES gait compared to the ACLD group during FES gait ($p=0.004$).

Table 5.9 Mean speed (m/s) of 8 control subjects, 4 ACL deficient subjects and 4 ACL reconstructed subjects (* $p < 0.05$)

Subject	Normal gait			FES gait ($p=0.047$)*		
	Control*	ACLD ($p=0.021$)*	ACLR	Control	ACLD ($p=0.023$)*	ACLR ($p=0.029$)*
1	0.32	0.20	0.27	0.27	0.20	0.23
2	0.39	0.24	0.29	0.33	0.20	0.25
3	0.28	0.33	0.40	0.23	0.29	0.35
4	0.31	0.23	0.36	0.29	0.21	0.33
5	0.35	-	-	0.31	-	-
6	0.32	-	-	0.33	-	-
7	0.40	-	-	0.39	-	-
8	0.33	-	-	0.29	-	-
Mean	0.34	0.26	0.33	0.31	0.23	0.29
SD	0.04	0.06	0.06	0.05	0.04	0.06

Table 5.10 Percentage difference between mean speed in normal gait and FES gait for all groups

Group	Control	ACLD	ACLR
Differences	-9.63%	-10.0%	-12.12%

The control group (0.34 ± 0.04 m/s) walks faster than the ACLD (0.26 ± 0.06 m/s) group in normal gait (Table 5.9; $p = 0.021$). The control group, the ACLD group and the ACLR group walk slower in FES gait compared to normal gait by 9.63% in control group ($p=0.020$), 10.0% in ACLD group and by 12.12% in ACLR group (Table 5.10).

Gluteus maximus muscle activation

The mean gluteus maximus muscle activation predicted from the model for the three groups are shown in Figure 5.15, Figure 5.16 and Figure 5.17. There is a significant difference in the first peak gluteus maximus muscle activation between groups for FES gait ($p=0.038$). There is significantly lower first peak gluteus maximus muscle activation in FES gait for the ACLD group compared to the ACLR group ($p=0.043$). The mean first peaks of gluteus maximus muscle activation during stance phase for the three groups are shown in Table 5.11.

Table 5.11 Peak gluteus maximus muscle activation for 8 control subjects, 4 ACLD subjects and 4 ACLR subjects (* $p < 0.05$)

Subject	Gluteus maximus muscle activation					
	Normal gait			FES gait ($p=0.038$)*		
	Control	ACLD	ACLR	Control	ACLD*	ACLR ($p=0.043$)*
1	0.0738	0.0706	0.0262	0.1058	0.0598	0.0641
2	0.0411	0.0120	0.0706	0.1069	0.0211	0.1115
3	0.0611	0.0646	0.0928	0.1080	0.0456	0.1154
4	0.0889	0.0583	0.0444	0.0906	0.0971	0.1137
5	0.0409	-	-	0.1024	-	-
6	0.0809	-	-	0.1577	-	-
7	0.0599	-	-	0.0991	-	-
8	0.0408	-	-	0.0000	-	-
Mean	0.0609	0.0514	0.0585	0.0963	0.0559	0.1012
SD	0.0191	0.0267	0.0293	0.0438	0.0318	0.0248

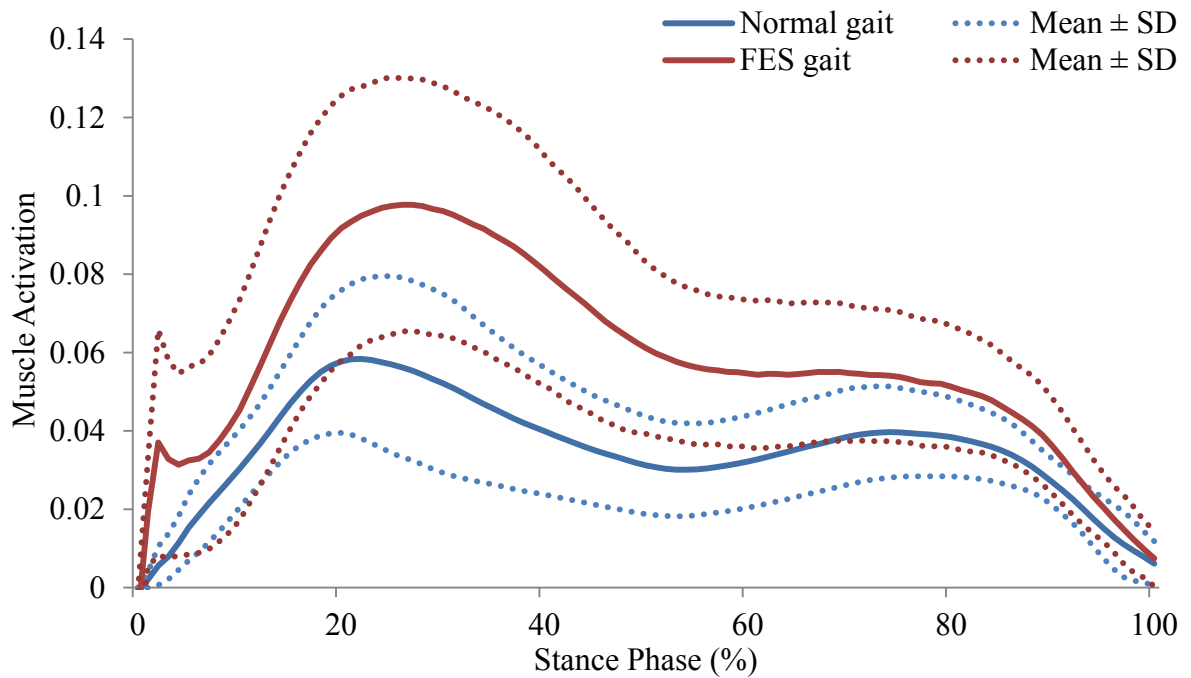


Figure 5.15 Gluteus maximus muscle activation (mean \pm SD) for 8 control subjects

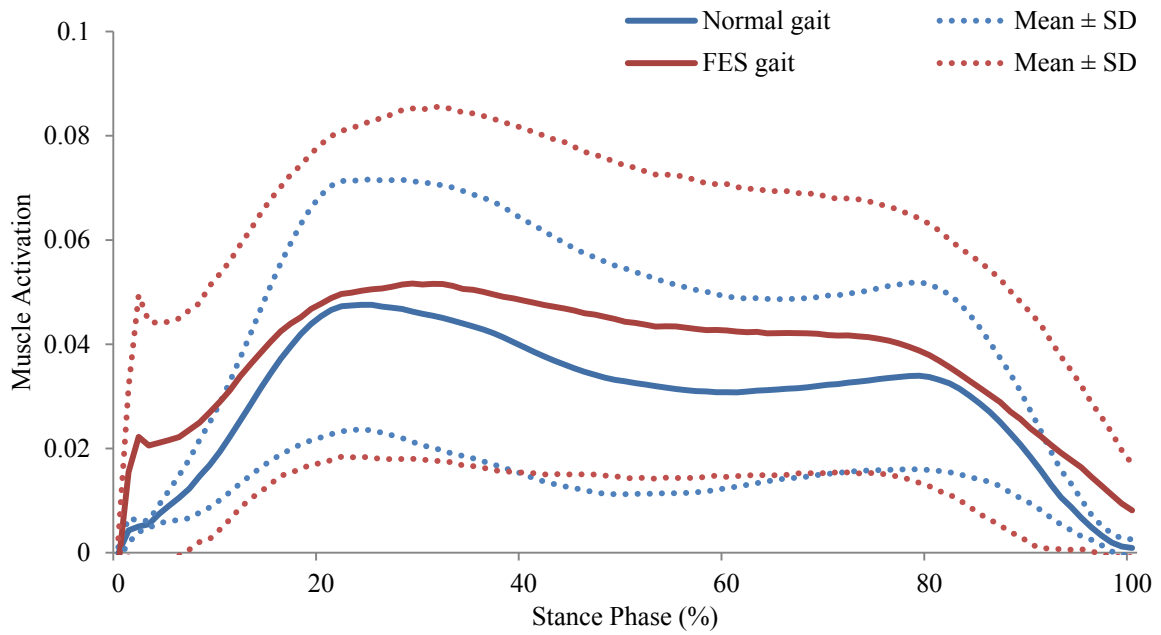


Figure 5.16 Gluteus maximus muscle activation (mean \pm SD) for 4 ACLD subjects

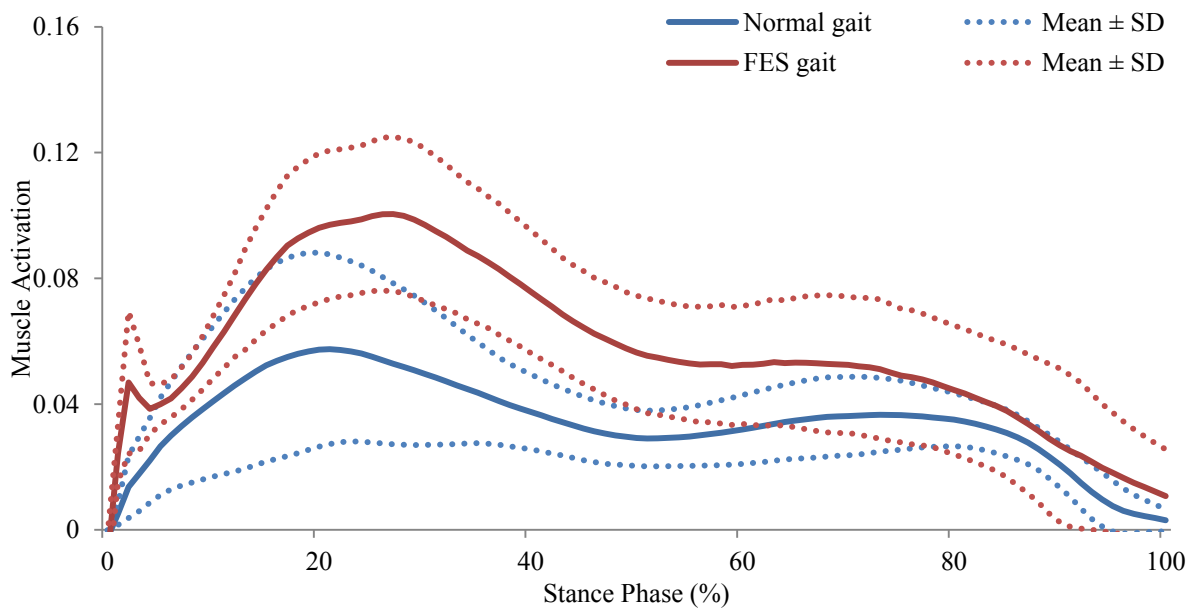


Figure 5.17 Gluteus maximus muscle activation (mean \pm SD) for 4 ACLR subjects

Gluteus medius muscle activation

The mean gluteus medius muscle activation for control, ACLD and ACLR subjects are shown in Figure 5.18, Figure 5.19 and Figure 5.20. There is a significant difference of the first peak gluteus medius muscle activation between groups for FES gait ($p=0.014$). There is significantly lower mean first peak gluteus medius muscle activation of the control group during normal gait (mean= 0.1021 ± 0.0180) compared to the ACLR group during FES gait (mean= 0.1693 ± 0.0928 ; $p=0.018$). The mean first peak curves of gluteus medius muscle activation during stance phase for the three groups are shown in Table 5.12.

Table 5.12 Peak gluteus medius activation for 8 control subjects, 4 ACLD subjects and 4 ACLR subjects (* $p < 0.05$)

Subject	Gluteus medius muscle activation					
	Normal gait			FES gait ($p=0.014$)*		
	Control*	ACLD	ACLR	Control	ACLD	ACLR ($p=0.018$)*
1	0.0708	0.0979	0.0938	0.0678	0.1234	0.1452
2	0.0892	0.1014	0.1625	0.1256	0.1313	0.2026
3	0.1041	0.0958	0.1286	0.1563	0.0650	0.1403
4	0.1007	0.1051	0.1280	0.0865	0.1342	0.1891
5	0.1040	-	-	0.1532	-	-
6	0.1289	-	-	0.1978	-	-
7	0.0976	-	-	0.1033	-	-
8	0.1214	-	-	0.0842	-	-
Mean	0.1021	0.1001	0.1282	0.1218	0.1135	0.1693
SD	0.0180	0.0536	0.0710	0.0445	0.0643	0.0928

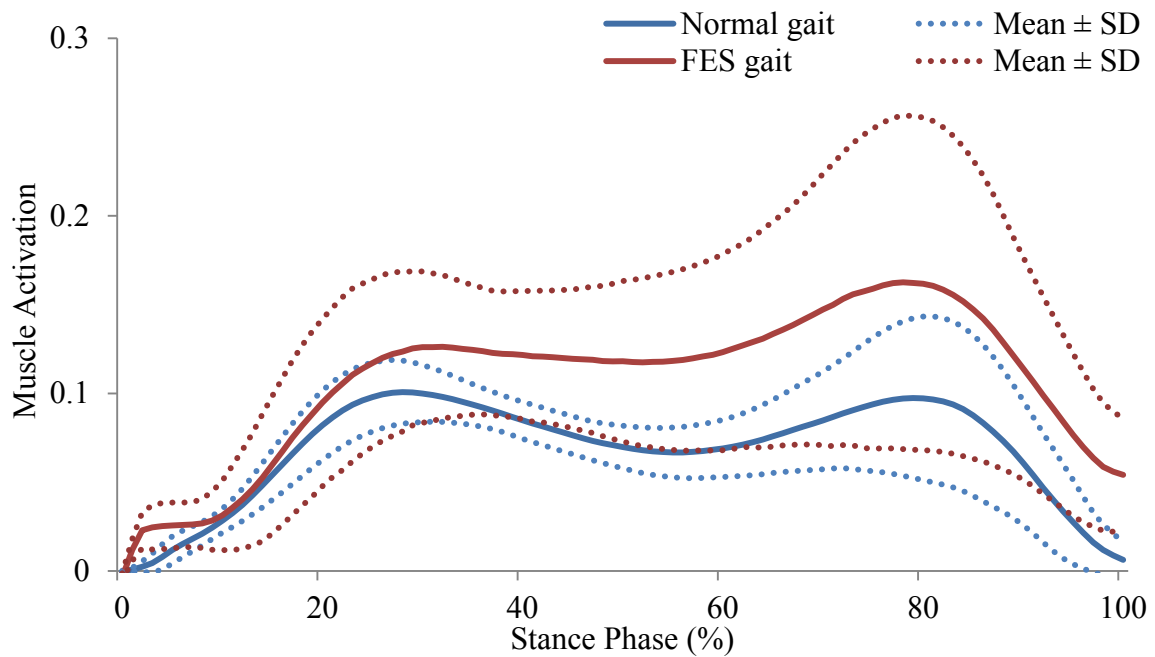


Figure 5.18 Gluteus medius muscle activation (mean \pm SD) for 8 control subjects

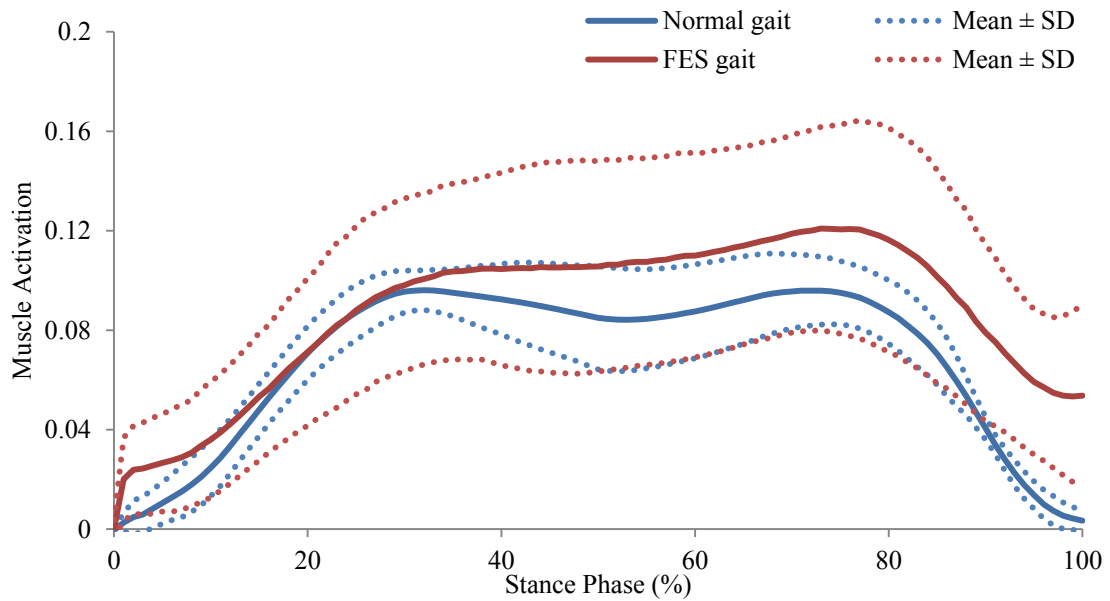


Figure 5.19 Gluteus medius muscle activation (mean \pm SD) for 4 ACLD subjects

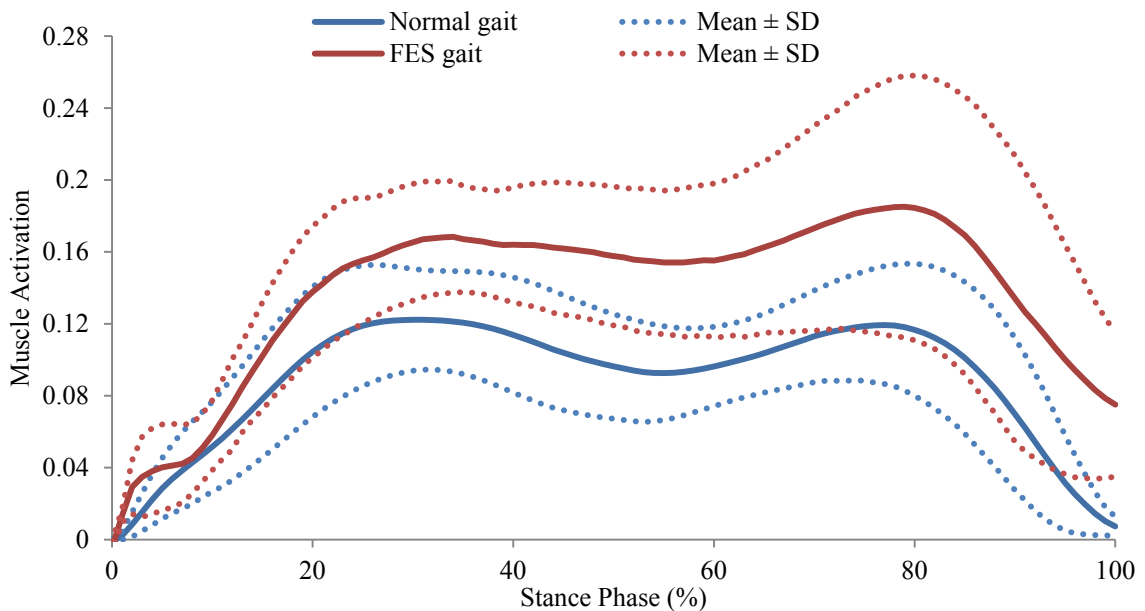


Figure 5.20 Gluteus medius muscle activation (mean \pm SD) for 4 ACLR subjects

Results summary

There is a significant difference between groups in peak internal rotation torque. Post hoc analysis found no pairwise differences. However, the Sprague and Geers metrics found that there are high differences in internal rotational torque curves between all two groups in terms of phase as shown in Table 5.7. Table 5.5 shows that the patient groups have lower internal rotation torque compared to the control group in normal gait. This result is counterintuitive, because the expectation of this study is that patients have knee instability with higher internal rotation torque compared to the control group. However, Table 5.6

shows that the BFLH stimulation with FES is able to reduce the internal rotation torque of the control group and the ACLD group but not in the ACLR group. This could be due to the ACLR group having tight ACL grafts which restricts the movement at the knee. Previous studies have shown that the surgical placement of the graft near to the central axis of the knee joint can have a significant effect on its resistance to rotatory loads (Kanamori et al., 2000; Woo et al., 2002; Yagi M, 2002).

There is a significant difference in peak anterior shear force between the control group during normal gait and the ACLD and ACLR groups during FES gait. There is a higher peak anterior shear force in the control group during normal gait compared to the ACLD group during FES gait. This result shows that the FES is successfully contracting the BFLH and reduced the peak anterior shear force of the ACLD group more than the ACLR group.

The FES stimulation of BFLH caused all groups to have slower gait compared to the normal gait. The control group has faster gait in normal gait and FES gait compared to the ACLD group in FES gait. The ACLD group has the slowest speed compared to other groups in both gaits. Table 5.9 shows that during normal gait the control group ($0.34\pm 0.04\text{m/s}$) walks faster compared to the patient groups. This would suggest kinematic differences between these groups; these were not analysed in this study. BFLH stimulation slows down the walking speed of all groups (Table 5.10).

The muscle activation results show that the ACLR group has the highest first peak gluteus muscle activation compared to the other groups. The FES stimulation of BFLH did not show any significant changes to the gluteus medius and gluteus maximus muscle activation of the ACLD group compared to other groups.

5.4 Discussion

ACL deficiency causes knee laxity in internal tibial rotation and anterior tibial translation. This is due to the shear and torque at the joint during activities of daily living not being adequately resisted by structures that can compensate for the ACL deficiency. Additionally, it is proposed that the joint position offset due to ACL deficiency increases the magnitude and effect of the shear and torque at the joint. The structures that may resist these loads include secondary ligamentous structures and muscles. BFLH is geometrically positioned to be able to apply posterior force on the tibia and increase the external rotational force to reduce the ACL deficient knee instability. Even ACLR patients may

have residual instabilities and, therefore, BFLH activation may also assist in these cases. This chapter tested, using a combined modelling and experimental approach, the hypothesis that activation of the BFLH can theoretically and practically reduce the anterior tibial shear, tibial internal rotation torque and speed of ACLD and ACLR subjects during the stance phase of gait. The hypothesis that activation of the BFLH can theoretically and practically increase the gluteus medius and gluteus maximus muscle activations is also discussed.

Internal rotation torque

There is a significant difference in the peak internal rotation torque between the three groups during normal gait ($p=0.040$). When stimulation of BFLH with FES is applied to the patient groups, they have a greater reduction in peak internal rotation torque compared to the control group ($p=0.038$). This indicates that FES reduces the internal rotation torque of both ACLD and ACLR patients.

The peaks of the tibial internal rotational torque for the three groups (Figure 5.1) took place at similar time frame, around 20% of stance phase, which is the transition from the end of loading response (4-19% of stance phase) to the beginning of the mid stance phase (20-50% of stance phase). This result is different from a study which claimed that the internal tibial rotational torque is during heel strike (Andriacchi et al., 2005). It is important to understand that the four sequential sub-phases in stance phase (initial contact, loading response, mid stance and terminal stance) are further grouped into weight acceptance (initial contact and loading response) and single limb support (mid stance and terminal stance) tasks (Perry et al., 2010). This means that the peak value of the tibial internal rotational torque occurred at the point of functional task transition weight acceptance (from weight bearing stability because of the initial double stance period) to the single limb support (progression over the stationary foot where the other foot starts to lift for swing). This transition causes instability at the knee joint where the tibia rotates more than usual. Thus, the exact time to reduce the peak tibial internal rotational torque of the patients by activating BFLH with FES is during this transition time.

Based on the Sprague and Geers' metric calculations, there was a positive phase error between the control group and the patients groups which indicate that the peak internal tibial rotational torque of the ACLD and ACLR groups has a time lag relative to the control group (Table 5.7). This means that the patients need the BFLH activation earlier

than the control group to support the progression of the single limb that is supporting the whole body weight. As expected, the magnitude of phase errors between these groups are highly dissimilar (Table 5.7) indicate that the patients tend to limit their internal tibial rotational movement during stance phase.

Surprisingly, there is no significant difference in peak internal rotation torque between the ACLD and ACLR groups during FES gait. This shows that the ACLR does not change much in terms of tibial internal rotation compared to the ACLD. However, there is phase error between the ACLD group during normal gait and ACLR group during FES gait which indicates that the ACLR group has a slight time lag relative to the ACLD group (Table 5.7).

In summary, the activation of BFLH with FES is able to reduce the peak of internal rotation torque in both ACLD and ACLR patients and occurs during the transition from weight acceptance task to single limb support task.

Anterior shear force

There is a significant difference in peak anterior shear force between the control group during normal gait and the ACLD and ACLR groups during FES gait ($p=0.002$). The stimulation of BFLH with FES on the ACLD group has a significantly smaller peak anterior shear force compared to the control group during normal gait ($p=0.003$). However, there is no significant difference in peak anterior shear force between the control group during normal gait and the ACLR group during FES gait. FES for the ACLD has successfully reduced the anterior shear force more than the ACLR group (Figure 5.6). It is hypothesised that this is due to more lateral laxity at the knee joint for the ACLD group compared to the ACLR group.

Based on the results obtained in this study, the peak of anterior shear force of all groups occurred during the transition from the weight bearing to single support limb task (approximately 20% of stance phase, Figure 5.6), similar to the occurrence of the peak of internal rotational torque. This corresponds to previous studies that found that the anterior shear force occurred during early stance phase (Lafortune et al., 1992) or during mid stance (Alkjaer et al., 2011; Gao et al., 2010). These results indicate that the activation of BFLH is needed most during this transition in order to stabilize the knee joint in both ACLD and ACLR patients.

It is interesting that patient ACLD1 (ACL full tear) (Figure 5.7) has a longer duration of anterior shear force compared to other ACLD subjects (Figure 5.8, Figure 5.9 and Figure 5.10). During loading response (3-19% of stance phase), the knee is flexed for shock absorption (from the instant foot drop during initial contact) with the help of the heel as a rocker (Perry et al., 2010). The body weight is aligned over the forefoot at the end of the mid stance phase (20-50% of stance phase). This subject may have increased the time of knee flexion (loading response) before having full knee extension in mid stance in order to support the full body weight gradually (Gao et al., 2010) at the same time avoiding quadriceps contraction (Berchuck et al., 1990). Moreover, patient ACLD1 has a longer duration of anterior shear force compared to other ACLD subjects; this may be explained by the shorter time after injury of this patient compared to other ACLD subjects. However, this study does not analyse the knee flexion angle during stance phase and this would be a good future study.

The spikes at the early stance phase in Figure 5.6 may be caused by co-contraction of other hamstrings muscles (biceps femoris short head, semitendinosus and semimembranosus - as has been shown by (Biscarini et al., 2013) during the activation of biceps femoris long head with FES. ACL deficient subject have been shown to have atypical hamstrings EMG profiles during stance phase (Boerboom et al., 2001).

Speed

The control group (0.34 ± 0.04 m/s) walks faster than the ACLD (0.26 ± 0.06 m/s) and ACLR (0.33 ± 0.06 m/s) groups in during normal gait (Table 5.9) and FES gait. This indicates that there is abnormality in the walking of the patients. The differences in FES gait can be explained by a number of factors, including that the FES activation was for the whole of the stance phase, including portions of the stance phase where an anteriorly directed shear force was not present and so the activation produced an elevated posterior shear force. In the future, the BFLH stimulation should be activated during the transition from the weight bearing to single support limb task. This would likely be more comfortable for the patient groups. The reason for overall reduction in walking speed for the patient groups even without FES can be explained from the literature in which it is known that they do not fully extend their knee during stance phase and so introduce a reduced stride length and slower gait (Gao et al., 2010).

Gluteus maximus and gluteus medius muscle activation

Gluteus maximus and gluteus medius are muscles that support the whole body during the mid stance phase (Anderson et al., 2003; Winter et al., 1987), whereby the peak of the tibial rotation torque and peak anterior shear force take place at the same time. During the mid stance phase, the first peak of both gluteus maximus and gluteus medius occurred. The high activation of BFLH is able to increase the gluteus maximus muscle activation which has been shown in Chapter 4. In this chapter, the stimulation of BFLH with FES is able to show that it affects the gluteus group muscle during mid stance.

The first peak of gluteus maximus muscle activation is significantly lower for the ACLD than ACLR group during FES gait ($p=0.043$) and first peak of gluteus medius muscle activation is significantly lower for the control than ACLR group during FES gait ($p=0.018$). Among the three groups, the ACLD group has the lowest peak gluteus medius and gluteus maximus muscle activation during both normal and FES gait. The reason for this could be that the ACLD group do not fully extend their knee during mid stance in order to restrict the gluteus muscles to fully support the whole body. This has been proposed elsewhere in the literature (Berchuck, 1990). The whole body of ACLD patients could be supported by the gluteus group of the contralateral leg during mid stance.

Limitations

This study shows a small mean value of the internal rotation torque of the three groups during the normal and FES gait. The findings suggest that there is no significant difference of peak anterior shear forces between the control group during normal gait and the ACLR group during FES gait. It may be that the study is underpowered to find a significant difference, and a power analysis could now be conducted to see what group sizes are required to follow on from this pilot study. Besides, there is a large gap in the duration time between the injury and surgery and the experiments were carried out at different times for both groups. Time and small sample size have an effect on the results of the test statistic used in this study. However, this study did show that the activation of BFLH with FES is able to reduce the anterior shear force of ACLD and ACLR group during stance phase. This finding is probably due to the variable degree of laxity of the ligaments and the different anatomic configuration of the knee between the subjects.

Comparing the knee instability of ACLD and ACLR leg with contralateral leg as a control could provide a better knowledge on the effect of the BFLH activation with FES. This is

because the compensatory strategy to stabilise the ruptured ACL could be supported by the contralateral leg. There is evidence that ACLD patients walk with a symmetrical gait that means that the unaffected limb reproduces the abnormal moment at the knee and at the hip (Berchuck et al., 1990). This would suggest that it may be possible that the activation of muscles on the contralateral leg could provide knee stability on the injured leg through creating a more physiological symmetrical gait.

The musculoskeletal model used in this study is a non-subject specific model. The anatomical model in this study is taken from a healthy subject and thus this model does not comprehensively simulate the conditions of ACLD and ACLR. It is known that after the loss of the ACL function, the axis of internal rotation of the knee that is normally at the middle of the tibial plateau surface is shifted to the medial side of the tibia. However, to find the exact position of the axis of rotation for each individual is quite challenging because it varies between individuals. The different morphologies of the tibial plateau surface with convexities, concavities and differences in posterior slope between medial and lateral sides (Hashemi et al., 2008; Lankester et al., 2008), also make it difficult to locate the axis of rotation for each subject.

Activating BFLH changes the movement pattern of other muscles and ligaments. For example, the medial collateral ligament (MCL) is the secondary stabiliser after ACL injury. The iliotibial band also acts as an anterolateral stabiliser of the tibia (Kwak et al., 2000), because of its attachment on the lateral tubercle of the tibia. These could all be investigated by looking at the changes in the activity of other muscles.

Besides, it is also interesting to explore the lower limb muscle activity in the whole gait cycle because the original muscle activity of BFLH is only at the early stance phase but in this study the activation of BFLH was increased beyond its natural levels. It is also important to note that the external tibial rotation reduction at the end of the swing phase causes the anterior tibial shear reduced for the ACLD knee (Andriacchi et al., 2005). Thus, the transition between swing phase and stance phase is also an important consideration in evaluating the ACLD knee (Beynon et al., 2002). Figure 5.6 shows that after 80% of stance phase the posterior shear forces became elevated. This mirrors the results found in Chapter 3 (Figures 3.21-3.32). Therefore, to mitigate any detrimental posterior forces, the recommendation from this work would be that stimulation should stop after 80% of stance phase and should not extend for the whole of the stance phase.

In the future, kinematics data should also be analysed; this would enable comprehensive analyses of the effect of BFLH stimulation with FES in both ACLD and ACLR patients. The contralateral leg should also be analysed to enable the questions of symmetry in pathological gait to be assessed.

5.5 Conclusion

This pilot study has shown the potential for activation of BFLH to reduce knee instability in both internal rotational torque and the anterior shear force specifically during the transition from the loading response to the mid stance phase for both ACLD and ACLR subjects. Treatment with FES during walking activity could potentially provide better knee stability and performance for ACL deficient and ACL reconstructed patients. The model used in this study can be improved to be applied in designing a rehabilitation device or a device to stimulate the correct muscle at a predefined time that can be used to assist ACLD and ACLR patients in undergoing their gait activity.

CHAPTER 6

Discussion and conclusions

This chapter summarises the key findings from this thesis and places them in the context of other work in the field. Future work is proposed and discussed by way of specific alternative musculoskeletal pathologies that may benefit from selective muscle activation through FES as defined by musculoskeletal modelling.

6.1 Key findings

This thesis has explored the ability of FES to provide knee stability for ACLD and ACLR patients through a series of three main studies utilising musculoskeletal modelling and in vivo studies. In Chapter 3, it was shown that the selective activation of the BFLH can reduce the tibial anterior shear force, a surrogate of ATT and the internal tibial rotational torque at the knee in healthy subjects. A musculoskeletal model was modified to enable this analysis to take place. The modelling cost function was modified from its standard form by assigning a weighting, c , to simulate BFLH stimulation. The peaks of reduction of tibial internal rotational torque occurred during weight acceptance, near full knee extension, which is the time when the ACL is loaded. The hamstrings on the medial side could also reduce anterior shear force and this has been shown in other modelling studies (Shelburne et al., 2005). The reduction of the tibial internal rotational torque also indirectly affects the value of the anterior shear force (More et al., 1993) as can be derived through a simple equivalent force analysis. The value of c for each subject that reduced anterior shear force to zero was found and the mean value of c across all was 0.208. According to Liu et al (2000), hamstring activation without FES has shown that 56% of the maximal hamstring muscle force could reduce the ATT to a normal level during the stance phase of gait. It is important to note that the knee joint force may increase by activating BFLH and thus provide additional stability at the knee through concavity-compression. The knee joint reaction force was not focussed in this chapter. However, based on a model by Catafalmo (2015), 50% stimulation of BFLH is more appropriate than 100% of BFLH stimulation because there will be less knee joint reaction force and could avoid further deterioration towards the surface of the tibia. The results from this chapter showed that the posterior pull of the extra activation of the BFLH by FES resulted in a slower speed than normal gait. The modified musculoskeletal model used in this chapter was then validated in Chapter 4.

In Chapter 4, the muscle forces calculated from the musculoskeletal model were validated non-invasively using electromyography (EMG). To avoid the problem of EMG signals being affected by the FES currents, a pair of muscles which are located a distant to each other were selected. The knee flexor muscle, BFLH was chosen as the stimulated muscle and its compensatory muscle for hip extensor (Kendall et al., 1993; Perry et al., 2010), gluteus maximus, was chosen as the EMG measuring muscle. The results showed that there was no FES artefact affecting the EMG signals. This study has found statistical correlations between peak and impulse of gluteus maximus activation between modelling

and EMG signals which provide a level of validation for the algorithm used in the musculoskeletal model and show that FES stimulation potentially can be tuned to a level to achieve different outcomes. Both mean peak gluteus maximus muscle activation predicted from the models and mean peak gluteus maximus activity from EMG measurement occurred during mid stance (20-50% of stance phase); prior work has also shown that this takes place in mid stance (Winter et al., 1987).

Interestingly, these results seem to contradict the literature which highlights that when the hamstrings action is reduced, the gluteus maximus activity should be increased during loading response to provide hip stability. In our study, the activation of BFLH caused the the gluteus maximus activity to increased. The reason for this could be because the BFLH and gluteus maximus actions are multi joint processes and there is a “sweet spot” of hamstrings activation that maintains a minimal gluteus maximus activation and if the hamstrings either over- or under-activate, then gluteus maximus has to provide compensation. A ‘sweet spot’ is a location at which maximum response can be produced due to a combination of factors and a given amount of effort. The gluteus maximus and hamstrings are the hip extensor and knee flexors respectively and have increasing activity in late swing to control the forward movement of the swinging lower limb (Winter et al., 1987). Moreover, the hip extensor muscles have two functions, firstly to decelerate the limb’s momentum in terminal swing to prepare for stance, and secondly to restrain the forward momentum of the pelvis and trunk as the limb is loaded (Perry et al., 2010). In addition, during stance phase, the primary muscles controlling the hip are the extensors and abductors, which include the gluteus maximus. The extra activation of the BFLH with FES in this study forced gluteus maximus activity to be activated from late mid swing through the loading response more than usual. As the hamstrings and gluteus maximus have a complementary role as the plantar flexors, this might also change not only the kinematics of the foot (Jonkers et al., 2003) but also of the knee and hip during early stance phase. Both BFLH and gluteus maximus also assist in lateral rotation of the tibia. These multi-joint actions provide an explanation for why the extra activation of BFLH with FES contributes to such large changes to gluteus maximus muscle activity and demonstrate the complexity of this “sweet spot” of activation.

The validated musculoskeletal model from Chapter 4 was used in Chapter 5 in a patient group. This study found that activation of BFLH with FES at the knee of the healthy, ACLD and ACLR groups was able to reduce the internal tibial rotational torque and

anterior tibial shear force specifically during the transition from the loading response to the mid stance phase and it could be applied to any type of ACLD and ACLR.

This model of muscular function and joint stability at the knee with the selective application of FES can potentially be used to plan and implement rehabilitation treatment. For example, rehabilitation is accelerated at a certain period after injury or surgery and FES could be incorporated in a device that can be used to assist in this rehabilitation by not only improving musculature before a return to more vigorous activities, but also to assist in muscle control through selective activation at particular points during an activity. This may enable ACL non-copers to become ACL copers.

6.2 The role of FES in rehabilitation

Today FES is available as a rehabilitation treatment for various conditions including spinal cord injury (SCI), ACLD/ACLR, cerebral palsy (CP) and osteoarthritis (OA).

Spinal cord injury (SCI)

SCI is caused by diseases that destroy the neurological tissue of the spinal cord which can result in a partial or total loss of sensory function, paralysis, or both to parts of the body below the level of the injury. Clinically, FES has been widely used to stimulate paralyzed or paretic muscles caused by upper motor neuron lesions experienced by SCI patients (Lynch et al., 2008).

FES stimulates and contracts one or more muscles to exert torques about a joint. By modulating the intensity of stimulation delivered to the flexor and extensor muscles, the resulting joint angle can be controlled to actuate the joint in opposite directions (Lynch et al., 2008). Large numbers of FES rehabilitation robots have been introduced to assist the SCI and stroke patients in functional activities. For example, rehabilitation orthosis LOKOMAT (Jezernik et al., 2003) and a hybrid neuroprosthesis that uses an electric motor-based wearable exoskeleton (Alibeji et al., 2015).

FES technology is designed to offer better mobility to the patients suffering from SCI. FES is now considered to be one of the safest techniques to apply currents to stimulate various human organs (e.g. assistance with respiration, bowel/bladder activity or some return of upper or lower limb function) of the body which is disabled due to SCI (Hamid et al., 2008). It is proven that the quality of life of SCI patients treated using FES increases due to restored mobility function.

The musculoskeletal modelling approach used in this thesis could also be applied to SCI, through the selective analysis of the effect of muscle stimulation on joint dynamics, joint mechanics, and muscle mechanics. However, the application of this approach to joints other than the knee would need validation; it is known that knee control is fundamentally a mechanically-mediated process that is amenable to musculoskeletal modelling, yet other joints may have other major factors driving the control of the joints and therefore musculoskeletal modelling might not be the most appropriate technique to assess FES stimulation.

ACLD and ACLR

Apart from SCI, FES is employed to restore quadriceps strength of the ACLD and ACLR patients. Quadriceps muscles are often affected by arthrogenic muscle inhibition and muscle atrophy after ACL reconstruction, which limits volitional contraction. To generate better quadriceps strength and improve knee functional outcome, voluntary exercise together with FES, which directly recruits the motor neurons, is highly recommended (Palmieri-Smith et al., 2008).

The rehabilitation treatment for ACLD and ACLR is focussing more on strengthening the quadriceps of the injured leg compared to the hamstring. To strengthen the quadriceps with FES, patients need to attend three rehabilitation sessions per week until the quadriceps maximal volitional isometric contraction is 80% of the uninvolved side (Adams et al., 2012). This thesis has proposed that this alone will not be able to provide stability to these patients, as the selective, timed, activation of the hamstrings can provide joint stability that wouldn't be provided by quadriceps strengthening alone. In fact, it may even be the case that quadriceps strengthening without hamstrings excitation (and, perhaps strengthening), could be detrimental.

Cerebral Palsy (CP)

FES is useful in CP treatment program to control selective muscle (Papavasiliou, 2009) or reducing spasticity of CP (Kerr et al., 2004). Children with CP are offered FES as an option for a treatment to achieve a direct "orthotic" effect during gait. Among FES functionality is to stimulate quadriceps to extend the knee during stance phase or to stimulate ankle dorsiflexors to lift the foot during swing phase. By employing FES within the treatment, the neural pathway will be improved. In long term, it reduces the tendency

for muscle atrophy and improved motor control (van der Linden et al., 2008). This improved motor control is tantalising and it follows that a hypothesis could be proposed that FES for ACLD and ACLR could improve motor control in the long run.

Osteoarthritis (OA)

Similar to ACLD, patients with osteoarthritis (OA) of the knee have quadriceps weakness and arthrogenic muscle inhibition. Knee OA is a painful condition causing disability and muscle weakness especially to the older people. FES combined with exercise routine could aid in increasing muscle strength. This leads to reduced pain, as well as decreased joint stiffness and muscle spasm (Durmus et al., 2007).

OA patients usually undergo total knee arthroplasty (TKA) to reduce pain and improve knee function. Yet, TKA could cause weak quadriceps after surgery. Thus, to strengthen the quadriceps activation failure and weakness experienced by patients, exercise that emphasize on strong muscle contraction and clinical tools while facilitating muscle activation, such as biofeedback and FES, may be necessary (Stevens et al., 2003).

Selective activation of muscles on the lateral aspect of the knee such as biceps femoris can also be used to delay medial knee osteoarthritis (Hodges et al., 2016) and prior musculoskeletal modelling work has shown that FES can altering joint loading at the knee to reduce the medial loading (Rane et al., 2016; Xu et al.). This selective muscle activation for OA is a direct comparison to the work presented in this thesis for ACLD and ACLR.

6.3 FES and muscle learning

It is known that there are synergistic relationships between ligaments and muscles in maintaining knee joint stability. The increasing length and tension in the ligament requires an increase in muscular force acting in the other direction in order to sustain joint stability. The sensory role of the ligaments via their inputs to the spinal cord motor units could provide balance to the antagonist muscle pair in an excitatory and inhibitory load. After ACL injury, this synergistic relationship between ACL and hamstring muscles might be reduced.

Ligaments also provide a source of reflex arc to relevant muscles through mechanoreceptors. The mechanoreceptors within the ACL and other knee ligaments transmit afferent information that may be processed as a reflex with the purpose of contracting musculature to decrease forces at the knee. It has been shown that this reflex

arc can be re-established after ligament reconstruction surgery, suggesting that mechanoreceptor have re-innervated the grafted ACL allowing for more normalized afferent function. This finding provides evidence that an ACL reflex exists, and can have both an excitatory and inhibitory component. It may be that this can be recovered in ACLD patients; Solomonow (2006) found that after only a few days' of use of a smart brace with FES, muscle re-learning occurs through which hamstring activation is elevated to prevent subluxation even if the 'smart brace' is deactivated. This tantalising result demonstrates that selective FES activation might be able to be used in rehabilitation only and might not be required for chronic use beyond a period of learning. This has been described as a "carry over" effect which occurs after stimulating a muscle with FES for a duration of time (Rushton, 2003), in which the 'carry over' effect may be short- or long-lasting. The study claimed that FES stimulation may somehow provide adaptive changes in cortical connectivity. This mechanism provides training or 'learning' of the muscles after stimulation by the FES (Waters, 1984). In SCI patients, Rushton (2003) deduced that FES stimulation must be simultaneously combined with voluntary effort activating the residual through a damaged pyramidal motor system, to help promote restorative synaptic modifications of these patients. This mechanism also indicates that the electrical stimulation applied at rest alone would not be expected to be beneficial to "train" the muscles (Rushton, 2003). This explains why some patients are not successful in recovering their leg functional movement while using the electrical stimulator device (Rushton, 2003).

6.4 Muscle learning and its application in medicine or physiotherapy

Based on the literature, the FES is able to improve muscle strength, improve flexibility and range of motion of the affected limb and reducing the amount of spasticity in CP patients. The treatment of the patients needs to be follow up for days or months to make sure that the FES has completely restored the functional limb. As shown above, there is a high possibility that a muscle can 'learn' after stimulation with FES. The understanding of learning and the 'carry over' effect on muscle after the FES stimulation also can be applied in rehabilitation programmes. The muscle learning process involves sensory organ which can transmit afferent information to the nervous system. However, it is a challenging task to find the right muscle or sensory organ to be stimulated during any functional activity. It is also difficult to find the most suitable time to successfully 'educate' the muscle during any functional activity. The biopotential feedback (e.g. EMG) could assist in predicting the suitable muscle for stimulation muscle and the right time during any rehabilitation activity.

6.5 Conclusions

The benefit of using FES in rehabilitation treatment has previously been shown in treating SCI, CP and OA and this work has expanded its potential utility still further. In this thesis, stimulating BFLH with FES was shown to be able to reduce the knee instability of ACLD and ACLR patients. Therefore, besides quadriceps, the rehabilitation treatment should focus on appropriate timed activation of the BFLH to improve the quality of life of patients. However, there are also other kinematic and kinetic changes to the lower limb during the FES stimulation that should be taken into consideration, these include speed of motion, joint reaction forces, and forces in other muscles. Harnessing the muscle ‘learning’ effect through FES stimulation is a tantalising prospect to improve and accelerate the rehabilitation treatment process and this should be further investigated.

APPENDIX A : Ethics

Imperial College
London

Imperial College Research Ethics Committee

Imperial College London
Room 5L10D, 5th Floor, Lab Block
Charing Cross Hospital
Fulham Palace Road
London
W6 8RF

Tel: +44 (0)203 331 0208 Fax: +44 (0) 203 311 0203

researchethicscommittee@imperial.ac.uk

Professor Antony Bull
Bioengineering Department
Imperial College London
London
SW7 2AZ

4th August 2014

Dear Professor Bull,

Study Title: Analysis and reduction of the4 medical contact force in the knee for medical compartment osteoarthritis.

ICREC reference: 14IC2134

The above study was approved by your Head of Department on 23rd June 2014 and by the Joint Research Compliance Office on the 31st July 2014.

Under the Imperial College Research Ethics Committee process, a study that has been reviewed by the Joint Research Compliance Office and Head of Division/Department (or Principal), where no significant ethical issues have been identified in the protocol or ethics application, can be approved without requiring it to go to full committee.

Documents

The documents reviewed were:

- ICREC Application form
- Study Protocol (V3 30/06/14)
- Participant Information sheet (V3 30/06/14)
- Consent Form (V3 30/06/14)
- Pain Questionnaire (V3 30/06/14)
- Recruitment email (V3 30/06/14)
- Recruitment advertisement (V3 30/06/14)
- Sponsorship and Insurance form

Yours sincerely,



Gary Roper,
Head of Regulatory Compliance,
Imperial College London

Imperial College of Science, Technology and Medicine

Prof Anthony Bull
Imperial College London
Department of Bioengineering,
Room 3.11, Royal School of Mines Building,
SW7 2AZ

Email: hra.approval@nhs.net

16 November 2016

Dear Professor Bull,

Letter of HRA Approval

Study title:	Musculoskeletal Modelling to Analyse and Treat Anterior Cruciate Ligament (ACL) deficiency
IRAS project ID:	190024
Protocol number:	N/A
REC reference:	16/LO/1646
Sponsor	Imperial College London

I am pleased to confirm that **HRA Approval** has been given for the above referenced study, on the basis described in the application form, protocol, supporting documentation and any clarifications noted in this letter.

Participation of NHS Organisations in England

The sponsor should now provide a copy of this letter to all participating NHS organisations in England.

Appendix B provides important information for sponsors and participating NHS organisations in England for arranging and confirming capacity and capability. **Please read *Appendix B* carefully**, in particular the following sections:

- *Participating NHS organisations in England* – this clarifies the types of participating organisations in the study and whether or not all organisations will be undertaking the same activities
- *Confirmation of capacity and capability* - this confirms whether or not each type of participating NHS organisation in England is expected to give formal confirmation of capacity and capability. Where formal confirmation is not expected, the section also provides details on the time limit given to participating organisations to opt out of the study, or request additional time, before their participation is assumed.
- *Allocation of responsibilities and rights are agreed and documented (4.1 of HRA assessment criteria)* - this provides detail on the form of agreement to be used in the study to confirm capacity and capability, where applicable.

Further information on funding, HR processes, and compliance with HRA criteria and standards is also provided.

It is critical that you involve both the research management function (e.g. R&D office) supporting each organisation and the local research team (where there is one) in setting up your study. Contact details and further information about working with the research management function for each organisation can be accessed from www.hra.nhs.uk/hra-approval.

Appendices

The HRA Approval letter contains the following appendices:

- A – List of documents reviewed during HRA assessment
- B – Summary of HRA assessment

After HRA Approval

The document “*After Ethical Review – guidance for sponsors and investigators*”, issued with your REC favourable opinion, gives detailed guidance on reporting expectations for studies, including:

- Registration of research
- Notifying amendments
- Notifying the end of the study

The HRA website also provides guidance on these topics, and is updated in the light of changes in reporting expectations or procedures.

In addition to the guidance in the above, please note the following:

- HRA Approval applies for the duration of your REC favourable opinion, unless otherwise notified in writing by the HRA.
- Substantial amendments should be submitted directly to the Research Ethics Committee, as detailed in the *After Ethical Review* document. Non-substantial amendments should be submitted for review by the HRA using the form provided on the [HRA website](http://www.hra.nhs.uk), and emailed to hra.amendments@nhs.net.
- The HRA will categorise amendments (substantial and non-substantial) and issue confirmation of continued HRA Approval. Further details can be found on the [HRA website](http://www.hra.nhs.uk).

Scope

HRA Approval provides an approval for research involving patients or staff in NHS organisations in England.

If your study involves NHS organisations in other countries in the UK, please contact the relevant national coordinating functions for support and advice. Further information can be found at <http://www.hra.nhs.uk/resources/applying-for-reviews/nhs-hsc-rd-review/>.

If there are participating non-NHS organisations, local agreement should be obtained in accordance with the procedures of the local participating non-NHS organisation.

User Feedback

The Health Research Authority is continually striving to provide a high quality service to all applicants and sponsors. You are invited to give your view of the service you have received and the application

IRAS project ID	190024
-----------------	--------

procedure. If you wish to make your views known please email the HRA at hra.approval@nhs.net. Additionally, one of our staff would be happy to call and discuss your experience of HRA Approval.

HRA Training

We are pleased to welcome researchers and research management staff at our training days – see details at <http://www.hra.nhs.uk/hra-training/>

Your IRAS project ID is **190024**. Please quote this on all correspondence.

Yours sincerely

Michael Higgs
Assessor

Email: hra.approval@nhs.net

*Copy to: Miss Ruth Nicholson, Imperial College London & Imperial College Healthcare NHS Trust
Miss Nur Liyana Azmi, Imperial College London*

IRAS project ID	190024
-----------------	--------

Appendix A - List of Documents

The final document set assessed and approved by HRA Approval is listed below.

<i>Document</i>	<i>Version</i>	<i>Date</i>
Copies of advertisement materials for research participants [Poster]	1	06 October 2016
Evidence of Sponsor insurance or indemnity (non NHS Sponsors only)		19 July 2016
GP/consultant information sheets or letters	1	01 July 2016
Instructions for use of medical device [Safety guideline using FES]	1	06 October 2016
IRAS Application Form [IRAS_Form_22082016]		22 August 2016
Non-validated questionnaire [Participant Data]	1	01 July 2016
Participant consent form	3	15 November 2016
Participant information sheet (PIS)	3	15 November 2016
Research protocol or project proposal [Protocol for nonCTIMPS]	5	01 July 2016
Summary CV for Chief Investigator (CI)		
Summary CV for student		
Summary CV for supervisor (student research)		
Validated questionnaire [Pain Questionnaire]	1	01 July 2016

Appendix B - Summary of HRA Assessment

This appendix provides assurance to you, the sponsor and the NHS in England that the study, as reviewed for HRA Approval, is compliant with relevant standards. It also provides information and clarification, where appropriate, to participating NHS organisations in England to assist in assessing and arranging capacity and capability.

For information on how the sponsor should be working with participating NHS organisations in England, please refer to the, *participating NHS organisations, capacity and capability and Allocation of responsibilities and rights are agreed and documented (4.1 of HRA assessment criteria) sections in this appendix.*

The following person is the sponsor contact for the purpose of addressing participating organisation questions relating to the study:

Name: Miss Ruth Nicholson
 Tel: 020 7594 1862
 Email: r.nicholson@imperial.ac.uk

HRA assessment criteria

Section	HRA Assessment Criteria	Compliant with Standards	Comments
1.1	IRAS application completed correctly	Yes	No comments
2.1	Participant information/consent documents and consent process	Yes	The sponsor amended the PIS and Consent Form to align with HRA Approval standards.
3.1	Protocol assessment	Yes	No comments
4.1	Allocation of responsibilities and rights are agreed and documented	Yes	This is a non-commercial single site study taking place in the NHS where that single NHS organisation's partner University is the study sponsor. A Statement of Activities or Schedule of Events is not expected to be used.
4.2	Insurance/indemnity arrangements assessed	Yes	Where applicable, independent contractors (e.g. General Practitioners) should ensure that the professional

Section	HRA Assessment Criteria	Compliant with Standards	Comments
			indemnity provided by their medical defence organisation covers the activities expected of them for this research study.
4.3	Financial arrangements assessed	Yes	No application for external funding has been made.
5.1	Compliance with the Data Protection Act and data security issues assessed	Yes	The sponsor amended the PIS and Consent Form to align with HRA Approval standards.
5.2	CTIMPS – Arrangements for compliance with the Clinical Trials Regulations assessed	Not Applicable	No comments
5.3	Compliance with any applicable laws or regulations	Yes	No comments
6.1	NHS Research Ethics Committee favourable opinion received for applicable studies	Yes	A REC favourable opinion was issued by the London – Queen Square Research Ethics Committee on 11 October 2016. Amended documents were submitted by the researchers to comply with HRA Approval standards. These were submitted as a non-substantial amendment.
6.2	CTIMPS – Clinical Trials Authorisation (CTA) letter received	Not Applicable	No comments
6.3	Devices – MHRA notice of no objection received	Not Applicable	No comments
6.4	Other regulatory approvals and authorisations received	Not Applicable	No comments

Participating NHS Organisations in England

This provides detail on the types of participating NHS organisations in the study and a statement as to whether the activities at all organisations are the same or different.

This is a non-commercial study where the only NHS site will act as a participant identification centre, at which members of potential participants care team will review medical records to identify potentially eligible patients. Recruitment posters will also be displayed in the NHS site. Research activity will take place at a non-NHS site.

If this study is subsequently extended to other NHS organisation(s) in England, an amendment should be submitted to the HRA, with a Statement of Activities and Schedule of Events for the newly participating NHS organisation(s) in England.

The Chief Investigator or sponsor should share relevant study documents with participating NHS organisations in England in order to put arrangements in place to deliver the study. The documents should be sent to both the local study team, where applicable, and the office providing the research management function at the participating organisation. For NIHR CRN Portfolio studies, the Local LCRN contact should also be copied into this correspondence. For further guidance on working with participating NHS organisations please see the HRA website.

If chief investigators, sponsors or principal investigators are asked to complete site level forms for participating NHS organisations in England which are not provided in IRAS or on the HRA website, the chief investigator, sponsor or principal investigator should notify the HRA immediately at hra.approval@nhs.net. The HRA will work with these organisations to achieve a consistent approach to information provision.

Confirmation of Capacity and Capability

This describes whether formal confirmation of capacity and capability is expected from participating NHS organisations in England.

This study has a single NHS PIC site with existing arrangements with its partner University. The R&D office will confirm to the CI when the study can start.

Principal Investigator Suitability

This confirms whether the sponsor position on whether a PI, LC or neither should be in place is correct for each type of participating NHS organisation in England and the minimum expectations for education, training and experience that PIs should meet (where applicable).

A Principal Investigator has been identified for the NHS PIC site.

GCP training is not a generic training expectation, in line with the [HRA statement on training expectations](#).

HR Good Practice Resource Pack Expectations

IRAS project ID	190024
-----------------	--------

This confirms the HR Good Practice Resource Pack expectations for the study and the pre-engagement checks that should and should not be undertaken

No staff not employed by the NHS Trust will be involved in activities at that site.

Other Information to Aid Study Set-up

This details any other information that may be helpful to sponsors and participating NHS organisations in England to aid study set-up.

The applicant has indicated that they do not intend to apply for inclusion on the NIHR CRN Portfolio.

APPENDIX B : Gluteus maximus muscle activations predicted from modelling and the measured EMG. These results are summarised in Chapter 4.

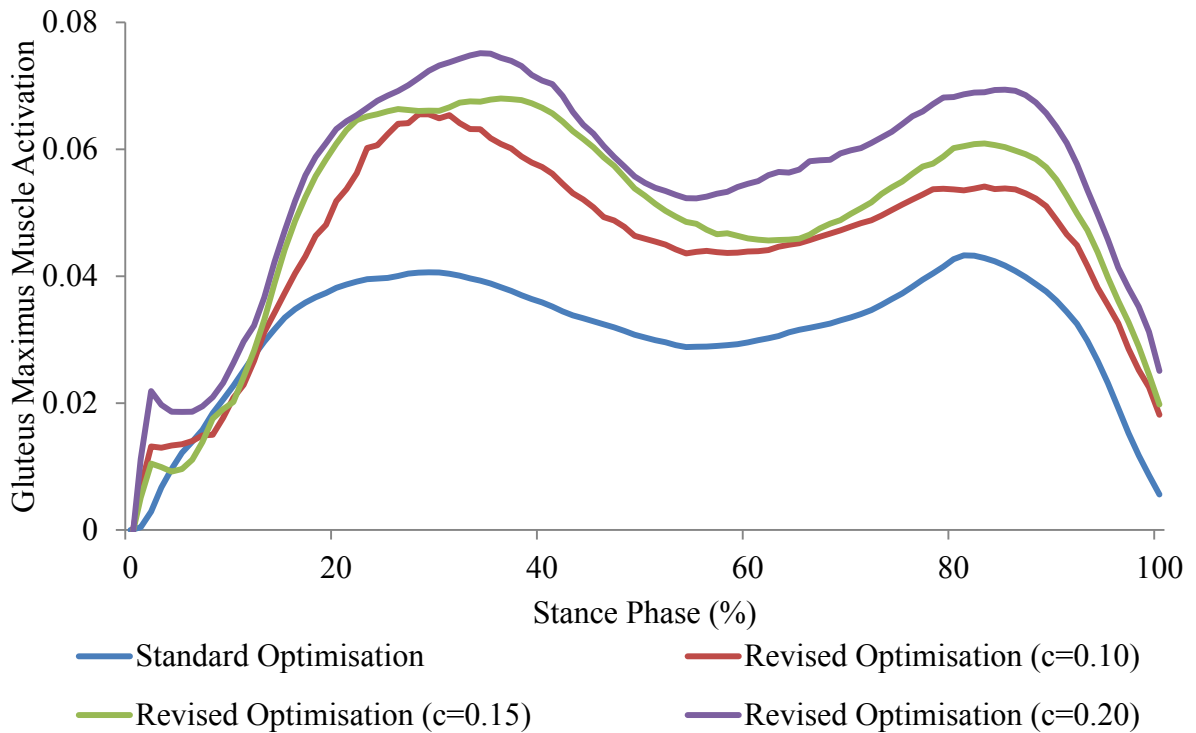


Figure B.1 Gluteus maximus model predictions of subject 1 in normal walking and FES applied walking

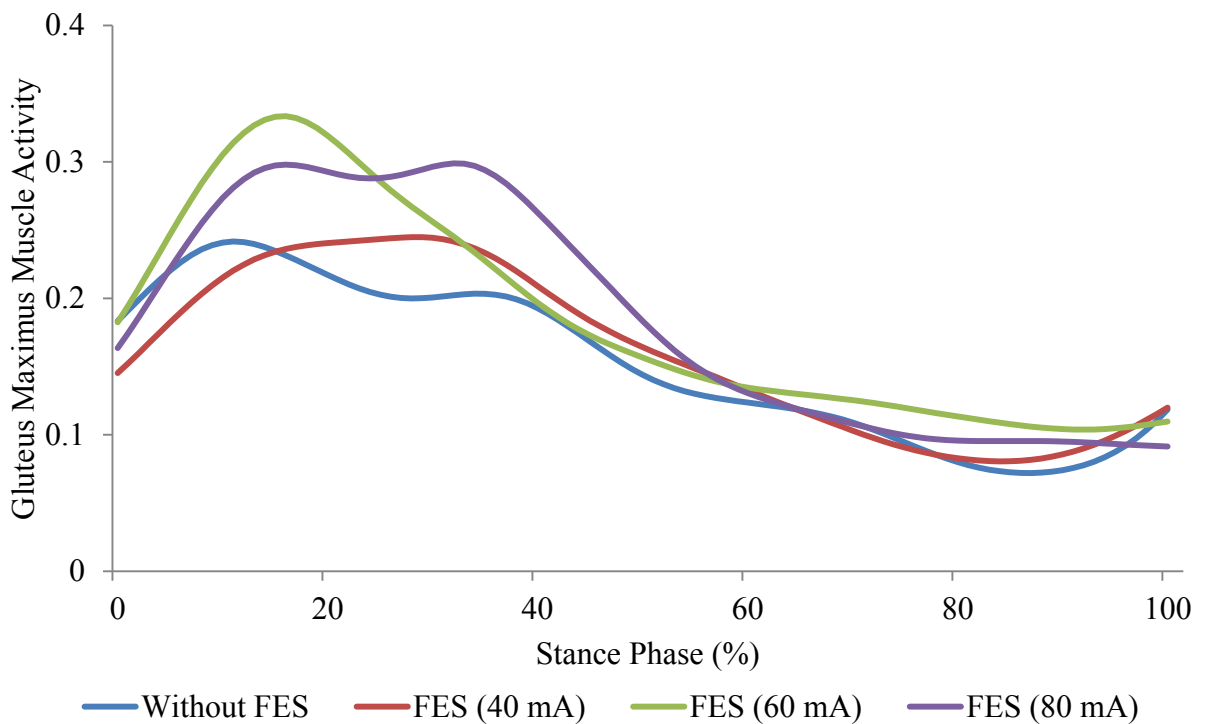


Figure B.2 Gluteus maximus EMG measurement of subject 1 in normal walking and FES applied walking

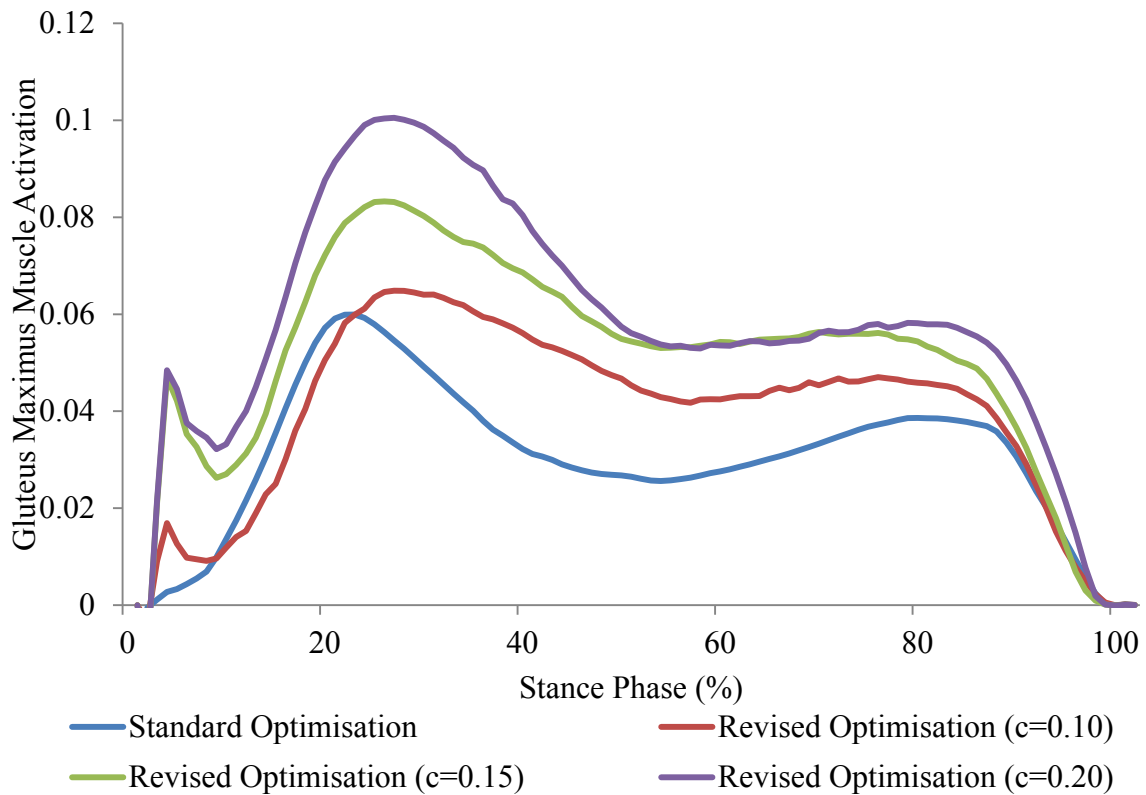


Figure B.3 Gluteus maximus model predictions of subject 2 in normal walking and FES applied walking

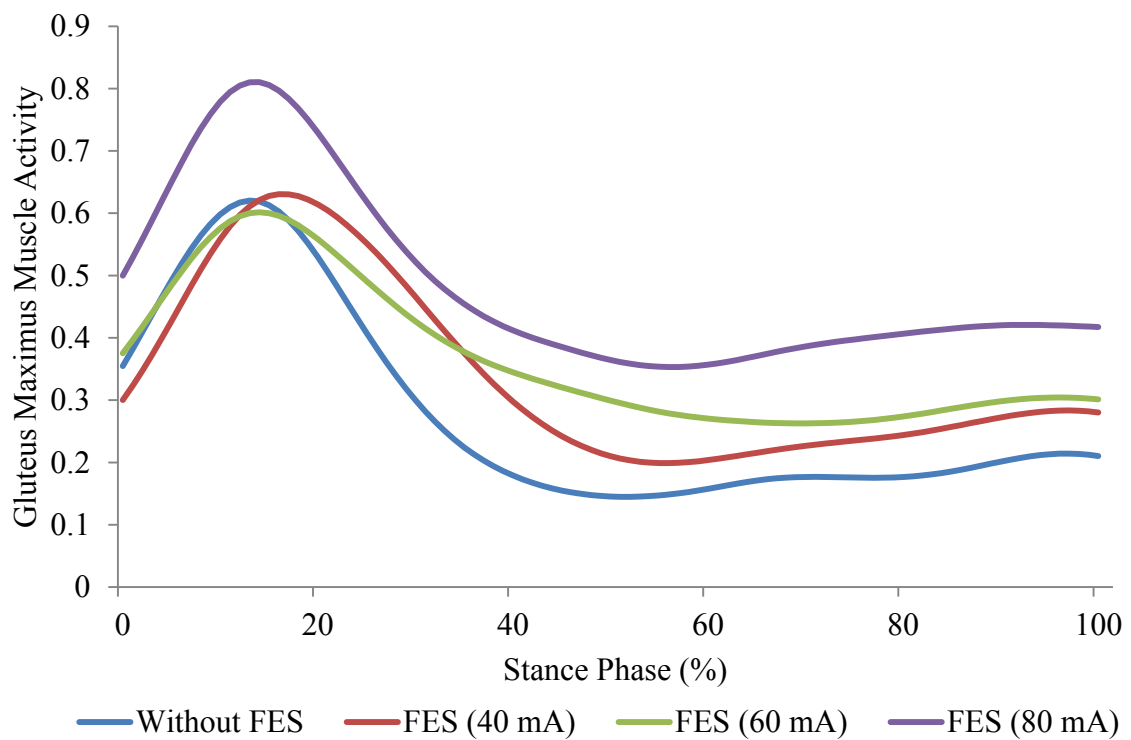


Figure B.4 Gluteus maximus EMG measurement of subject 2 in normal walking and FES applied walking

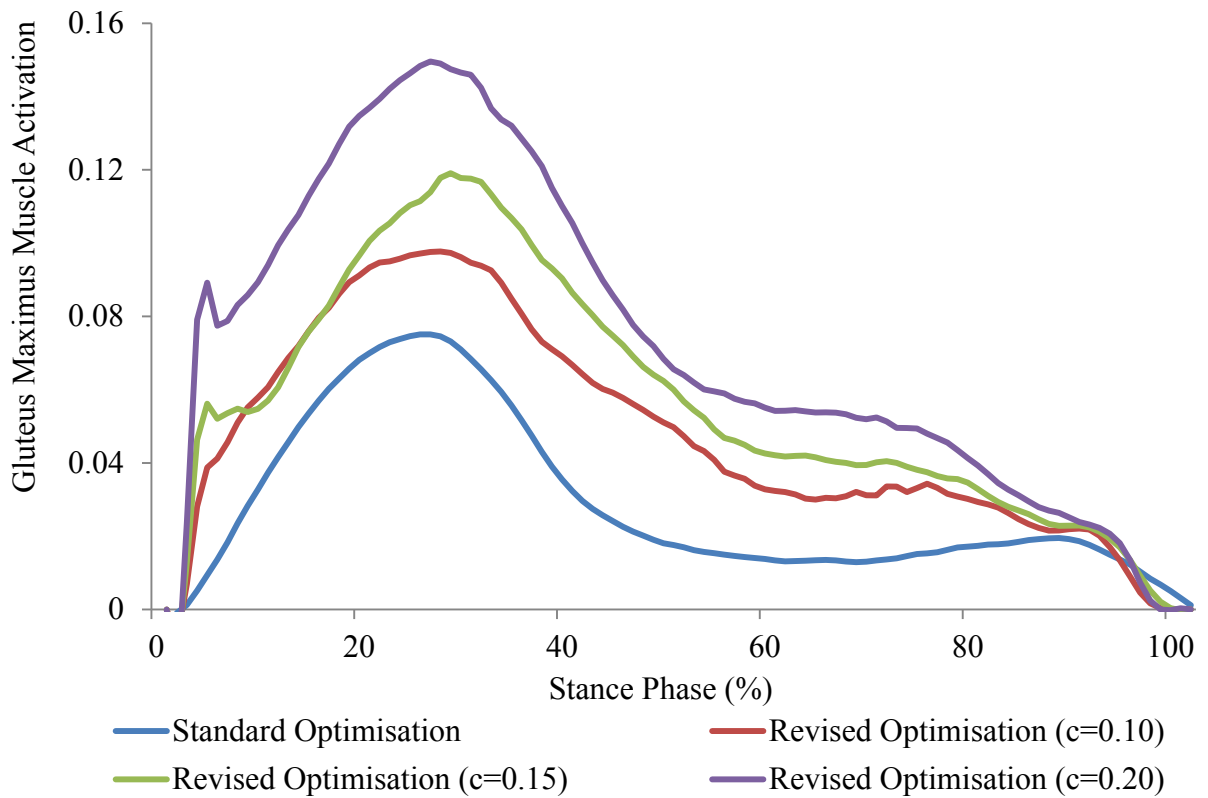


Figure B.5 Gluteus maximus model predictions of subject 3 in normal walking and FES applied walking

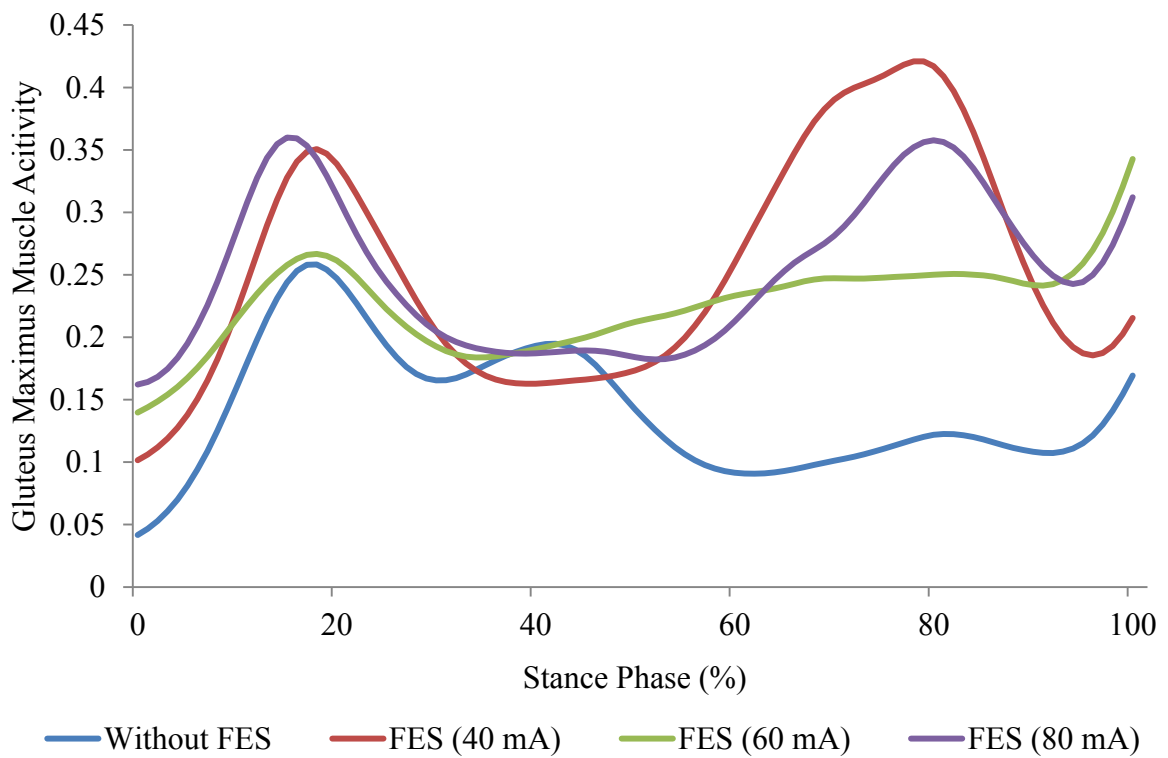


Figure B.6 Gluteus maximus EMG measurement of subject 3 in normal walking and FES applied walking

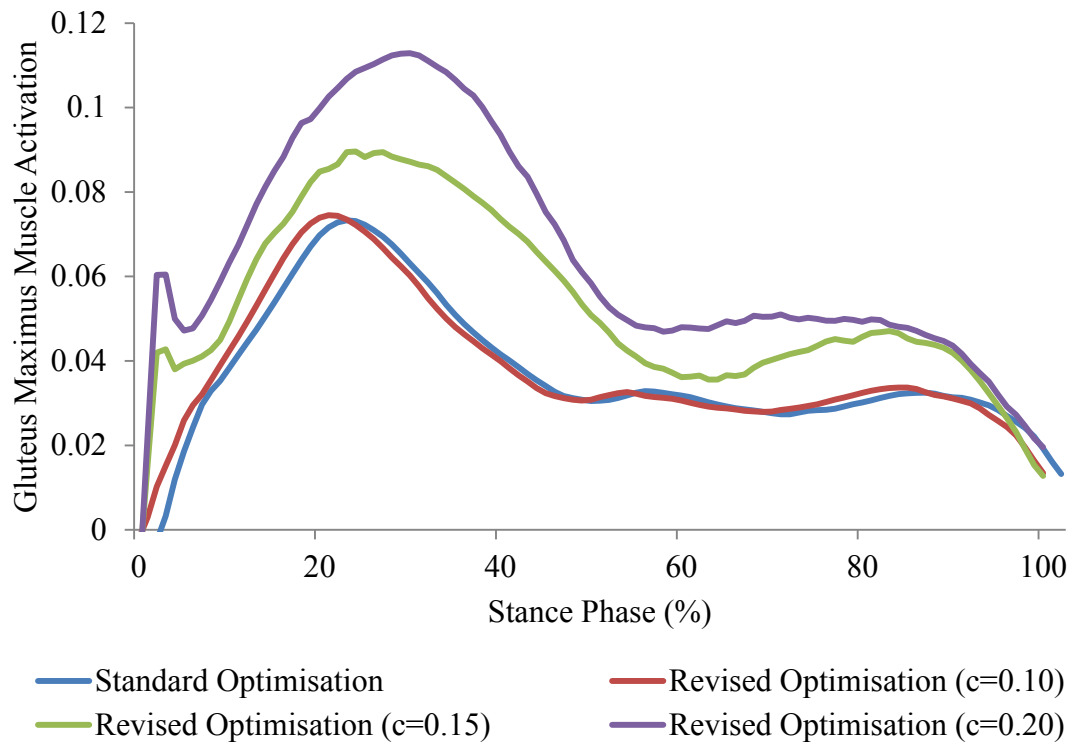


Figure B.7 Gluteus maximus model predictions of subject 4 in normal walking and FES applied walking

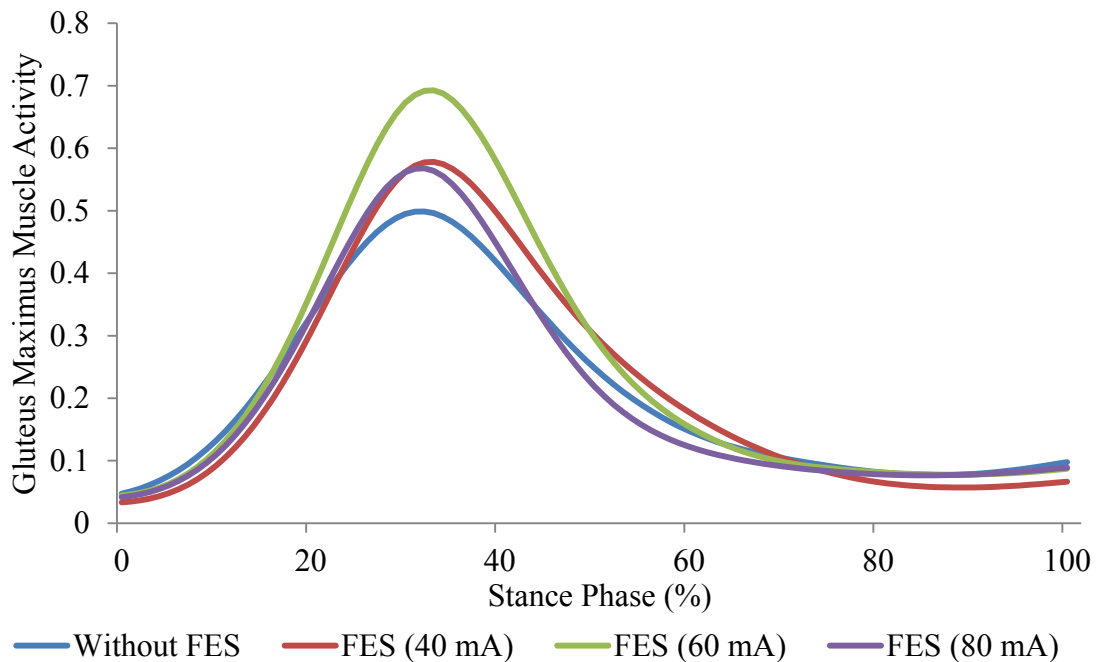


Figure B.8 Gluteus maximus EMG measurement of subject 4 in normal walking and FES applied walking

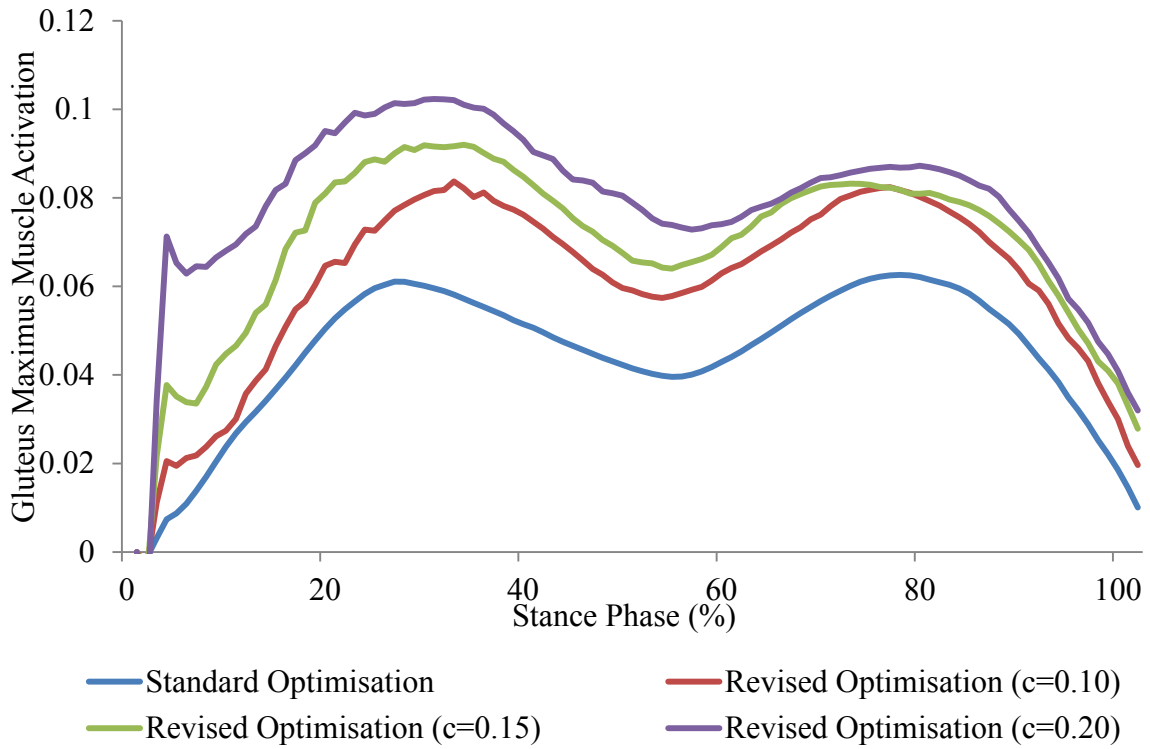


Figure B.9 Gluteus maximus model predictions of subject 5 in normal walking and FES applied walking

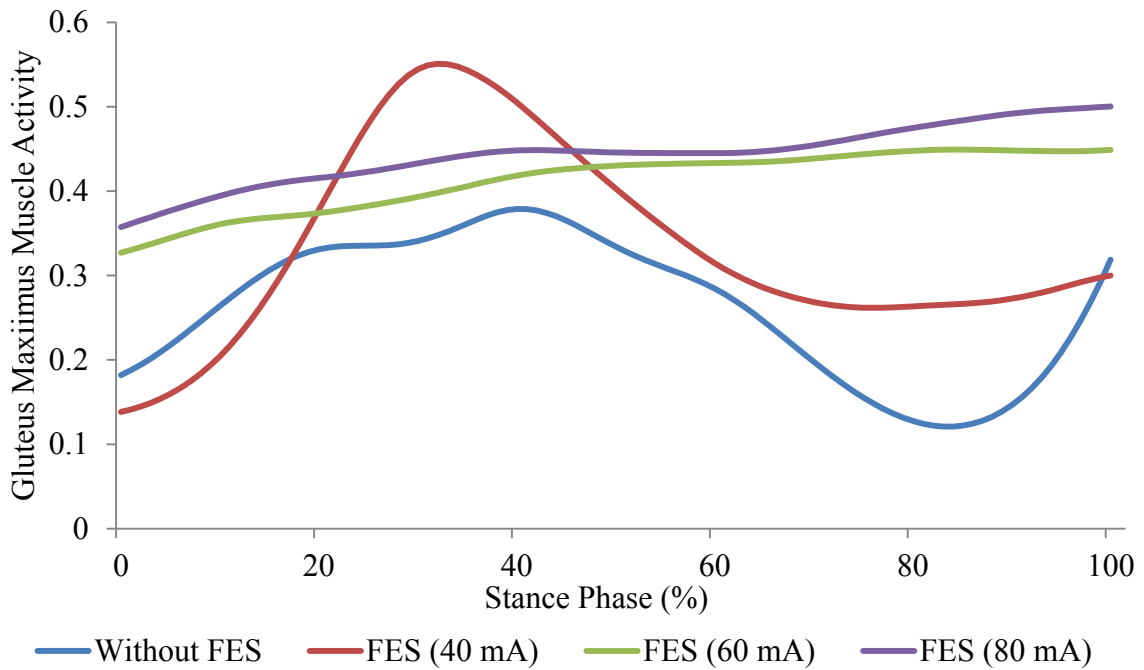


Figure B.10 Gluteus maximus EMG measurement of subject 5 in normal walking and FES applied walking

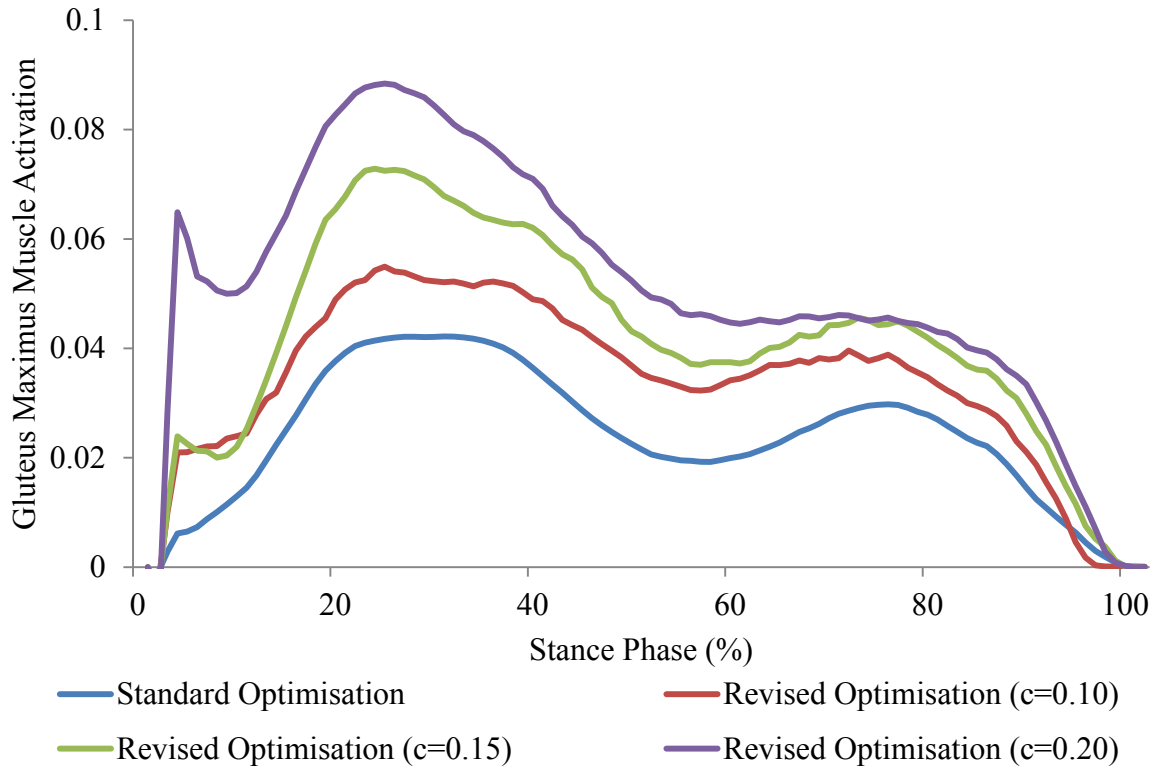


Figure B.11 Gluteus maximum model predictions of subject 6 in normal walking and FES applied walking

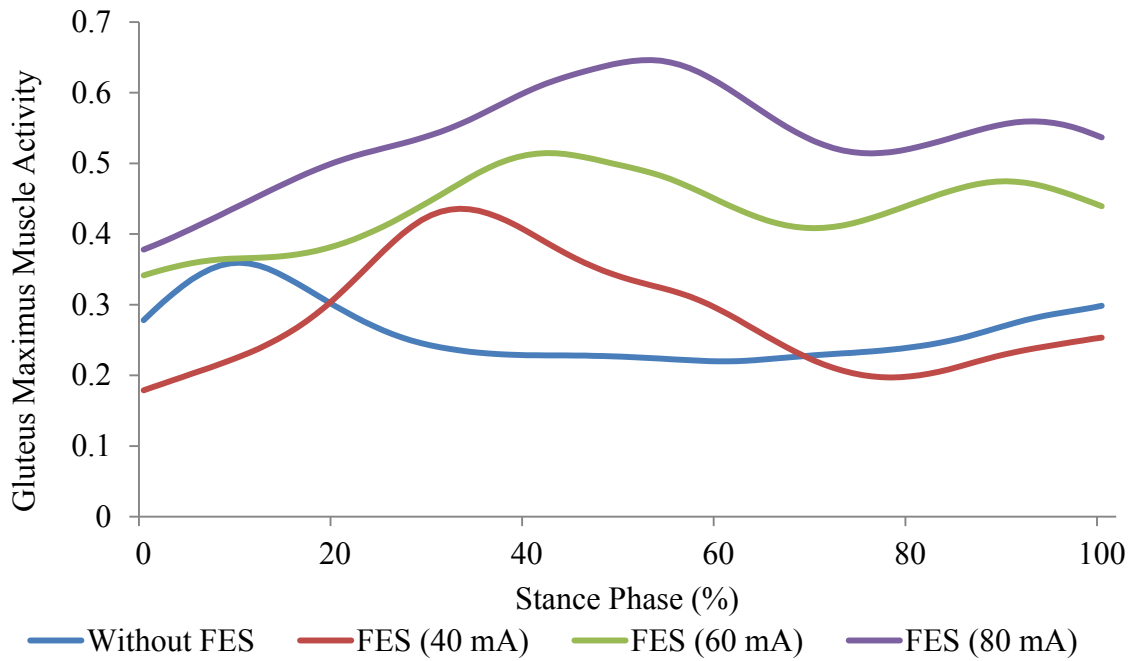


Figure B.12 Gluteus maximum EMG measurement of subject 6 in normal walking and FES applied walking

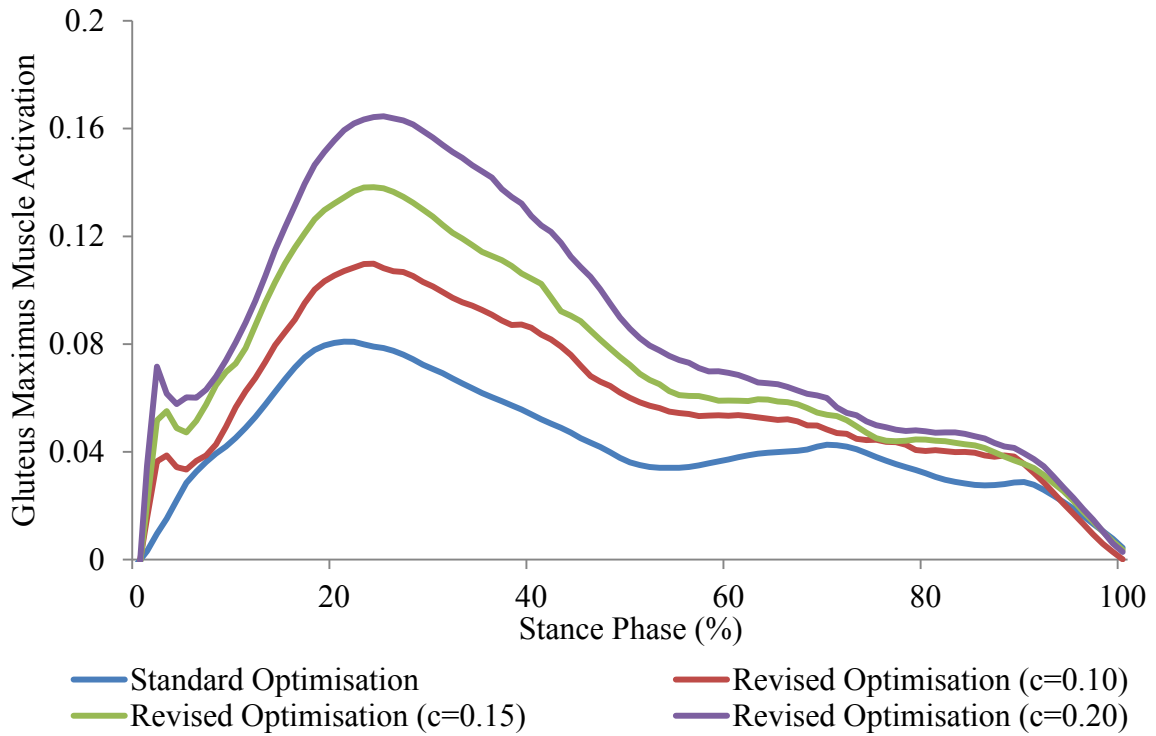


Figure B.13 Gluteus maximus model predictions of subject 7 in normal walking and FES applied walking

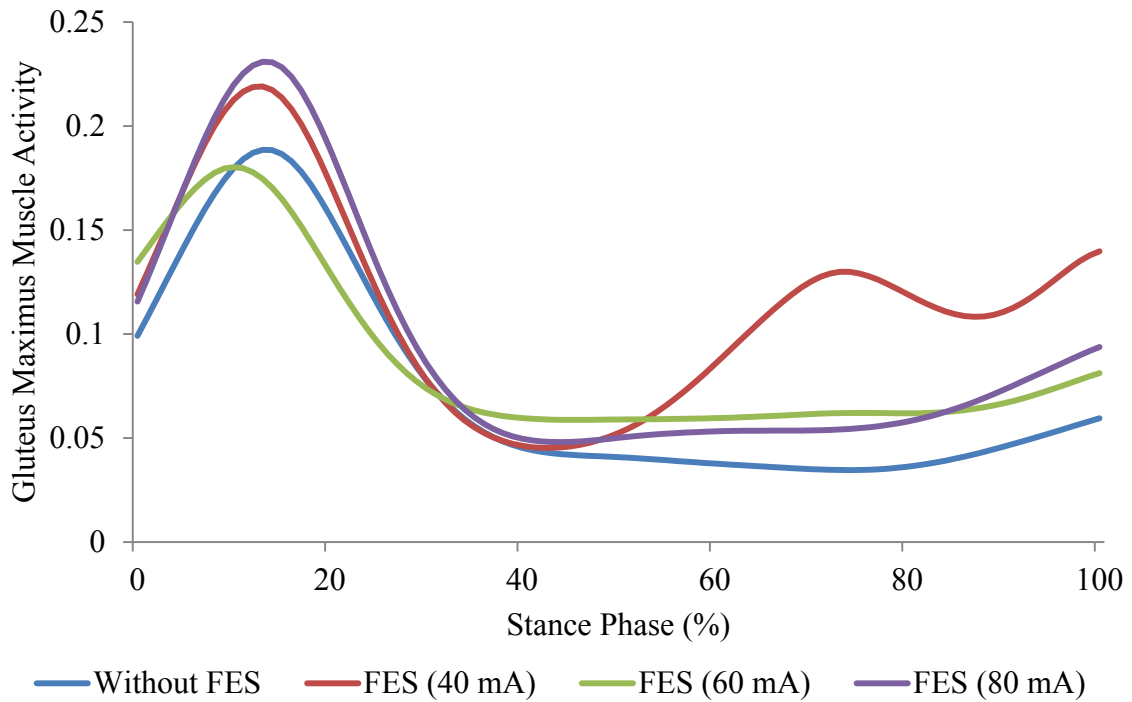


Figure B.14 Gluteus maximus EMG measurement of subject 7 in normal walking and FES applied walking

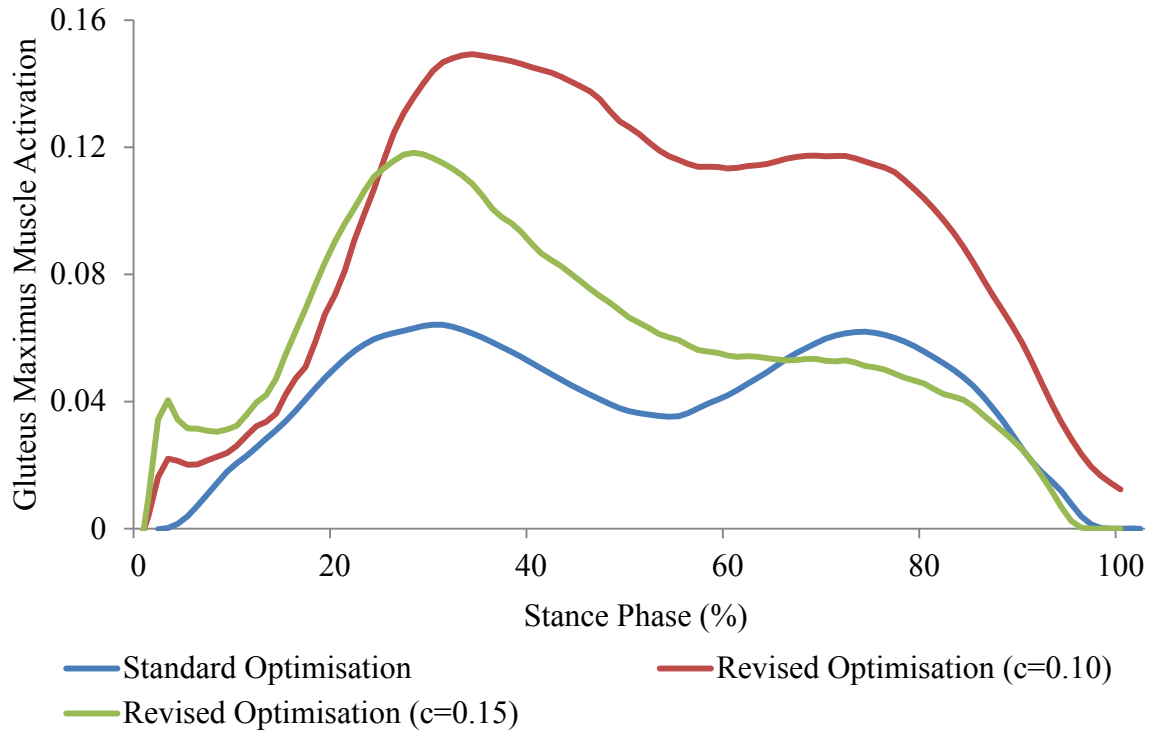


Figure B.15 Gluteus maximus model predictions of subject 8 in normal walking and FES applied walking

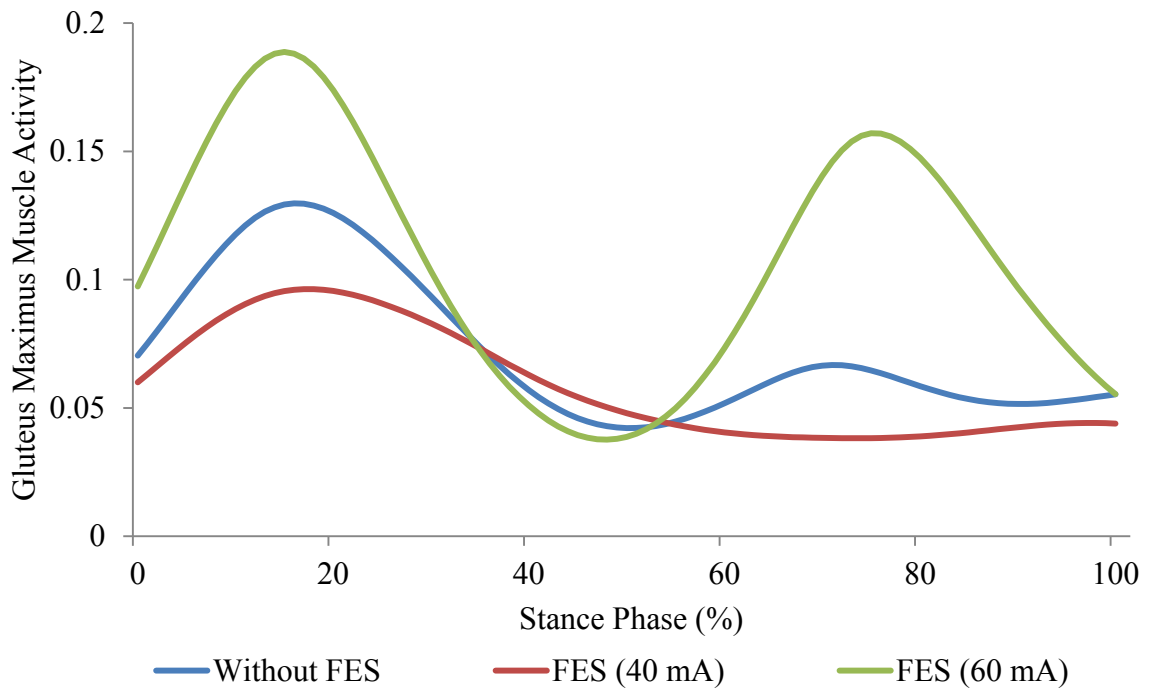


Figure B.16 Gluteus maximus EMG measurement of subject 8 in normal walking and FES applied walking

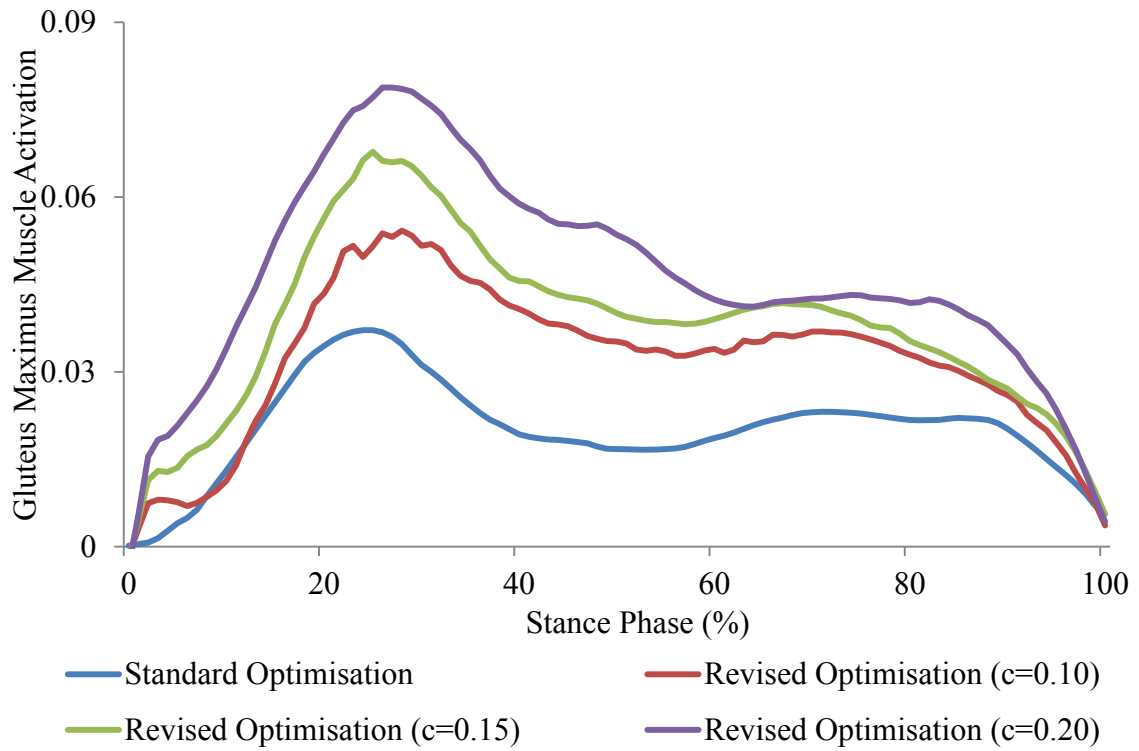


Figure B.17 Gluteus maximus model predictions of subject 9 in normal walking and FES applied walking

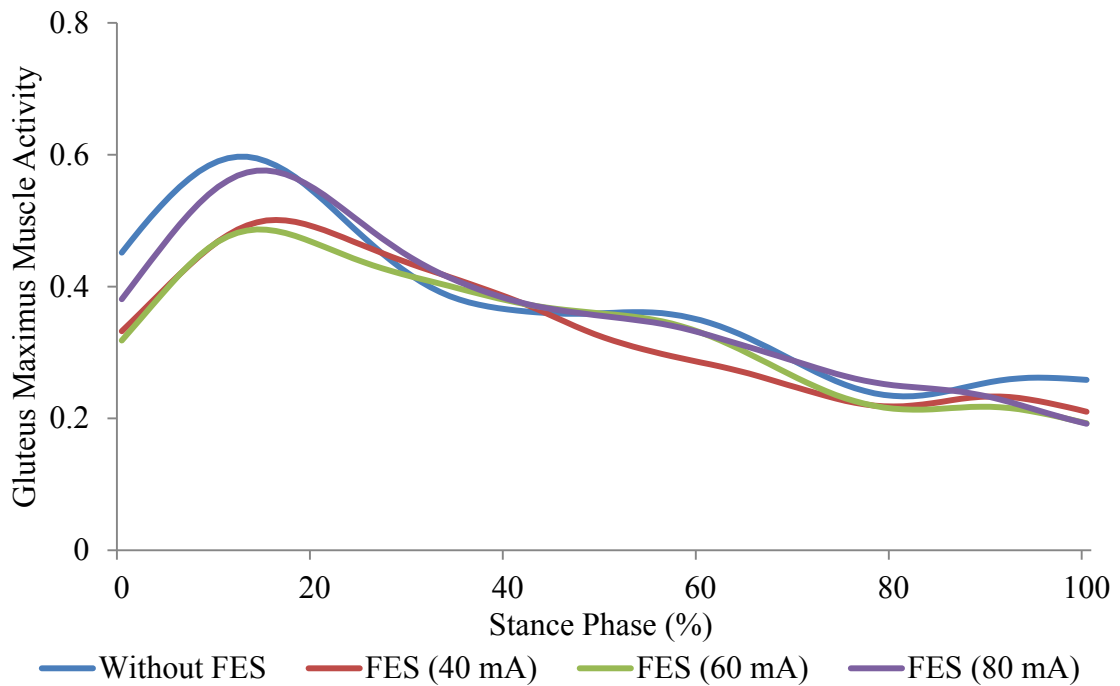


Figure B.18 Gluteus maximus EMG measurement of subject 9 in normal walking and FES applied walking

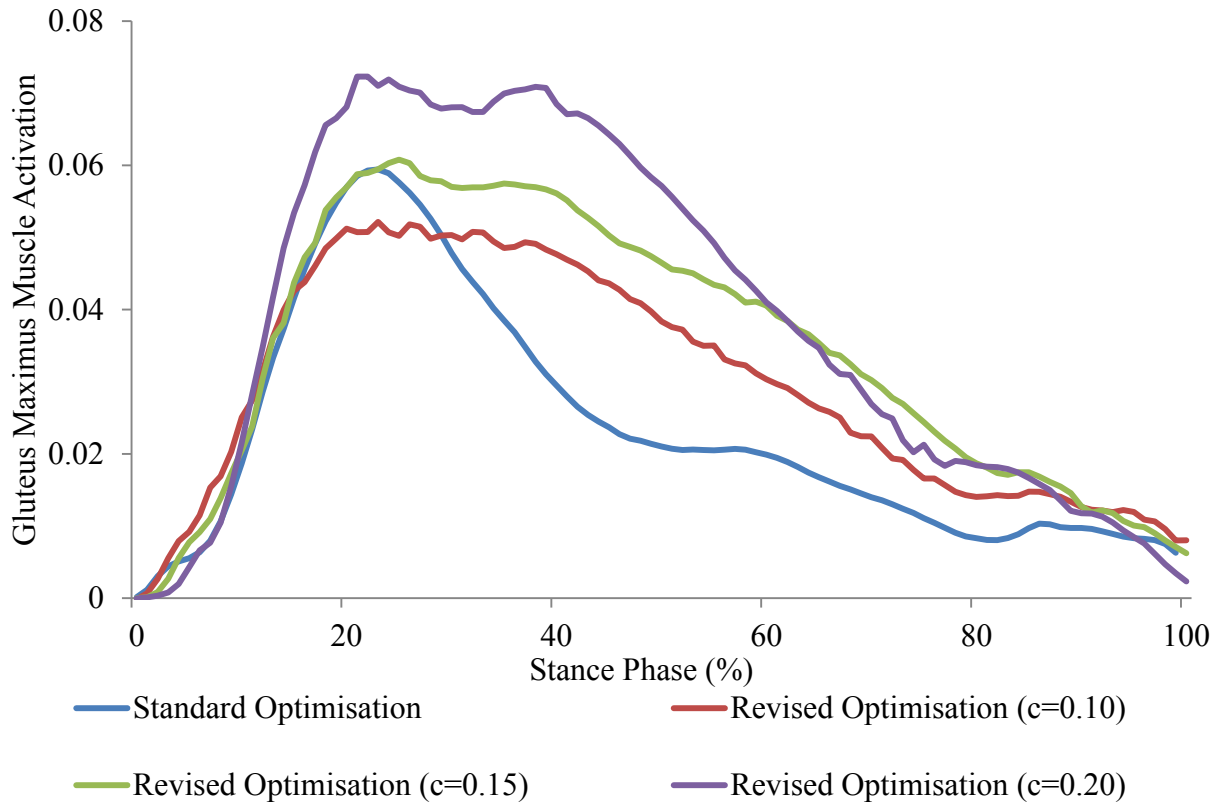


Figure B.19 Gluteus maximus model predictions of subject 10 in normal walking and FES applied walking

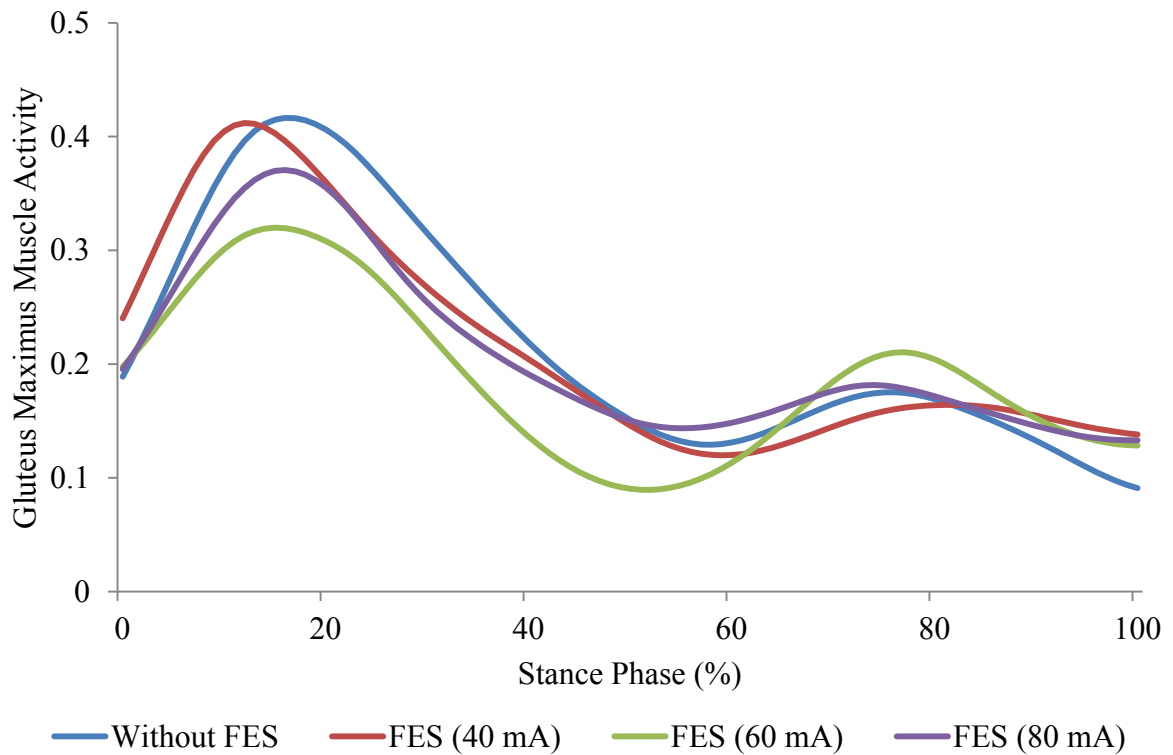


Figure B.20 Gluteus maximus EMG measurement of subject 10 in normal walking and FES applied walking

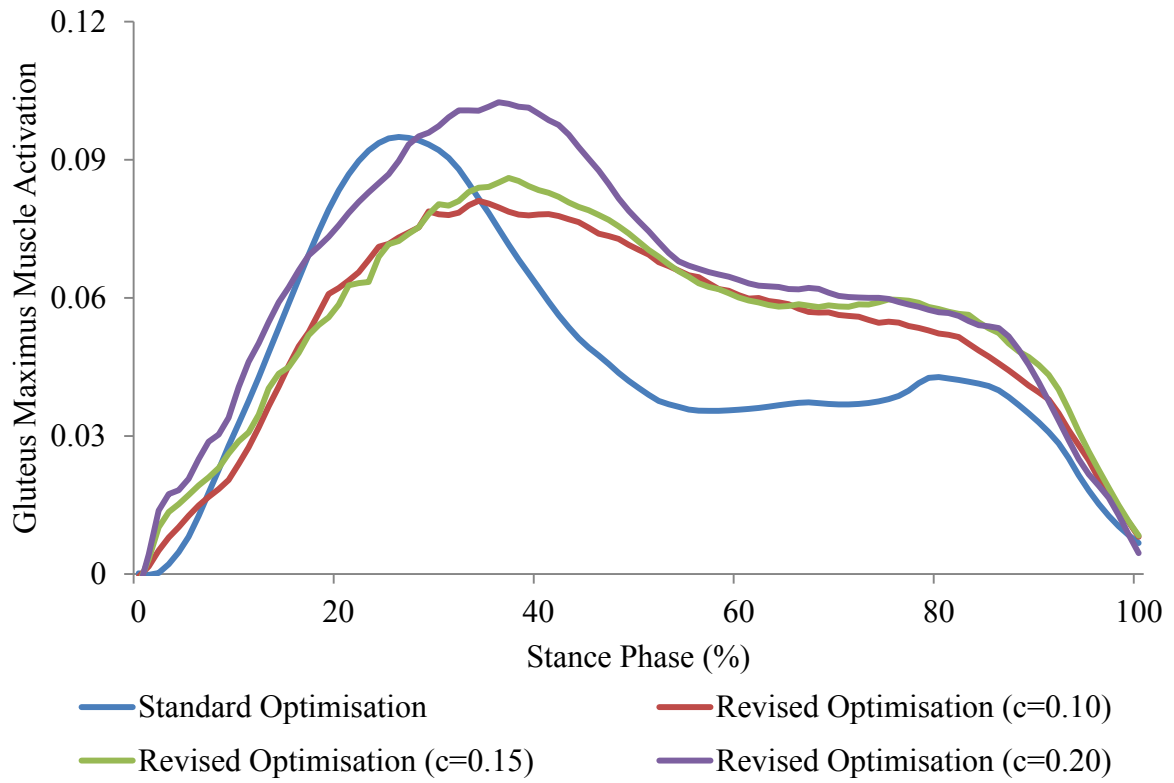


Figure B.21 Gluteus maximus model predictions of subject 11 in normal walking and FES applied walking

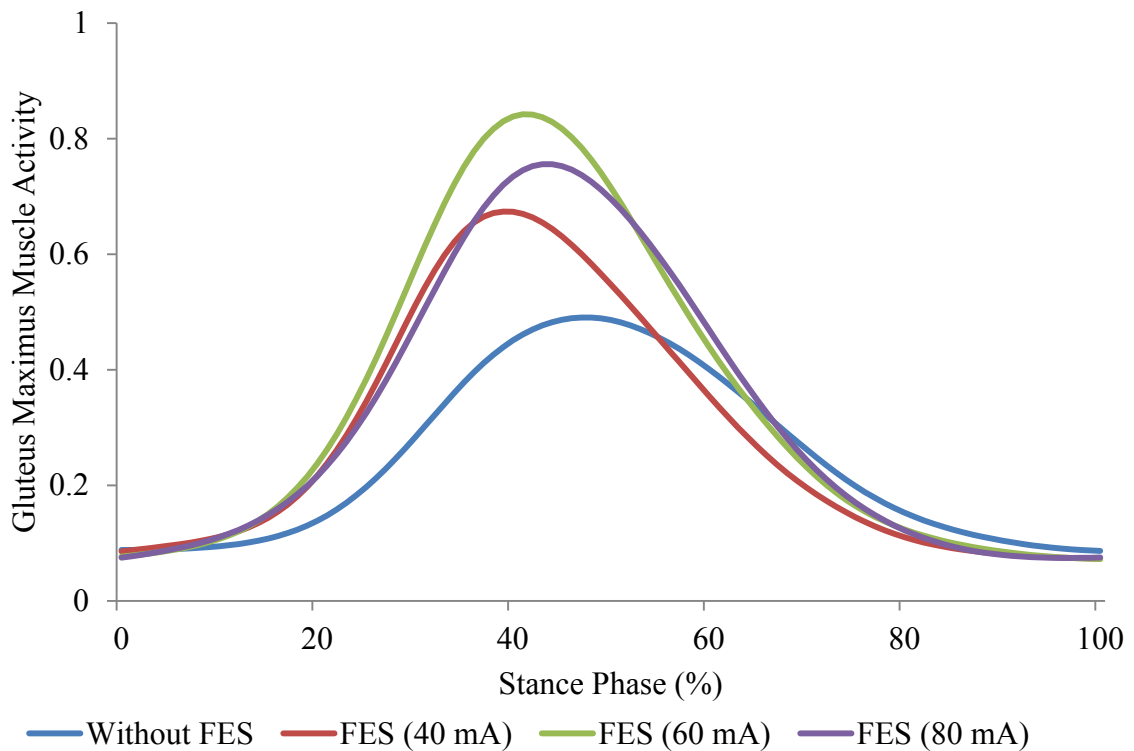


Figure B.22 Gluteus maximus EMG measurement of subject 11 in normal walking and FES applied walking

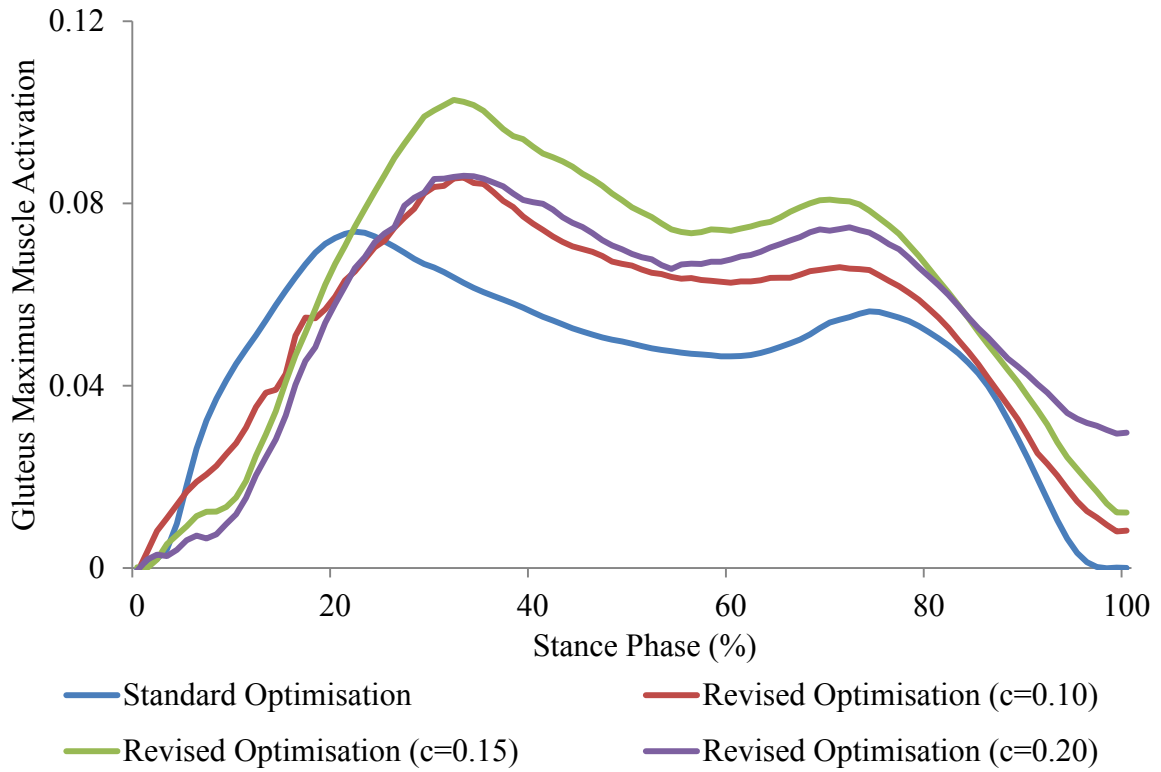


Figure B.23 Gluteus maximus model predictions of subject 12 in normal walking and FES applied walking

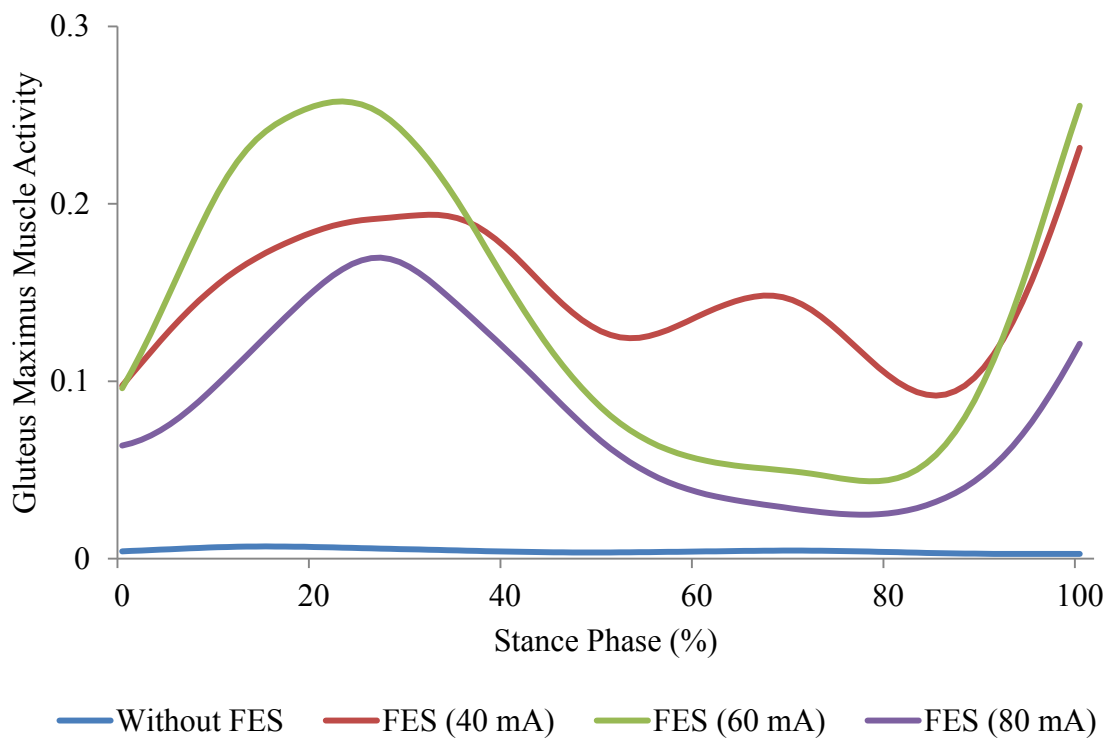


Figure B.24 Gluteus maximus EMG measurement of subject 12 in normal walking and FES applied walking

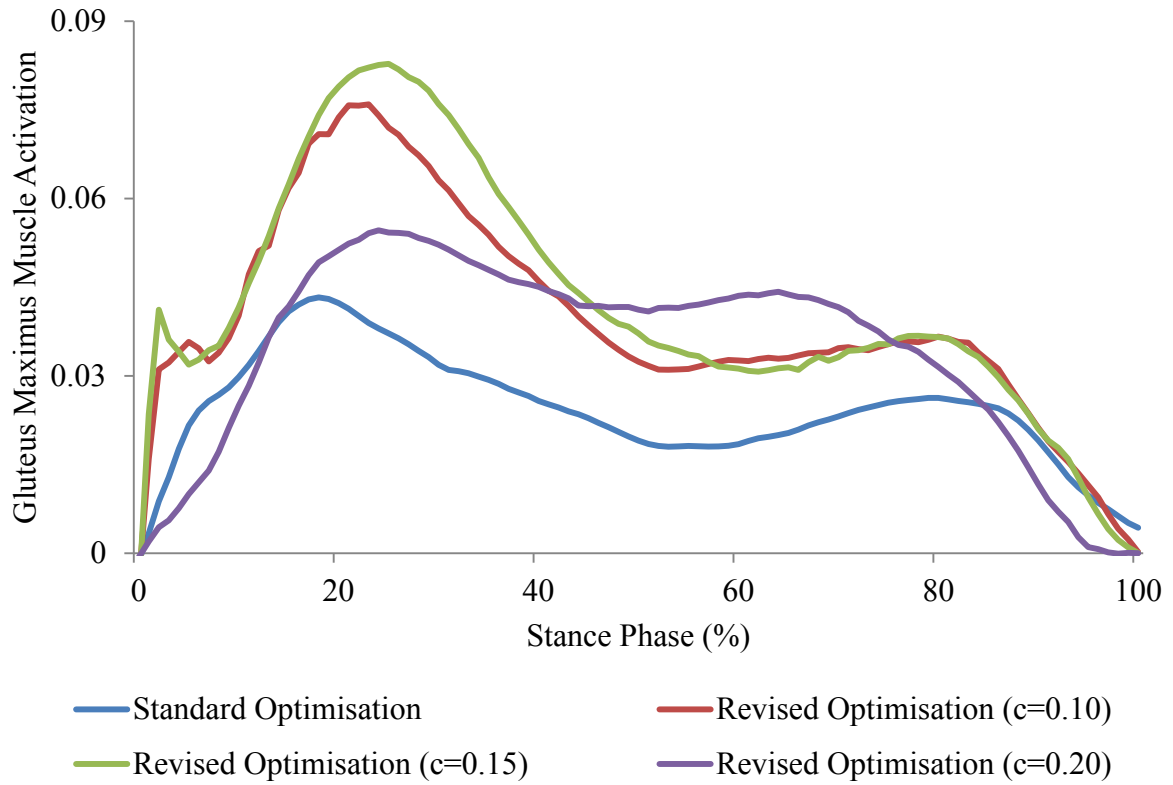


Figure B.25 Gluteus maximus model predictions of subject 13 in normal walking and FES applied walking

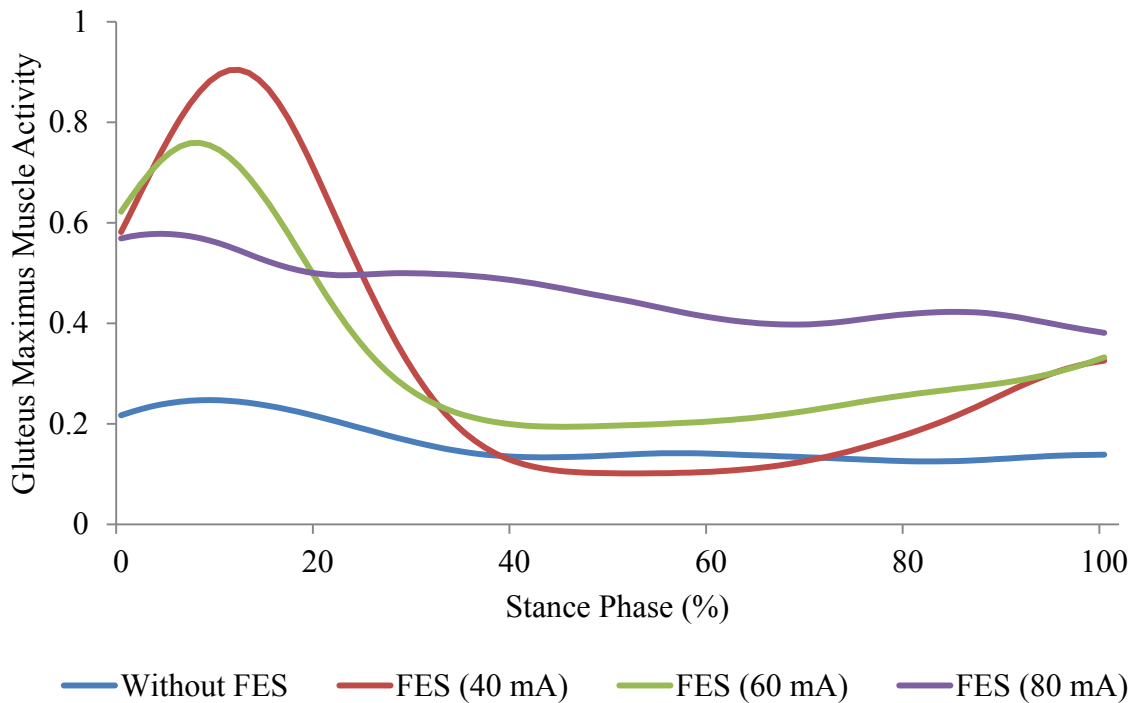


Figure B.26 Gluteus maximus EMG measurement of subject 13 in normal walking and FES applied walking

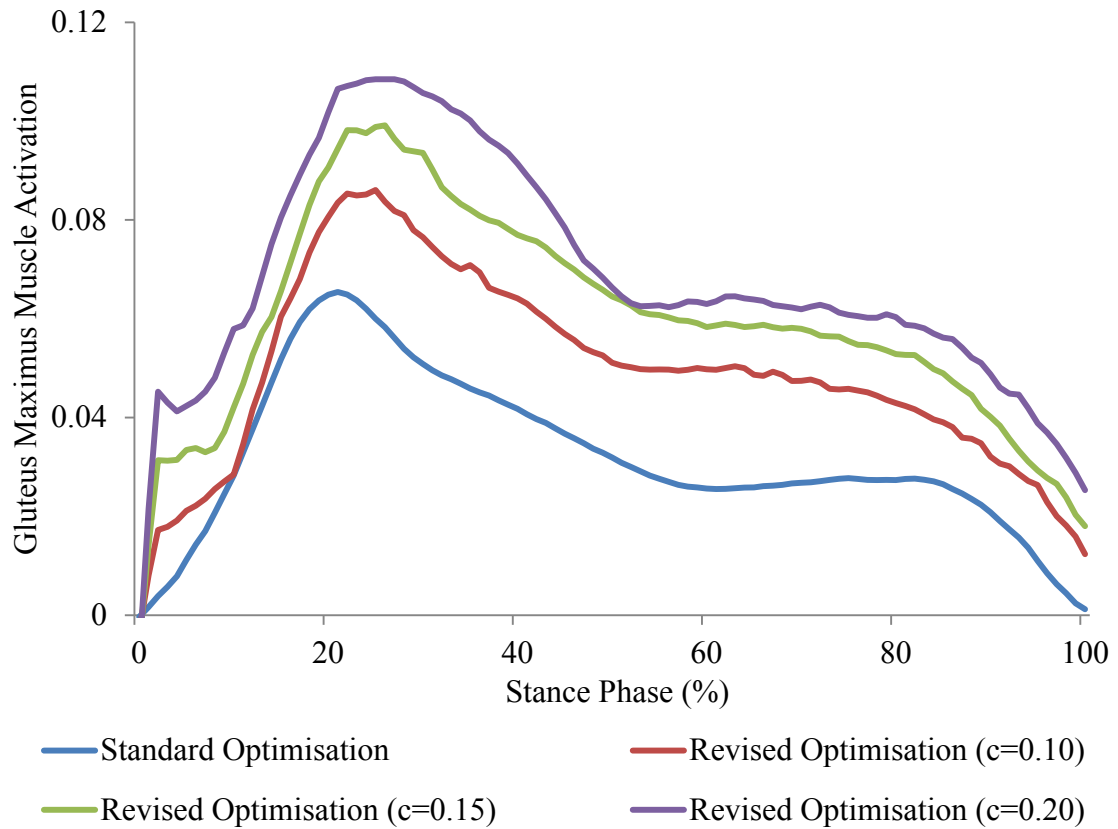


Figure B.27 Gluteus maximus model predictions of subject 14 in normal walking and FES applied walking

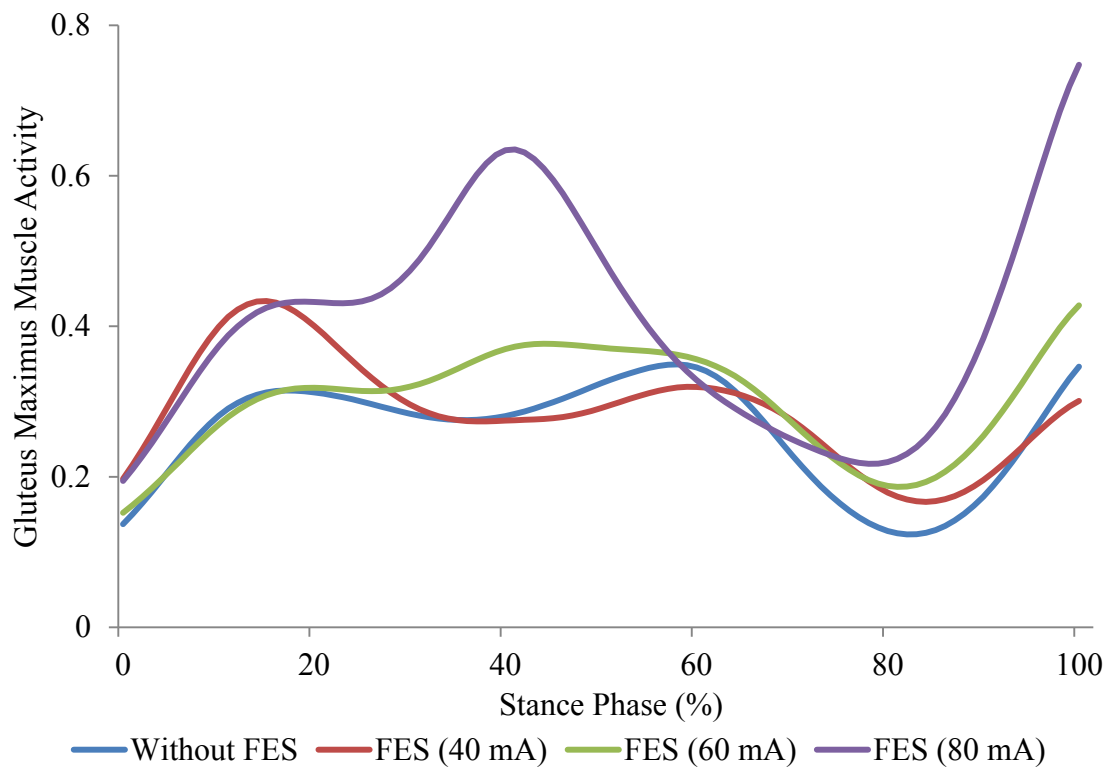


Figure B.28 Gluteus maximus EMG measurement of subject 14 in normal walking and FES applied walking

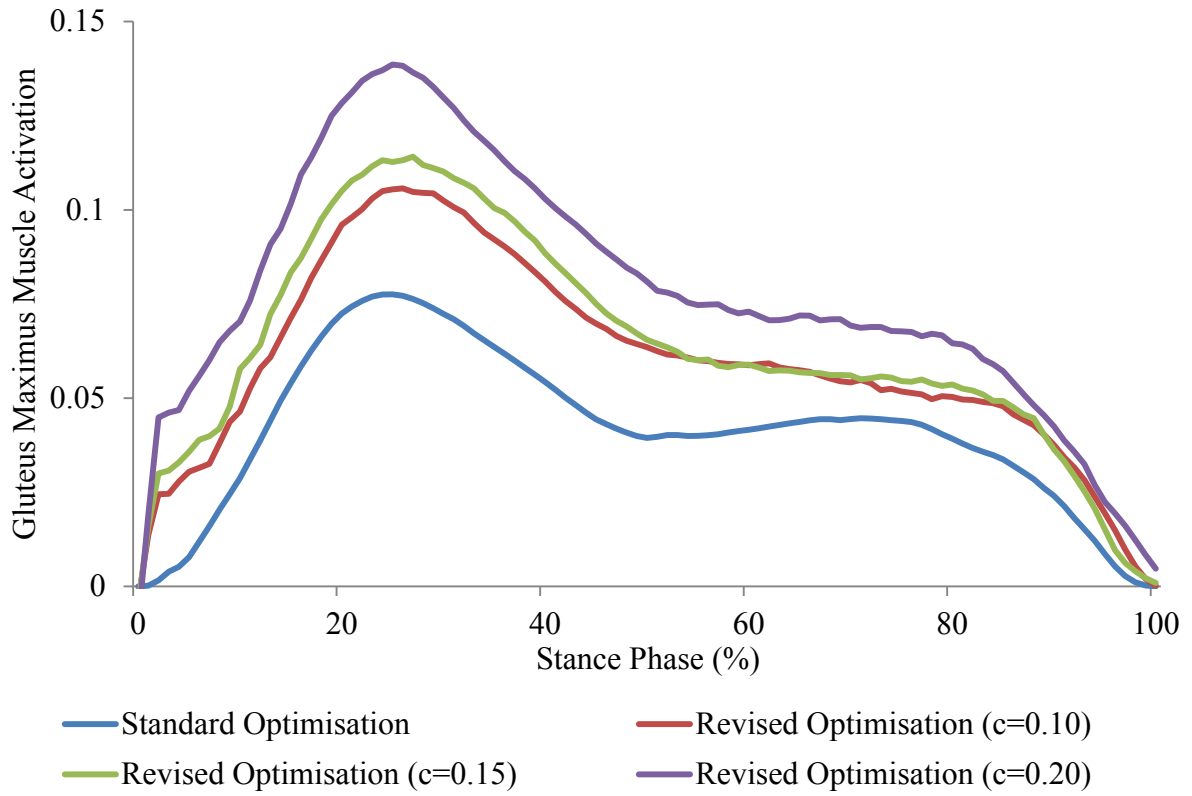


Figure B.29 Gluteus maximus model predictions of subject 15 in normal walking and FES applied walking

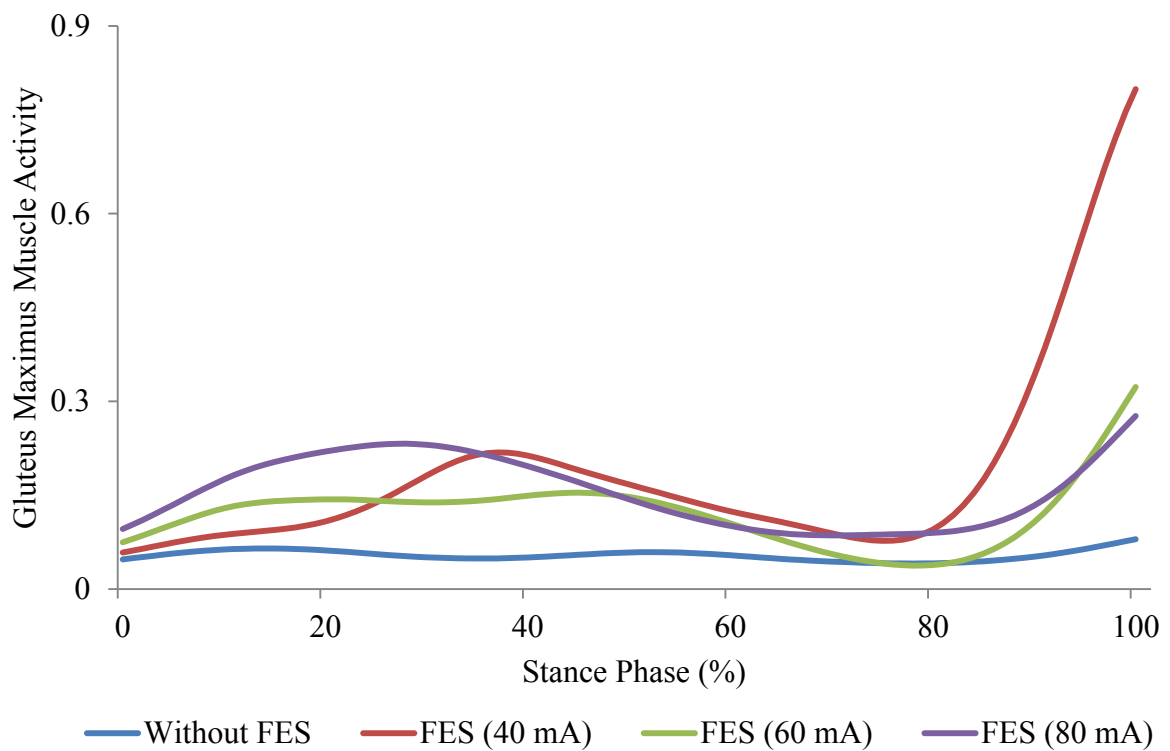


Figure B.30 Gluteus maximus EMG measurement of subject 15 in normal walking and FES applied walking

DISSEMINATION

Conference Presentations:

Azmi, N.L., Ding, Z. & Bull, A.M.J (2016). Activation of Biceps Femoris Can Reduce Tibiofemoral Anterior Shear Force and Mitigate Anterior Cruciate Ligament Deficiency. *22nd Congress of the European Society of Biomechanics (ESB)*, Lyon, France (Podium).

Azmi, N.L., Ding, Z., Xu, R. & Bull, A.M.J (2016). Activation of Biceps Femoris: A Target for Ligament Injury Rehabilitation. *MEIbioeng16*, Oxford, United Kingdom (Podium).

Azmi, N.L., Ding, Z., Xu, R. & Bull, A.M.J (2015). Muscles Can Negate, or Exacerbate The Effects of Anterior Cruciate Ligament Insufficiency. *MEIbioeng15*, Leeds, United Kingdom (Poster, 2nd Best Poster Award).

Peer Reviewer Journal Publications:

Azmi NL, Ding Z, Xu R, Bull AMJ (2018) Activation of biceps femoris long head reduces tibiofemoral anterior shear force and tibial internal rotation torque in healthy subjects. *PLoS ONE* 13(1): e0190672. <https://doi.org/10.1371/journal.pone.0190672>

Azmi, N.L., Ding, Z. & Bull, A.M.J. Validation of a musculoskeletal gait model to study the role of functional electrical stimulation. *In submission IEEE Transactions on Biomedical Engineering*

REFERENCES

- Adams, D., Logerstedt, D. S., Hunter-Giordano, A., Axe, M. J., & Snyder-Mackler, L. (2012). Current concepts for anterior cruciate ligament reconstruction: a criterion-based rehabilitation progression. *J Orthop Sports Phys Ther*, 42(7), 601-614. doi:10.2519/jospt.2012.3871
- Aglietti, P., Giron, F., Losco, M., Cuomo, P., Ciardullo, A., & Mondanelli, N. (2009). Comparison Between Single- and Double-Bundle Anterior Cruciate Ligament Reconstruction. *The American Journal of Sports Medicine*, 38(1), 25-34. doi:10.1177/0363546509347096
- Alibeji, N. A., Kirsch, N. A., & Sharma, N. (2015). A Muscle Synergy-Inspired Adaptive Control Scheme for a Hybrid Walking Neuroprosthesis. *Front Bioeng Biotechnol*, 3, 203. doi:10.3389/fbioe.2015.00203
- Alkjaer, T., Henriksen, M., & Simonsen, E. B. (2011). Different knee joint loading patterns in ACL deficient copers and non-copers during walking. *Knee Surg Sports Traumatol Arthrosc*, 19(4), 615-621. doi:10.1007/s00167-010-1302-2
- Alkjaer, T., Simonsen, E. B., Jorgensen, U., & Dyhre-Poulsen, P. (2003). Evaluation of the walking pattern in two types of patients with anterior cruciate ligament deficiency: copers and non-copers. *Eur J Appl Physiol*, 89(3-4), 301-308. doi:10.1007/s00421-002-0787-x
- Amis, A. A., Bull, A. M. J., & Lie, D. T. (2005). Biomechanics of rotational instability and anatomic anterior cruciate ligament reconstruction. *Oper Tech Orthop*, 15(1), 29-35. doi:10.1053/j.oto.2004.10.009
- Andersen, H. N., & Dyhre-Poulsen, P. (1997). The anterior cruciate ligament does play a role in controlling axial rotation in the knee. *Knee Surg Sports Traumatol Arthrosc*, 5, 145-149.
- Anderson, F. C., & Pandy, M. G. (2001). Static and dynamic optimization solutions for gait are practically equivalent. *J Biomech*, 34, 153-161.
- Anderson, F. C., & Pandy, M. G. (2003). Individual muscle contributions to support in normal walking. *Gait & Posture*, 17(2), 159-169. doi:10.1016/s0966-6362(02)00073-5
- Andriacchi, T. P. (1990). Dynamics of the Pathological Motion: Applied to the Anterior Cruciate Deficient Knee. *Biomechanics*, 23, 99-105.
- Andriacchi, T. P., & Dyrby, C. O. (2005). Interactions between kinematics and loading during walking for the normal and ACL deficient knee. *J Biomech*, 38(2), 293-298. doi:10.1016/j.jbiomech.2004.02.010
- Ardern, C. L., Webster, K. E., Taylor, N. F., & Feller, J. A. (2011). Return to sport following anterior cruciate ligament reconstruction surgery: a systematic review and meta-analysis of the state of play. *Br J Sports Med*, 45(7), 596-606. doi:10.1136/bjism.2010.076364
- Ardestani, M. M., & Moazen, M. (2016). How human gait responds to muscle impairment in total knee arthroplasty patients: Muscular compensations and articular perturbations. *J Biomech*, 49(9), 1620-1633. doi:10.1016/j.jbiomech.2016.03.047
- Arnold, E. M., Hamner, S. R., Seth, A., Millard, M., & Delp, S. L. (2013). How muscle fiber lengths and velocities affect muscle force generation as humans walk and run at different speeds. *J Exp Biol*, 216(Pt 11), 2150-2160. doi:10.1242/jeb.075697
- Bax, L., Staes, F., & Verhagen, A. (2005). Does neuromuscular electrical stimulation strengthen the quadriceps femoris? *Sports Medicine*, 35(3), 191-212.
- Beard, D., Soundarapandian, R., O'Connor, J., & Dodd, C. (1996). Gait and electromyographic analysis of anterior cruciate ligament deficient subject. *Gait & Posture*, 4, 83-88.
- Benedetti, M. G., Bonato, P., Catani, F., D'Alessio, T., Knaflitz, M., Marcacci, M., & Simoncini, L. (1999). Myoelectric activation pattern during gait in total knee replacement relationship with kinematics, kinetics and clinical outcome. *IEEE T REHABIL ENG*, 7(2), 140-149.
- Berchuck, M., Andriacchi, T. P., Bach, B. R., & Reider, B. (1990). Gait adaptations by patients who have a deficient anterior cruciate ligament. *J Bone Joint Surg Am.*, 72(6), 871-877.
- Besier, T. F., Lloyd, D. G., & Ackland, T. R. (2003). Muscle activation strategies at the knee during running and cutting maneuvers. *Med Sci Sports Exerc*, 35(1), 119-127. doi:10.1249/01.MSS.0000043608.79537.AB

- Beynon, B., Fleming, B., Labovitch, R., & Parsons, B. (2002). Chronic anterior cruciate ligament deficiency is associated with increased anterior translation of the tibia during the transition from non-weightbearing to weightbearing. *J Orthop Res*, *20*, 332-337.
- Beynon, B. D., Johnson, R. J., Abate, J. A., Fleming, B. C., & Nichols, C. E. (2005). Treatment of anterior cruciate ligament injuries, part I. *Am J Sports Med*, *33*(10), 1579-1602. doi:10.1177/0363546505279913
- Biscarini, A., Botti, F. M., & Pettorossi, V. E. (2013). Selective contribution of each hamstring muscle to anterior cruciate ligament protection and tibiofemoral joint stability in leg-extension exercise: a simulation study. *Eur J Appl Physiol*, *113*(9), 2263-2273. doi:10.1007/s00421-013-2656-1
- Boerboom, A. L., Hof, A. L., Halbertsma, J. P., van Raaij, J. J., Schenk, W., Diercks, R. L., & van Horn, J. R. (2001). Atypical hamstrings electromyographic activity as a compensatory mechanism in anterior cruciate ligament deficiency. *Knee Surg Sports Traumatol Arthrosc*, *9*(4), 211-216. doi:10.1007/s001670100196
- Brand, J., Weiler, A., Caborn, D., Brown, C., & Johnson, D. (2000). Graft fixation in cruciate ligament reconstruction. *Am J Sports Med*, *28*(5), 761-774.
- Brandsson, S., Karlsson, J., Sward, L., Kartus, J., Eriksson, B. I., & Karrholm, J. (2002). Kinematics and laxity of the knee joint after anterior cruciate ligament reconstruction: pre- and postoperative radiostereometric studies. *Am J Sports Med*, *30*(3), 361-367. doi:10.1177/03635465020300031001
- Buchanan, T. S., Lloyd, D. G., Manal, K., & Besier, T. F. (2004). Neuromusculoskeletal modeling: estimation of muscle forces and joint moments and movements from measurements of neural command. *J Appl Biomech*, *20*(4), 367-395.
- Bull, A., & Amis, A. (1998). The pivot-shift phenomenon: a clinical and biomechanical perspective. *The Knee*, *5*(3), 141-158.
- Bull, A., Earnshaw, P., Smith, A., Katchburian, M., Hassan, A., & Amis, A. (2002). Intraoperative measurement of knee kinematics in reconstruction of the anterior cruciate ligament. *Bone & Joint Journal*, *84*(7), 1075-1081.
- Bull, A. M. J., Andersen, H. N., Basso, O., Targett, J., & Amis, A. A. (1999). Incidence and mechanism of the pivot shift: An in vitro study. *Clin Orthop Relat Res*, *363*, 219-231.
- Bull, A. M. J., Reilly, P., Wallace, A. L., Amis, A. A., & Emery, R. J. H. (2005). A novel technique to measure active tendon forces: application to the subscapularis tendon. *Knee Surg Sports Traumatol Arthrosc*, *13*(2), 145-150. doi:10.1007/s00167-004-0556-y
- Carmick, J. (1997). Guidelines for the Clinical Application of Neuromuscular Electrical Stimulation (NMES) for Children with Cerebral Palsy. *Pediatric Physical Therapy*, *9*(3), 128-136.
- Catalfamo, P. F., Aguiar, G., Curi, J., & Braidot, A. (2010). Anterior cruciate ligament injury: Compensation during gait using hamstring muscle activity. *Open Biomed Eng J*, *4*, 99-106.
- Chen, C. F., Kuo, Y. H., Luh, J. J., Chen, Y. J., Chen, S. W., Kuo, T. S., & Lai, J. S. (2013). Reducing anterior tibial translation by applying functional electrical stimulation in dynamic knee extension exercises: Quantitative results acquired via marker tracking. *Clin Biomech*, *28*(5), 549-554. doi:<http://dx.doi.org/10.1016/j.clinbiomech.2013.03.007>
- Ciccotti, M. G., Kerlan, G. K., Perry, J., & Pink, M. (1994). An electromyographic analysis of the knee during functional activities, Part II: The anterior cruciate ligament-deficient and -reconstructed profiles. *Am J Sports Med*, *22*, 651-658.
- Cleather, D. J., & Bull, A. M. J. (2015). The development of a segment-based musculoskeletal model of the lower limb: introducing FreeBody. *R Soc Open Sci*, *2*, 140449. doi:10.1098/rsos.140449
- Collins, D. (2007). Central contributions to contractions evoked by tetanic neuromuscular electrical stimulation. *Exercise and sport sciences reviews*, *35*(3), 102-109.
- Crowninshield, R. D., & Brand, R. A. (1981). A physiologically based criterion of muscle force prediction in locomotion. *J Biomech*, *14*(11), 793-801.
- Czerniecki, J., Lippert, F., & Olerud, J. (1988). A biomechanical evaluation of tibiofemoral rotation in anterior cruciate deficient knees during walking and running. *Am J Sports Med*, *16*(4), 327-331.

- Damsgaard, M., Rasmussen, J., Christensen, S. T., Surma, E., & de Zee, M. (2006). Analysis of musculoskeletal systems in the AnyBody Modeling System. *Simulation Modelling Practice and Theory*, *14*(8), 1100-1111. doi:10.1016/j.simpat.2006.09.001
- Delp, S. L., Anderson, F. C., Arnold, A. S., Loan, P., Habib, A., John, C. T., . . . Thelen, D. G. (2007). OpenSim: open-source software to create and analyze dynamic simulations of movement. *IEEE Trans Biomed Eng*, *54*(11), 1940-1950. doi:10.1109/TBME.2007.901024
- DeSantana, J., Walsh, D., Vance, C., Rakel, B., & Sluka, K. (2008). Effectiveness of transcutaneous electrical nerve stimulation for treatment of hyperalgesia and pain. *Curr Rheumatol Rep.*, *10*, 492-499.
- Devita, P., Hortobagyi, T., & Barrier, J. (1998). Gait biomechanics are not normal after anterior cruciate ligament reconstruction and accelerated rehabilitation. *Medicine and Science in Sports and Exercise*, *30*, 1481-1488.
- Ding, Z., Nolte, D., Tsang, C. K., Cleather, D. J., Kedgley, A. E., & Bull, A. M. J. (2016). In vivo knee contact force prediction using patient-specific musculoskeletal geometry in a segment-based computational model. *J Biomech Eng*, *138*(2), 021018. doi:10.1115/1.4032412
- Donnelly, C. J., Lloyd, D. G., Elliott, B. C., & Reinbolt, J. A. (2012). Optimizing whole-body kinematics to minimize valgus knee loading during sidestepping: implications for ACL injury risk. *J Biomech*, *45*(8), 1491-1497. doi:10.1016/j.jbiomech.2012.02.010
- Duffell, L. D., Hope, N., & McGregor, A. H. (2014). Comparison of kinematic and kinetic parameters calculated using a cluster-based model and Vicon's plug-in gait. *Proc Inst Mech Eng H*, *228*(2), 206-210. doi:10.1177/0954411913518747
- Dumas, R., Aissaoui, R., & de Guise, J. A. (2004). A 3D generic inverse dynamic method using wrench notation and quaternion algebra. *Comput Methods Biomech Biomed Engin*, *7*(3), 159-166. doi:10.1080/10255840410001727805
- Durmus, D., Alayli, G., & Canturk, F. (2007). Effects of quadriceps electrical stimulation program on clinical parameters in the patients with knee osteoarthritis. *Clin Rheumatol*, *26*(5), 674-678. doi:10.1007/s10067-006-0358-3
- Duthon, V. B., Barea, C., Abrassart, S., Fasel, J. H., Fritschy, D., & Menetrey, J. (2006). Anatomy of the anterior cruciate ligament. *Knee Surg Sports Traumatol Arthrosc*, *14*(3), 204-213. doi:10.1007/s00167-005-0679-9
- Dyrby, C. O., & Andriacchi, T. P. (2004). Secondary motions of the knee during weight bearing and non-weight bearing activities. *J Orthop Res*, *22*(4), 794-800. doi:10.1016/j.jorthres.2003.11.003
- Elias, J. J., Faust, A., Chu, Y., Chao, E., & Cosgarea, A. (2003). The soleus muscle acts as an agonist for the anterior cruciate ligament an in vitro experimental study. *Am J Sports Med*, *31*(2), 241-246.
- Erdemir, A., McLean, S., Herzog, W., & van den Bogert, A. J. (2007). Model-based estimation of muscle forces exerted during movements. *Clin Biomech (Bristol, Avon)*, *22*(2), 131-154. doi:10.1016/j.clinbiomech.2006.09.005
- Escamilla, R. F., Macleod, T. D., Wilk, K. E., Paulos, L., & Andrews, J. R. (2012). Anterior cruciate ligament strain and tensile forces for weight-bearing and non-weight-bearing exercises: a guide to exercise selection. *J Orthop Sports Phys Ther*, *42*(3), 208-220. doi:10.2519/jospt.2012.3768
- Ferrarin, M., & Pedotti, A. (2000). The relationship between electrical stimulus and joint torque a dynamic model. *IEEE Transactions on Rehabilitation Engineering*, *8*(3), 342-352.
- Fitzgerald, G. K., Axe, M. J., & Snyder-Mackler, L. (2000). Proposed practice guidelines for nonoperative anterior cruciate ligament rehabilitation of physically active individuals. *J Orthop Sports Phys Ther*, *30*(4), 194-203.
- Frank, C., & Jackson, B. (1997). Current concepts review The science of reconstruction of the anterior cruciate ligament. *J Bone Joint Surg*, *79-A*(10), 1556-1576.
- Fregly, B. J., Besier, T. F., Lloyd, D. G., Delp, S. L., Banks, S. A., Pandy, M. G., & D'Lima, D. D. (2012). Grand challenge competition to predict in vivo knee loads. *J Orthop Res*, *30*(4), 503-513. doi:10.1002/jor.22023

- Frigo, C., Ferrarin, M., Frasson, W., Pavan, E., & Thorsen, R. (2000). EMG signals detection and processing for on-line control of functional electrical stimulation. *J Electromyogr Kinesiol*, *10*(5), 351-360.
- Fukuda, Y., Woo, S., Loh, J., Tsuda, E., Tang, P., McMahon, P., & Debski, R. (2003). A quantitative analysis of valgus torque on the ACL: a human cadaveric study. *Journal of Orthopaedic Research*, *21*(6), 1107-1112.
- Gabriel, M., Wong, E., Woo, S., Yagi, M., & Debski, R. (2004). Distribution of in situ forces in the anterior cruciate ligament in response to rotatory loads. *J Orthop Res*, *22*(1), 85-89.
- Gao, B., & Zheng, N. N. (2010). Alterations in three-dimensional joint kinematics of anterior cruciate ligament-deficient and -reconstructed knees during walking. *Clin Biomech*, *25*(3), 222-229. doi:10.1016/j.clinbiomech.2009.11.006
- Geers, T. (1984). An objective error measure for the comparison of calculated and measured transient response histories *Shock and Vibration Information Center The Shock and Vibration Bull*, *54*(2), 99-108.
- Georgoulis, A., Papadonikolakis, A., Papageorgiou, C., Mitsou, A., & Stergiou, N. (2003). Three dimensional tibiofemoral kinematics of the ALCD and ALCR knee during walking. *Am J Sports Med*, *31*(1), 75-79.
- Girgis, F., Marshall, J., & Jem, A. (1975). The Cruciate Ligaments of the Knee Joint: Anatomical, Functional and Experimental Analysis. *Clinical orthopaedics and related research*, *106*, 216-231.
- Gregory, C. M., & Bickel, C. S. (2005). Recruitment patterns in human skeletal muscle during electrical stimulation. *Physical Therapy*, *85*(4), 358-364.
- Griffin, L. Y., Albohm, M. J., Arendt, E. A., Bahr, R., Beynon, B. D., Demaio, M., . . . Yu, B. (2006). Understanding and preventing noncontact anterior cruciate ligament injuries: a review of the Hunt Valley II meeting, January 2005. *Am J Sports Med*, *34*(9), 1512-1532. doi:10.1177/0363546506286866
- Grindem, H., Eitzen, I., Engebretsen, L., Snyder-Mackler, L., & Risberg, M. A. (2014). Nonsurgical or Surgical Treatment of ACL Injuries: Knee Function, Sports Participation, and Knee Reinjury: The Delaware-Oslo ACL Cohort Study. *J Bone Joint Surg Am*, *96*(15), 1233-1241. doi:10.2106/JBJS.M.01054
- Hamid, S., & Hayek, R. (2008). Role of electrical stimulation for rehabilitation and regeneration after spinal cord injury: an overview. *Eur Spine J*, *17*(9), 1256-1269. doi:10.1007/s00586-008-0729-3
- Hashemi, J., Chandrashekar, N., Gill, B., Beynon, B. D., Slauterbeck, J. R., Schutt, R. C., Jr., . . . Dabiezies, E. (2008). The geometry of the tibial plateau and its influence on the biomechanics of the tibiofemoral joint. *J Bone Joint Surg Am*, *90*(12), 2724-2734. doi:10.2106/JBJS.G.01358
- Hermens, H. J., Freriks, B., Disselhorst-Klug, C., & Rau, G. (2000). Development of recommendations for SEMG sensors and sensor placement procedures. *J Electromyogr Kines*, *10*, 361-374.
- Hewett, T. E., Di Stasi, S. L., & Myer, G. D. (2013). Current concepts for injury prevention in athletes after anterior cruciate ligament reconstruction. *Am J Sports Med*, *41*(1), 216-224. doi:10.1177/0363546512459638
- Hirokawa, S., Solomonow, M., Yun, L., Zong-Ping, L., & D'ambrosia, R. (1992). Anterior-Posterior and Rotational Displacement of The Tibia Elicited By Quadriceps Contraction. *The American Journal of Sports Medicine*, *20*(3), 299-306.
- Hodges, P. W., van den Hoorn, W., Wrigley, T. V., Hinman, R. S., Bowles, K. A., Cicuttini, F., . . . Bennell, K. (2016). Increased duration of co-contraction of medial knee muscles is associated with greater progression of knee osteoarthritis. *Man Ther*, *21*, 151-158. doi:10.1016/j.math.2015.07.004
- Imoto, A., Peccin, S., Almeida, G., Saconato, H., & Atallah, A. (2011). Effectiveness of electrical stimulation on rehabilitation after ligament and meniscal injuries: a systematic review. *Sao Paulo Med J*, *129*(6), 414-423.

- Jezernik, S., Colombo, G., Keller, T., Frueh, H., & Morari, M. (2003). Robotic orthosis lokomat: A rehabilitation and research tool. *Neuromodulation: Technology at the neural interface*, 6(2), 108-115.
- Jonkers, I., Stewart, C., & Spaepen, A. (2003). The complementary role of the plantarflexors, hamstrings and gluteus maximus in the control of stance limb stability during gait. *Gait Posture*, 17(3), 264-272. doi:10.1016/s0966-6362(02)00102-9
- Kanamori, A., Woo, S. L., Ma, C. B., Zeminski, J., Rudy, T. W., Li, G., & Livesay, G. A. (2000). The forces in the anterior cruciate ligament and knee kinematics during a simulated pivot shift test: A human cadaveric study using robotic technology. *Arthroscopy*, 16(6), 633-639. doi:10.1053/jars.2000.7682
- Kendall, F. P., McCreary, E. K., Provance, P. G., Rodgers, M. M., & Romani, W. A. (1993). *Muscles: Testing and Function with Posture and Pain* (5th ed.). United States of America: Lippincott William & Wilkins.
- Kerr, C., McDowell, B., & McDonough, S. (2004). Electrical stimulation in cerebral palsy a review of effects on strength and motor function. *Dev Med Child Neurol*, 46, 205-213.
- Kiapour, A., & Murray, M. (2014). Basic science of anterior cruciate ligament injury and repair. *Bone and Joint Research*, 3(2), 20-31.
- Kim, K. M., Croy, T., Hertel, J., & Saliba, S. (2010). Effects of neuromuscular electrical stimulation after anterior cruciate ligament reconstruction on quadriceps strength, function, and patient-oriented outcomes: a systematic review. *J Orthop Sports Phys Ther*, 40(7), 383-391. doi:10.2519/jospt.2010.3184
- Komura, T., & Nagano, A. (2004). Evaluation of the influence of muscle deactivation on other muscles and joints during gait motion. *J Biomech*, 37(4), 425-436. doi:10.1016/j.jbiomech.2003.09.022
- Kondo, E., Yasuda, K., Azuma, H., Tanabe, Y., & Yagi, T. (2008). Prospective clinical comparisons of anatomic double-bundle versus single-bundle anterior cruciate ligament reconstruction procedures in 328 consecutive patients. *Am J Sports Med*, 36(9), 1675-1687.
- Koo, S., & Andriacchi, T. P. (2008). The knee joint center of rotation is predominantly on the lateral side during normal walking. *J Biomech*, 41(6), 1269-1273. doi:10.1016/j.jbiomech.2008.01.013
- Kvist, J. (2004). Rehabilitation following anterior cruciate ligament injury. *Sports Medicine*, 34(4), 269-280.
- Kwak, S., Ahmad, C., Gardner, T., Grelsamer, R., Henry, J., Blankevoort, L., . . . Mow, V. (2000). Hamstrings and iliotibial band forces affect knee kinematics and contact pattern. *J Orthop Res*, 18(1), 101-108.
- Lafortune, M., Cavanagh, P., Sommer, H., & Kalenak, A. (1992). Three-dimensional kinematics of the human knee during walking. *J Biomech*, 25(4), 347-357.
- Lankester, B., Cottam, H., Pinskerova, V., Eldridge, J., & Freeman, M. (2008). Variation in the anatomy of the tibial plateau. *Bone & Joint Journal*, 90(3), 330-333. doi:10.1302/0301-620X.90B3
- Levine, J. W., Kiapour, A. M., Quatman, C. E., Wordeman, S. C., Goel, V. K., Hewett, T. E., & Demetropoulos, C. K. (2013). Clinically relevant injury patterns after an anterior cruciate ligament injury provide insight into injury mechanisms. *Am J Sports Med*, 41(2), 385-395. doi:10.1177/0363546512465167
- Li, G., Rudy, T., Sakane, M., Kanamori, A., Ma, C., & Woo, S.-Y. (1999). The importance of quadriceps and hamstring muscle loading on knee kinematics and in-situ forces in the ACL. *J Biomech*, 32, 395-400.
- Liu, W., & Maitland, M. E. (2000). The effect of hamstring muscle compensation for anterior laxity in the ACL-deficient knee during gait. *J Biomech*, 33(7), 871-879.
- Logan, M., Dunstan, E., Robinson, J., Williams, A., Gedroyc, W., & Freeman, M. (2004a). Tibiofemoral kinematics of the anterior cruciate ligament (ACL)-deficient weightbearing, living knee employing vertical access open "interventional" multiple resonance imaging. *Am J Sports Med*, 32(3), 720-726. doi:10.1177/0095399703258771

- Logan, M., Williams, A., Lavelle, J., Gedroyc, W., & Freeman, M. (2004b). What really happens during the Lachman test? A dynamic MRI analysis of tibiofemoral motion. *Am J Sports Med*, 32(2), 369-375. doi:10.1177/0095399703258698
- Lohmander, L. S., Englund, P. M., Dahl, L. L., & Roos, E. M. (2007). The long-term consequence of anterior cruciate ligament and meniscus injuries: osteoarthritis. *Am J Sports Med*, 35(10), 1756-1769. doi:10.1177/0363546507307396
- Lynch, C. L., & Popovic, M. R. (2008). Functional electrical stimulation. *IEEE Contr Syst Mag*, 28(2), 40-50. doi:10.1109/mcs.2007.914689
- MacWilliams, B., Wilson, D., DesJardins, J., Romero, J., & Chao, E. (1999). Hamstrings cocontraction reduces internal rotation, anterior translation and anterior cruciate ligament load in weight-bearing flexion. *J Orthop Res*, 17, 817-822.
- Maffiuletti, N. A. (2010). Physiological and methodological considerations for the use of neuromuscular electrical stimulation. *Eur J Appl Physiol*, 110(2), 223-234. doi:10.1007/s00421-010-1502-y
- Markolf, K. L., O'Neill, G., Jackson, S. R., & McAllister, D. R. (2004). Effects of applied quadriceps and hamstrings muscle loads on forces in the anterior and posterior cruciate ligaments. *Am J Sports Med*, 32(5), 1144-1149. doi:10.1177/0363546503262198
- Marra, M., Vanheule, V., Fluit, R., Koopman, B., Rasmussen, J., Verdonschot, N., & Andersen, M. (2015). A Subject-Specific Musculoskeletal Modeling Framework to Predict In Vivo Mechanics of Total Knee Arthroplasty. *ASME. J Biomech Eng.*, 137(2), 020904-020904-020912. doi:10.1115/1.4029258]
- Marshall, S. W. (2010). Recommendations for Defining and Classifying Anterior Cruciate Ligament Injuries in Epidemiologic Studies. *Journal of Athletic Training*, 45(5), 516-518.
- Masouros, S. D., Bull, A. M. J., & Amis, A. A. (2010). (i) Biomechanics of the knee joint. *Orthopaedics and Trauma*, 24(2), 84-91. doi:10.1016/j.mporth.2010.03.005
- Matsumoto, H. (1990). Mechanism of the pivot shift. *J Bone Joint Surg*, 72-B, 816-821.
- Matsunaga, T., Shimada, Y., & Sato, K. (1999). Muscle fatigue from intermittent stimulation with low and high frequency electrical pulses. *Archives of physical medicine and rehabilitation*, 80(1), 48-53.
- Micheo, W., Hernandez, L., & Seda, C. (2010). Evaluation, management, rehabilitation, and prevention of anterior cruciate ligament injury: current concepts. *PM R*, 2(10), 935-944. doi:10.1016/j.pmrj.2010.06.014
- Mohr, T., Andersen J.L., Biering-Sørensen, F., Galbo, H., Bangsbo, J., Wagner, A., & Kjaer, M. (1997). Long term adaptation to electrically induced cycle training in severe spinal cord injury individuals. *Spinal cord*, 35(1).
- Monaghan, B., Caulfield, B., & O'Mathuna, D. P. (2010). Surface neuromuscular electrical stimulation for quadriceps strengthening pre and post total knee replacement. *Cochrane Database Syst Rev*(1), CD007177. doi:10.1002/14651858.CD007177.pub2
- More, R., Karras, B., Neiman, R., Fritschy, D., Woo, S., & Daniel, D. (1993). Hamstring an anterior cruciate ligament protagonist. *Am J Sports Med*, 21(2), 231-237.
- Murray, J. R., Lindh, A. M., Hogan, N. A., Trezies, A. J., Hutchinson, J. W., Parish, E., . . . Cross, M. V. (2012). Does anterior cruciate ligament reconstruction lead to degenerative disease?: Thirteen-year results after bone-patellar tendon-bone autograft. *Am J Sports Med*, 40(2), 404-413. doi:10.1177/0363546511428580
- Neptune, R. R., & Sasaki, K. (2005). Ankle plantar flexor force production is an important determinant of the preferred walk-to-run transition speed. *J Exp Biol*, 208(Pt 5), 799-808. doi:10.1242/jeb.01435
- Nolte, D., Tsang, C. K., Zhang, K. Y., Ding, Z., Kedgley, A. E., & Bull, A. M. J. (2016). Non-linear scaling of a musculoskeletal model of the lower limb using statistical shape models. *J Biomech*, 49(14), 3576-3581. doi:10.1016/j.jbiomech.2016.09.005
- Noyes, F. R., & Barber-Westin, S. D. (2006). Anterior cruciate ligament revision reconstruction: results using a quadriceps tendon-patellar bone autograft. *Am J Sports Med*, 34(4), 553-564. doi:10.1177/0363546505281812

- Noyes, F. R., Bassett, R. W., Grood, E. S., & Butler, D. L. (1980). Arthroscopy in acute traumatic hemarthrosis of the knee. Incidence of anterior cruciate tears and other injuries. *J Bone Joint Surg Am*, 62(5), 687-695, 757.
- Noyes, F. R., Matthews, D. S., Mooar, P. A., & Grood, E. S. (1983a). The symptomatic anterior-cruciate deficient knee. Part II: the results of rehabilitation, activity modification, and counseling on functional disability. *J Bone Joint Surg Am*, 65(2), 163-174.
- Noyes, F. R., Mooar, L. A., Moorman III, C. T., & McGinnis, G. H. (1989). Partial tears of the anterior cruciate ligament. *J Bone Joint Surg*, 71-B, 825-833.
- Noyes, F. R., Mooar, P. A., Matthews, D. S., & Butler, D. L. (1983b). The symptomatic anterior cruciate-deficient knee. Part I: the long-term functional disability in athletically active individuals. *J Bone Joint Surg Am*, 65(2), 154-162.
- Paillard, T. (2008). Combined application of neuromuscular electrical stimulation and voluntary muscular contractions. *Sports Medicine*, 38(2), 161-177.
- Palmieri-Smith, R. M., Thomas, A. C., & Wojtys, E. M. (2008). Maximizing quadriceps strength after ACL reconstruction. *Clin Sports Med*, 27(3), 405-424, vii-ix. doi:10.1016/j.csm.2008.02.001
- Papannagari, R., Gill, T. J., Defrate, L. E., Moses, J. M., Petruska, A. J., & Li, G. (2006). In vivo kinematics of the knee after anterior cruciate ligament reconstruction: a clinical and functional evaluation. *Am J Sports Med*, 34(12), 2006-2012. doi:10.1177/0363546506290403
- Papavasiliou, A. S. (2009). Management of motor problems in cerebral palsy: a critical update for the clinician. *Eur J Paediatr Neurol*, 13(5), 387-396. doi:10.1016/j.ejpn.2008.07.009
- Paterno, M. V., Schmitt, L. C., Ford, K. R., Rauh, M. J., Myer, G. D., Huang, B., & Hewett, T. E. (2010). Biomechanical measures during landing and postural stability predict second anterior cruciate ligament injury after anterior cruciate ligament reconstruction and return to sport. *Am J Sports Med*, 38(10), 1968-1978. doi:10.1177/0363546510376053
- Peckham, P. H. (1987). Functional electrical stimulation: current status and future prospects of applications to the neuromuscular system in spinal cord injury. *Paraplegia*, 25(3), 279-288. doi:10.1038/sc.1987.52
- Perry, J., & Burnfield, J. (2010). *Gait Analysis: Normal and Pathological Function* (2nd ed.). New Jersey: SLACK Incorporated.
- Rane, L., & Bull, A. M. J. (2016). Functional electrical stimulation of gluteus medius reduces the medial joint reaction force of the knee during level walking. *Arthritis Res Ther*, 18(1), 255. doi:10.1186/s13075-016-1155-2
- Renstrom, P., Arms, S. W., Stanwyck, T. S., Johnson, R. J., & Pope, M. H. (1986). Strain within the anterior cruciate ligament during hamstring and quadriceps activity. *Am J Sports Med*, 14(1), 83-87.
- Risberg, M., Lewek, M., & Snyder-Mackler, L. (2004). A systematic review of evidence for anterior cruciate ligament rehabilitation: how much and what type? *Physical Therapy in Sport*, 5(3), 125-145. doi:10.1016/j.ptsp.2004.02.003
- Rudolph, K. S., Axe, M. J., Buchanan, T. S., Scholz, J. P., & Snyder-Mackler, L. (2001). Dynamic stability in the anterior cruciate ligament deficient knee. *Knee Surg Sports Traumatol Arthrosc*, 9(2), 62-71. doi:10.1007/s001670000166
- Rudolph, K. S., Eastlak, M. E., Axe, M. J., & Snyder-Mackler, L. (1998). 1998 Basmajian Student Award Paper: Movement patterns after anterior cruciate ligament injury: a comparison of patients who compensate well for the injury and those who require operative stabilization. *J Electromyogr Kinesiol*, 8(6), 349-362.
- Rushton, D. N. (2003). Functional Electrical Stimulation and rehabilitation—an hypothesis. *Medical Engineering & Physics*, 25(1), 75-78. doi:10.1016/s1350-4533(02)00040-1
- Schwer, L. E. (2007). Validation metrics for response histories: perspectives and case studies. *Engineering with Computers*, 23(4), 295-309. doi:10.1007/s00366-007-0070-1
- Sennels, S., Biering-Sørensen, F., Andersen, O. T., & Hansen, S. D. (1997). Functional neuromuscular stimulation controlled by surface electromyographic signals produced by volitional activation of the same muscle: adaptive removal of the muscle response from the recorded EMG-signal. *IEEE T on Rehabil Eng*, 5(2), 195-205.

- Shao, Q., MacLeod, T. D., Manal, K., & Buchanan, T. S. (2011). Estimation of ligament loading and anterior tibial translation in healthy and ACL-deficient knees during gait and the influence of increasing tibial slope using EMG-driven approach. *Ann Biomed Eng*, 39(1), 110-121. doi:10.1007/s10439-010-0131-2
- Shelburne, K. B., Pandy, M. G., & Torry, M. R. (2004). Comparison of shear forces and ligament loading in the healthy and ACL-deficient knee during gait. *J Biomech*, 37(3), 313-319. doi:10.1016/j.jbiomech.2003.07.001
- Shelburne, K. B., Torry, M. R., & Pandy, M. G. (2005). Effect of muscle compensation on knee instability during ACL-deficient gait. *Med Sci Sports Exerc*, 37(4), 642-648. doi:10.1249/01.mss.0000158187.79100.48
- Shimokochi, Y., & Shultz, S. J. (2008). Mechanisms of noncontact anterior cruciate ligament injury. *J Athl Train*, 43(4), 396-408.
- Sinkjaer, T., & Arendt-Nielsen, L. (1991). Knee stability and muscle coordination in patients with anterior cruciate ligament injuries: An electromyographic approach. *J Electromyogr Kinesiol*, 1(3), 209-217.
- Smith, G. V., Alon, G., Roys, S. R., & Gullapalli, R. P. (2003). Functional MRI determination of a dose-response relationship to lower extremity neuromuscular electrical stimulation in healthy subjects. *Exp Brain Res*, 150(1), 33-39. doi:10.1007/s00221-003-1405-9
- Snyder-Mackler, L., De Luca, P., Williams, P., Eastlack, M., & Bartolozzi, r. A. (1994). Reflex inhibition of the quadriceps femoris muscle after injury or reconstruction of the anterior cruciate ligament. *J Bone Joint Surg*, 76(4), 555-560.
- Snyder-Mackler, L., Delitto, A., Bailey, S. L., & Stralka, S. W. (1995). Strength of the quadriceps femoris muscle and functional recovery after reconstruction of the anterior cruciate ligament. *J Bone Joint Surg*, 77(8), 1166-1173.
- Snyder-Mackler, L., Lladin, Z., Schepsis, A., & Young, J. (1991). Electrical stimulation of the thigh muscles after reconstruction of the ACL. *J Bone Joint Surg*, 73-A(7), 1025-1036.
- Solomonow, M. (2006). Sensory-motor control of ligaments and associated neuromuscular disorders. *J Electromyogr Kinesiol*, 16(6), 549-567. doi:10.1016/j.jelekin.2006.08.004
- Sprague, M., & Geers, T. (2003). Spectral elements and field separation for an acoustic fluid subject to cavitation. *Journal of Computational Physics*, 184(1), 149-162.
- Stevens, J. E., Mizner, R. L., & Snyder-Mackler, L. (2003). Quadriceps strength and volitional activation before and after total knee arthroplasty for osteoarthritis. *J Orthop Res*, 21(5), 775-779. doi:10.1016/s0736-0266(03)00052-4
- Thorsen, R., Ferrarin, M., Spadone, R., & Frigo, C. (1999). Functional control of the hand in tetraplegics based on residual synergistic EMG activity. *Artif Organs*, 23(5), 470-473.
- van der Linden, M. L., Hazlewood, M. E., Hillman, S. J., & Robb, J. E. (2008). Functional electrical stimulation to the dorsiflexors and quadriceps in children with cerebral palsy. *Pediatr Phys Ther*, 20(1), 23-29. doi:10.1097/PEP.0b013e31815f39c9
- van Eck, C. F., Lesniak, B. P., Schreiber, V. M., & Fu, F. H. (2010). Anatomic single- and double-bundle anterior cruciate ligament reconstruction flowchart. *Arthroscopy*, 26(2), 258-268. doi:10.1016/j.arthro.2009.07.027
- Victor, J., Labey, L., Wong, P., Innocenti, B., & Bellemans, J. (2010). The influence of muscle load on tibiofemoral knee kinematics. *J Orthop Res*, 28(4), 419-428. doi:10.1002/jor.21019
- Waters, R. L. (1984). The enigma of "carry-over". *International Rehabilitation Medicine*, 6(1), 9-12. doi:10.3109/09638288409166960
- Wen, L., & Maitland, M. E. (2000). The effect of hamstring muscle compensation for anterior laxity in the ACL-deficient knee during gait. *Journal of Biomechanics*, 33, 871-879.
- Winter, D. A., & Yack, H. J. (1987). EMG profiles during normal human walking: stride-to-stride and inter-subject variability. *Electroen Clin Neuro*, 67, 402-411.
- Woo, S. L., Abramowitch, S. D., Kilger, R., & Liang, R. (2006). Biomechanics of knee ligaments: injury, healing, and repair. *J Biomech*, 39(1), 1-20. doi:10.1016/j.jbiomech.2004.10.025
- Woo, S. L., Kanamori, A., Zeminski, J., Yagi, M., Papageorgiou, C., & Fu, F. H. (2002). The effectiveness of reconstruction of the anterior cruciate ligament with hamstrings and patellar tendon: a cadaveric study comparing anterior tibial and rotational loads. *J Bone Joint Surg*, 84(6), 907-914.

- Wright, R., Preston, E., Fleming, B., Amendola, A., Andrish, J., Bergfeld, J., . . . McCarty, E. (2008). A Systematic Review of Anterior Cruciate Ligament Reconstruction Rehabilitation—Part II: Open Versus Closed Kinetic Chain Exercises, Neuromuscular Electrical Stimulation, Accelerated Rehabilitation, and Miscellaneous Topics. *The journal of knee surgery*, *21*(3), 225-234.
- Wu, J.-L., Jong Keun, S., Gadikota, H. R., Hosseini, A., Sutton, K. M., Gill, T. J., & Guoan, L. (2009). In Situ Forces in the Anteromedial and Posterolateral Bundles of the Anterior Cruciate Ligament Under Simulated Functional Loading Conditions. *Am J Sports Med*, *38*(3), 558-563. doi:10.1177/0363546509350110
- Xu, R., Ming, D., Ding, Z., & Bull, A. M. J. Extra Excitation of Biceps Femoris or Lateral Gastrocnemius during NMES Reduces Knee Medial Loading. *in submission*.
- Yagi, M., Kuroda, R., Nagamune, K., Yoshiya, S., & Kurosaka, M. (2007). Double-bundle ACL reconstruction can improve rotational stability. *Clin Orthop Relat Res*, *454*, 100-107. doi:10.1097/BLO.0b013e31802ba45c
- Yagi M, W. E., Kanamori A, Debski RE, Fu FH, Woo SL. . (2002). Biomechanical analysis of an anatomic anterior cruciate ligament reconstruction. *Am J Sports Med*, *30*(5), 660-666.
- Yamaguchi, G. T. (2001). *Dynamic modeling of musculoskeletal motion: A vectorized approach for biomechanical analysis in three dimensions*. (Vol. ISBN: 978-0-387-28750-8). New York: Springer.
- Yanagawa, T., Shelburne, K., Serpas, F., & Pandy, M. (2002). Effect of hamstrings muscle action on stability of the ACL-deficient knee in isokinetic extension exercise. *Clin Biomech.*, *17*, 705–712.
- Zantop, T., Herbort, M., Raschke, M. J., Fu, F. H., & Petersen, W. (2007). The role of the anteromedial and posterolateral bundles of the anterior cruciate ligament in anterior tibial translation and internal rotation. *Am J Sports Med*, *35*(2), 223-227. doi:10.1177/0363546506294571